T-1418

EFFECTS OF NICKELOUS ION ON THE ELECTRODEPOSITION OF COPPER

by

John C. Gathje

ProQuest LLC.
789 East Eisenhower Parkway
P.O. Box 1346
Ann Arbor, MI 48106 – 1346

T-1418

A thesis respectfully submitted to the Faculty and the Board of Trustees of the Colorado School of Mines in partial fulfillment of the requirements for the degree of Master of Science in Metallurgical Engineering.

Signed: John C. Gathje
John C. Gathje

Golden, Colorado
Date: Dec. 13, 1971

Approved:
T. Balberyszski
Thesis Advisor

J. P. Hager
Head of Department
Metallurgical Engineering

Golden, Colorado
Date: DEC. 13, 1971

ABSTRACT

A kinetic and an empirical study of the effects of nickelous ion on the deposition process of copper in a copper sulfate+sulfuric acid system was made.

The empirical experiments indicate that nickel ion has no effect on the current efficiency of the deposition process nor on the purity of the deposit. It does have an effect on the morphology of the deposit and the cell voltage. A system of grading the quality of the deposit was developed. This system results in a Reference Number, R, which describes the experimental conditions of deposition. The quality of the surface of the deposit is given by the Surface Index, Q. Correlation between R and Q are given along with the four divisions of the qualities of the deposits.

An increase in the nickel concentration gives deposits that are less satisfactory. This effect becomes greatest at high current densities. At a current density of 19.1 amps/ft^2, good deposits are obtained at all nickel concentrations regardless of the copper concentration. At 37.0 and 56.1 amps/ft^2 the control of the copper concentration becomes critical and less satisfactory deposits are obtained when the copper concentration is below a certain minimum.

All concentrations of the nickel ion increase the cell voltage at a current density of 19.1 amps/ft^2. It is lowered at 37.0 amps/ft^2 if the nickel concentration is not above 1 gram per liter. At concentrations higher than 1 gram per liter the cell voltage is increased. At a current

density of 50.1 amps/ft^2 the nickel concentration lowers the cell voltage. All increases and decreases in the cell voltage are relative to the cell voltage when no nickel is present in the electrolyte. At all current densities the nickel stabilized the cell voltage at a value that was independent of the copper concentration.

The kinetic studies indicate that nickel increases the exchange current density of the copper + copper sulfate + sulfuric acid system. These studies indicate that the nickel influences the amount of energy required for the charge-transfer process. It lowers this energy requirement and thus allows the reaction to proceed by a one-step charge-transfer process at nickel concentrations of approximately 10 grams per liter. This concentration is independent of the copper concentration. The reaction reverts back to a two-step charge-transfer process at high nickel concentrations (approximately 15 grams per liter).

A theory is proposed to explain this behavior. This theory proposes that the lowering in the energy is accomplished through either or a combination of two factors: 1) the stretching of the copper-water bond by the presence of nickel ions, and/or 2) the lowering of the work function of the metal electrode in the presence of nickel ions. It is also proposed that the nickel ions build up in concentration near the cathode and act as a barrier that affects the mobility of the copper ions. The energy lowering effect and the barrier effect join to produce forces that influence the system so that it acts in the manner that was experimentally determined.

TABLE OF CONTENTS

LIST OF FIGURES

LIST OF TABLES

ACKNOWLEDGMENTS

The author wishes to express his appreciation and thanks to Dr. T. Balberyszski, Associate Professor, Department of Metallurgical Engineering, Colorado School of Mines, for his valuable guidance and assistance throughout the course of this investigation.

The author would also like to extend his gratitude to his committee, Dr. P.G. Herold and Dr. W. Copeland.

Thanks also goes to the author's fellow students Mr. V.F.Campos for his many helpful discussions, aid in computer programming and photography; and to Mr. R. Roberts for his assistance with much of the polarization experimental equipment, and for his valuable aid and guidance during this phase of the work.

The author would also like to thank the Colorado School of Mines Foundation and the American Metals Climax Corporation for providing the financial assistance necessary to carry out this investigation.

The author would also like to thank Dr. N.C. Schieltz for his valuable help in much of the photography work.

Last but not least, the author would also like to thank his wife, Judy for her kind and gentle patience during this course of study.

INTRODUCTION

In a recent publication (Rosenbaum, 1968), the Research Director of the Salt Lake City Metallurgy Research Center, Mr. J. B. Rosenbaum stated:

> "There is little prospect for the displacement of concentrate smelting by electrometallurgy. However, leaching of copper from ores and waste dumps is increasing sharply. Most of the copper so dissolved is removed from solution by cementation on scrap iron and charged to the smelter. An alternative route, receiving increasing attention, is to prepare and enriched solution for copper electrowinning by solvent extraction of the dilute leach solution or by dissolving the cement copper in cell electrolyte."

The two important words to take note of from the above quote are- copper electrowinning. It was the intent of this author to conduct research which would be of practical value to both the copper electrowinning and electrorefining industries.

In the last ten years the total production of refined copper has grown from 1,679,362 tons in 1961 to 1,985,202 tons in 1969. However, the copper produced by electrolytic means has dropped during this same time period. In 1961 electrolytic copper accounted for 90.4% of the refined copper output of the United States. This figure dropped to 88.3% in 1969. These figures can be compared to the figures of 1950 which show that electrolytic copper accounted for 93.5% of the refined copper output.

During this same time period the price of electrolytic copper increased sharply. At the end of 1961 the price was 31.00 cents per

pound whereas in September 1969 the price had risen to 52.12 1/2 cents per pound. This is almost a twofold increase during a very short time period.

Many reasons can be given for the increase in price and decrease in production of electrolytic copper. It is not the intent of this author nor of this research to investigate the economics of copper production. However, it is necessary to point out that with such a state of affairs it behooves the copper industry to know as much as possible about their operating parameters.

It is also important to show the increasing tendency and need of the copper industry to go to hydrometallurgical processes for producing copper. Many new plants using primarily hydrometallurgy and specifically electrowinning of copper as a recovery means have been developed in recent years. In Zambia, Africa, the Chambishi RLE plant was recently built and uses the Chambishi Process for the roasting, leaching and electrowinning of copper (Verney, 1968).

In March of 1968 the first commercial copper liquid ion exchange and electrowinning plant was opened in the Bluebird Mine in Miami, Arizona (Power, 1970). In its first year it produced 9,000,000 pounds of cathode copper.

There are also many copper refineries throughout the world. These refineries encounter many of the same problems that are encountered at electrowinning operations. In a typical refinery there are eight major impurities to cope with. They are: gold, silver, selenium, tellurium, arsenic, antimony, lead and nickel. These same impurities also show up in many electrowinning plants. Table 1 shows some

typical electrolyte analysis from various plants.

Table 1: Impurity Levels of Refinery Electrolytes

Impurity	Plant					
	Mufulira (gpl)	Ndola (gpl)	Chambishi (gpl)	1* (gpl)	2* (gpl)	3* (gpl)
Bi	0.16	0.14	0.04	----	----	----
Ni	2.0	4.0	0.6	21.49	18.09	5.15
As	0.3	----	----	13.72	16.80	6.96
Fe	0.6	0.8	10.0	3.00	3.00	3.65
Cl	0.04	0.02	----	----	----	----
Co	----	----	3.0	----	----	----
Ti	----	----	0.06	----	----	----
Mn	----	----	2.0	----	----	----
Se	----	----	0.7ppm	----	----	----

Table 2 shows some typical nickel analysis of copper anodes used in electrorefining (Mantell, 1950).

Various effects of many of these impurities have been known for many years. In the refinery process Se and Te go into the slimes and are recovered later. Lead precipitates as $PbSO_4$. Arsenic remains in the electrolyte as arsenic acid. Antimony can form H_3SbO_3 which reacts with the arsenic to produce basic antimonious arsenate compounds. Nickel remains in the electrolyte as a sulfate.

Table 2: Typical Nickel Analysis of Copper Anodes Used In Electrorefining.

	% Ni
American Smelting and Refining, Barber, N.J.	0.038
American Smelting and Refining, Baltimore, Md.	0.08
American Smelting and Refining, Tacoma, Wash.	0.14
Anaconda Copper Mining Co., Great Falls, Mont.	0.030
International Nickel Company of Canada, Ltd., Copper Cliff, Ontario	0.48

It is obvious from the foregoing that nickel is usually present in both electrowinning and electrorefining. Very little work has actually been done to determine just what effects the nickel has on copper electrodeposition. It is known that with an increase in the nickel ion content of the electrolyte, there is an increase in nickel in the finished product. This is shown in Figure 2. This nickel in turn has an injurious effect on the conductivity of the final copper product. This is shown in Figure 1 which shows a plot of the percent conductivity of copper as a function of the amount of added nickel.

Kern and Chang (Kern and Chang, 1922) conducted research in 1922 in which they found that arsenic, iron and nickel decreased the conductivity of a $CuSO_4$ - H_2SO_4 electrolyte. The results of their work indicated that the iron and nickel content of the electrolyte should be kept as low as possible.

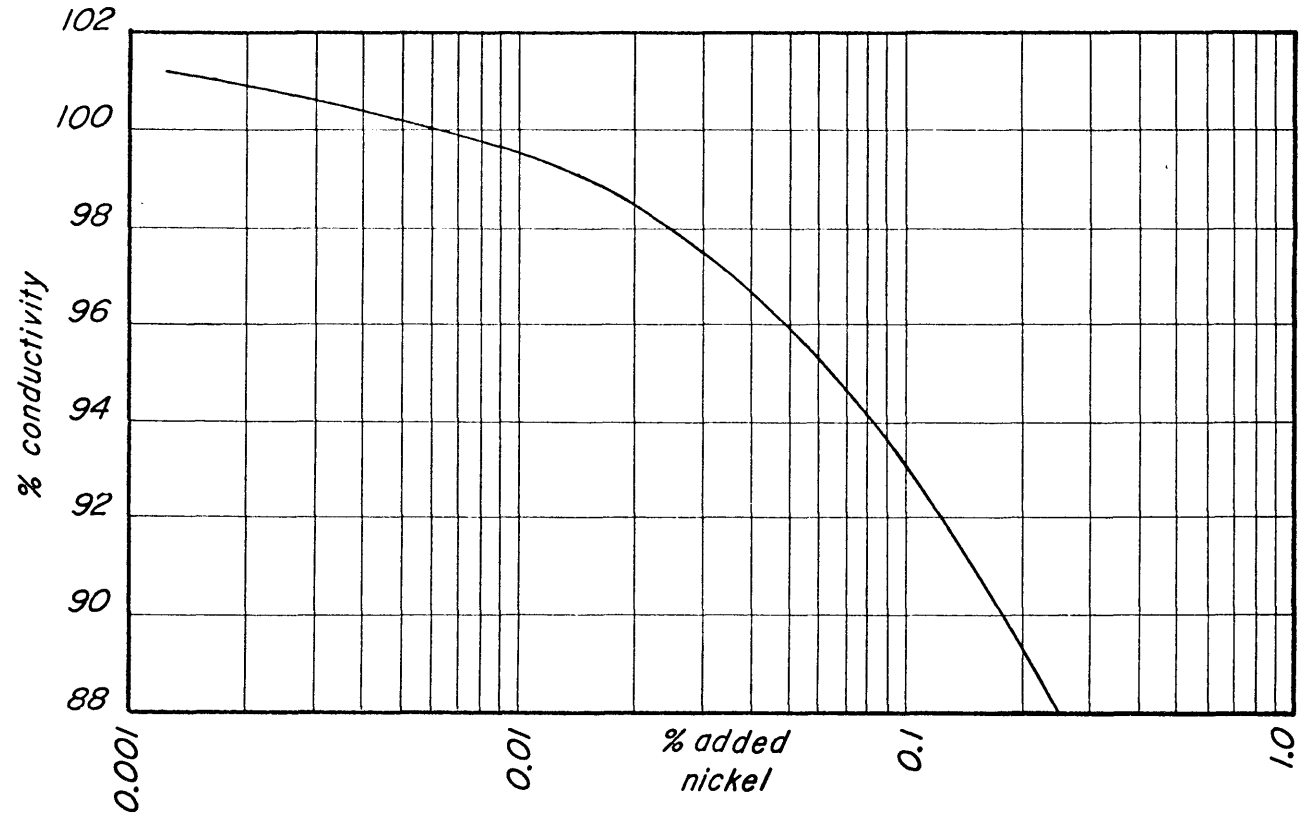

EFFECT OF NICKEL ON COPPER CONDUCTIVITY

FIGURE 1

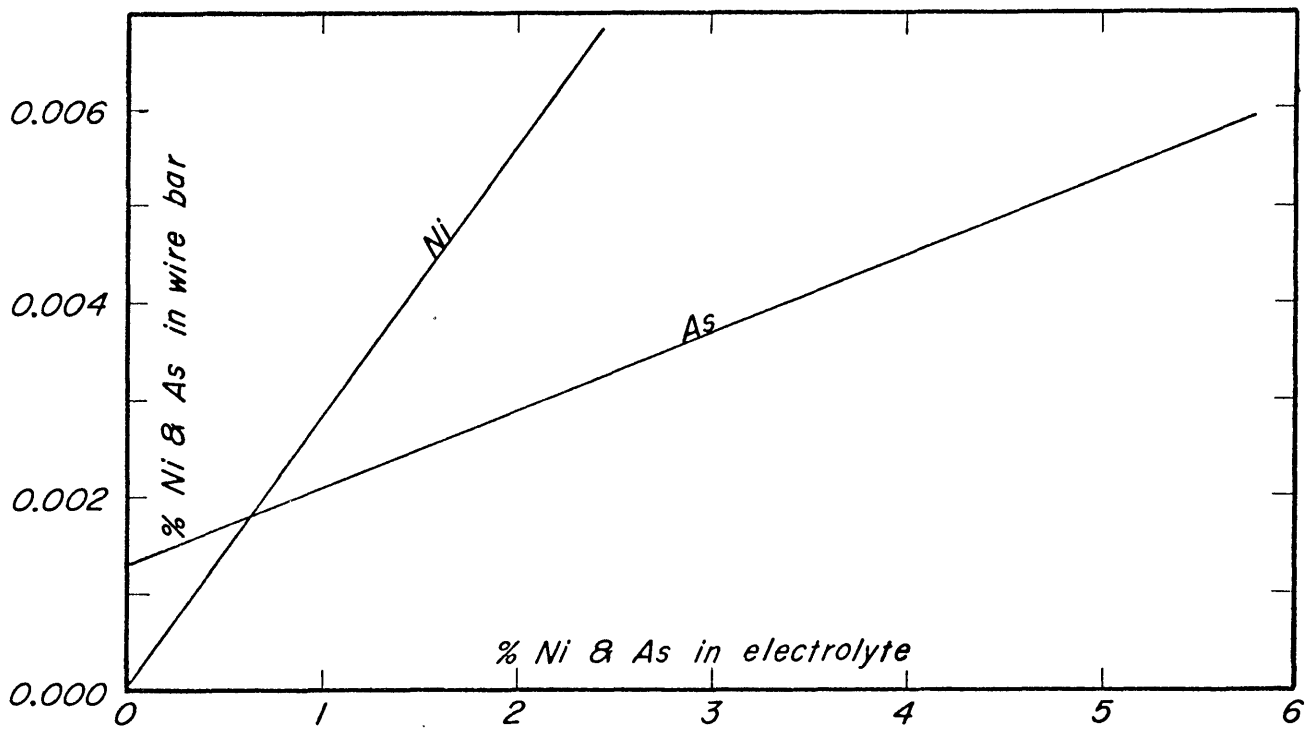

EFFECT OF NICKEL AND ARSENIC ON PURITY OF COPPER WIRE BAR

FIGURE 2

Skowronski and Reinoso (Skowronski and Reinoso, 1927) repeated the work of Kern and Chang. They were able to derive equations for predicting the increase in resistivity of a H_2SO_4 electrolyte with various additions of copper, nickel iron and arsenic. Using a standard electrolyte of 150 gpl H_2SO_4 at a temperature of 55 °C, each one gram of added nickel, copper, iron and arsenic produced the increase in resistivity shown in Table 3.

Table 3: Percent Increase In Resistivity Of An H_2SO_4 Electrolyte

Element	% Increase
Cu	0.657
Ni	0.766
Fe	0.818
As	0.0725

In none of the previous research was there any indication of what effects nickelous ion has on the morphology of the deposit or the efficiency of the process. Nor was there any work that illustrated how important nickel is to the basic deposition process. It was the intention of this research to investigate these factors.

SURVEY OF THE LITERATURE

Much of the earlier work conducted in the field of electrodeposition of copper has been concentrated in the area of studying such impurities as those that are added intentionally in order to produce a certain type of deposit, i.e. gelatin and other organic additives. These additives are used to produce either bright or smooth deposits. In the study of the kinetics of electrode reactions all of the work concerned with copper has concentrated on systems using solutions having only copper as the main cation present in solution.

Organic Additives

A great deal of work has been done on the effects of organic additives in the copper electrodeposition process. It was not the purpose of this work to investigate any organic substances. The reader however, can be referred to several fine works on this subject. These works provide a good starting point for studying "inhibitors" (Bockris and Razumney, 1967) and (Vetter, 1967).

Cation And Anion Impurities

Conductivity and Cell Voltage Measurements

Some work has been done in finding what effects certain anions and cations have on various aspects of the electrodeposition process. Most, if not all of this earlier work dealt with the effect each

impurity had on the properties of the electrolyte, e.g. specific conductivity. Kern and Chang (Kern and Chang, 1922) published a paper in 1922 in which they gave detailed information on the conductivity of electrolytes used in copper refining. They studied the effects of arsenic, nickel sulfate and ferrous sulfate upon the conductivity of the electrolyte. They found in their work that the presence of nickel sulfate depressed the conductivity of the electrolyte.

Skowronski and Reinoso (Skowronski and Reinoso, 1926) in 1926 took the work of Kern and Chang a step further. In their work they also studied the effects of copper, nickel, iron and arsenic on the conductivity of the electrolyte. However, they were able to obtain relationships which enabled them to provide a means of calculating the conductivity of an electrolyte given its chemical analysis. Their calculated values for the conductivity gave results which were within ±1% of the actual measured conductivity.

Rouse and Aubel (Rouse and Aubel, 1927) in 1927 published a paper concerned with the cell voltages in copper refining. In their work they investigated the effects of temperature, acid concentration, copper, nickel and arsenic concentration and also the effect of glue. They found that the addition of the metal impurities increased the resistance of the electrolyte. However, they also found that in the case of nickel there was a decrease in the polarization voltages (as nickel was added to solution) which overcame the increase in the electrolyte resistance. This produced voltages which were lower than would be expected. They found that this effect reached a minimum (minimum in

total cell voltage). Then an increase in nickel concentration produced an increase in resistance which was more than the depolarizing effect of the nickel and therefore, the total cell voltage again increased. This was the first case in which a behavior such as this had been noted.

Other work has also been done in the area of voltage studies of copper refining electrolytes. In particular the work of Fink and Philippi in 1926 (Fink and Philippi, 1926). Their main concern and that of others was the effect of acid, temperature and copper concentration on the total cell voltages. No attempt was made to introduce any impurities.

Electrodeposition

Very little work on the actual copper electrodeposition process with impuities other than organic ones has been done. Gauvin and Winkler (Gauvin and Winkler, 1952) in 1952 published a paper concerned with the effect of chloride ions in the electrodeposition of copper.

Sheir and Smith (Sheir and Smith, 1952) in 1952 published a series of papers concerned with cathodic polarization during copper electrodeposition. Although their work was not directed at investigating the effects of any impurities it gave some very interesting results. They found that the methods of preparation and storage of an electrolyte solution and the time of storage had a definite effect on the "constant state polarization potential". They found that freshly prepared solutions gave a fine copper deposit with a high polarization value. Whereas

those solutions stored prior to use resulted in a coarse deposit and a lower value for the polarization potential. They suggested that these effects were due to the presence of an oxidizable sulfur compound.

Edwards and Wall (Edwards and Wall, 1966) in 1966 studied the effects of certain impurities on the energy requirements for copper electrodeposition. They found that the presence in solution of typical refinery impurities had no significant effect on the energy requirements.

Tuddenham and Sorensen (Tuddenham and Sorensen, 1969) conducted work to investigate the effects of copper, iron, aluminum and acid concentrations on the quality of electrowon copper. They demonstrated that the effects of these impurities were dependent on the type of circulation present in the cell.

Electrode Kinetics

General Kinetics

Except for a few early papers on the subject, electrode kinetics has been a subject that has evolved only within the last 20 years. In 1938 Agar and Bowden (Agar and Bowden, 1938) published a paper on the subject of the kinetics of electrode reactions. Their paper set forth some of the very basic concepts dealing with electrode kinetics.

In 1951 Parsons (Parsons, 1951) attempted to deal with the subject on a purely theoretical basis and derive some general equations to describe the rate determining step in any electrode process.

Conway and Bockris (Conway and Bockris, 1958) in 1958 published a paper in which they discussed the mechanism of electrodeposition. Their main concern was the investigation of the most likely path a depositing ion would follow.

Kinetics of Copper Electrodeposition

Mattsson and Bockris (Mattsson and Bockris, 1959) in 1959 investigated the kinetics of copper deposition and dissolution in a copper sulfate solution using galvanostatic techniques. Their results indicated that at low current densities the rate controlling step was the surface diffusion of adions. Whereas at higher current densities the rate controlling step was the charge-transfer process between Cu^{++} and Cu^{+}.

This same system was investigated in more detail by Bockris and Kita (Bockris and Kita, 1962) in 1962. They investigated the dependence of the charge-transfer and surface diffusion steps on the nature of the surface. They found that at low current densities the rate determining step for electrodeposited and oxide film surfaces was a combination of both surface diffusion and charge-transfer. However, at higher current densities the rate determining step is predominantly charge-transfer.

For surfaces prepared by quenching the copper in either a helium or hydrogen atmosphere they found that the rate determining step at low current densities is surface diffusion and at high current densities it is charge-transfer.

In 1962, Hurlen (Hurlen, 1962) investigated the kinetics of iron, zinc and copper electrodes. His findings are concerned with a transition-state theory of activation controlled reactions at the electrode. He considered both electrodeposition and dissolution. His findings are in conflict with those of Bockris and Kita and of Mattsson and Bockris.

None of the foregoing investigations have dealt with the problem of what effect a second ion has on the kinetics of the electrode reaction.

Anodic Dissolution of Copper

Some work has been done in the field of corrosion that deals with the area of anodic dissolution of copper. Most of this work deals primarily with the environment(s) that most readily produce or reduce the corrosion of copper. Although these studies are not directed at the kinetics of dissolution they are helpful.

Ives and Rawson (Ives and Rawson, 1962) published a paper concerned with copper corrosion. Their paper is a very detailed one in which they explore four areas of copper corrosion : 1) thermodynamics, 2) kinetic studies, 3) the electrochemical theory of general corrosion, and 4) the effects of saline additions. However, their main concern was that of investigating the corrosion products when dissolved oxygen and carbon dioxide were present in solution.

Jenkins and Stiegler (Jenkins and Stiegler, 1962) in 1962 conducted work on the anodic dissolution of single crystalline copper. Their work indicated that the rate of dissolution was dependent upon the defect structure of the electrode.

A more diverse study by Valeev and Khlopotina (Valeev and Khlopotina, 1969) was conducted in order to study the relationship of the mechanism of dissolution and the diffusion layer. Their work indicated that there is a light-sensitive film on the electrode surface which plays an important part in the mechanism of smoothing of the macrorelief of the surface.

In 1970 Leckie (Leckie, 1970) conducted research on the anodic polarization behavior of copper. His research was directed at investigating the polarization behavior of copper under various pH environments. His findings are important in that they indicate that in acid solution there is no formation of a protective film on the copper surface.

The anodic dissolution of copper at high current densities was investigated by Landolt, Müller and Tobias (Landolt, Müller and Tobias, 1971). However, the main aim of their research was to find a satisfactory method of experimentally determining the anodic behavior at high current densities.

EXPERIMENTAL APPARATUS AND PROCEDURES

This investigation was conducted in two separate phases: 1) empirical experiments and, 2) polarization experiments. The empirical experiments were conducted in order to obtain information on the effects of nickelous ion on the purity and morphology of the deposit. The effects of nickelous ions on the cell voltage and current efficiency was also determined. The polarization experiments were conducted in order to obtain basic information helpful in determining the kinetics of the electrode reaction with nickelous ions present.

Empirical Experiments

Equipment

A schematic diagram of the equipment is shown in Figure 3 and a photograph of the set-up is shown in Figure 4. The constant current source was a Hewlett-Packard, D.C. power supply, Model 6201B. The ammeter was a Weston, Model No. 1. A plot of cathode to anode voltage was made using a Speedomax, Type G recorder. Since this recorder was made to handle only 50 millivolts full-scale load, it had to be connected to the electrodes through a voltage divider. This enabled the recorder to record voltages of 0 to 4 volts. This voltage divider is not shown in Figure 3, but is placed between the recorder and the electrodes. Cathode to anode voltages were also measured using a Hewlett-Packard digital voltmeter Model 3430A. The timer shown was used in order to

calculate the current efficiency of each test. It was connected in series with the power to the d.c. power supply. This was done in order that the timing of the tests would start the instant power was supplied to the electrodes. The timer was capable of reading to ±0.01 minute.

The constant temperature bath consisted of a concrete container two feet deep by two feet wide by two feet long with walls one inch thick. The heating medium was water and was circulated by means of a submersible pump located in the center of the bath. Heating was provided by two, 250-watt immersible heaters. Power to the heaters was controlled by a Versatherm Electronic Temperature Control Relay Model 2149 which was connected to a JUMO temperature sensor. The temerature sensor itself was located in the cell. This equipment was capable of maintaining cell temperatures constant to within ±0.5 °C. All empirical tests were run at 25 °C.

The electrolysis cell consisted of a plexiglas box as shown in Figure B.1, Appendix B. The electrode holders are also shown in Appendix B, Figure B.2. The magnetic stirrer consisted of a laboratory model magnetic stirrer which was encased in a waterproof plexiglas box. It was designed (see Appendix B, Figures B.4 and B.5) so that a repeatable positioning of the electrolysis cell could be made upon it. This was done in order to assure constant stirring characteristics between tests and during the complete set of empirical experiments. The speed of the magnetic stirrer was controlled by a Variac a.c. transformer. The stirring bar was Teflon coated to avoid contamination of the solution. Conductivity measurements were made using a conductivity

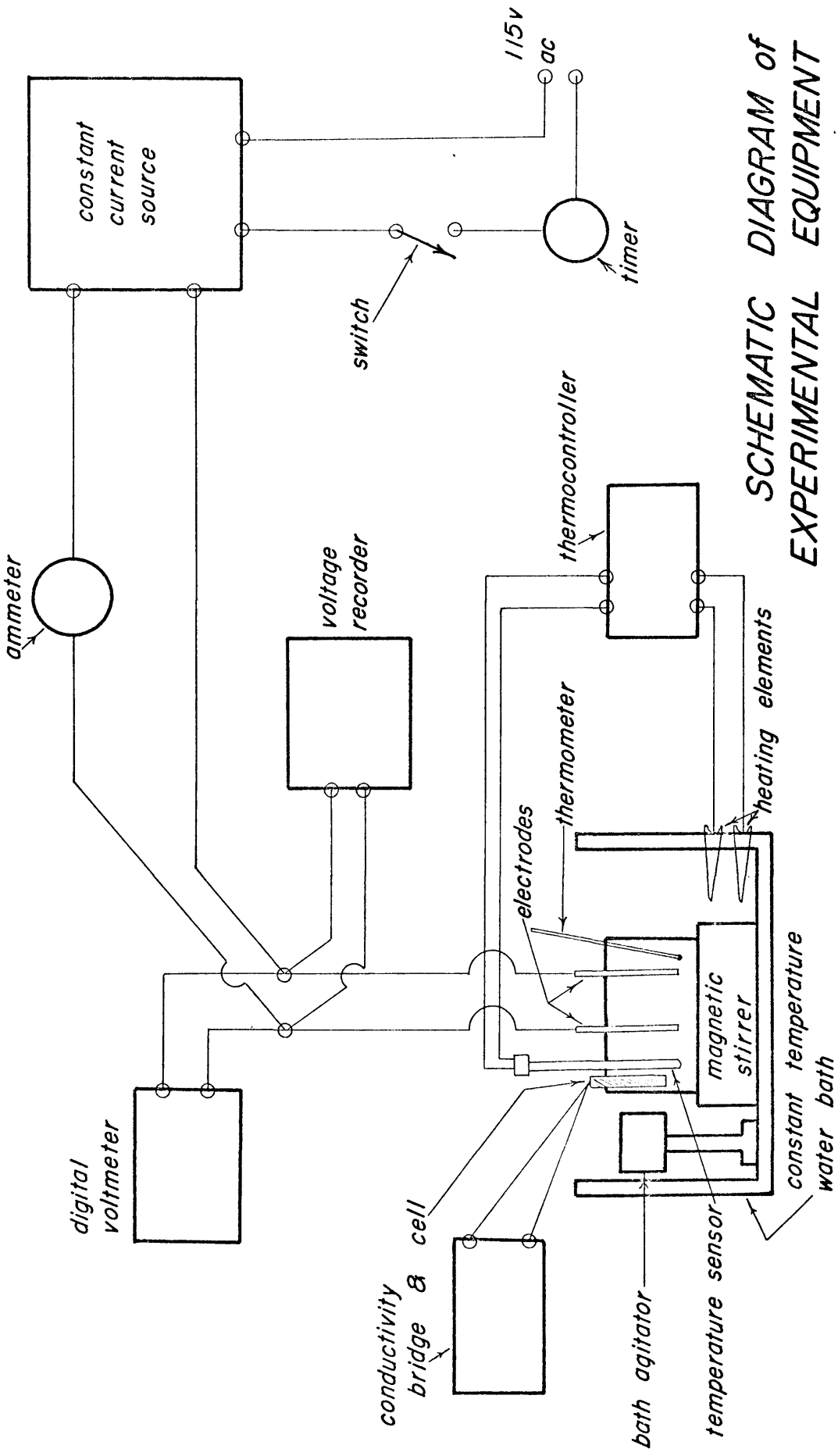

SCHEMATIC DIAGRAM of EXPERIMENTAL EQUIPMENT

Figure 3

FIGURE 4: Photograph of Empirical Tests Set-up.

bridge and a Leeds-Northrup conductivity cell with platinized electrodes and a cell constant of 1.096 cm^{-1}.

Materials

The cathodes consisted of copper reagent foil 0.005 inches in thickness. The purity of the foil was 99.95 to 99.99% copper with an analysis as shown in Table 4.

Table 4: Analysis of Copper Foil Used for Empirical Electrodes.

Element	Percentage
Cu	99.95
Insoluble in HNO_3	0.004
Sn	0.005
As	0.0002
Fe	0.003
Pb	0.003
Mn	0.0003
P	0.0004
Ag	0.0002

The anode consisted of pure platinum foil 0.003 inches in thickness. All chemicals used were of reagent grade. The source of copper in solution was cupric sulfate, $CuSO_4 \cdot 5H_2O$. The source of nickelous ion

was from nickelous sulfate, $NiSO_4 \cdot 6H_2O$. All water used was triple distilled and then deionized by passing it through Amberlite MB-3, a cationic and anionic exchange resin.

Procedure

At the start of the investigation tests were run with one anode located between two cathodes. Difficulties arose from this arrangement and the procedure was abandoned. These difficulties are reviewed in Appendix G. The next stage in the investigation was to use only one cathode. The procedure was to run a test at a specified initial copper, nickel and acid concentration using a specified current density and depositing one gram of copper. Difficulties were encountered using this procedure and it was also abandoned. These difficulties are reviewed in Appendix G. The following procedure was finally used and worked satisfactorily. The empirical results of this investigation are based on data obtained using this procedure.

A prepared sample was loaded into the cell (see Appendix D for detailed information on sample preparation and loading). The cell was then filled with 1400 ml of electrolyte which had previously been allowed to reach the operating temperature by being placed in the constant temperature bath for 4 to 8 hours.

The loaded cell was then fastened into the magnetic stirrer and a measurement of the conductivity was made. Power connections to the cell were then made and the test started by switching on the power. The test was run for such a length of time that theoretically five grams of copper should have been deposited. (This was done assuming 100%

current efficiency). The power was then cut-off and the sample removed and washed. The sample was then dried in a desicator for 24 hours before a final weight measurement was made. A second sample was then loaded into the cell using the same electrolyte and five more grams of copper were deposited. This procedure was repeated using successive samples until the deposit obtained was of a powdery nature. The electrolyte was then replaced with one having a different chemical analysis. During the course of each series of tests, make-up water was added to keep the volume of electrolyte constant at 1400 ml.

Analysis of Solutions

The analysis of nickel in both the final and initial solutions was done by atomic absorption using a Techtron Atomic Absorption Spectrophotometer, Type AA4. Analysis for copper was done by a wet chemical analysis using a standard procedure.

The determination of pH values was done using a Sargent Model DR digital pH meter and either a Beckman combination pH electrode or a Sargent combination pH electrode. The pH meter was standardized before each use and several times during the series of determinations.

Polarization Experiments

Equipment

The polarization experiments were conducted in a U-tube cell as shown schematically in Figure 5. Photographs of the U-tube and electrode holder are shown in Figures 6, 7, and 8. Appendix C gives detailed

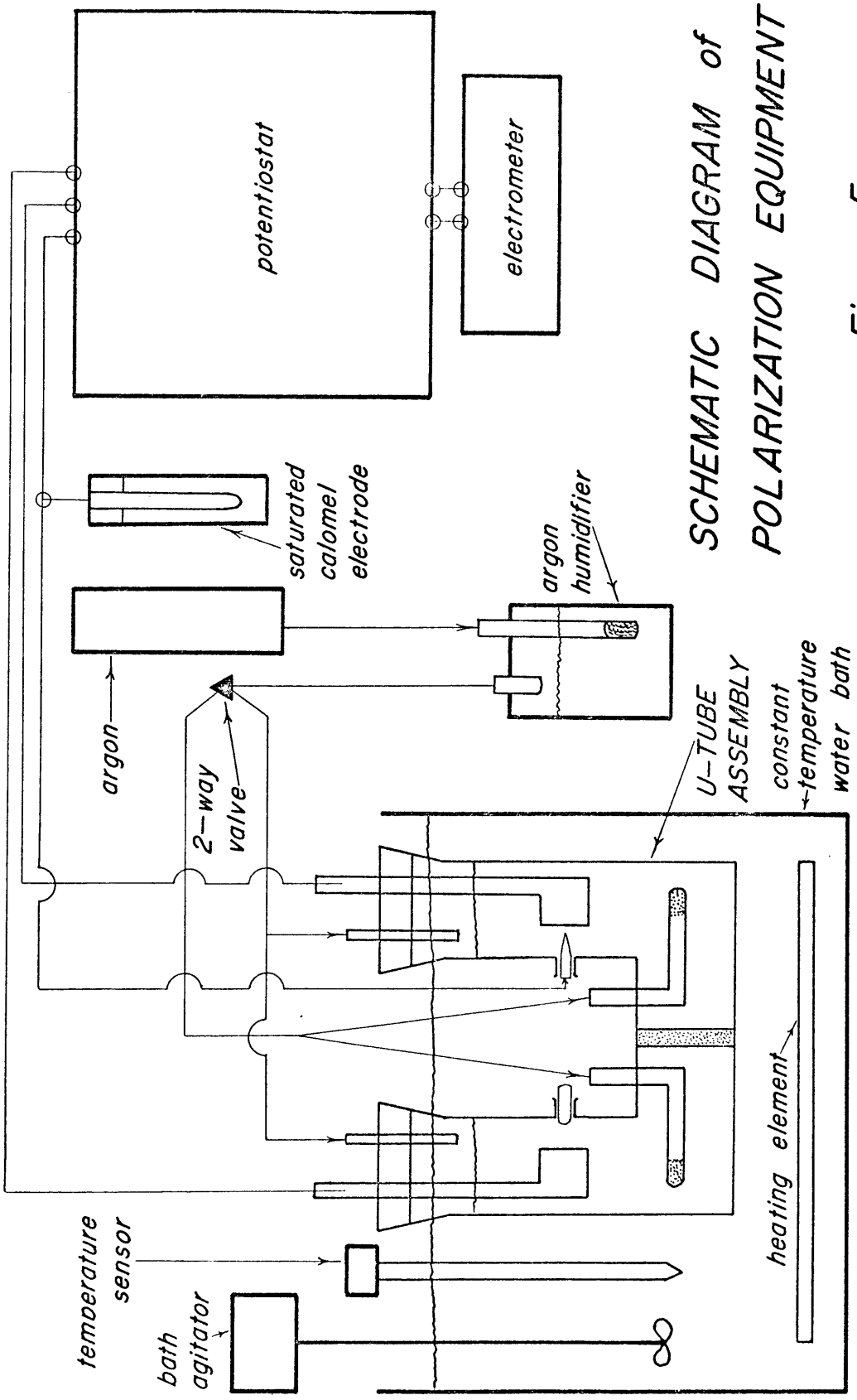

SCHEMATIC DIAGRAM of POLARIZATION EQUIPMENT

Figure 5

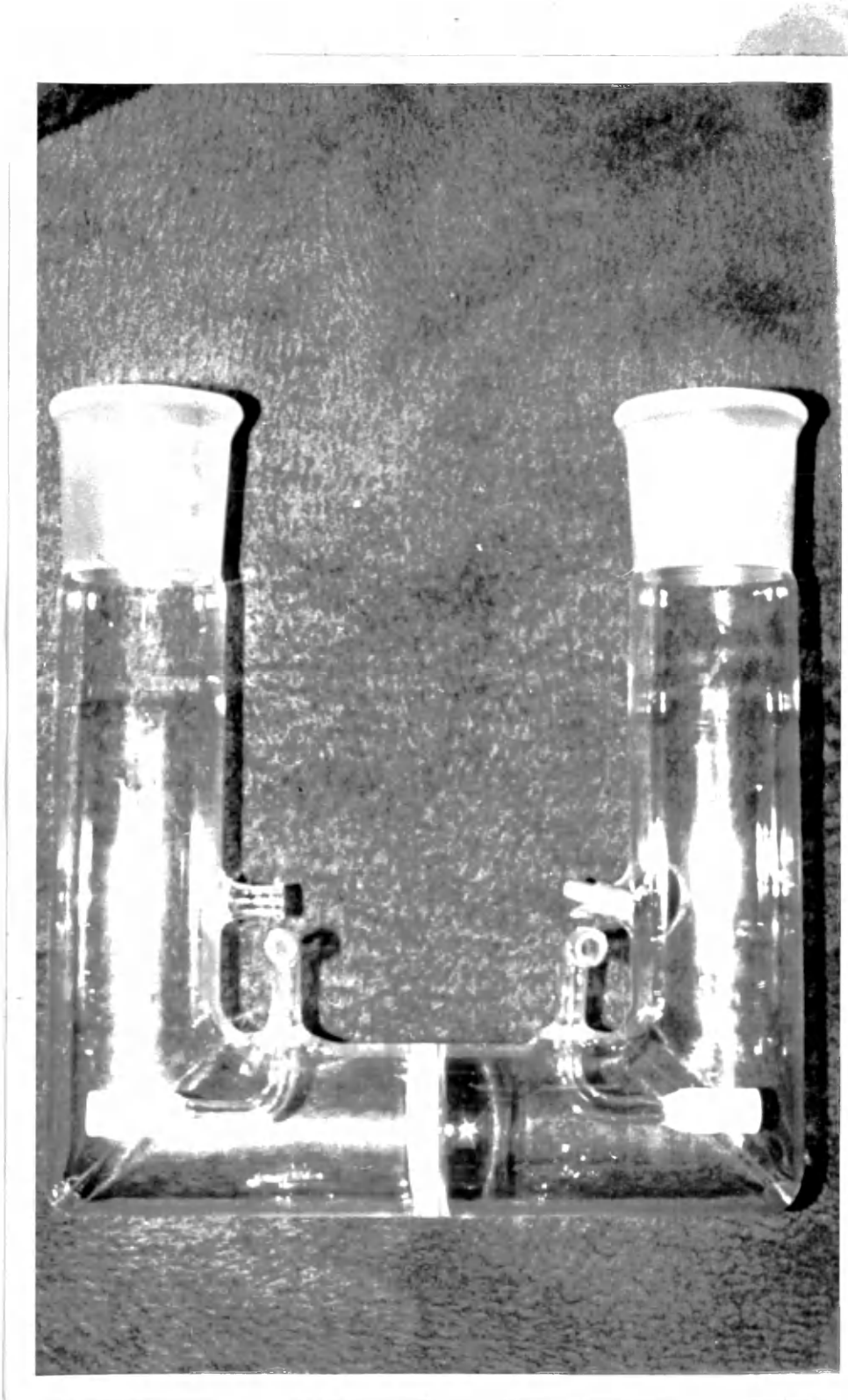

FIGURE 6: Photograph of U-tube Polarization Cell

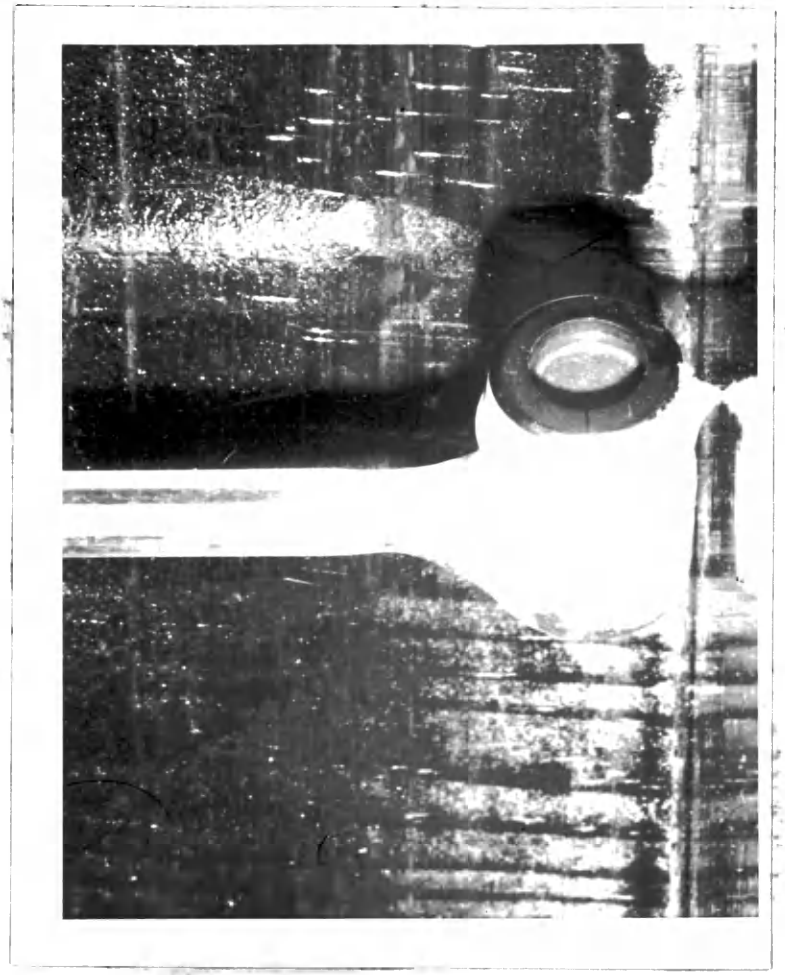

FIGURE 8: Close-up Photograph of Electrode Holder

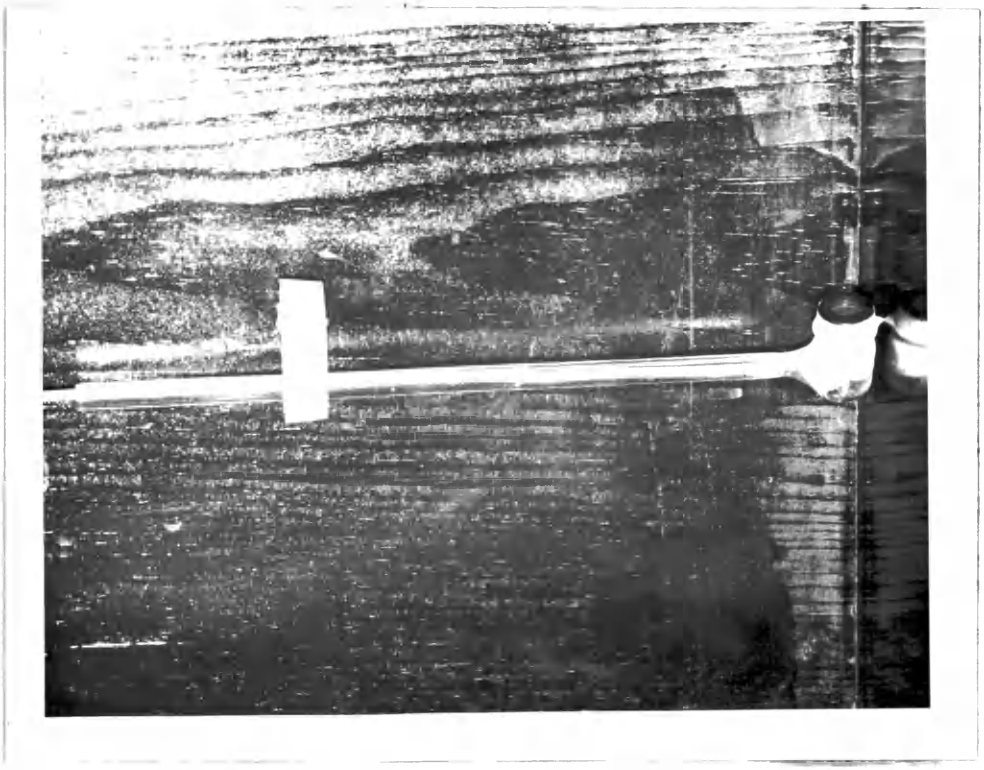

FIGURE 7: Photograph of Electrode Holder

information on and drawings of the U-tube. Polarization potentials were supplied by a Magna Potentiostat (Research Model 4700M). Potentials were measured using an E-H Research Laboritories Electrometer, Model 230. This electrometer was connected to the system via the potentiostat to avoid any ground loops. A provision for this type of circuit was built into the potentiostat.

The constant temperature water bath was controlled by a Versatherm Electronic Temperature Control Relay working through a JUMO temperature sensor and controlling power to a 250-watt immersion heater. This system was capable of maintaining the temperature constant to within ±0.5 °C.

Materials

All chemicals used were of an analytical reagent grade. The water was double distilled (but with no deionization through an ion exchange resin). All weight measurements were made using a Mettler H-Model analytical balance.

The copper used for both the anodes and the cathodes was from a commercial electrolytically pure,cold rolled copper sheet, 0.025 inches thick. Samples were made by punching out circular discs 0.530 inches in diameter.

Procedure

The following procedure was used in running each test. The potentiostat was allowed a warm-up time of at least one hour prior to each test. The electrometer was kept running continuously throughout

the polarization experiments in order to keep a stable calibration. The U-tube cell was fastened into the constant temperature bath and 300 ml of electrolyte was poured into each arm of the cell (the electrolyte had previously been allowed to reach the operating temperature by keeping it immersed in the constant temperature bath for 8 to 10 hours previous to the test). Purging was then started and allowed to continue for 45 minutes.

The argon used for purging was commercially pure and dry bottled argon. To prevent evaporation of the electrolyte during purging the argon was saturated with water vapor prior to entering the U-tube cell. The saturation was accomplished by bubbling the argon through distilled water using a fritted glass tube to produce as many small argon bubbles as possible in the water.

The reference electrode used was a saturated calomel electrode. It was connected to the U-tube cell via a salt bridge made as shown in Figure C.3, Appendix C. A Luggin-Haber probe was used to obtain potentials of the working electrode. The Luggin-Haber probe consisted of a glass tube with an inside diameter of 0.20 inches which was drawn to a fine tip having an inside diameter of 0.05 inches. This glass probe was filled with a special agar gel as described in Appendix H. Connection between the probe and saturated calomel electrode was completed using Tygon tubing filled with saturated potassium chloride. This tube was then connected to a glass vessel in which the saturated calomel electrode was immersed in saturated potassium chloride.

At the end of the 45 minute purging period the electrode holder containing a prepared sample was inserted into each arm of the U-tube cell. A sample was prepared by first cleaning with acetone and rinsing in distilled water. The cleaned sample was then inserted into the electrode holder. It was then etched with a nitric acid etchant (1:1, water: nitric acid). It was allowed to etch for a period of 15 seconds. The sample was then rinsed in distilled water and dried in a blast of air. The purging was then allowed to continue for another 15 to 20 minutes. This time period allowed the sample to thermally equilibrate.

The purging was then stopped and the two-way valve shown in Figure 5 was turned so that the same purging atmosphere entered through the glass tubes in the top of the electrode holders as shown in Figure 5. This kept an inert atmosphere over the solution and prevented any oxygen from re-entering the electrolyte.

The test was then started by applying a potential using the potentiostat. Each test was started at a potential that resulted in a measured current of 0.0 to 0.1 milliamps (anodic current). This anodic current was then increased by raising the potential in successive steps, with the system allowed to reach equilibrium for 2 to 5 minutes at each step.

The test was continued until the limiting current was reached. At this time the power was cut and the samples removed and re-cleaned. The solution was then re-purged using the same procedure as outlined above. The test was then repeated using the same sample. This procedure was repeated for each electrolyte and temperature condition.

EXPERIMENTAL RESULTS

The experimental results from this investigation have been divided into two separate categories: 1) empirical results , and 2) polarization results.

Empirical Results

Effect of Nickelous Ion on the Current Efficiency

It was found that the presence of nickelous ion had no measurable effect on the current efficiency of the deposition process. Efficiency measurements were made by calculating the amount of copper that should have been deposited theoretically and comparing the experimental amount to this value. The amount of copper that theoretically should have been deposited was calculated by determining the length of time that current was supplied to the cell under a condition of constant current. Through this calculation it was possible to find the number of coulombs that had passed through the cell. Since 3.2924×10^{-4} grams of copper are deposited per coulomb it was then possible to calculate the theoretical amount of copper that should have been deposited.

Experimentally, it was found that the current efficiencies varied from 97% to 99% with no indication of nickelous ion having any important effect. It was also found that neither the amount of copper in solution (within experimental limits of 15 - 40 gpl) nor current density had any

discernible effect on the current efficiency. The current density varied from 19.1 to 56.1 asf with nickelous ion present and from 19.1 to 93.3 asf with no nickelous ion present.

When looking at the data in Appendix A it can be seen that at the lowest current density, i.e. 19.1 asf, the current efficiencies were lower than for those at higher current densities, i.e. 37.0 and 56.1 asf. This result is contrary to all other previous experimental work. An explanation for this behavior is given in Appendix G.

Effect of Nickelous Ion on the Morphology

A visual inspection of the deposits revealed that nickelous ions did have an effect on the morphology of the deposit. It was also shown that current density had a noticeable effect on the morphology.

The aforementioned inspection indicated that there was a noticable pattern to the outward appearance of the deposits. In order to systematically assemble and correlate the conditions of deposition and the resulting morphology, two methods for a qualitative description of the deposit were devised.

The first method defines the experimental conditions of deposition. It takes into account the initial copper concentration, the initial nickel concentration and the current density. Such factors as temperature, acid concentration, stirring rate and electrode spacing were not accounted for since they remained constant throughout all the experimental tests. This method is based on the definition of a "Reference Number", R, calculated in the following way:

$$R = \frac{[\ Cu^{++}_{in} + Ni^{++}\ ]}{Cu^{++}_{in}} \times \frac{Cu^{++}_{ref}}{Cu^{++}_{in}} \times \frac{C.D._{act}}{C.D._{ref}} \qquad (1)$$

Where:

Cu^{++}_{in} = Initial copper concentration (gpl).

Cu^{++}_{ref} = A copper concentration used as a standard of comparison (gpl). For this investigation all values of R were calculated using a value of 40 gpl for Cu^{++}_{ref}.

Ni^{++} = Nickel concentration (gpl).

$C.D._{act}$ = The actual current density used for a test (asf).

$C.D._{ref}$ = A current density (asf) used as a standard of comparison. For this investigation all values of R were calculated using a value of 19.1 asf for $C.D._{ref}$.

The Reference Number will increase as, 1) the nickel concentration increases, 2) the copper concentration decreases, and 3) the current density increases, in relation to the standard conditions.

A different method was used to describe the nature of the surface for each deposit. It was based on a visual comparison of the deposit obtained in each test with a deposit obtained under standard conditions (40 gpl copper, 0 gpl nickel and 19.1 asf) and by ascribing to it a "Surface Index", Q, ranging from 1.0 (standard conditions) to 25.0. Hence, an increasing Surface Index indicates a progressively less satisfactory deposit.

Table 5 shows a tabulation of R values for various copper and nickel concentrations at 19.1 asf. These values are plotted in Figure 9 and show how R changes with the copper and nickel concentrations.

Table 5: Reference Number, R, As A Function Of Copper And Nickel Concentration.

Nickel Conc. (gpl)	Copper Concentration (gpl)						
	40	35	30	25	20	15	10
	R	R	R	R	R	R	R
0	1.000	1.142	1.333	1.600	2.000	2.666	4.000
1	1.025	1.175	1.375	1.663	2.100	2.845	4.400
5	1.125	1.305	1.555	1.920	2.500	3.550	6.000
10	1.250	1.470	1.778	2.240	3.000	4.440	8.000
15	1.375	1.633	2.000	2.560	3.500	5.330	10.000
20	1.500	1.795	2.220	2.880	4.000	6.225	12.000

Values for R at the two higher current densities (37.0 and 56.1 asf) would follow the same pattern. However, they would have values approximately 2 and 3 times as large as for the low current density.

Deposit Quality

Four qualities of deposits, depending upon their Surface Index, were defined as shown in Table 6. Table 7 shows a tabulation of the Reference Numbers and Surface Indices for a representative number of tests. Photographs of actual electrode surfaces with their Surfaces Indices are given in Appendix J.

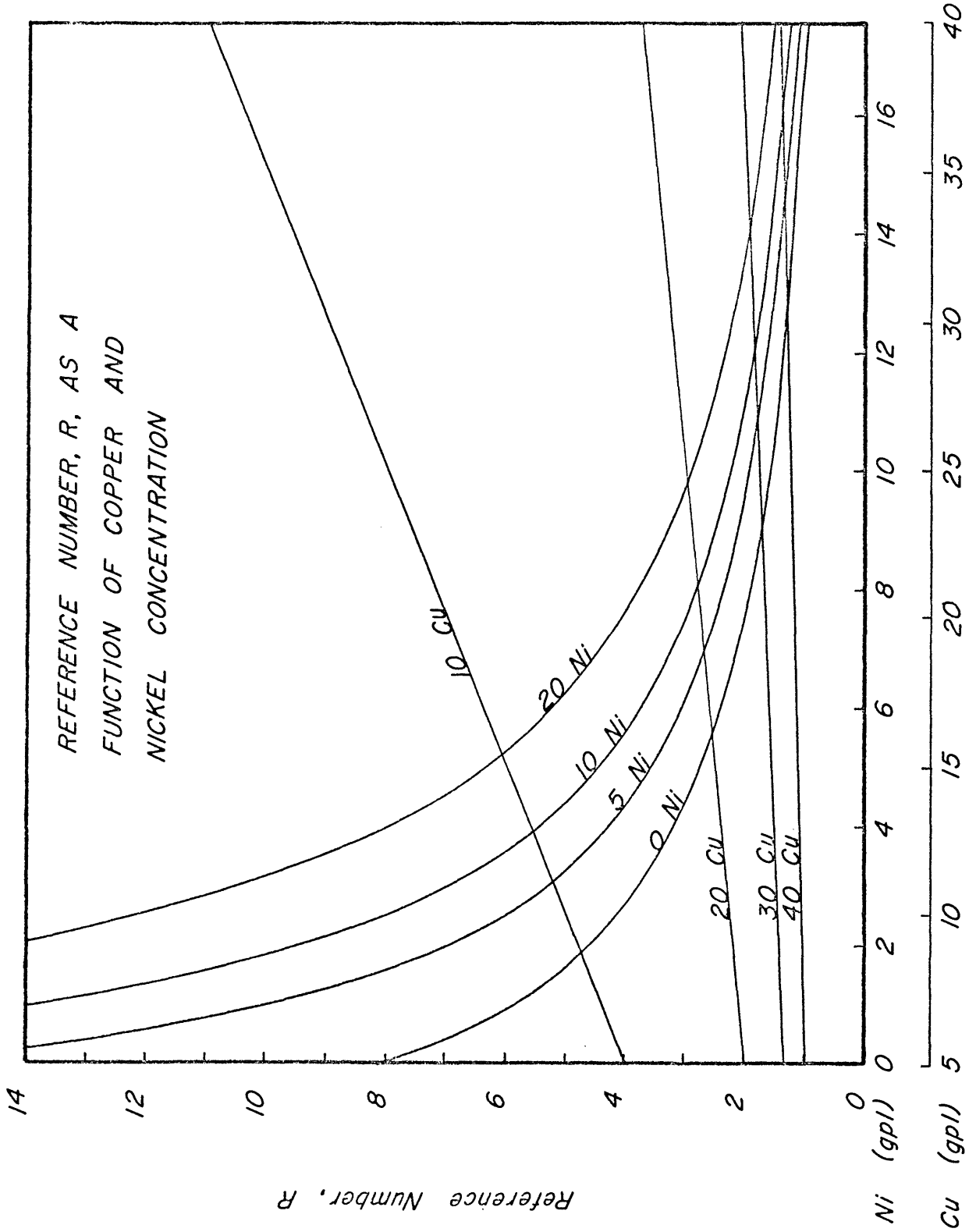
REFERENCE NUMBER, R, AS A FUNCTION OF COPPER AND NICKEL CONCENTRATION
Reference Number, R
14
12
10
8
6
4
2
0
Ni (gpl)
0
2
4
6
8
10
12
14
16
Cu (gpl)
5
10
15
20
25
30
35
40
10 Cu
20 Ni
10 Ni
5 Ni
0 Ni
20 Cu
30 Cu
40 Cu

FIGURE 9

Table 6: Quality Of Deposit As A Function Of The Surface Index

Surface Index, Q	Quality Of Deposit	Characteristics Of The Deposit
1.0 to 2.0	Good	Very smooth, very adherent, very compact
2.1 to 5.0	Acceptable	Smooth, adherent, Compact
5.1 to 10.0	Poor	Rough, less adherent, less compact
10.1 to 25.0	Unacceptable	Very rough, poorly adherent, slightly powdery

Surface Index As A Function Of The Initial Copper Concentration-19.1 asf

Figures 10,11 12 and 13 show the effect of initial copper concentration on the Surface Index. These figures show that for a current density of 19.1 asf and with 0 to 15 gpl nickel, a good deposit could be expected as long as the copper concentration did not fall below approximately 22 gpl. For these same conditions an acceptable deposit could be expected as long as the copper concentration did not fall below approximately 15 gpl.

Surface Index As A Function Of The Initial Copper Concentration-37.0 asf

For 37.0 asf Figure 10 shows that a good deposit could be expected at copper concentrations of 27 gpl and above when no nickel is present.

Table 7: Surface Indices And Reference Numbers For Actual Experimental Tests - 19.1 amps/ft^2.

Test No.	Initial Copper (gpl)	Initial Nickel (gpl)	Reference Number, R	Surface Index, Q
76	39.8	0.00	0.995	1.0
83	40.2	0.99	1.020	1.1
91	40.2	5.10	1.122	1.1
99	40.2	17.66	1.432	1.1
79	30.3	0.00	1.320	1.2
86	31.3	0.99	1.320	1.1
94	30.5	5.10	1.530	1.1
102	29.1	17.66	2.210	1.3
81	22.0	0.00	1.820	1.5
88	22.3	0.99	1.874	1.6
96	23.3	5.10	2.090	1.7
104	20.9	17.66	3.530	2.0
82	17.7	0.00	2.260	6.0
90	14.6	0.99	2.925	6.0
98	14.6	5.10	3.690	5.0
106	13.5	17.66	6.830	9.0

Table 7: Surface Indices And Reference Numbers For Actual Experimental Tests - 37.0 amps/ft^2.

Test No.	Initial Copper (gpl)	Initial Nickel (gpl)	Reference Number, R	Surface Index, Q
69	39.4	0.00	2.250	1.1
107	40.1	1.01	2.145	1.1
114	40.1	6.24	2.415	1.0
122	39.3	13.38	2.855	1.8
72	27.9	0.00	3.000	1.9
110	29.5	1.01	2.935	3.0
117	28.3	6.24	3.615	3.5
125	29.8	13.38	4.070	4.2
74	20.8	0.00	4.020	5.0
112	21.4	1.01	4.090	5.7
119	21.2	6.24	5.110	8.0
127	18.6	13.38	7.750	8.0
75	16.7	0.00	5.020	16.0
113	17.6	1.01	5.030	16.0
120	17.4	6.24	6.540	16.5
128	17.4	13.38	8.510	18.0
124	37.2	13.38	2.830	2.5
126	25.5	13.38	4.640	4.2

Table 7: Surface Indices And Reference Numbers For Actual Experimental Tests - 56.1 amps/ft^2.

Test No.	Initial Copper (gpl)	Initial Nickel (gpl)	Reference Number, R	Surface Index, Q
61	39.0	0.00	3.010	4.2
129	40.3	1.26	3.010	4.3
135	40.1	6.27	3.392	4.5
141	39.7	14.93	4.070	5.8
64	30.1	0.00	3.900	5.0
131	32.2	1.26	3.790	5.0
137	32.3	6.27	4.340	4.9
143	32.0	14.93	4.230	4.2
66	23.8	0.00	4.940	17.0
133	24.0	1.26	5.150	18.0
140	21.2	6.27	7.180	20.0
146	22.7	14.93	8.580	20.0
63	33.8	0.00	3.475	4.8
65	27.9	0.00	4.210	5.8
132	27.5	1.26	4.470	8.0
134	20.2	1.26	6.180	25.0
139	24.7	6.27	5.960	15.0
138	28.6	6.27	5.010	7.0
136	36.4	6.27	3.890	4.5

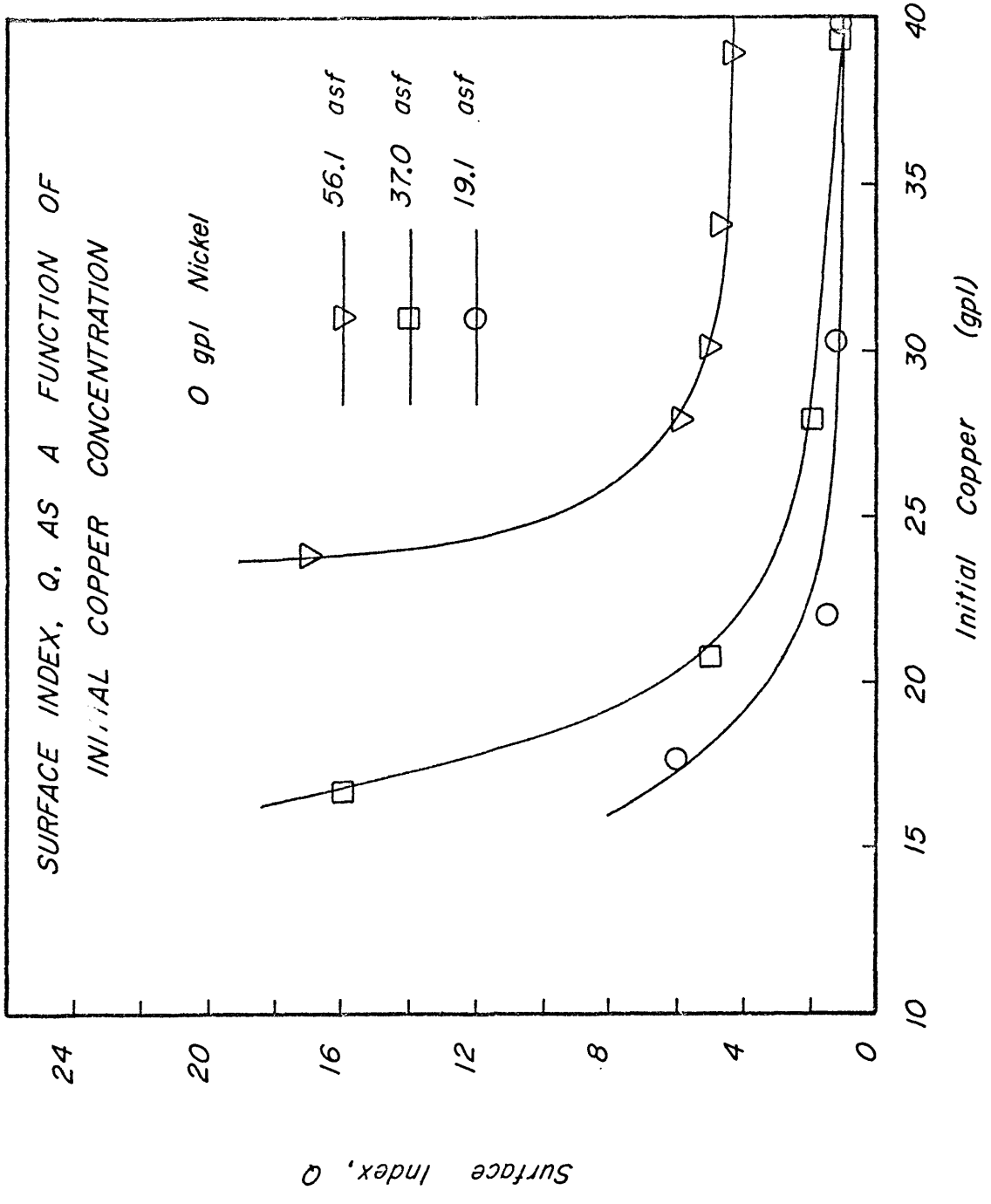
SURFACE INDEX, Q, AS A FUNCTION OF
INITIAL COPPER CONCENTRATION
0 gpl Nickel
56.1 asf
37.0 asf
19.1 asf
Surface Index, Q
Initial Copper (gpl)
0
4
8
12
16
20
24
10
15
20
25
30
35
40

FIGURE 10

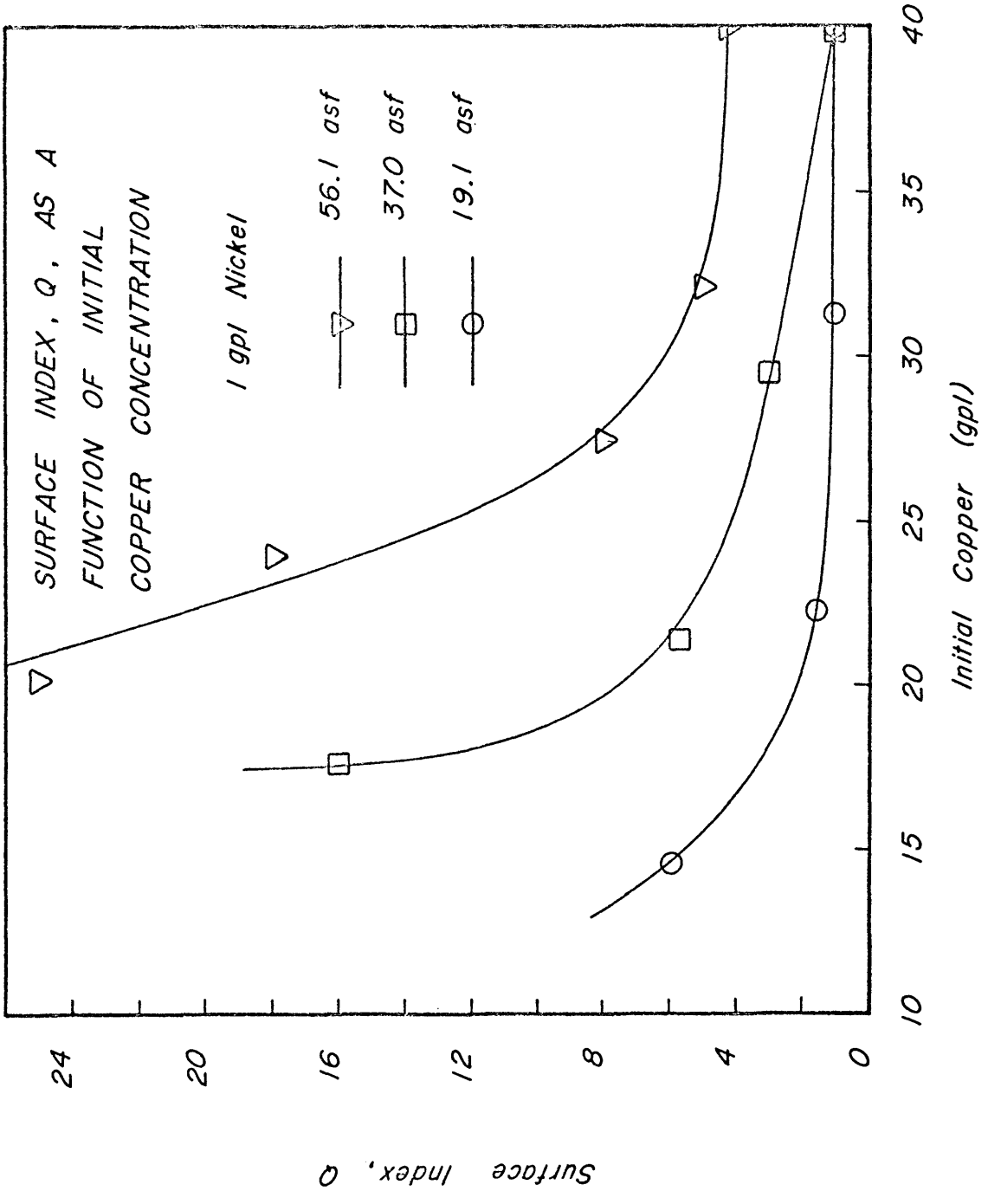
SURFACE INDEX, Q, AS A FUNCTION OF INITIAL COPPER CONCENTRATION
1 gpl Nickel
56.1 asf
37.0 asf
19.1 asf
Surface Index, Q
Initial Copper (gpl)
0
4
8
12
16
20
24
10
15
20
25
30
35
40

FIGURE 11

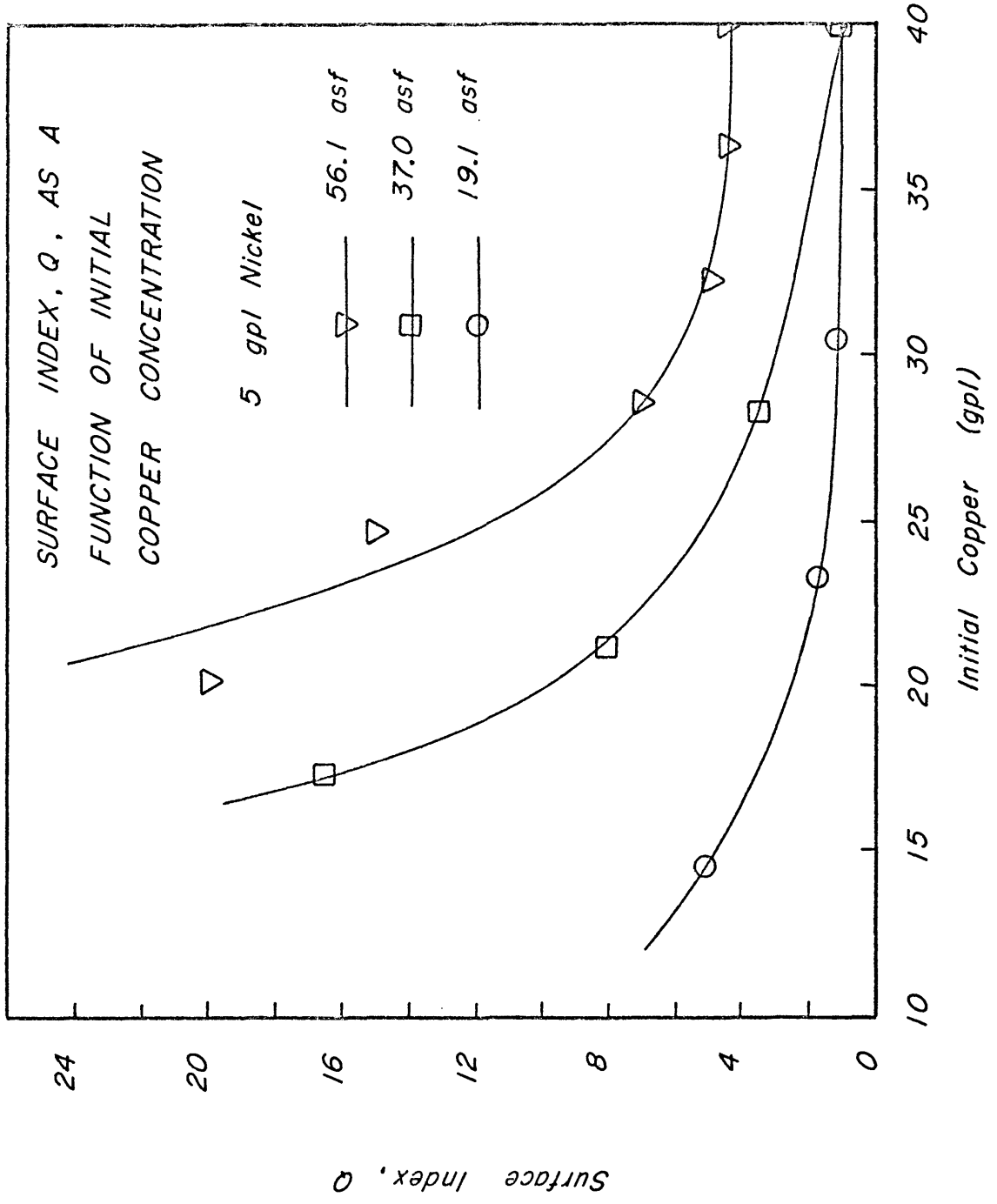
SURFACE INDEX, Q, AS A
FUNCTION OF INITIAL
COPPER CONCENTRATION
5 gpl Nickel
56.1 asf
37.0 asf
19.1 asf
Surface Index, Q
Initial Copper (gpl)
0
4
8
12
16
20
24
10
15
20
25
30
35
40

FIGURE 12

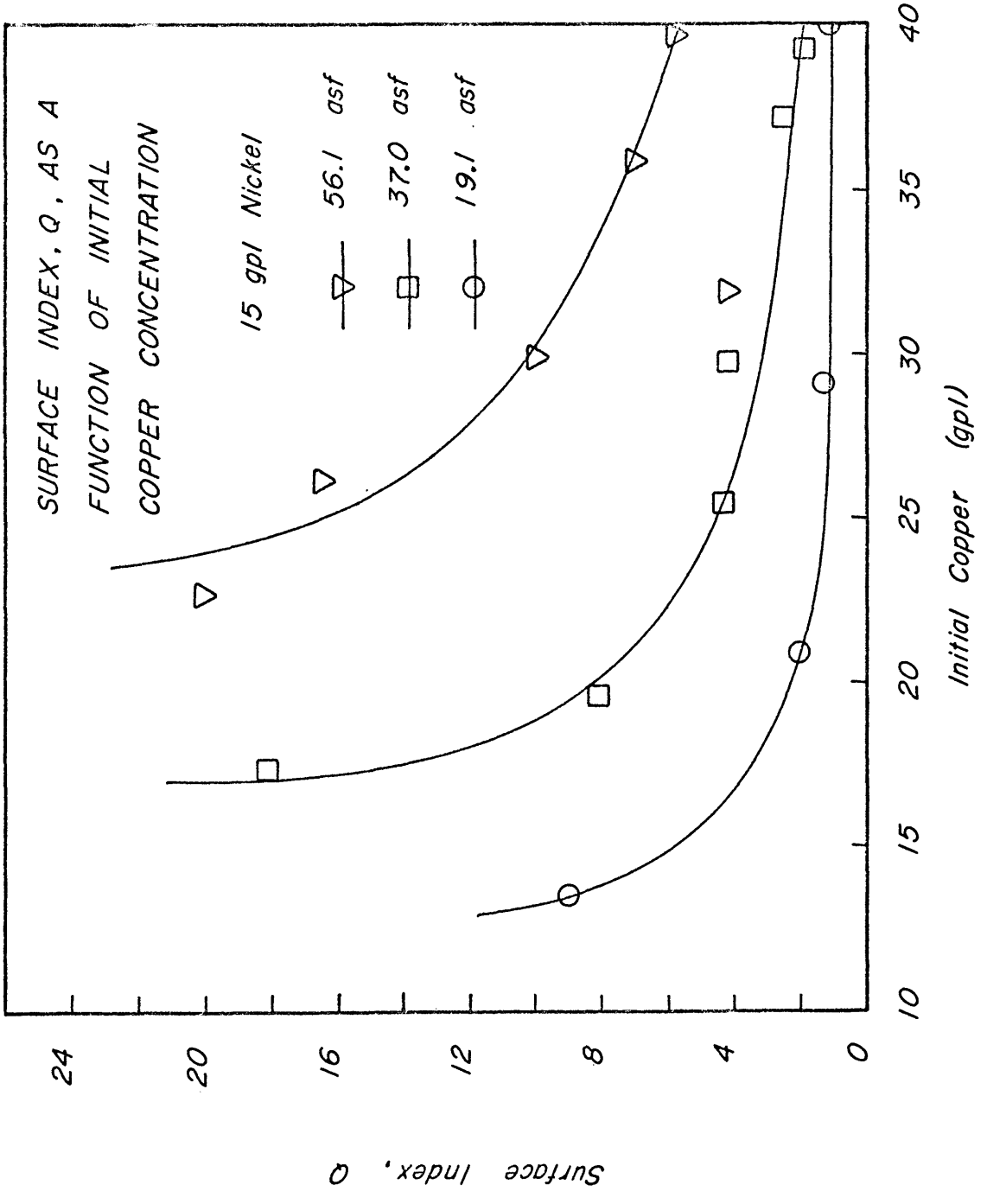
SURFACE INDEX, Q, AS A
FUNCTION OF INITIAL
COPPER CONCENTRATION
15 gpl Nickel
56.1 asf
37.0 asf
19.1 asf
Surface Index, Q
0
4
8
12
16
20
24
10
15
20
25
30
35
40
Initial Copper (gpl)

FIGURE 13

Figure 11 however, shows that the introduction of nickel at a concentration of 1 gpl raises the amount of copper that has to be present in solution in order to obtain a good deposit. This limit is approximately 35 gpl copper. As the nickel concentration goes up, Figure 12 shows that the limit for the copper concentration is about the same for 5 gpl nickel as it was for 1 gpl nickel. Figure 13 shows that for 15 gpl nickel the limit is again raised, this time to approxiamtely 39 gpl copper. These figures also show that to obtain an acceptable deposit the lower limit for the copper concentration is raised as the nickel concentration is raised.

Surface Index as a Function of the Initial Copper Concentration-56.1 asf

Figure 10 shows that for a current density of 56.1 asf a good deposit can never be expected even when no nickel is present in solution. An acceptable deposit, however, can be expected for copper concentrations as low as approximately 30 gpl. With 1 and 5 gpl nickel, Figures 11 and 12, this copper concentration limit is raised to approximately 33 gpl. For 15 gpl nickel, Figure 13, the limit is raised to a point that is higher than 40 gpl, which was the highest copper concentration used experimentally.

Surface Index as a Function of Current Density

Figure 14 shows several curves which indicate the influence of current density on the surface index. With an initial copper concentration of 40 gpl and with nickel concentrations of 1, 0 and 5 gpl there is very little influence of current density until the current density

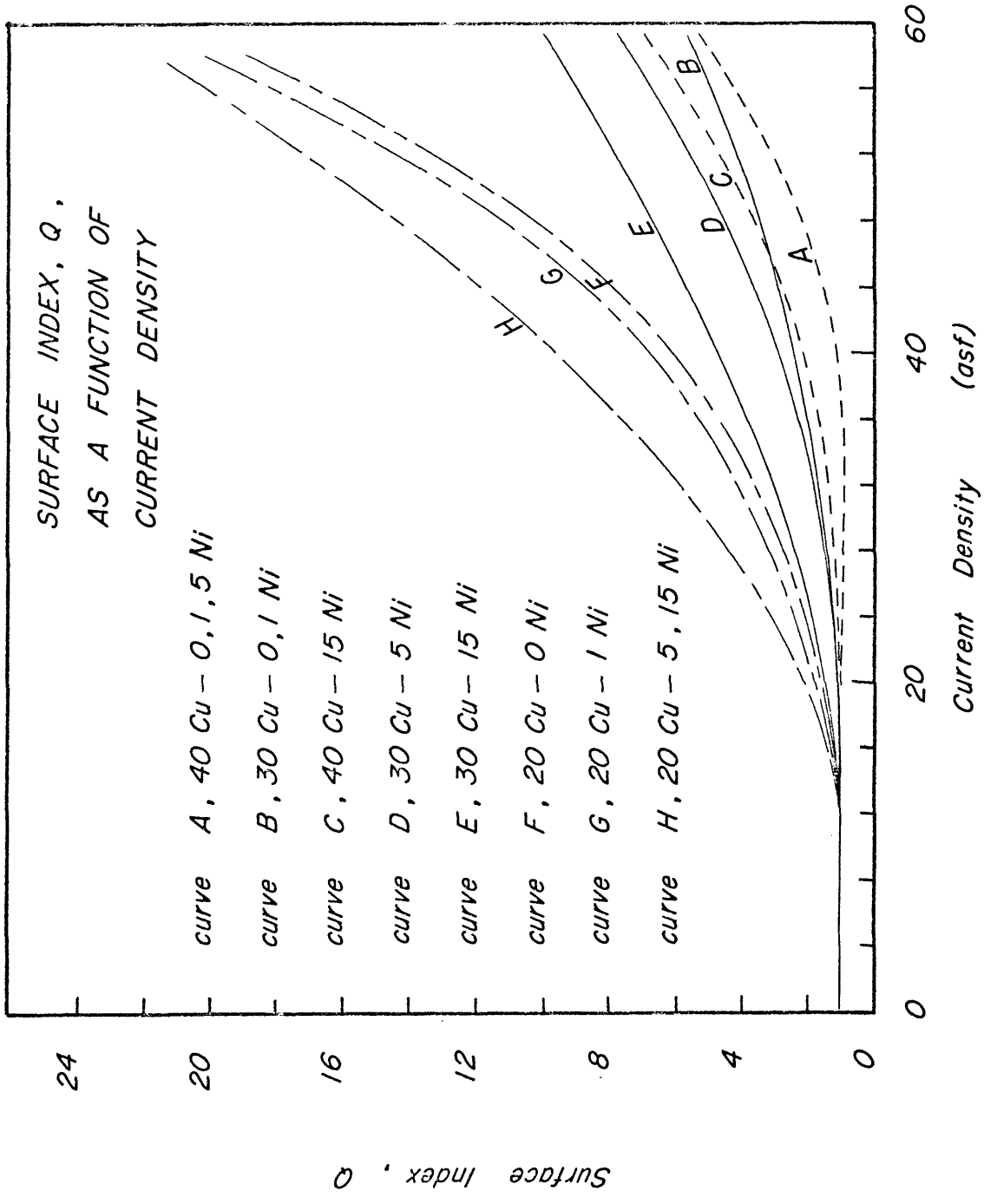
SURFACE INDEX, Q,
AS A FUNCTION OF
CURRENT DENSITY
curve A, 40 Cu – 0,1,5 Ni
curve B, 30 Cu – 0,1 Ni
curve C, 40 Cu – 15 Ni
curve D, 30 Cu – 5 Ni
curve E, 30 Cu – 15 Ni
curve F, 20 Cu – 0 Ni
curve G, 20 Cu – 1 Ni
curve H, 20 Cu – 5, 15 Ni
Surface Index, Q
Current Density (asf)
0
4
8
12
16
20
24
0
20
40
60
A
B
C
D
E
F
G
H

FIGURE 14

reaches a value of approximately 40 asf. At this point the surface index starts to increase. However, the deposit remains good up to a current density of 47 asf. With the same copper concentration but with a higher nickel concentration (15 gpl) the quality of the deposit begins to decrease at any current density greater than 19 asf and remains good only up to a current density of 38 asf (as shown by curve C, Figure 14). So, an additional 10 gpl nickel lowered the working current density by 10 asf in order to obtain a good deposit.

As the copper concentration is lowered to 30 gpl the influence of nickel concentration starts at a lower nickel concentration. This is shown by Curve B, Figure 14, which shows that for a nickel concentration of 0 to 1 gpl a good deposit is obtained for current densities up to 37 asf. However, for nickel concentrations of 5 and 15 gpl (Curves D and E respectively) the highest limits for the current density at which a good deposit will be formed are 32 and 25 asf respectively.

As the copper concentration decreases to 20 gpl Curves F, G and H in Figure 14 show that the effect of nickel is still more pronounced. Curve F shows that even with no nickel a good deposit can only be obtained at current densities lower than 22 asf. Whereas, with 1 gpl nickel this limit is lowered to 20 asf and with nickel concentrations higher than 1 gpl- the current density limit is lower than any used experimentally (i.e. 19.1 asf).

A comparison of Curves B and C, Figure 14, shows that adding 15 gpl nickel to a solution having 40 gpl copper (Curve C) has approximately the same effect as lowering the copper concentration, with no nickel, from 40 gpl to 30 gpl (Curve B). Both conditions result in a

current density limit of approximately 38 asf in order to obtain a good deposit.

Surface Index as a Function of Nickel Concentration - 19.1 asf

Curves A through I, Figure 15, show the influence of nickel concentration on the surface index. These curves show that as the current density increases and as the copper concentration decreases, the influence of nickel concentration on the surface index becomes greater (as indicated by the increase in the slope of the curves in going from Curve A to Curve I).

Curve A shows that for a current density of 19.1 asf and for copper concentrations of 30 and 40 gpl, the nickel concentration has little or no effect on the surface index. However, as the copper concentration is lowered to 20 gpl (Curve C), the nickel concentration begins to effect the surface index. At this low copper concentration a good deposit is obtained for nickel concentrations as high as 15 gpl.

Surface Index as a Function of Nickel Concentration - 37.0 asf

At a current density of 37.0 asf the nickel concentration had an effect at all copper concentrations studied, i.e. 20, 30 and 40 gpl. This is shown in Curves B, D and G, Figure 15. It can be seen that Curves D and G have approximately the same slope. This slope is greater than the slope for Curve B, which indicates that at 30 and 20 gpl copper the amount of nickel present in solution has a larger influence than it does at a copper concentration of 40 gpl.

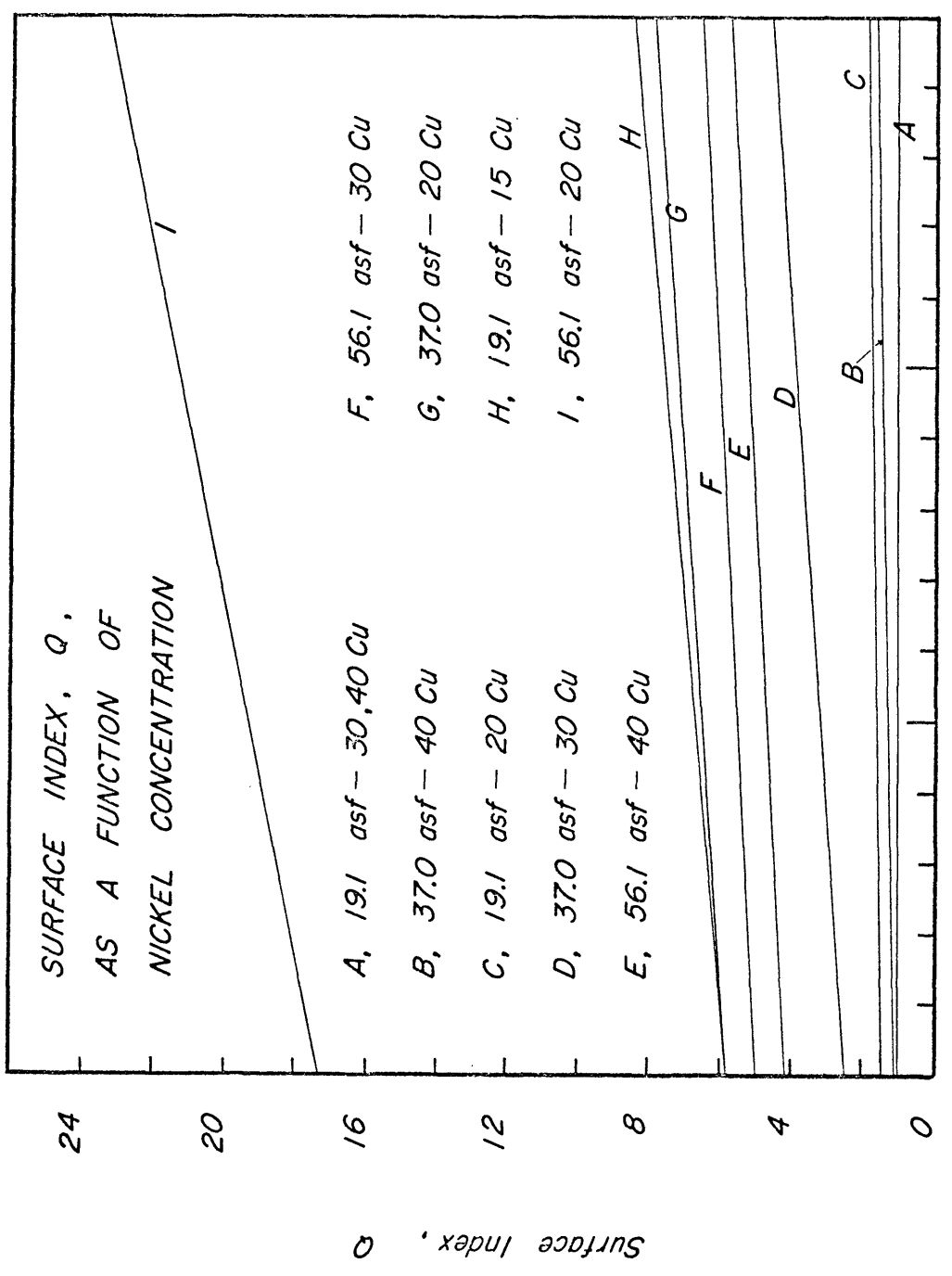
SURFACE INDEX, Q,
AS A FUNCTION OF
NICKEL CONCENTRATION
A, 19.1 asf – 30,40 Cu
B, 37.0 asf – 40 Cu
C, 19.1 asf – 20 Cu
D, 37.0 asf – 30 Cu
E, 56.1 asf – 40 Cu
F, 56.1 asf – 30 Cu
G, 37.0 asf – 20 Cu
H, 19.1 asf – 15 Cu
I, 56.1 asf – 20 Cu
Surface Index, Q
Nickel Concentration (gpl)
0
4
8
12
16
20
24
0
5
10
15

FIGURE 15

A comparison of Curves B and C shows that they also have a slope that is approximately the same. This indicates that a deposit would be obtained at 20 gpl copper and 19.1 asf which would be very similar to a deposit obtained at 40 gpl copper and 37.0 asf when they have approximately equal levels of nickel present. The same could be said if Curves G and H are compared. A deposit at 15 gpl copper and 19.1 asf would be similar to a deposit made at 20 gpl copper and 37.0 asf.

Surface Index as a Function of Nickel Concentration - 56.1 asf

With a current density of 56.1 asf, the same general trend is noted as shown in Curves E, F and I, Figure 15. However, Curve I shows that when the copper concentration is lowered to 20 gpl there is a large change in the surface index over that which was found for a copper concentration of 30 gpl. Curve I also has a much steeper slope than any of other curves. This indicates that at this current density the effect of nickel concentration is much greater than at the lower current densities.

Surface Index as a Function of the Reference Number

The relationship between the surface index and the reference number R, is shown in Figure 16. This curve shows a general trend that as the reference number increases the surface index also increases. The area between the dashed lines in this curve indicates a region in which a certain quality of deposit would be expected when experimental conditions resulted in a certain reference number. For example, an experiment with a reference number of 4.0 would result in a deposit having a

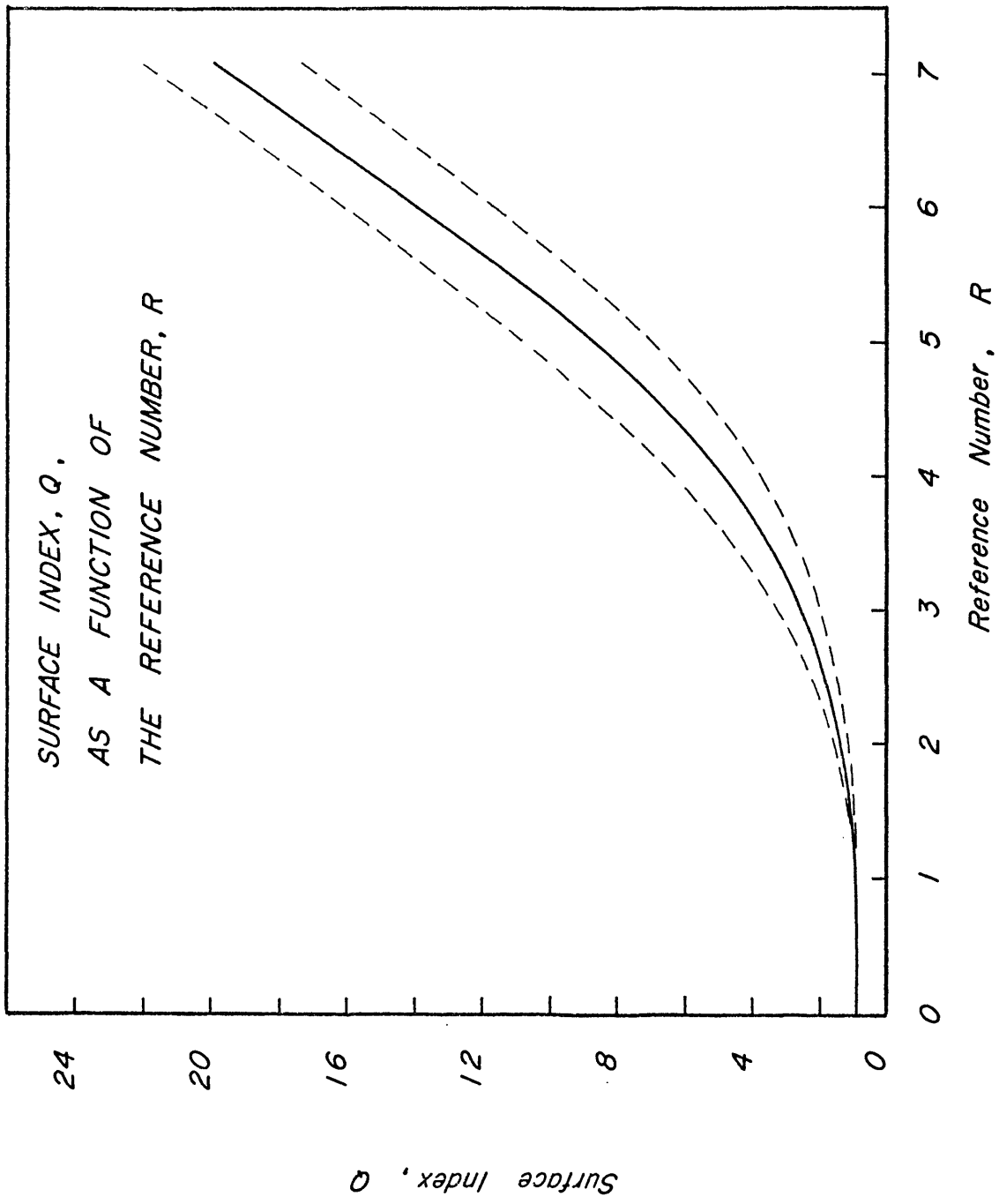
SURFACE INDEX, Q,
AS A FUNCTION OF
THE REFERENCE NUMBER, R
Surface Index, Q
0
4
8
12
16
20
24
Reference Number, R
0
1
2
3
4
5
6
7

FIGURE 16

surface index of from 3.75 to 5.75. In other words, a deposit having a quality of somewhere between "acceptable" and "poor" would be expected.

Effect of Copper and Nickel Concentration on the Total Cell Voltage

Figures 17 to 20 show various curves which indicate the effect of both copper and nickel concentration on the total cell voltage. Figure 17 shows five curves representing cell voltage as a function of copper concentration at five various current densities. These curves show a general trend of a decrease in total cell voltage as the copper concentration decreases to an approximate value of 30 gpl. At this point the total cell voltage starts to reach a steady state value and remains nearly constant down to a copper concentration of 15 gpl (which was the lower experimental limit). These curves show that the initial decrease in the cell voltage is faster at the higher current densities (93.3, 74.5 and 56.1 asf). But, at the two lower current densities the decrease is slow and very small. At 19.1 asf there is actually very little change in the cell voltage. These curves represent cell voltages with no nickel present in solution.

Effect of Copper and Nickel Concentration on Cell Voltage - 19.1 asf

At 19.1 asf and with various nickel concentrations Figure 18 shows that the nickel had little effect on the cell voltage. The curves in this figure indicate that the nickel tended to raise the cell voltage by a very slight amount. The curves also show that the concentration of the nickel was not important and only a small amount was needed to

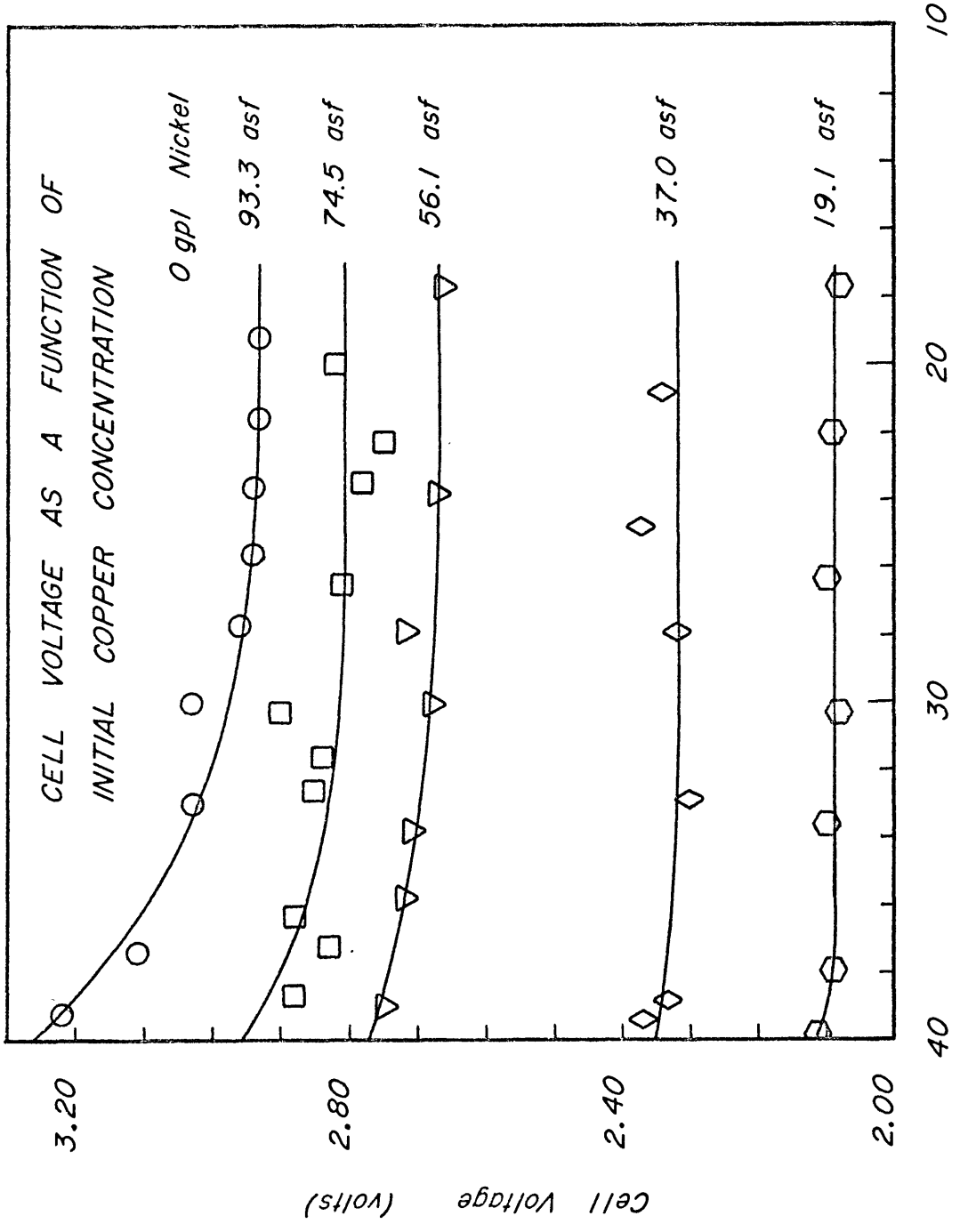
CELL VOLTAGE AS A FUNCTION OF
INITIAL COPPER CONCENTRATION
0 gpl Nickel
93.3 asf
74.5 asf
56.1 asf
37.0 asf
19.1 asf
3.20
2.80
2.40
2.00
Cell Voltage (Volts)
10
20
30
40
Initial Copper (gpl)

FIGURE 17

produce the noticed effect. Larger amounts of nickel produced the same effect and the changes were of the same magnitude, so for 1, 5 and 15 gpl nickel there was only one curve which represented the effect of nickel.

Effect of Copper and Nickel Concentration on Cell Voltage - 37.0 asf

At 37.0 asf Figure 19 shows that the effects of nickel were more drastic. It can be seen that for a nickel concentration of 1 gpl the cell voltage is lowered slightly below that when no nickel is present. However, for 5 and 15 gpl nickel a single curve is obtained which shows that the cell voltage is raised slightly over that when no nickel is present.

Effect of Copper and Nickel Concentration on Cell Voltage - 56.1 asf

At 56.1 asf Figure 20 shows that the concentration of nickel had still greater effects. It can be seen (lower curve) that a nickel concentration of 1 gpl had the greatest effect on the cell voltage. At this nickel concentration and at a copper concentration of 40 gpl, the cell voltage was lowered by approximately 210 millivolts from the cell voltage at the same copper concentration but with no nickel. At 25 gpl copper, 1 gpl of nickel lowered the cell voltage by 100 millivolts below the no nickel value.

For 5 and 15 gpl nickel the lowering of the cell voltage was less than for 1 gpl. It can be seen that at 15 gpl nickel and at copper concentrations below 25 gpl there was actually very little difference in the

cell voltage as compared to the no nickel values.

In Figures 18 to 20 it is important to note one thing. Unlike the cell voltages for tests in which no nickel was present (Figure 17) when nickel was present in solution it stabilized the cell voltage so that it remained constant over 11 of the copper concentrations studied. Whereas when no nickel was present the cell voltage decreased a certain amount before it stabilized.

Effect of Current Density on the Cell Voltage

The curves in Figure 21 show how the current density affected the cell voltage. The curves show a general trend of an increase in cell voltage as the current density is increased. The curves show that for no nickel, the cell voltage for a solution of 40 gpl copper is higher at any given current density than for a solution with 20 and 30 gpl copper. These curves actually represent the same situations as mentioned in the three previous sections.

Effect of Nickelous Ion on Deposit Purity

The purity of the deposit was checked by monitoring the amount of nickel present in the initial and final electrolyte solutions during each test. In no case was there any indication that any nickel had been removed from the solution.

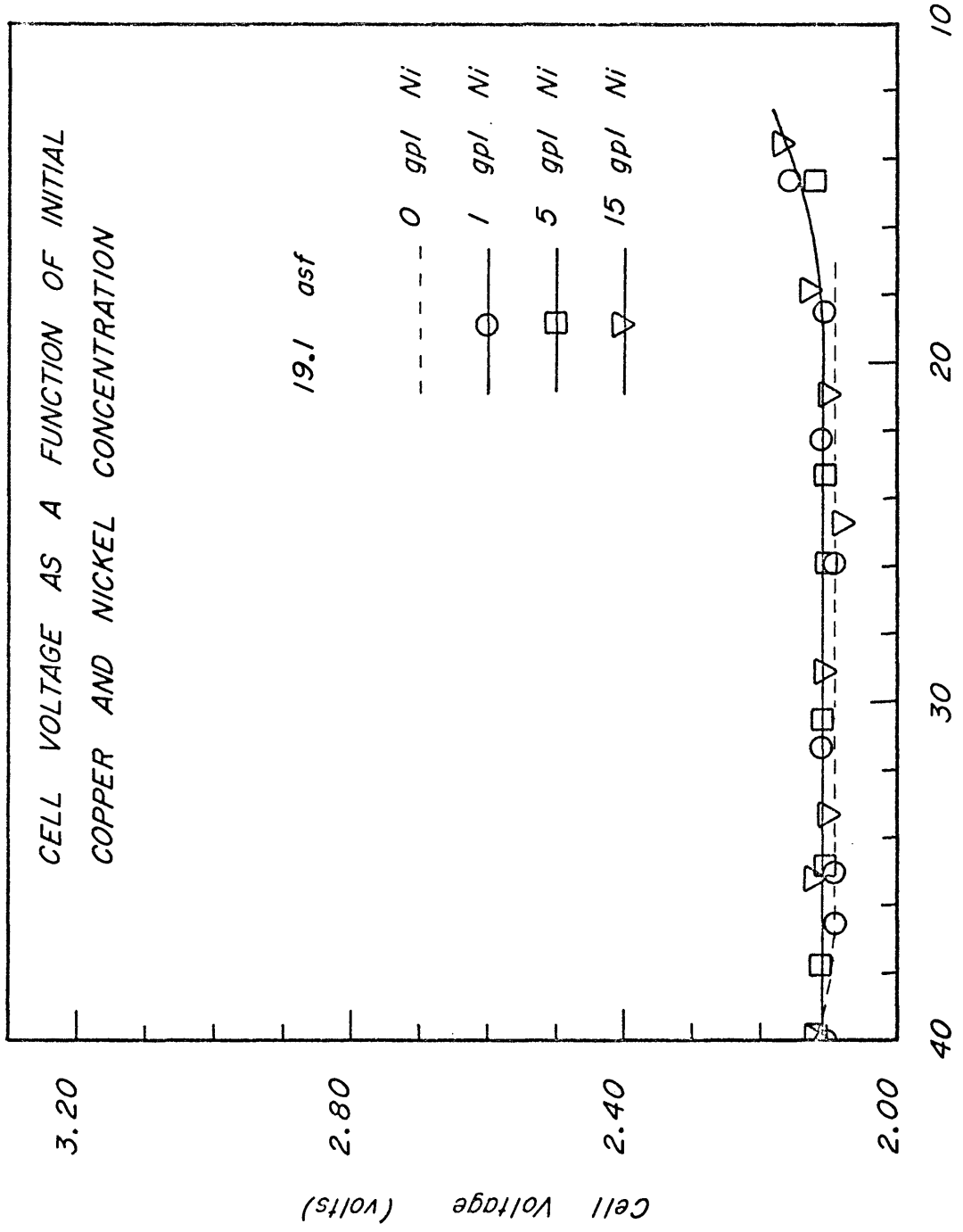
CELL VOLTAGE AS A FUNCTION OF INITIAL COPPER AND NICKEL CONCENTRATION
19.1 asf
0 gpl Ni
1 gpl Ni
5 gpl Ni
15 gpl Ni
Cell Voltage (volts)
3.20
2.80
2.40
2.00
10
20
30
40
Initial Copper (gpl)

FIGURE 18

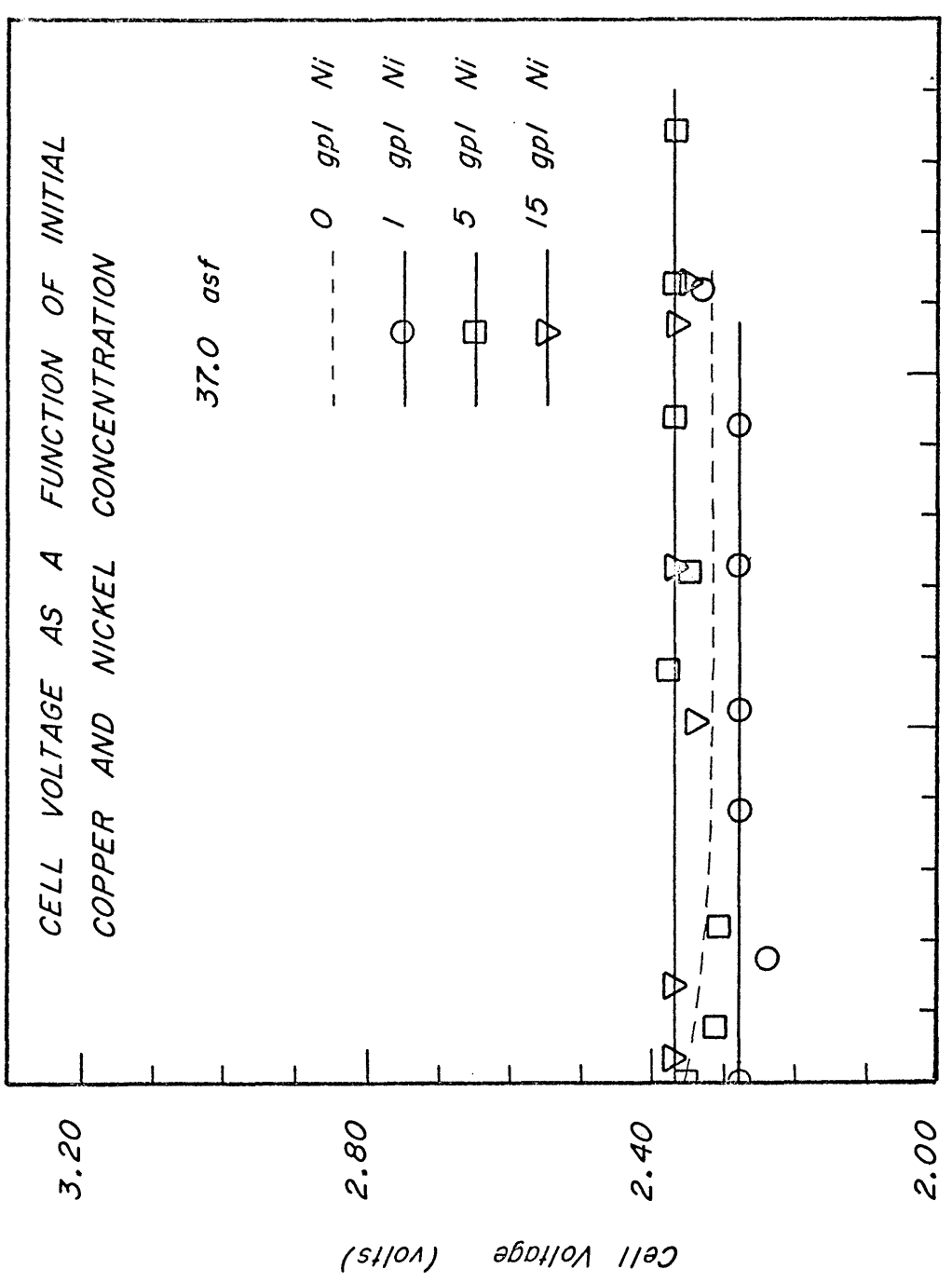
CELL VOLTAGE AS A FUNCTION OF INITIAL COPPER AND NICKEL CONCENTRATION
37.0 asf
0 gpl Ni
1 gpl Ni
5 gpl Ni
15 gpl Ni
Cell Voltage (volts)
3.20
2.80
2.40
2.00
10
20
30
40
Initial Copper (gpl)

FIGURE 19

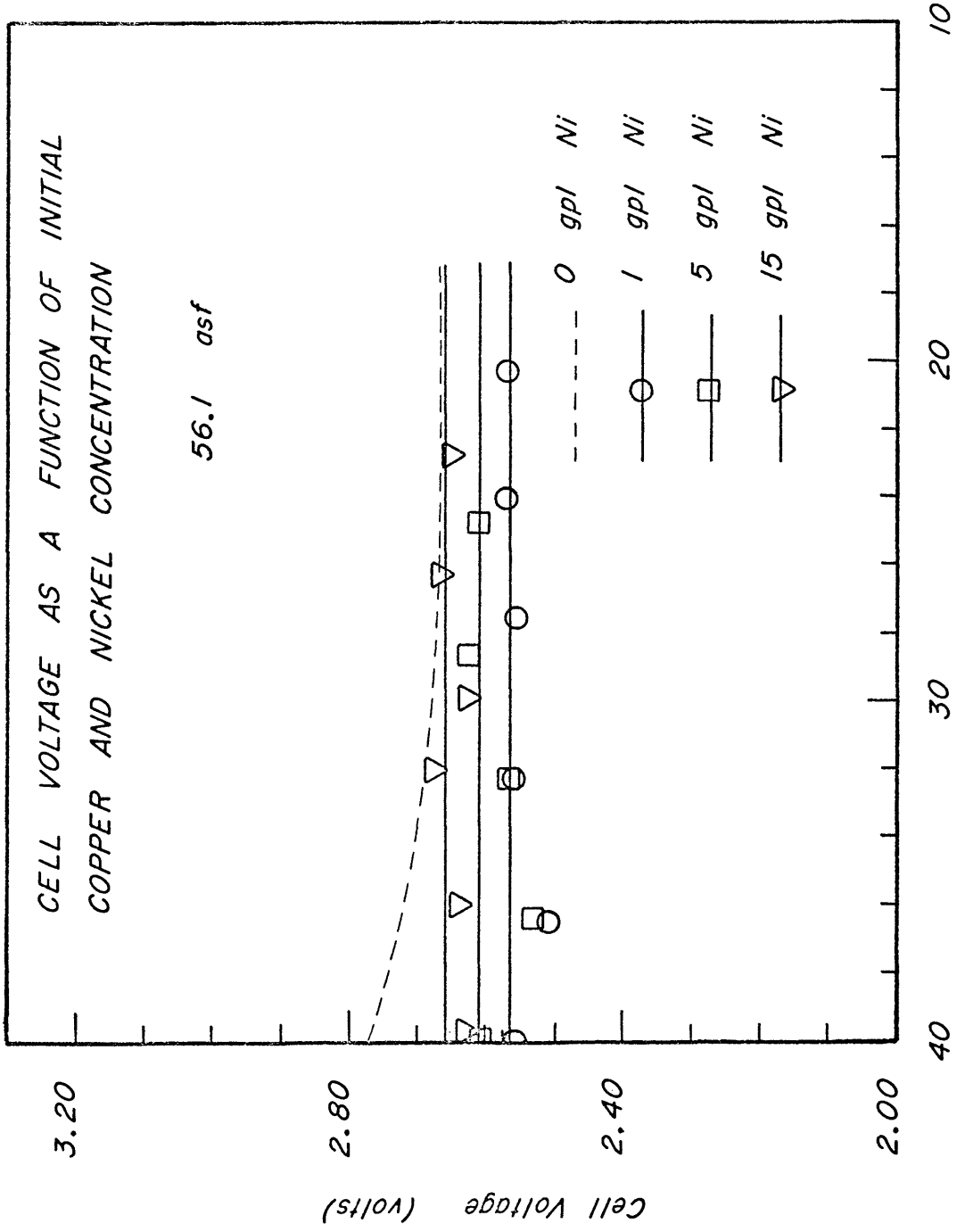
CELL VOLTAGE AS A FUNCTION OF INITIAL COPPER AND NICKEL CONCENTRATION
56.1 asf
0 gpl Ni
1 gpl Ni
5 gpl Ni
15 gpl Ni
Cell Voltage (volts)
3.20
2.80
2.40
2.00
40
30
20
10
Initial Copper (gpl)

FIGURE 20

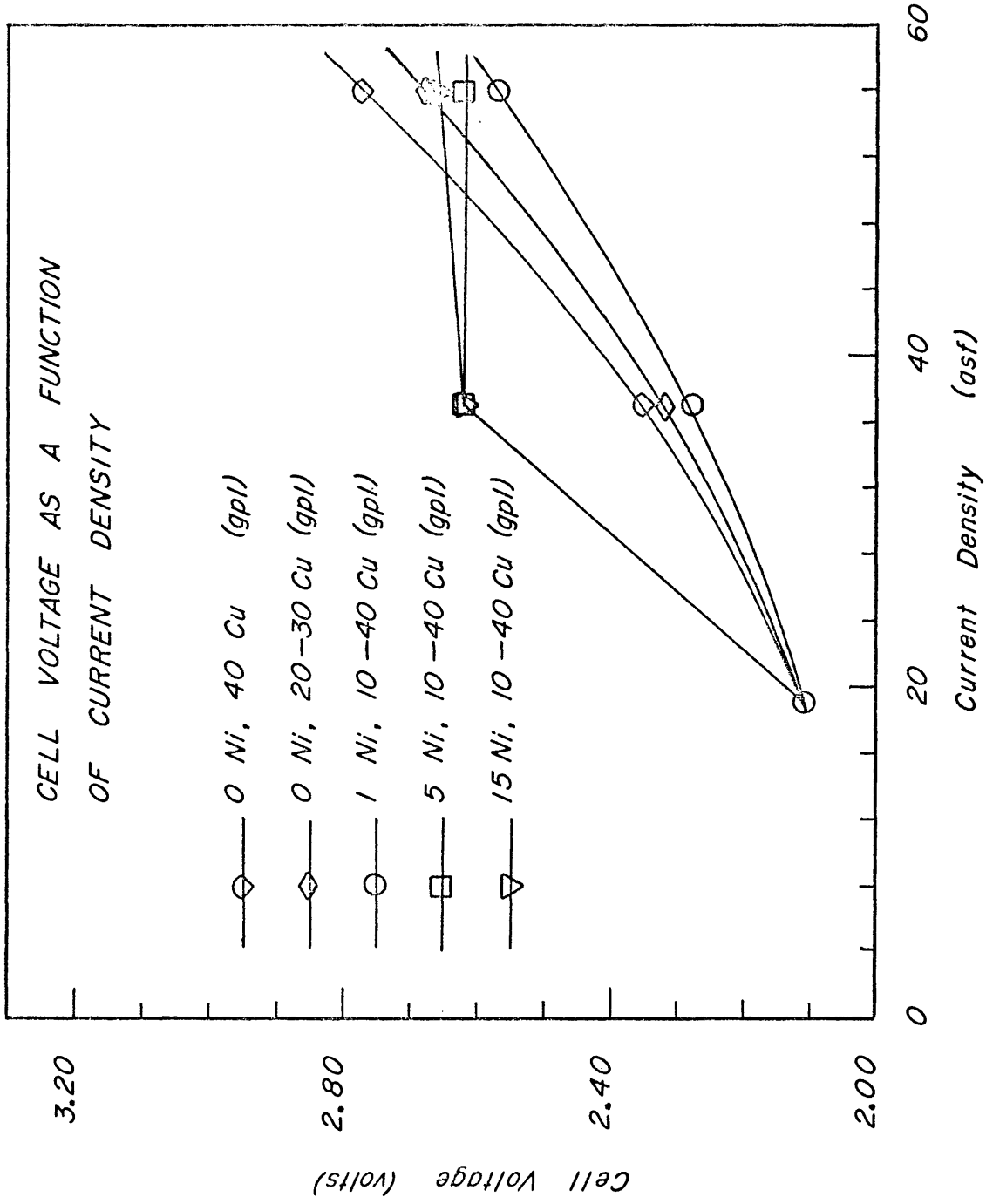
CELL VOLTAGE AS A FUNCTION
OF CURRENT DENSITY
0 Ni, 40 Cu (gpl)
0 Ni, 20-30 Cu (gpl)
1 Ni, 10-40 Cu (gpl)
5 Ni, 10-40 Cu (gpl)
15 Ni, 10-40 Cu (gpl)
Cell Voltage (volts)
3.20
2.80
2.40
2.00
0
20
40
60
Current Density (asf)

FIGURE 21

Polarization Results

The main result of these tests was the determination of the exchange current density, i_0, under various experimental conditions. These conditions were selected in order to parallel those used in the empirical section of the investigation.

Effect of Nickel on the Exchange Current Density

Figure 22 shows what effect nickel had on the exchange surrent density at two copper concentrations. The data used to construct the curves in this Figure are tabulated in Table 8. The curves in Figure 22 are for experimentally determined exchange current densities. These exchange current densities were determined by plotting the corrected data (see Appendix I) as, overvoltage versus log i, where i is the experimental current density. The straight line portion of this curve was then extrapolated to zero overvoltage. This intersection gave the value of the exchange current density.

Figure 22 shows that as the nickel concentration increases the exchange current density also increases and reaches a peak at a nickel concentration of approximately 10 gpl. This is true regardless of the copper concentration. After reaching this peak the exchange current density gradually decreases. These curves also show that as the copper concentration increases the exchange current density increases.

Theoretical and Calculated Values of the Exchange Current Density

Earlier work on this system has shown that it is controlled by

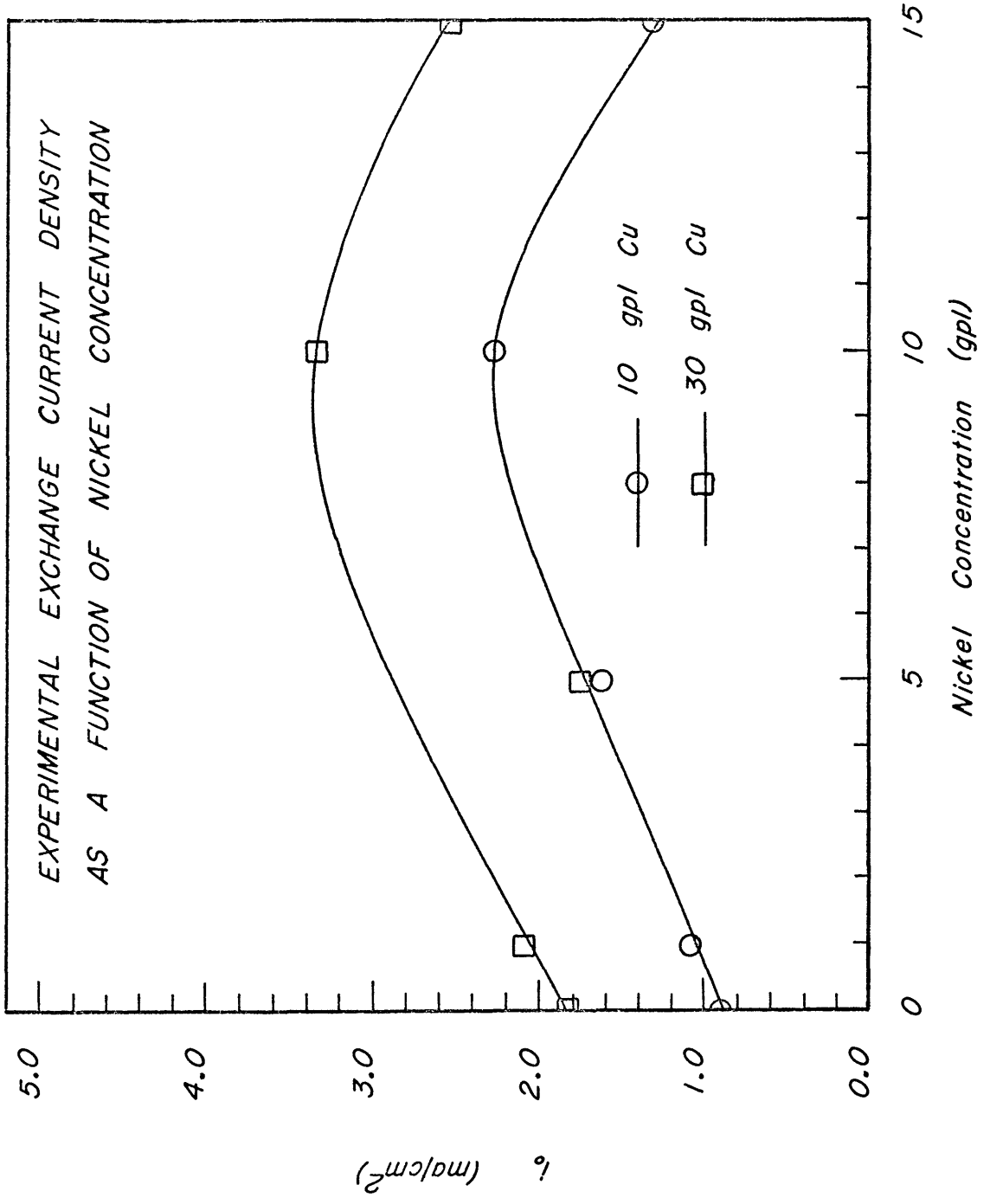
EXPERIMENTAL EXCHANGE CURRENT DENSITY
AS A FUNCTION OF NICKEL CONCENTRATION
10 gpl Cu
30 gpl Cu
i_o (ma/cm^2)
5.0
4.0
3.0
2.0
1.0
0.0
0
5
10
15
Nickel Concentration (gpl)

FIGURE 22

Table 8: Experimental Exchange Current Densities

Test No.	Temp. (°C)	Copper (gpl)	Nickel (gpl)	Acid (gpl)	i_0 (ma/cm^2)	Average i_0 (ma/cm^2)
1	25	0.0	0.0	49.0	0.87	
2	25	0.0	0.0	49.0	0.80	
3	25	0.0	0.0	49.0	0.89	0.86
4	25	0.0	0.0	100.0	0.55	
5	25	0.0	0.0	100.0	0.46	0.50
6	25	10.0	0.0	100.0	0.94	
7	25	10.0	0.0	100.0	0.90	
8	25	10.0	0.0	100.0	----	
9	25	10.0	0.0	100.0	0.86	0.90
10	25	10.0	1.0	100.0	0.98	
11	25	10.0	1.0	100.0	1.17	
12	25	10.0	1.0	100.0	0.40*	1.08
13	25	10.0	5.0	100.0	0.39*	
14	25	10.0	5.0	100.0	1.63	1.63
15	25	10.0	10.0	100.0	1.96	
16	25	10.0	10.0	100.0	2.41	2.18

*Values considered to be unreliable and were not used in any calculations or graphs.

Table 8: Experimental Exchange Current Densities

Test No.	Temp. (°C)	Copper (gpl)	Nickel (gpl)	Acid (gpl)	i_0 (ma/cm^2)	Average i_0 (ma/cm^2)
17	25	10.0	15.0	100.0	1.29	
18	25	10.0	15.0	100.0	1.34	1.31
19	25	30.0	0.0	100.0	1.92*	
20	25	30.0	0.0	100.0	1.83	
21	25	30.0	0.0	100.0	1.43*	1.83
22	25	30.0	1.0	100.0	2.23	
23	25	30.0	1.0	100.0	1.92	2.08
24	25	30.0	5.0	100.0	1.18*	
25	25	30.0	5.0	100.0	1.74	1.74
26	40	30.0	5.0	100.0	3.12	
27	40	30.0	5.0	100.0	3.79*	3.12
28	40	30.0	10.0	100.0	2.66	2.66
29	25	30.0	10.0	100.0	3.39	
30	25	30.0	10.0	100.0	3.30	3.35
31	25	30.0	15.0	100.0	2.55	
32	25	30.0	15.0	100.0	2.50	2.53

Table 8: Experimental Exchange Current Densities

Test No.	Temp. (°C)	Copper (gpl)	Nickel (gpl)	Acid (gpl)	i_0 (ma/cm^2)	Average i_0 (ma/cm^2)
33	40	30.0	15.0	100.0	3.93	
34	40	30.0	15.0	100.0	3.30	3.62
35	60	30.0	15.0	100.0	10.51	
36	60	30.0	15.0	100.0	10.51	10.51
37	30	4.76	0.0	49.0	3.62	3.62

charge-transfer overvoltage (Mattsson and Bockris, 1959) and (Bockris and Kita, 1962). From theoretical considerations it can be shown (Vetter, 1967) that the relationship between the exchange current density, the apparent current density and the overvoltage is given by:

$$i = i_0 [\exp(\alpha z F \eta / RT) - \exp\{-(1-\alpha) z F \eta / RT\}] \quad (2)$$

Where:

i = apparent current density (ma/cm^2).

i_0 = exchange current density (ma/cm^2)

α = charge-transfer coefficient.

z = charge-transfer valence.

F = Faraday constant (96,493 coulombs).

R = Universal gas constant (8314 millivolt-soulombs/deg).

T = absolute temperature (°K).

η = overvoltage (millivolts).

This equation can be simplified for high anodic currents, i.e. when $|\eta| >> RT/zF$, to give the following equation:

$$i = i_0 \cdot \exp(\alpha z F \eta / RT) \qquad (3)$$

Equation 3 can be rewritten as:

$$\eta = - (RT/\alpha zF) \cdot \ln i_0 + (RT/\alpha zF) \cdot \ln i \qquad (4)$$

The above equation has the form of a Tafel equation and can be rewritten as:

$$\eta = a + b \cdot \ln i \qquad (5)$$

The factor (RT/αzF) can be calculated from the known values of R, T and F and assuming that α= 0.5. This is a generally accepted value for the charge-transfer coefficient (Bauer, 1968), (Bockris and Kita, 1962), (Bockris and Kazumney, 1967), (Hampel, 1964), (Hurlen, 1962) and (Vetter, 1967). The parameter z will have the value of 2 (for copper deposition or dissolution).

Using experimental overvoltages and current density measurements and with α, z, F, R and T having the values previously mentioned, it is possible to calculate theoretical exchange current densities. This was done using a computer (Program Number 5, Appendix F). The results are listed in Table 9 as Theo. i_0.

The above calculation resulted in several values for the exchange current density for each test. An average value of these exchange current densities was then used in Equation 4 in order to calculate the theoretical overvoltage values for each particular test. Example values of a typical test are tabulated in Table 10 as "Theoretical Overvoltages".

Equation 5 is the equation of a straight line with a slope of b and an intercept of a. Using experimental values for both the slope and the intercept it was possible to calculate another set of overvoltage values. Example values are tabulated in Table 10 and are listed as "Experimental Calculated Overvoltages". These calculations were done using the computer and Program Number 5 listed in Appendix F.

The experimental slope and intercept values for this calculation were obtained as follows. For each test the straight line portion of the overvoltage versus log i curve was extrapolated to zero overvoltage. An example of this is shown in Figure I.2, Appendix I. The intersection of this straight line with the x-axis gave the experimental value for the exchange current density as was previously mentioned.

For all tests the straight line portion of the curve fell between 10 and 100 milliamps/cm^2. Therefore, the intercept value used for the

calculation was not the intersection of the straight line portion with the zero overvoltage axis but the intersection of this line with the 10 milliamp/cm^2 line. The slope value used was the slope of this straight line. For example the straight line portion of the curve in Figure I.2 has an intercept value of approximately 17 millivolts and a slope of approximately 0.52 mv/ma.

Using these experimental calculated overvoltages together with the experimental current density and experimental slope another set of exchange current densities was calculated. The results of these calculations are tabulated in Table 9 as "Exp. i_0". These calculations were again done using the computer Program Number 5 listed in Appendix F.

The final calculation was to use the experimental values for the slope, the intercept and overvoltages to again calculate exchange current densities. These values are also listed in Table 9 as "Exp.* i_0". Program Number 5, Appendix F was also used for these calculations.

Exchange Current Density Calculated From Experimental Overvoltages

Figure 23 is similar to Figure 22 except that the exchange current densities used are those calculated using experimental slope, intercept and overvoltage values (Exp.*i_0). It can be seen that the curves in this figure show the same trend as seen in Figure 22, i.e. the exchange current density increases with nickel concentration up to a peak at approximately 10 gpl nickel and then decreases. It also shows that the exchange current density increases with copper concentration.

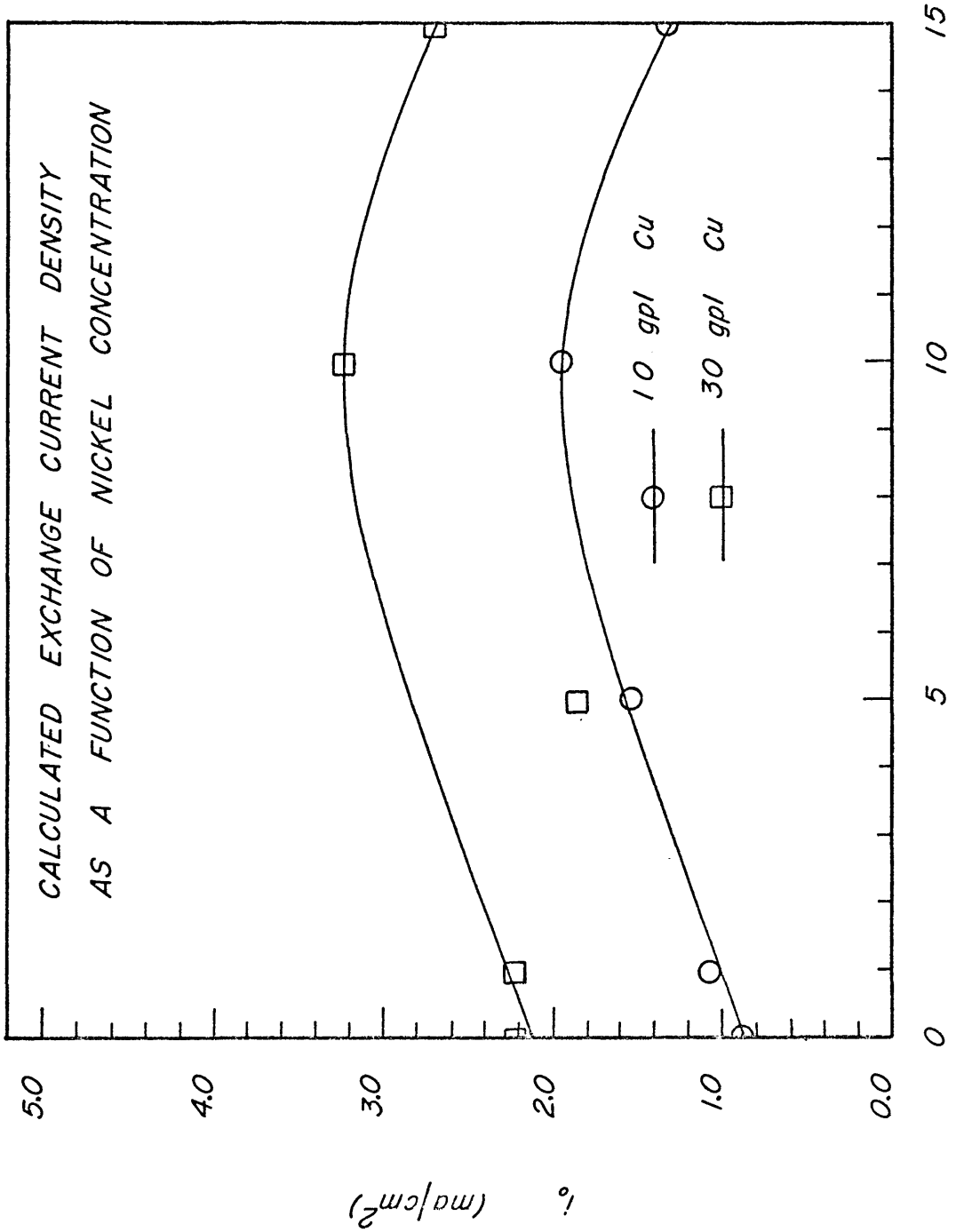
CALCULATED EXCHANGE CURRENT DENSITY
AS A FUNCTION OF NICKEL CONCENTRATION
10 gpl Cu
30 gpl Cu
Nickel Concentration (gpl)
i_o (ma/cm²)
0.0
1.0
2.0
3.0
4.0
5.0
0
5
10
15

FIGURE 23

Table 9: Theoretical and Calculated Exchange Current Densities

Test No.	Theo. i_0	Avg. Theo. i_0	Exp.* i_0	Avg. Exp.* i_0	Exp. i_0	Avg. Exp. i_0
1	0.49		0.94		0.93	
2	0.61		0.61		0.63	
3	0.44	0.51	0.22	0.59	0.17	0.58
4	0.73		0.14		0.14	
5	0.40	0.57	0.35	0.25	0.36	0.25
6	1.64		1.04		0.96	
7	2.41		0.94		0.88	
8	----		----		----	
9	2.58	2.31	0.86	0.95	0.81	0.88
10	3.14		0.80		0.84	
11	2.38		1.32		1.29	
12	2.85*	2.76	0.47*	1.06	0.45*	1.07
13	2.99*		0.39*		0.40*	
14	3.03	3.03	1.55	1.55	1.54	1.54
15	2.02		1.81		1.76	
16	2.13	2.07	2.26	2.03	2.15	1.96

*Values considered to be unreliable and were not used in any calculations or graphs.

Table 9: Theoretical and Calculated Exchange Current Densities

Test No.	Theo. i_0	Avg. Theo. i_0	Exp.* i_0	Avg. Exp.* i_0	Exp. i_0	Avg. Exp. i_0
17	2.43		1.64		1.50	
18	2.53	2.48	1.16	1.40	1.13	1.32
19	4.20*		1.38*		1.35*	
20	3.12		2.23		2.09	
21	3.85*	3.12	1.43*	2.23	1.35*	2.09
22	3.33		2.23		2.32	
23	3.05*	3.33	1.64*	2.23	1.70*	2.32
24	3.73*		0.97*		1.38*	
25	3.64	3.64	1.87	1.87	1.87	1.87
26	5.83		1.76		4.44	
27	5.66*	5.83	3.79*	1.76	3.90*	4.44
28	7.24	7.24	3.10	3.10	3.16	3.16
29	2.45*		4.96*		4.41*	
30	2.87	2.87	3.23	3.23	3.40	3.40
31	2.68		2.88		2.17	
32	2.70	2.69	2.49	2.68	2.51	2.39

Table 9: Theoretical and Calculated Exchange Current Densities

Test No.	Theo. i_0	Avg. Theo. i_0	Exp.* i_0	Avg. Exp.* i_0	Exp. i_0	Avg. Exp. i_0
33	7.52		2.74		2.90	
34	7.30	7.41	2.86	2.80	2.74	2.82
35	12.74		11.45		10.74	
36	12.61	12.67	8.94	10.20	8.57	9.66
37	1.94	1.94	1.94	1.94	1.96	1.96

Exchange Current Density Calculated from Calculated Overvoltages

Figure 24 shows curves similar to those in Figures 22 and 23. However, the exchange current densities used for these curves are those calculated using the overvoltages mentioned previously (Exp. i_0). Again the same trends as before are evident.

Comparison of Experimental and Calculated Exchange Current Densities

Figure 25 shows how the three previously mentioned exchange current densities compare. Curves A and B are those exchange current densities obtained experimentally using the intercept value for i_0. Curves C and D are those exchange current densities (Exp.* i_0) obtained by calculation using experimental overvoltages, experimental slope and experimental intercept values. Curves E and F represent those exchange

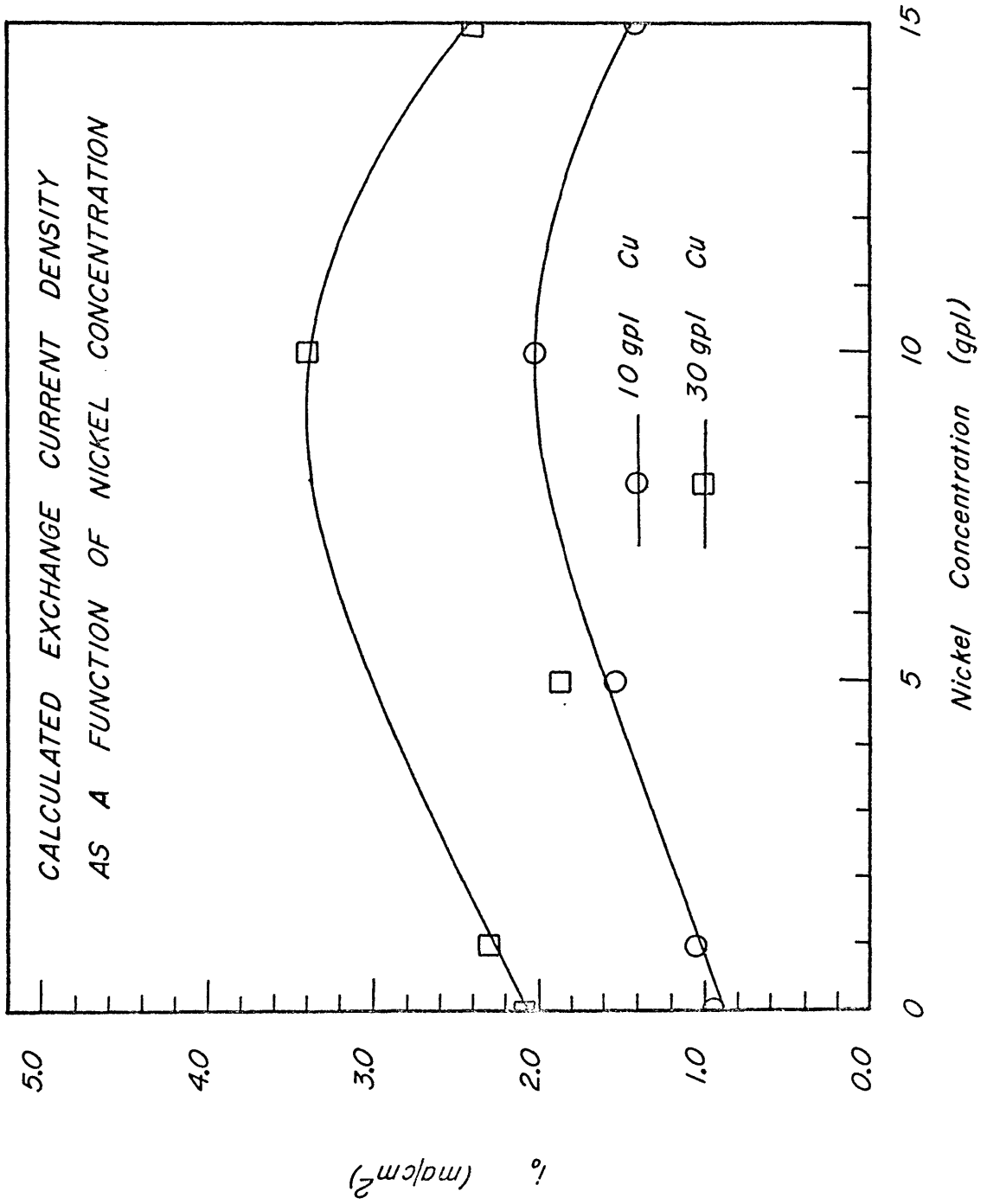
CALCULATED EXCHANGE CURRENT DENSITY
AS A FUNCTION OF NICKEL CONCENTRATION
10 gpl Cu
30 gpl Cu
Nickel Concentration (gpl)
i₀ (ma/cm²)
0.0
1.0
2.0
3.0
4.0
5.0
0
5
10
15

FIGURE 24

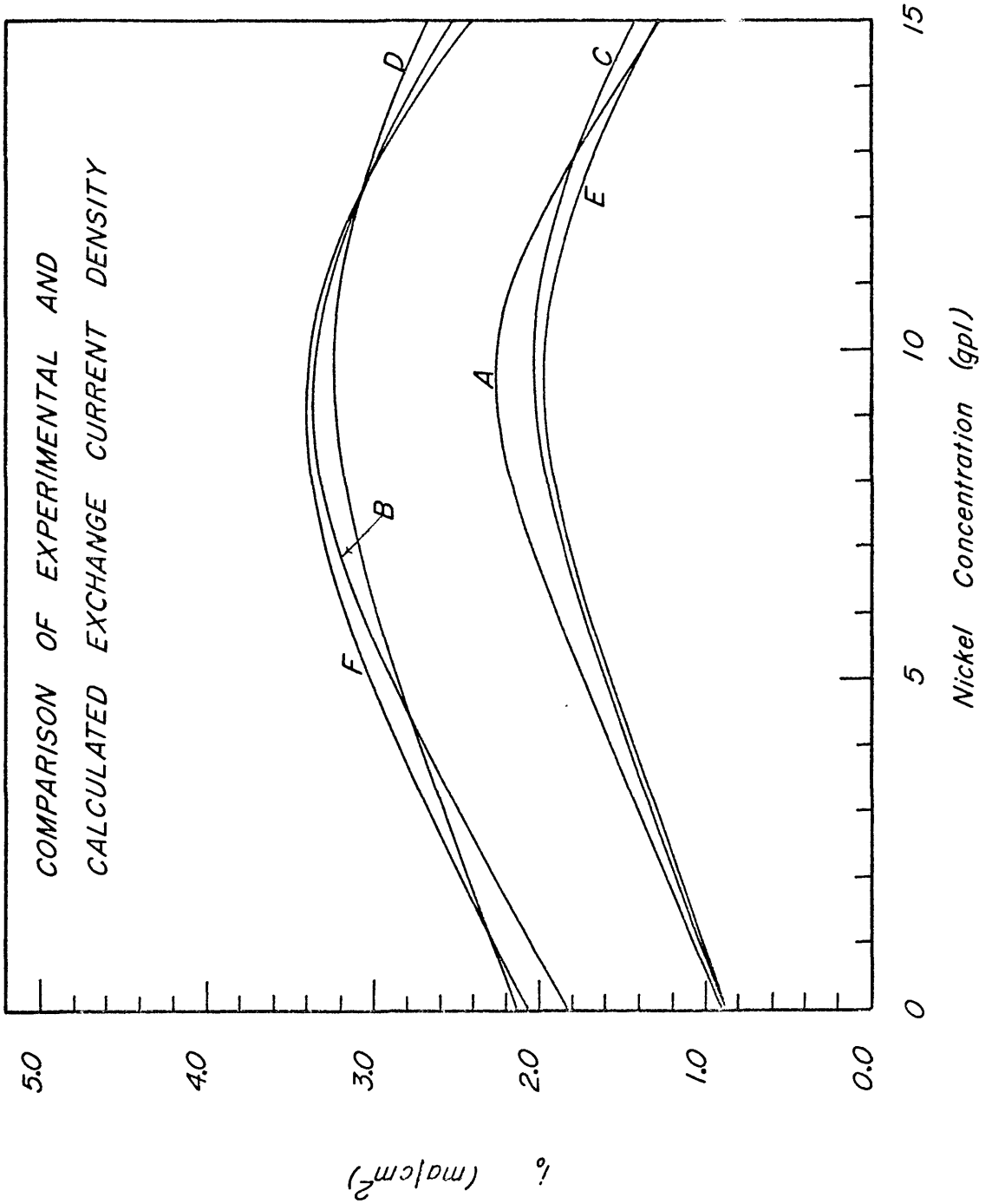
COMPARISON OF EXPERIMENTAL AND
CALCULATED EXCHANGE CURRENT DENSITY
A
B
C
D
E
F
5.0
4.0
3.0
2.0
1.0
0.0
i (ma/cm²)
0
5
10
15
Nickel Concentration (gpl)

FIGURE 25

current densities (Exp. i_0) obtained by calculation using calculated values for the overvoltages, experimental slope and experimental intercept values. It can be seen that all three curves for both copper concentrations agree very well.

Average Exchange Current Density

Figure 26 shows two curves plotted using the average of the previous three exchange current densities. The values used to plot these curves are tabulated in Table 11.

Effect of Temperature on the Exchange Current Density

The curves in Figure 27 show how temperature effects the exchange current density. Data for these curves is tabulated in Table 9. The curve for a solution having a copper concentration of 30 gpl and a nickel concentration of 15 gpl, shows that as the temperature is increased, the exchange current density also increases in a non-linear manner.

The curve for a solution having a copper concentration of 30 gpl and a nickel concentration of 5 gpl shows a lower exchange current density as compared to the 15 gpl nickel curve. It also shows the same trend, an increase in exchange current density with an increase in temperature.

However, the curve for a nickel concentration of 10 gpl indicates a decrease in the exchange current density when the temperature is increased. It also seems to indicate a linear relationship between the exchange current density and temperature.

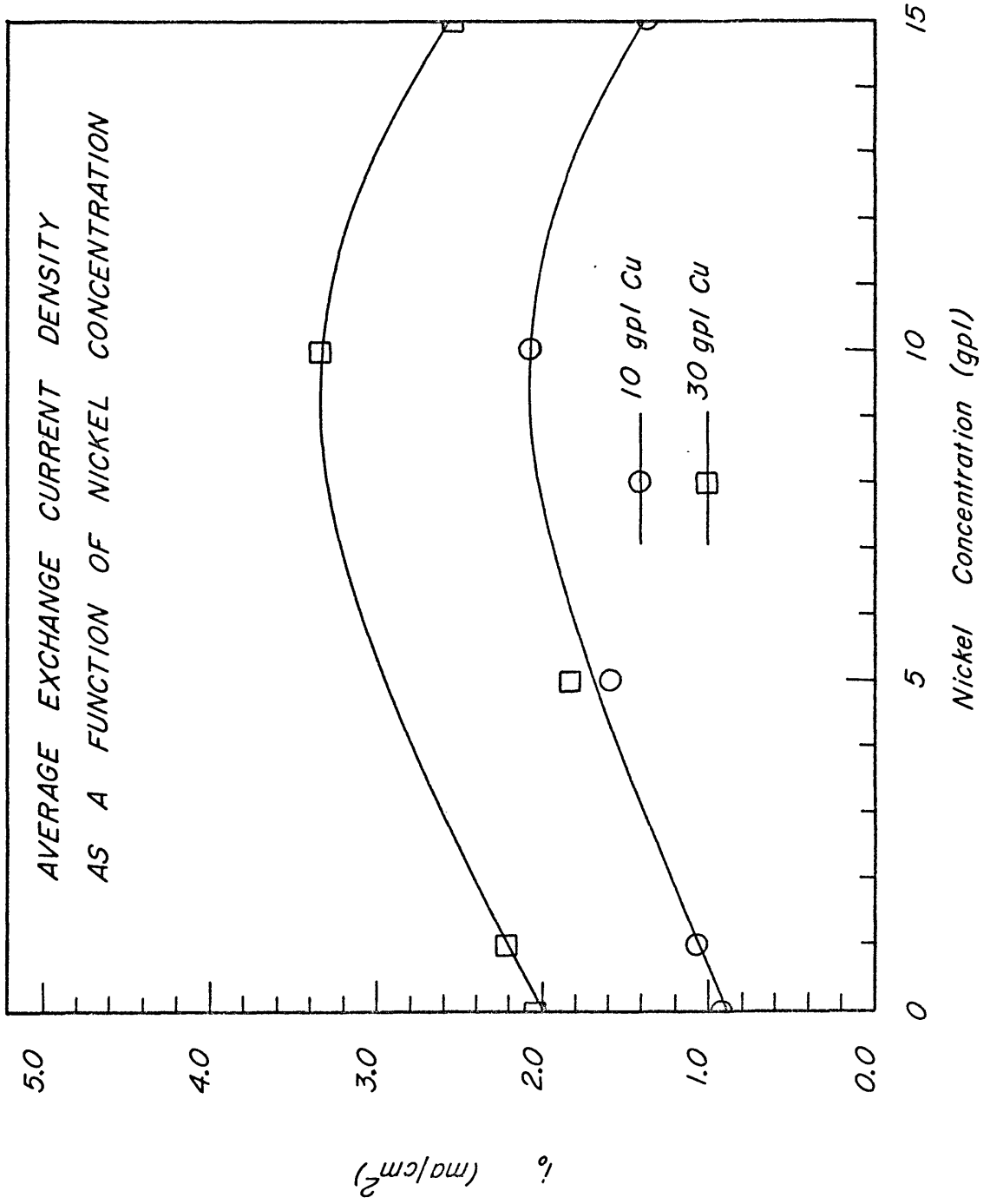
AVERAGE EXCHANGE CURRENT DENSITY
AS A FUNCTION OF NICKEL CONCENTRATION
10 gpl Cu
30 gpl Cu
Nickel Concentration (gpl)
i₀ (ma/cm²)
0.0
1.0
2.0
3.0
4.0
5.0
0
5
10
15

FIGURE 26

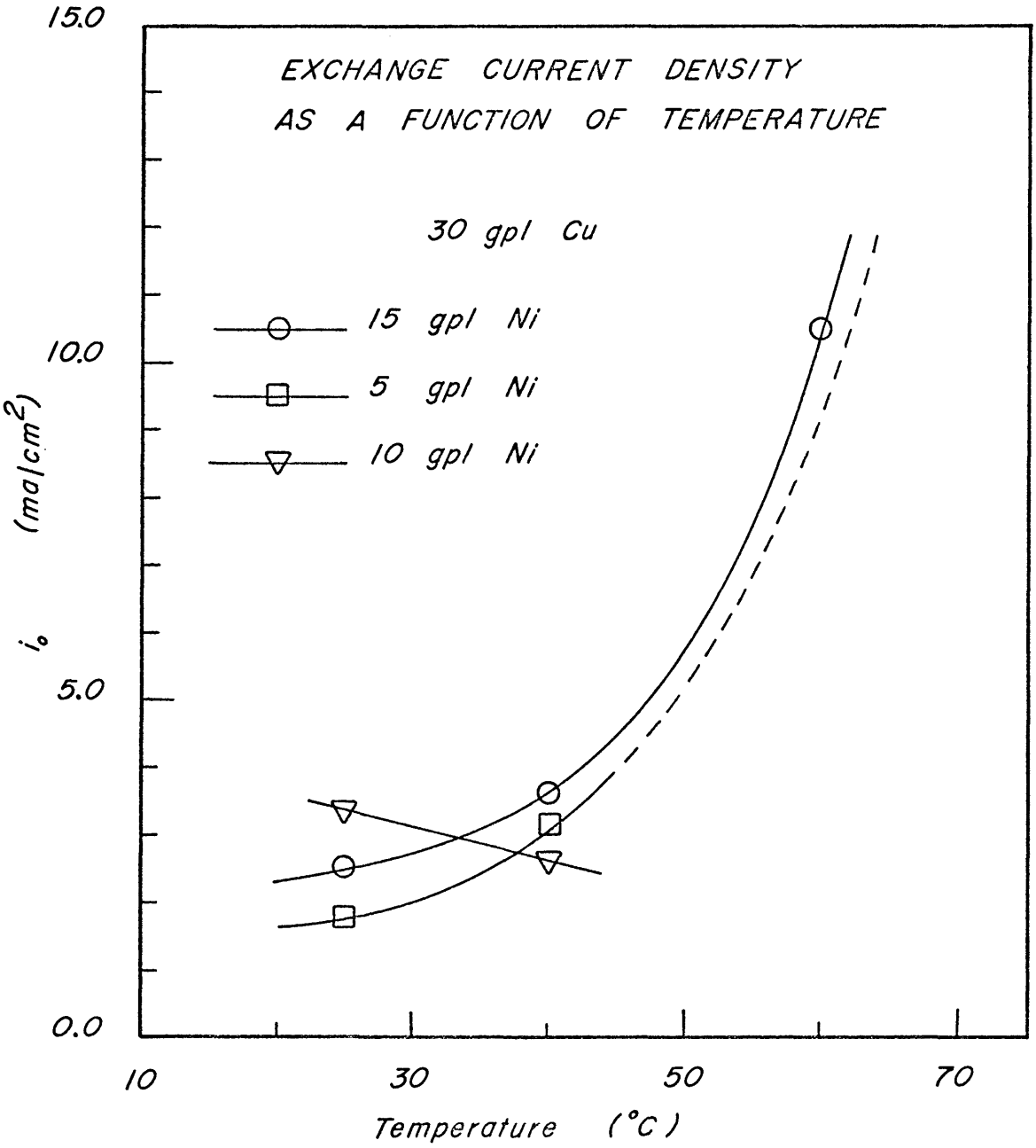
EXCHANGE CURRENT DENSITY
AS A FUNCTION OF TEMPERATURE
30 gpl Cu
15 gpl Ni
5 gpl Ni
10 gpl Ni
15.0
10.0
5.0
0.0
i_o (ma/cm^2)
10
30
50
70
Temperature (°C)

FIGURE 27

Table 10: Experimental and Calculated Overvoltages for Test Number 33

Experimental Overvoltage (mv)	Theoretical Overvoltage (mv)	Experimental Calculated Overvoltage (mv)
33.31	23.32	32.40
36.98	29.34	36.38
40.22	34.26	39.63
43.09	38.42	42.38
45.62	42.02	44.76
47.85	45.19	46.86
49.83	48.03	48.74
51.58	50.61	50.44
53.15	52.95	51.99
54.56	55.11	53.42
55.83	57.11	54.74
57.01	58.97	55.97
58.12	60.71	57.12
59.17	62.35	58.20
60.20	63.89	59.22
61.21	65.35	60.19
62.24	66.73	61.10
63.29	68.04	61.97
64.78	69.30	62.80

Table 11: Average Exchange Current Densities

Tests No.	Average Exchange Current Density (ma/cm^2)
1 to 3	0.68
4 to 5	0.33
6 to 9	0.91
10 to 12	1.07
13 to 14	1.57
15 to 16	2.06
17 to 18	1.34
19 to 21	2.05
22 to 23	2.21
24 to 25	1.84
26 to 27	3.11
28	3.97
29 to 30	3.33
31 to 32	2.53
33 to 34	3.08
35 to 36	10.12
37	2.51

DISCUSSION OF RESULTS

The discussion of the polarization results will be given first, in order to establish certain basic fundamentals which, inturn, will permit a better understanding of the empirical results.

Polarization Results

Exchange Current Density

The main concern of the polarization experiments was the determination of the "exchange current density". This quantity was first introduced by Bowden and Agar in 1938 (Bowden and Agar, 1938). If equilibrium exists in a heterogeneous system, such as an electrode in contact with an electrolyte, there is a situation in which there is no "macroscopic" changes, i.e. no flow of current. However, there is always the probability that some metal ions will leave the metal lattice and enter the solution. Metal ions in the solution also have a probability of leaving the solution and entering the metal lattice. So that, on the microscopic level there is always an exchange of "charge carriers" (ions or electrons). This exchange is equal in both directions. That is to say,the electrons produced by the anodic reaction will be consumed by the cathodic reaction. Therefore, for the heterogeneous system of an electrode and an electrolyte, the " anodic partial current" will be equal in magnitude but opposite in direction

to the "cathodic partial current".

These two partial currents compensate for each other so that no externally measurable current flows through the system. The magnitude of these two compensating current densities is called the "exchange current density, i_0". By definition the exchange current density is always positive. It is a measure of the rate of attainment of the equilibrium potential. The situation is shown in Figure 28. The arrows represent the direction and relative magnitude of the currents involved.

At a potential greater than the equilibrium potential ($\varepsilon > \varepsilon_0$ with $\eta>0$) there exists a flow of anodic current and metal ions (Me^{z+}) will enter the electrolyte. In this case $i_+>i_-$. For the reverse case of $i_-> i_+$ ($\varepsilon<\varepsilon_0$ with $\eta<0$) there will be a net flow of current in the opposite direction and metal ions (Me^{z+}) will be deposited on the metal surface.

Compact Double-Layer and the Diffuse Layer

A second concept that is useful when discussing the interface between an electrode and an electrolyteis that of the "compact double-layer" and the "diffuse layer". This situation is shown very simply in Figure 29.

The diffuse layer consists of a region, in close proximity to the electrode, in which the ions are held in place by non-specific coulombic forces between the charge on the ions and the charge on the electrode (and also the charge on the compact double-layer). In this interphase the ions are not held in a rigid position. Figure 29 shows that in this region the ions are more highly concentrated toward the

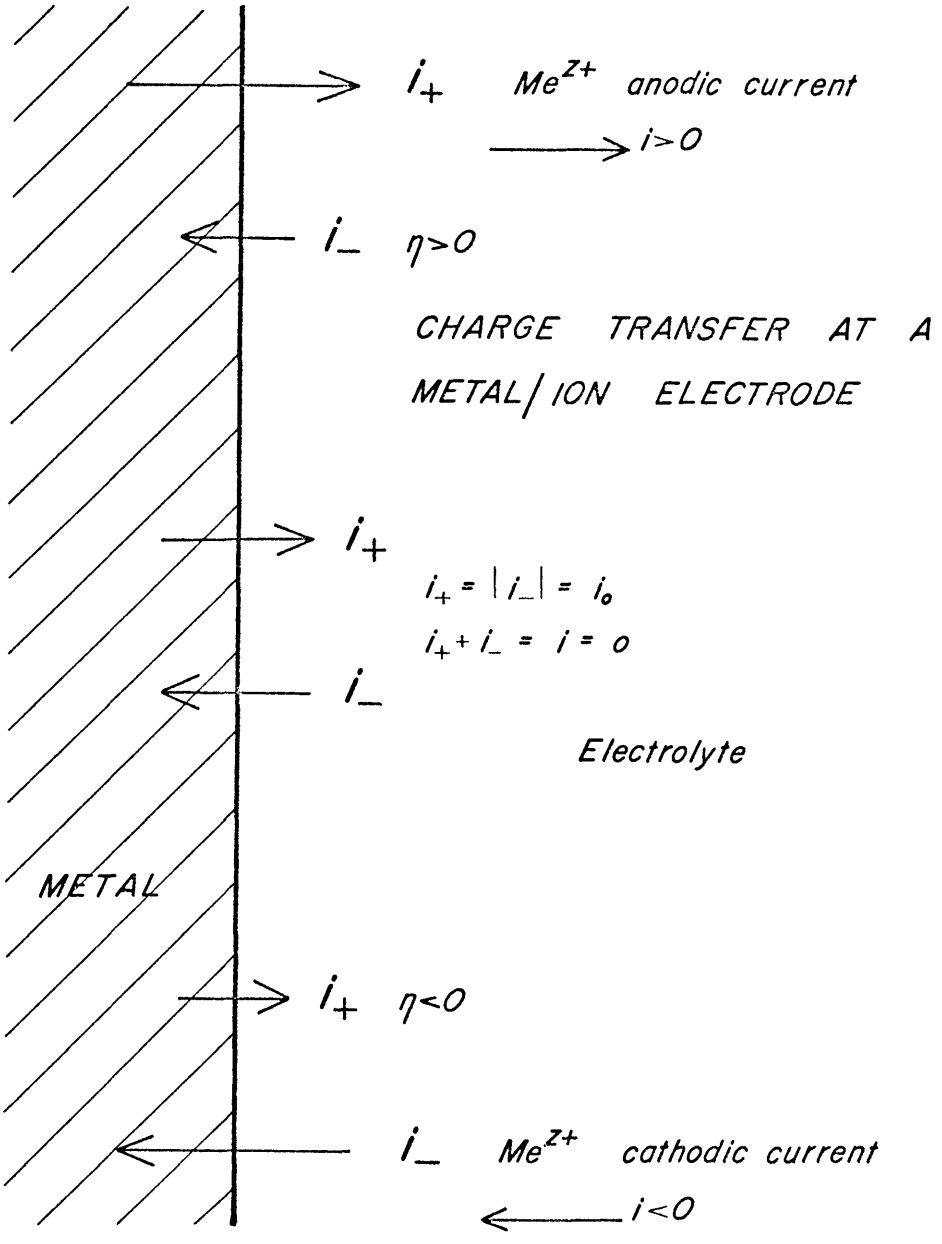
i_+ Me^{z+} anodic current
$i>0$
i_- $\eta>0$
CHARGE TRANSFER AT A METAL/ION ELECTRODE
i_+
$i_+ = |i_-| = i_o$
$i_+ + i_- = i = 0$
i_-
Electrolyte
METAL
i_+ $\eta<0$
i_- Me^{z+} cathodic current
$i<0$

Figure 28

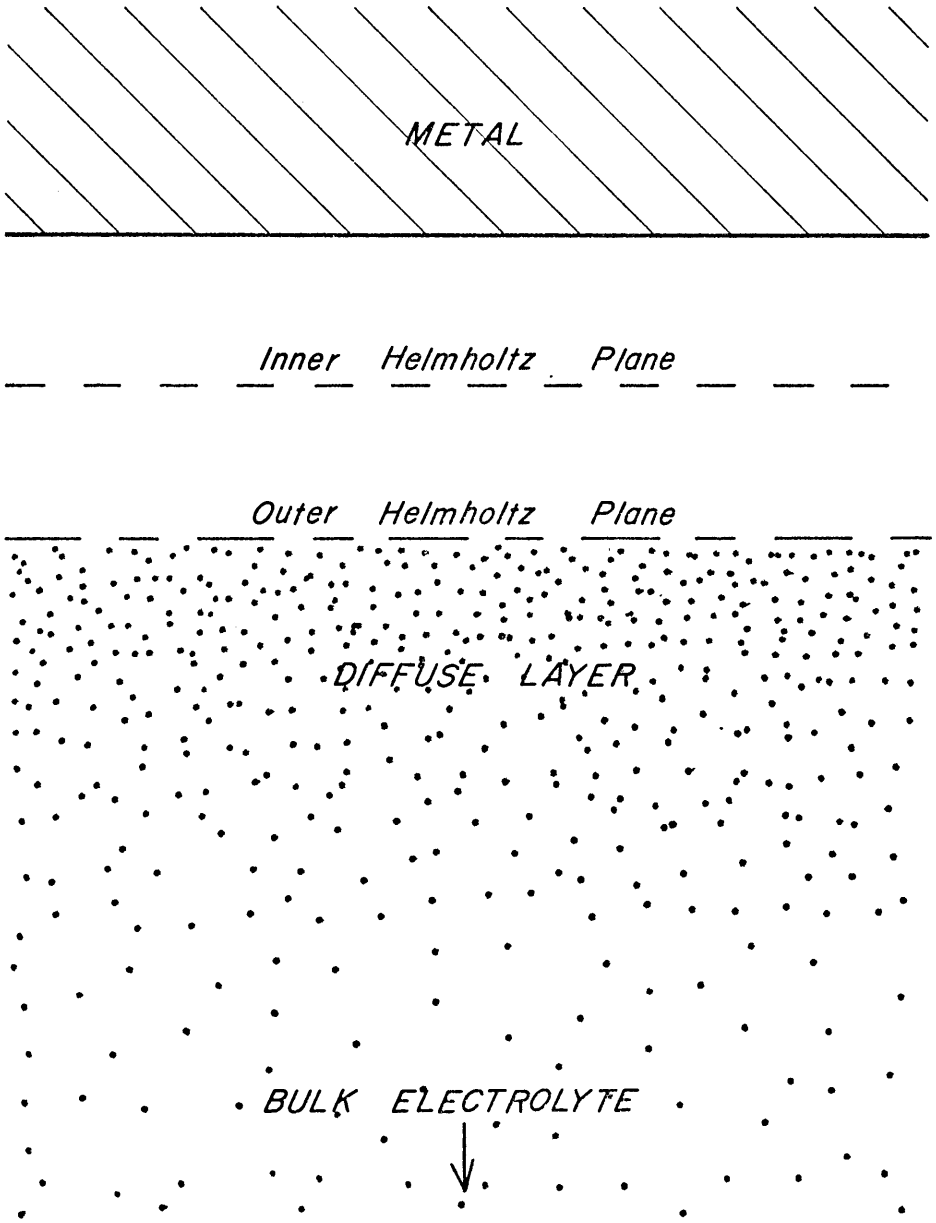

SCHEMATIC OF DOUBLE LAYER

Figure 29

electrode and then seem to diffuse to a concentration that is lower and which is known as the bulk concentration.

The compact double-layer is a layer that is 1 to 2 molecular diameters in thickness. In this interphase the ions are held in place by specific coulombic forces acting between the ions and the electrode. Figure 29 shows this layer to be further subdivided into two more layers. These layers are separated by the "inner Helmholtz plane". The diffuse layer and the compact double-layer are likewise separated by the "outer Helmholtz plane".

This situation is better shown in Figure 30 and it is seen that the inner Helmholtz plane is a plane passing through the centroid of the specifically adsorbed anions. The outer Helmholtz plane is a plane passing through the centroid of the solvated cations. This figure also shows that the actual separation between the diffuse layer and the compact double-layer is not as distinct as was shown in Figure 29. It can be seen that the diffuse layer actually follows the irregular boundary shown in Figure 30.

Figure 30 shows that in the interphase at the electrode surface there are both adsorbed water dipoles and anions. These adsorbed species can play an important part in the charge-transfer steps and the type of crystal growth that can occur at the electrode. Bockris states (Bockris and Razumney, 1967) that these adsorbed species can act as inhibitors and as such can "effect the growth of crystals on the electrodes". He also states that they could modify the free energy of activation for the elementary charge-transfer steps occuring at the electrode. This factor

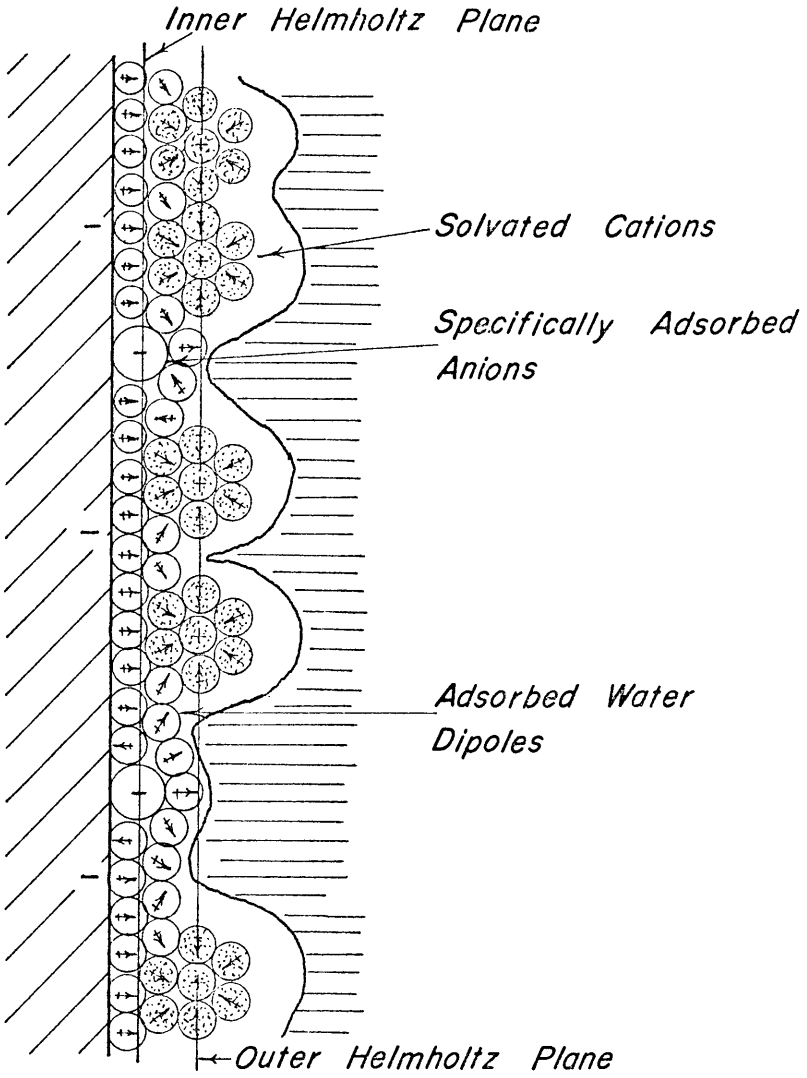

DETAILED MODEL OF DOUBLE LAYER

Figure 30

directly affects the exchange current density, the rate-determining step of the reaction and even the path that the ions and electrons pursue during the charge-transfer step. These adsorbed species will also reduce the amount of area available for reduction of the ions.

Experimental and Theoretical Exchange Current Density

It was shown in Figures 22 through 26 that the experimental exchange current density increased with both an increase in the copper concentration and with an increase in the nickel concentration. This experimental exchange current density was a measure of the rate of exchange between copper ions in solution and electrons from the copper electrode. There should have been no exchange of any nickel ions. It is easy to see that with an increase in copper concentration the exchange current density should increase since there is an increase in the probability of exchange. This has also been shown to be true experimentally by Mattsson and Bockris (Mattsson and Bockris, 1959).

The experimental work conducted by Mattsson and Bockris (Mattsson and Bockris, 1959) and by Bockris and Kita (Bockris and Kita, 1962) show this reaction to be primarily controlled by the charge-transfer reaction. With this consideration and with the present system having an excess of an inert electrolyte (sulfuric acid) then it can be shown theoretically (Vetter, 1967) that the exchange current density is proportional to the concentration of the species under going charge-transfer. Which would be in this case copper ions. Thus for the anodic and cathodic exchange currents the following equations are derived:

$$i_+ = k_+ \cdot c_M \cdot c_r \cdot \exp (\alpha z F \epsilon / RT) \rightarrow \text{anodic current} \quad (6)$$

$$i_- = - k_- \cdot c_0 \cdot \exp [-(1-\alpha) z F \epsilon / RT] \rightarrow \text{cathodic current} \quad (7)$$

Where:

i_+ = anodic partial current density.

i_- = cathodic partial current density.

k_+ = reaction rate constant for the anodic reaction.

k_- = reaction rate constant for the cathodic reaction.

c_M = concentration of the reduced species in the charge-transfer reaction (intermediate species).

c_r = concentration of the reduced species in the charge-transfer reaction (final state).

c_0 = concentration of the oxidized species in the charge-transfer reaction.

α = charge-transfer coefficient.

z = charge-transfer valence.

F = Faraday constant.

R = Universal gas constant.

T = absolute temperature.

ϵ = potential difference.

Since $i_+ = i_- = i_0$ = exchange current density, these equations show that the exchange current density does indeed increase with an increase in the concentration of the involved species.

However, since only the copper ions are considered to be taking any part in any charge-transfer, the increase in the exchange current density with an increase in nickel concentration while at the same time keeping the copper concentration constant can not be explained by any present theories. This behavior was shown in Figures 22 to 26.

Two-Step and One-Step Charge-Transfer

It has been previously mentioned that in this system the rate controlling step is that of charge-transfer. It has also been shown both experimentally (Bockris and Kita, 1962) and theoretically (Bockris and Razumney, 1967) that this reaction proceeds by a two-step charge-transfer mechanism. It has been ruled highly improbable on theoretical considerations (Bockris and Razumney, 1967) that this reaction could proceed by a one-step charge-transfer mechanism. This is because of the high energy barrier that has to be surmounted in order for the one-step mechanism to proceed.

With this fact in mind the type of behavior as shown in Figures 31 and 32 again demonstrate a type of behavior that is not explained by any present theory. Curve B, Figure 31, shows a plot of the experimental exchange current density (this is the same plot given in Figure 22). The three other curves shown in Figure 31 were arrived at in the following manner. The top curve, Curve A, is a plot of the theoretical exchange current density. The procedure for obtaining these values was outlined in the Results section and are tabulated in Table 9 as, "Theo. i_0". These values are calculated assuming a one-step charge-transfer reaction. If on the other hand, a two-step charge-transfer reaction is

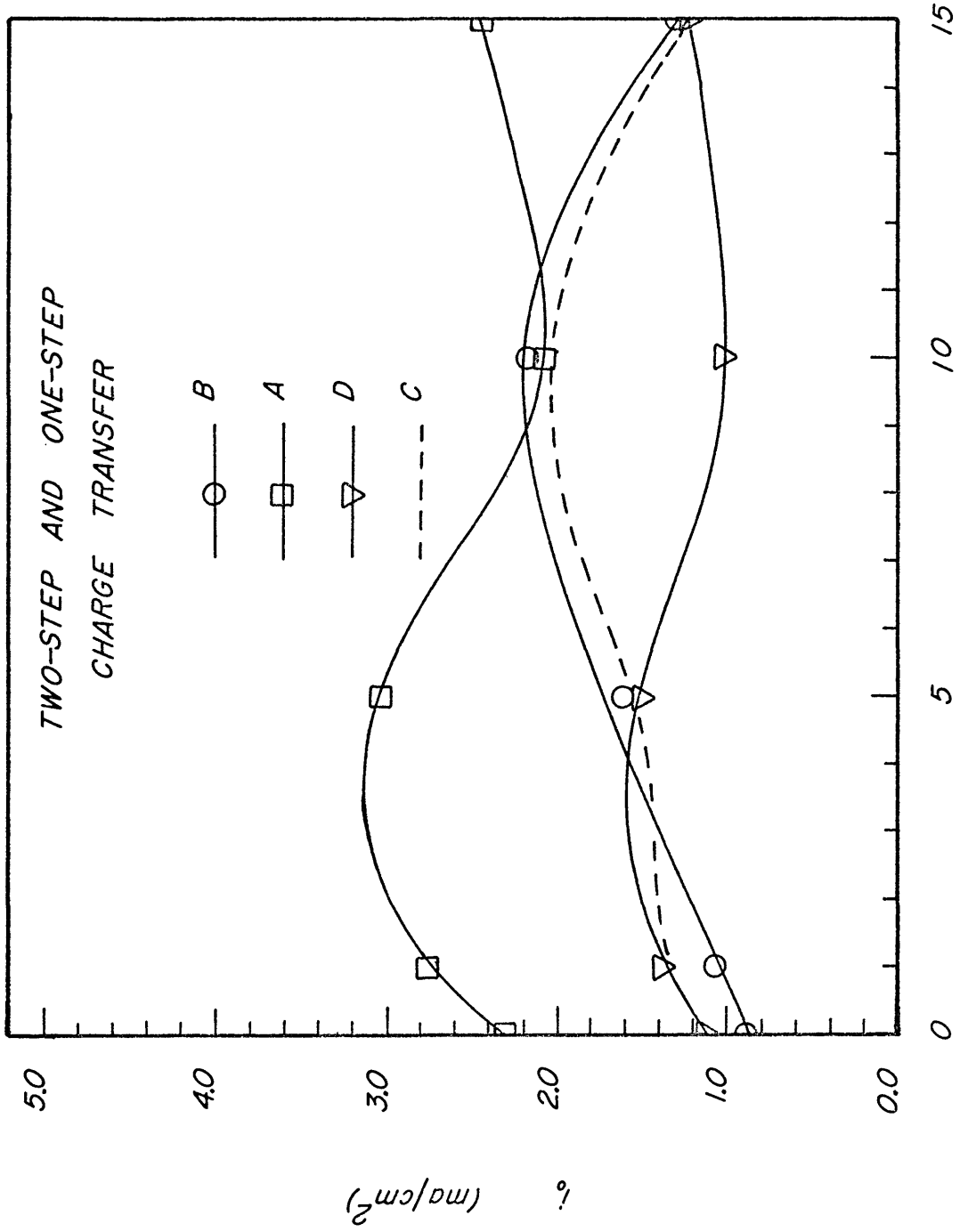
TWO-STEP AND ONE-STEP
CHARGE TRANSFER
B
A
D
C
5.0
4.0
3.0
2.0
1.0
0.0
i₀ (ma/cm²)
0
5
10
15
Nickel Concentration (gpl)

FIGURE 31

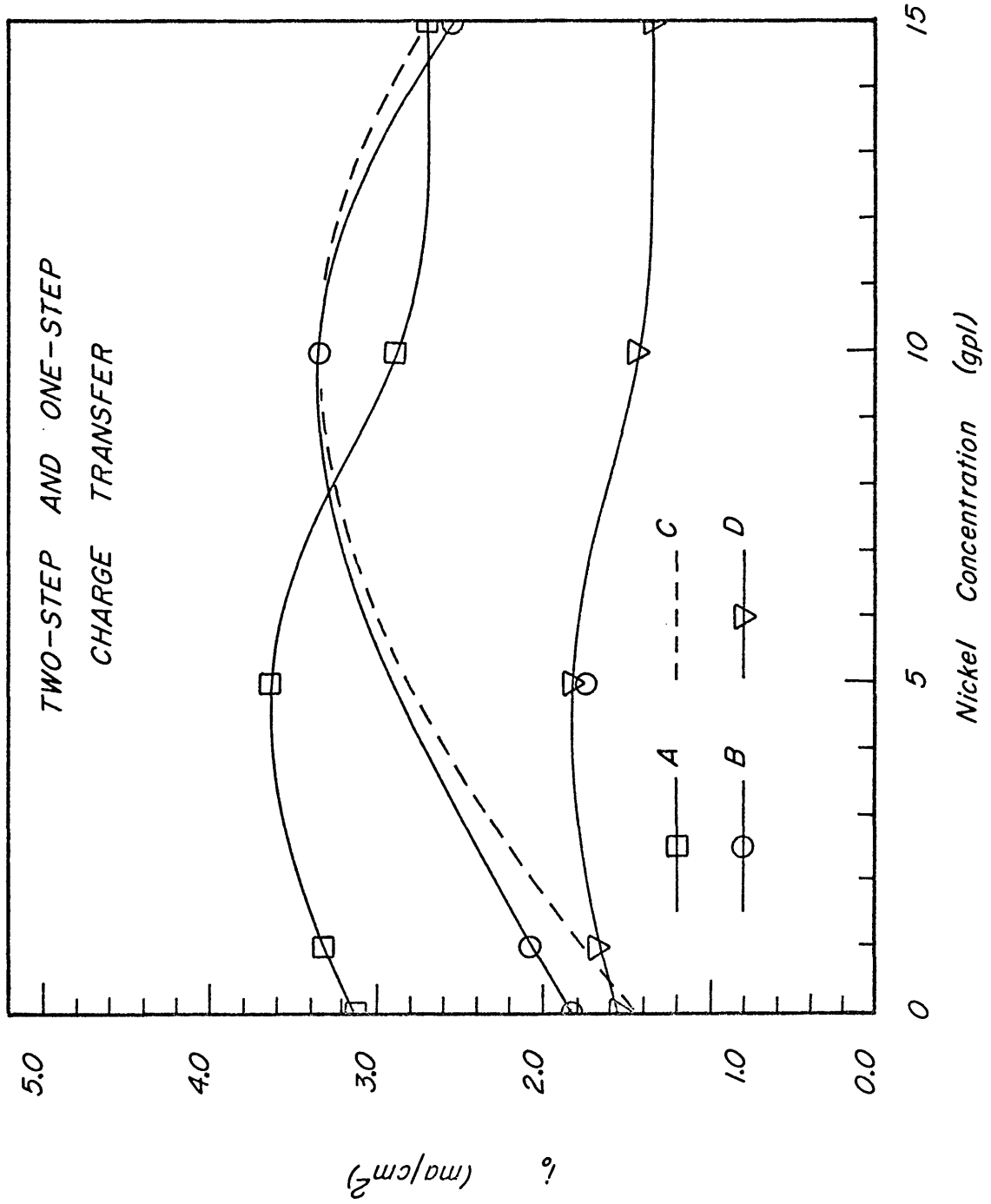
TWO-STEP AND ONE-STEP
CHARGE TRANSFER
A
B
C
D
5.0
4.0
3.0
2.0
1.0
0.0
0
5
10
15
Nickel Concentration (gpl)
i. (ma/cm²)

FIGURE 32

assumed to be occuring (and as mentioned this is indeed the case) then the values of the theoretical exchange current densities will be exactly one-half of the values tabulated for a one-step charge-transfer.

Curve D in Figure 31, then shows the plotted values for a two-step charge-transfer reaction. This curve shows that the theoretical values for the exchange current density are in good agreement with the experimental values for nickel concentrations of 0, 1, 5 and 15 gpl. However, for a nickel concentration of 10 gpl the theoretical and experimental values differ greatly. Therefore another curve, Curve C, was plotted through all of the theoretical values for a two-step charge-transfer for the nickel concentrations of 0, 1, 5 and 15 gpl, and through the theoretical value considering a one-step charge-transfer for a nickel concentration of 10 gpl. It can now be seen that Curve C is in close agreement with the experimental curve.

The same procedures were carried out in plotting the four curves shown in Figure 32, except in this case the copper concentration was 30 gpl. Again the same type of behavior is obtained. It therefore seems, that there is a situation in which a change takes place from a two-step mechanism at lower nickel concentrations (0 to 5 gpl nickel) to a one-step mechanism at a higher nickel concentration (10 gpl nickel) and then again another change to a two-step mechanism at even higher nickel concentrations (15 gpl nickel). This change is not a sudden one but is gradual.

This behavior along with the fact that the exchange current density increases with the nickel concentration can not be explained by any present single theory. To explain these facts several pieces of various

other theories must be employed. These theories are outlines in the following sections.

Hydrogen Evolution Reaction

For several years there was a considerable amount of controversy concerning the kinetics of the reaction occuring during the evolution of hydrogen at a cathode. In 1931 R. W. Gurney (Gurney, 1931) published a paper concerned with the problem. His theory helped to explain several factors that were in doubt concerning the hydrogen evolution reaction (h.e.r.). However, there were still some experimental facts which his theory could not explain. For this reason his work went largely neglected for several years although several people were aware of it and two tried to improve upon it (Butler, 1936) and (Gerischer, 1960).

The most notable addition to Gurney's original theory however, has come in recent years and is by Bockris and Matthews (Bockris and Matthews, 1966) and (Bockris and Conway, 1971). In their original paper Bockris and Matthews give a detailed theoretical investigation of the charge-transfer reaction occuring at the electrode during the h.e.r. They considered three aspects of the problem: 1) classical electron transfer, 2) quantum mechanical electron transfer, and 3) classical proton transfer.

Theory of Bockris and Matthews

For reasons of brevity only a general outline of the procedure and results of the work of Bockris and Matthews will be given here.

Bockris and Matthews consider a system in which cations such as the H_3O^+ ions are adsorbed in a hydrated state on the surface of the electrode. This same surface is also covered with adsorbed water dipoles which when the surface potential is negative to the potential of zero charge (p.z.c.) are oriented with their positive end toward the electrode. This was previously shown in Figure 30.

Bockris and Matthews first consider the case of classical electron transfer. They constructed a potential energy - distance profile for electron transfer from a metal electrode to the proton in solution. They found that the energy of transfer depended on several factors (they actually considered only the change in enthalpy and not the change in free energy). These factors are: 1) R, the repulsive force between the hydrogen atom and the water molecule, 2) A, the attractive force between the metal and the hydrogen atom, 3) J, the ionization potential of the atom, 4) L_o, the solvation energy of the ion, and 5) Φ, the electronic work function of the metal. Their findings were that the energy barrier, ${}_o\Delta H_o(e)$, for the electron transfer from the Fermi level of the metal electrode to the electron level of the proton (when the system is in its ground state) was as follows:

$$ {}_o\Delta H_o(e) = R - A - J - L_o + \Phi \qquad (8) $$

The next step they took was to consider the case of classical proton transfer. The same energy profile as was used in the electron transfer is used. In this case they considered that neutralization of the proton may occur by electron tunneling from the Fermi level of the metal

to the proton. Their conclusions were that charge-transfer does occur by the process of electron tunneling between particles in the solution and the metal. The rate of this tunneling is dependent upon the amount of displacement of the ion-solvent sheath. This enables empty electron energy levels in the ion-solvent sheath to become equal in energy to full energy levels in the metal.

The final step in the analysis of Bockris and Matthews was to consider the combination of classical proton transfer and electron tunneling. This case is shown in Figure 33. Curve A shows the variation in energy with internuclear distance of the system $e^-(M)$-H^+-OH_2 and Curve B the variation in energy with internuclear distance of the system M-H-OH_2. Where $e^-(M)$ is the electron in the metal, H^+-OH_2 is the H_3O^+ ion, M is the metal and H-OH_2 is the hydrogen-water combination.

The point at which the curves cross, X, is the point at which the condition of electron tunneling is most likely to take place since at this point $\Delta H_0(e)$ is zero. This point should correspond to the electron in the Fermi level of the metal since at this level there is the lowest activation energy.

Point X can be shifted by one or a combination of two methods: 1) by activating the electron, and/or 2) by activating the H^+-OH_2 bond. Either method of activation will result in point X being shifted to a lower potential energy. So, if either or both methods of activation are used there is the possibility of lowering the amount of energy required for the electron transfer, and thus the rate of the reaction increases.

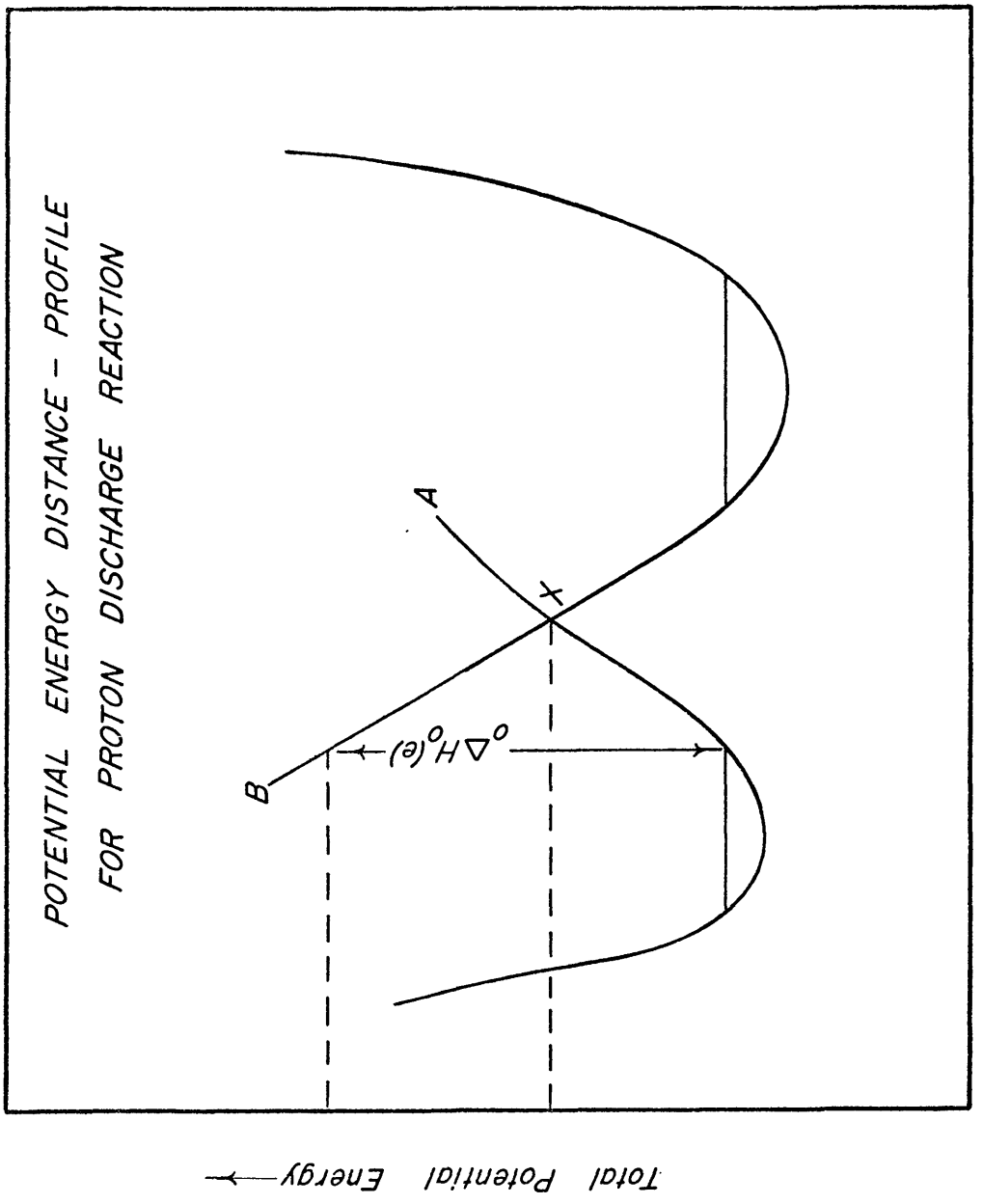
POTENTIAL ENERGY DISTANCE - PROFILE
FOR PROTON DISCHARGE REACTION
A
B
$\Delta H^o_{(e)}$
Total Potential Energy
Internuclear Distance

Figure 33

Bockris and Matthews concluded that for the h.e.r. the rate controlling process was the stretching of the H^+-OH_2 bond. They also concluded that the theory may be generally applied to other electrode reactions such as metal deposition and redox reactions.

In order to properly set forth a theory which may explain the experimental behavior, the theory of Bockris and Matthews must be combined with two other areas of pertinent information: 1) the electronic work function, and 2) the hydration of the copper and nickel ions.

The Electronic Work Function

A small amount of work on the electronic work function in relation to electrode reactions has been done. In 1947 Bockris (Bockris, 1947) published a short article concerned with the hydrogen overpotential and the thermionic work function. In this paper he states that since the work function is a measure of the electron affinity of a metal then it must also be a measure of the tendency of the metal to take an electron away from the hydrogen atom and bind this electron to itself. Thus the ability of a metal to adsorb atomic hydrogen should be proportional to its work function.

Conway and Bockris (Conway and Bockris, 1957) published a paper in 1957 concerned with the kinetics of hydrogen evolution and its relation to the electronic and adsorptive properties of the metal. They found a direct correlation between the electronic work function of a metal and the corresponding value for the exchange current density for that metal. They found that for the metals Mo, W, Fe, Ni, Cu, Au, Ag, Pd and Rh as the electronic work function increased the exchange current

density also increased. They were able to derive a linear relationship for this observation.

Kittel reports (Kittel, 1962) that in the case of tungsten the electronic work function is lowered when positive ions are adsorbed on its surface. He attributes this to the formation of an electric double layer (dipole layer) at the surface of the tungsten due to the attracting force that the positive ions exert on the conduction electrons of the tungsten metal.

Gurney's original theory predicted that an increase in the work function would decrease the current density at any given potential. If the inverse were also true then the current density at any given potential would increase as the work function decreased. It is also proposed in Gurney's theory that the work function may enter indirectly in the hydrogen evolution reaction by influencing the heat of adsorption of hydrogen on the metal.

The Hydration Of Copper and Nickel Ions

As J. O'M. Bockris states in his book on electrocrystallization (Bockris and Razumney, 1967), "the knowledge of the hydration sheath that surrounds the metal ion in solution is not one of the strongest points in electrochemistry". He considers the hydrated ion to be surrounded by a primary hydration sheath. This sheath is in turn surrounded by another sheath called the secondary hydration sheath. An ion during deposition will retain part of its hydration sheath if during this time it retains part of its ionic character. So, the adsorbed anion will have some of its hydration sheath associated with it.

During the charge-transfer process the ion has to displace part of its hydration sheath. How much displacement must occur will depend upon the type of site at which the charge-transfer process takes place.

The energy of hydration of both copper and nickel is not an easily measured quantity. Indeed there is no data available which would enable either energy to be known with a small amount of uncertainty. However, certain concepts and data can be useful in ascertaining which ion has the strongest affinity for water dipoles.

According to Gold (Gold, 1954) the heat of hydration at 25 °C and relative to hydrogen for copper and nickel are 19.45 kcal and 18.1 kcal respectively. He gives the free energy of solvation (in aqueous solution) for copper as 23.77 kcal and under the same conditions no free energy values for nickel are given.

Basolo and Pearson (Basolo and Pearson, 1967) give several pieces of data which are useful in leading to a conclusion concerning the hydration of copper and nickel. For instance, they give values for the hydration of gaseous ions of copper and nickel which both have a value of -507 kcal. They also state that the water and amine complexes for nickel and copper have bond strengths that are comparable. They then give the heat of solvation for both copper and nickel in a hexamine complex as both being - 410 kcal.

They also state that the heat of hydration varies inversely with the ionic radius. Therefore, copper with a smaller ionic radius should have a higher heat of hydration than nickel. However, this can be disputed since there is a great deal of uncertainty about the ionic radius for both copper and nickel. Basolo and Pearson give ionic radii for

copper and nickel as 0.72 A° and 0.78 A° respectively. Weast (Weast, 1968) gives the respective values of 0.72 A° and 0.69A° for copper and nickel. Lange (Lange, 1961) gives still different values of 0.70 A° for copper and from 0.69 A° to 0.78 A° for nickel. From this consideration it then seems probable that both ions would have approximately the same heat of hydration.

Basolo and Pearson also give the reactivity order of certain metal complexes which indicate that the nickel complexes are generally more stable than the corresponding copper complexes. These nickel complexes also have a higher heat of activation than the copper complexes. They also show that the rate constants for the exchange of water molecules from the first coordination sphere of copper is 3×10^5 times faster than for nickel. The energy of activation for this reaction is 12.2 kcal for nickel and 5.6 kcal for copper. This implies that the nickel complex with water is much stronger than the same complex for copper. This information leads to a reaction order that puts nickel as being more stable than copper.

Proposed Theory

Consideration of all the afore mentioned facts will result in a theory which can be used to explain the experimental results. From the work of Gurney, and Bockris and Matthews it is now evident that the rate of the metal deposition process can be increased by lowering the total amount of energy that is needed to complete the reaction and allow a transfer of charge to take place. This can be accomplished by either or a combination of two ways. First, the electron can be activated by

lowering the amount of energy required to remove an electron from the metal electrode and make it available to an ion. This can be achieved through the reduction of the electronic work function. This in turn is achieved through the presence of nickel ions. In a manner similar to the reduction of the electronic work function of tungsten when positive ions are adsorbed on its surface, the presence of nickel which is adsorbed on the electrode surface could lower the electronic work function. This would in turn lower the energy barrier as can be seen from Equation 8.

The second method of activation would be stretching of the $Cu-H_2O$ bond. This could be achieved again through the presence of nickel. Nickel with its higher affinity for water dipoles could aid in stretching this bond and thus lower the amount of energy required for the charge-transfer. Both of these factors may work together to actually lower the energy barrier and thus enable the charge-transfer to proceed at a much higher rate than in the absence of nickel. This would explain why the presence of nickel tends to increase the exchange current density which is a measure of the rate of charge-transfer.

Secondly it is proposed by this author that the nickel ions can actually act as a barrier to the incoming copper ions. Since the nickel ions are attracted to the cathode in the same manner as the copper ions it is probable that they build up in the diffuse layer. This building up of the nickel ions would increase with an increase in nickel concentration up to some point. At this point the build up would reach a "steady state" concentration.

In this manner the nickel ions act as a sieve limiting the mobility of the copper ions. This barrier of nickel ions could not stop the progress of the copper ions (since the flow of copper ions is a necessary condition for the flow of current) but could make it more difficult for the copper ions to reach the region of the compact double-layer.

This factor can now be used to explain why the exchange current density decreases after a certain nickel concentration is reached. The situation is shown in Figure 34. Curve A shows how the energy required for the charge-transfer decreases with an increase in the nickel concentration while at the same time the barrier effect of nickel increases with an increase in nickel as shown by Curve B. The resultant curve upon adding these two curves is Curve C. This curve can be seen to have the same general shape as the experimental curves for the exchange current density as a function of the nickel concentration.

It is possible that since the energy for the charge-transfer is becoming less with an increase in the nickel concentration faster than the barrier effect is occuring that this lowering of the energy is sufficient to allow the charge-transfer to proceed by a one-step process at a point near the maximum in the energy effect curve. This is noted by the region D in Figure 34. In the regions E and F there is less probability that this may be happening. This is because in the region E the lowering of the energy required for the one-step process is not yet sufficient to enable it to take place with a sufficient magnitude that is detectable experimentally. Whereas,in the region F although the lowering of the energy would be sufficient by itself, it is now insufficient since the barrier effect is now much stronger. This explains why there

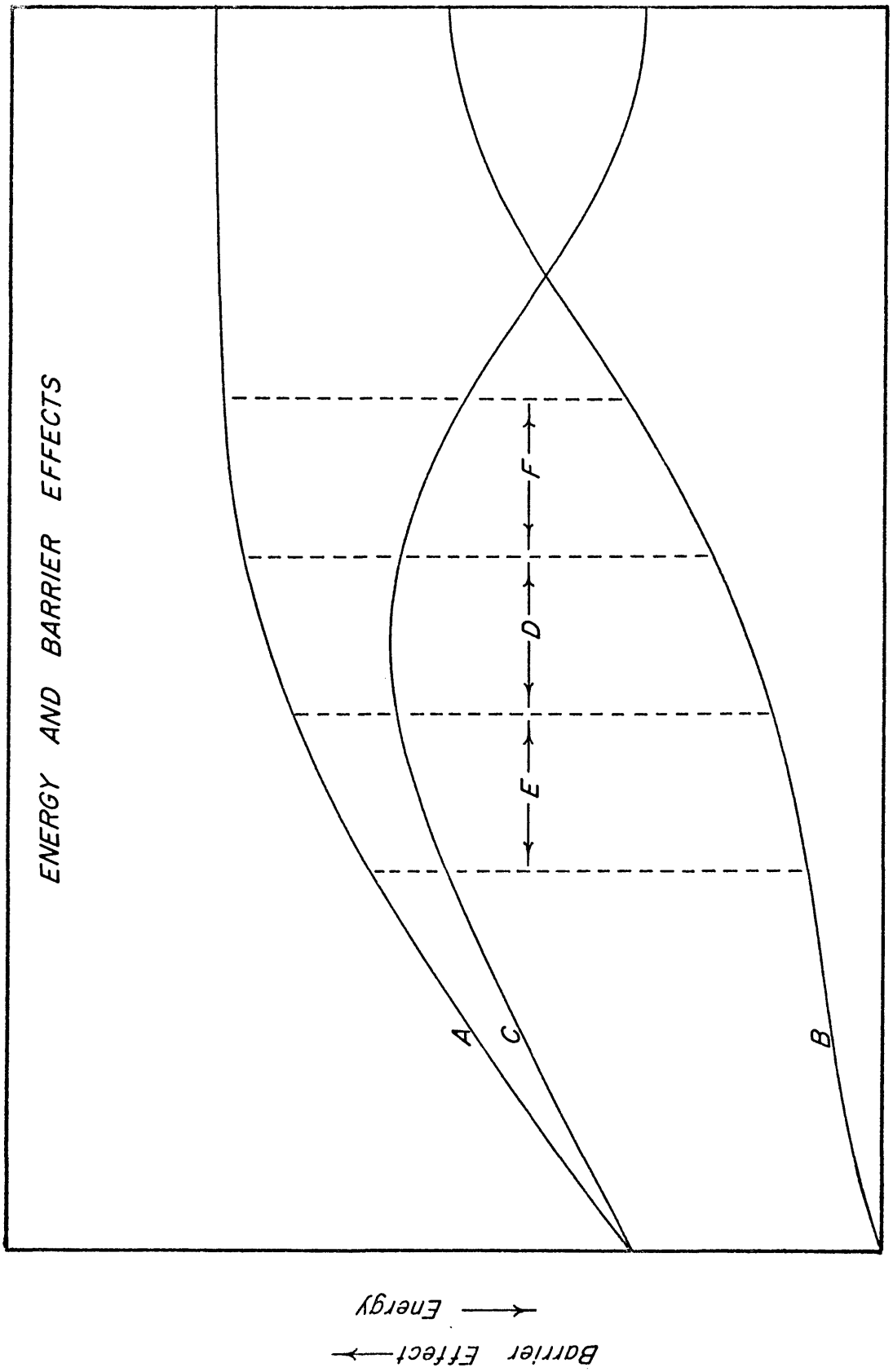
ENERGY AND BARRIER EFFECTS
F
D
E
A
C
B
Nickel Concentration
Barrier Effect
Energy

Figure 34

seems to be a gradual change from a two-step charge-transfer to a one-step charge-transfer and then again to a two-step charge-transfer as was shown in Figures 31 and 32.

Effects of Temperature

Although there was very little work done on the effects of temperature the results of what was done was shown in Figure 27. These curves show an interesting trend. For nickel concentrations of 5 and 15 gpl the exchange current density increases with an increase in the temperature. However, for a nickel concentration of 10 gpl the exchange current density goes down with an increase in temperature.

The data for the temperature of 40 °C in Figure 27 can be replotted to produce the bottom curve in Figure 35. In this figure the exchange current density at 40 °C is plotted against the nickel concentration. This curve shows the same trend as was shown in Figure 27- a decrease in the exchange current density at a nickel concentration of 10 gpl. The top curve in this figure was obtained by plotting one-half of the theoretical exchange current density as was listed in Table 9 as "Theo. i_0". Again the value of one-half of this theoretical exchange current density would correspond to a two-step charge-transfer reaction.

As can be seen in Figure 34 the values of the experimental exchange current density an one-half of the theoretical exchange current density agree very well at the nickel concentrations of 5 and 15 gpl. But at a nickel concentration of 10 gpl there is a large difference between the two values.

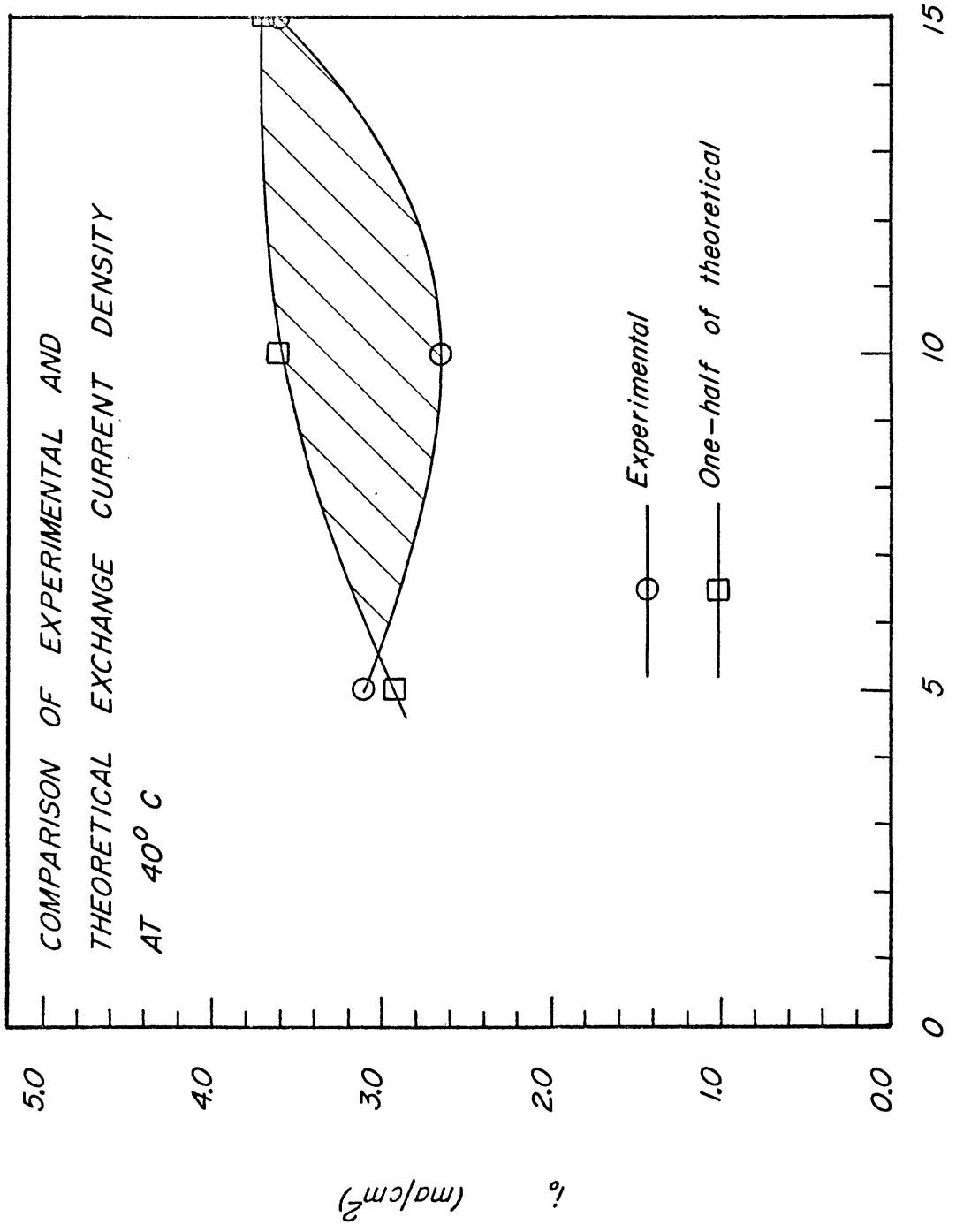
COMPARISON OF EXPERIMENTAL AND
THEORETICAL EXCHANGE CURRENT DENSITY
AT 40° C
Experimental
One-half of theoretical
i₀ (ma/cm²)
5.0
4.0
3.0
2.0
1.0
0.0
0
5
10
15
Nickel Concentration (gpl)

Figure 35

Although there is not enough experimental data to make any definite conclusions the curves in Figure 35 seem to indicate that there is a region between the nickel concentrations of 5 and 15 gpl in which the charge-transfer reaction changes from a two-step mechanism to a mixed mechanism and then back to a two-step mechanism in much the same way as shown before. However, there is an important difference. At the higher temperature , unlike at the temperature of 25 °C, it is not possible to say that the mechanism changes to a one-step charge-transfer process between 5 and 15 gpl nickel. Instead it must be stated that it changes to a "mixed mechanism". The reason being that the one-step theoretical exchange current density value for a nickel concentration of 10 gpl is much greater than the experimental value (7.24 ma/cm^2 as opposed to 2.66 ma/cm^2).

Comparison of these two values rules out the possibility of a one-step charge-transfer but comparison of experimental and one-half of the theoretical also seems to rule out the possibility of a two-step charge-transfer. So, at this nickel concentration (10 gpl) there might posibly be a mixture of the two mechanisms or there might possibly be another mechanism entering the picture.

Empirical Results

Current Efficiency

It should be expected that the presence of small amounts of nickelous ion in solution would have very little if any effect on the current efficiency. The current efficiency as calculated was a measure of the amount of copper being reduced per unit time. The experiments were conducted under a condition of constant current which meant that the rate of copper reduction had to proceed at a given rate. Since nickel is not reduced under the experimental conditions the only other reaction capable of occuring at the cathode and therefore capable of reducing the current efficiency was the reduction of hydrogen. However, the amount was quite small owing to the excellent stirring conditions that were present. This greatly reduced any concentration polarization effects which would in turn have lowered the current efficiency by limiting the amount of copper ions available for reduction at the cathode. If any significant concentration effects were present the impressing of a constant current would have required the potential to increase to such a point that the reduction of hydrogen would have proceeded at a much greater rate. This would then have lowered the current efficiency.

Morphology of the Deposit

It was shown in the results that an increase in the current density and an increase in the nickel concentration both had the same effect of producing a less satisfactory deposit. It has been known for years that

an increase in the current density produced deposits which were rougher and less coherent than deposits made in the same solution at lower current densities. No universely accepted reason for this behavior is available. However, it is thought that with the increased current density the ions are reaching the electrode at a much faster rate and with a higher energy. They are therefore able to form more sites of nucleation. These nucleation sites are not the same sites the ions would have chosen had they been able to reach the electrode under more favorable conditions. With the rapid rate of nucleation the activity of the surface changes. This change produces a deposit which is not as good as it would be under conditions of a lower current density.

With the presence of nickel a similar process is occuring. The depositing ions because of the lowering of the amount of energy required for charge-transfer are able to reach the electrode surface with a much higher energy than in the absence of nickel. This has the same effect as increasing the current density. The activity of the deposited surface is such that a gradually worsening deposit is obtained.

Cell Voltage

Figure 36 shows a curve representing the cell voltage. This curve is very similar to those obtained experimentally. The shape of this curve is easily explained by looking at two factors that influence the cell voltage. The cell voltage is composed of two main parts: 1) the IR drop between the two electrodes due to the resistance of the electrolyte, and 2) the polarization phenomena occuring at the electrode surfaces. Figure 36 shows IR drop of an electrolyte plotted as a

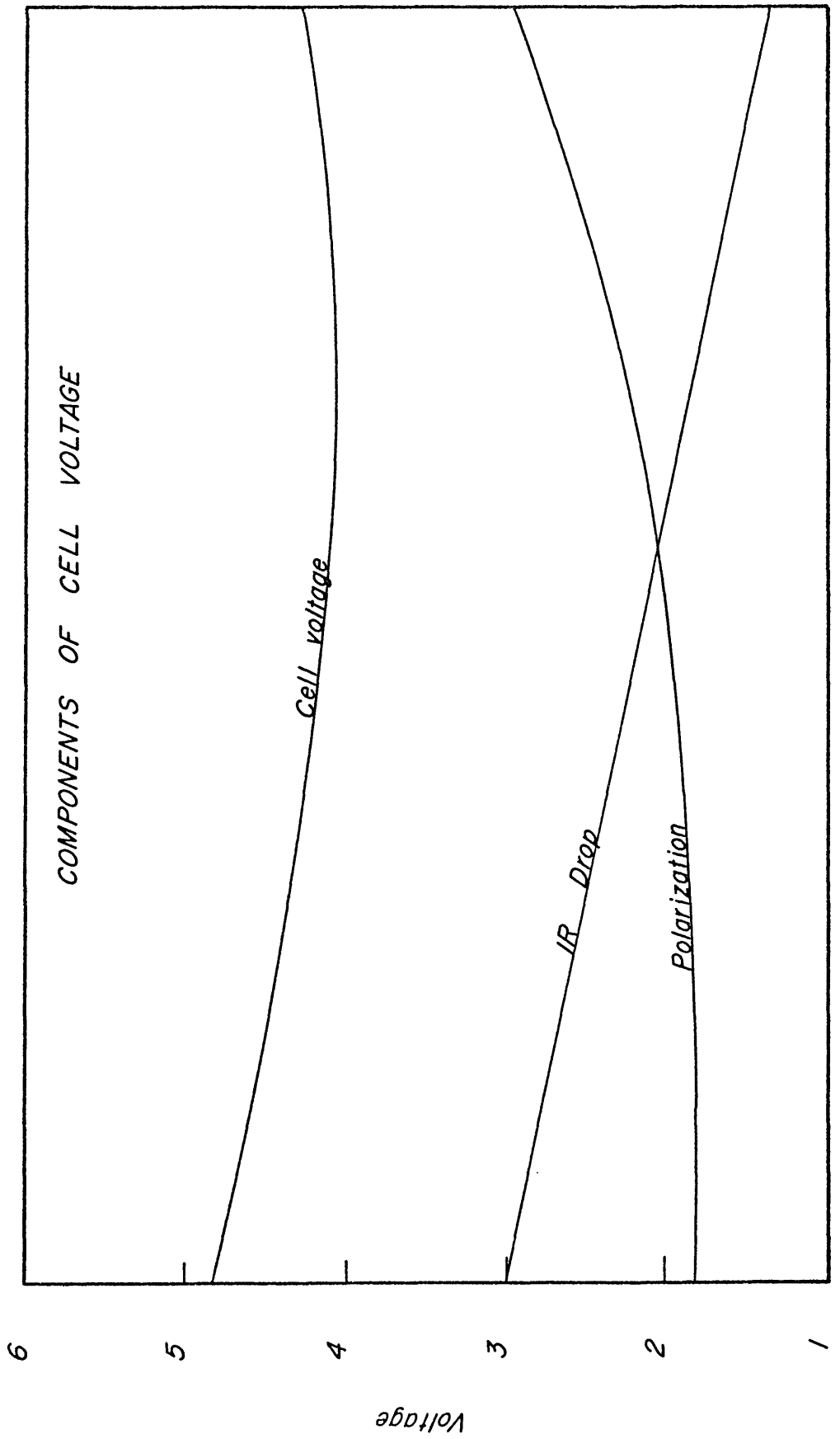
COMPONENTS OF CELL VOLTAGE
Cell voltage
IR Drop
Polarization
Copper (gpl)
Voltage
6
5
4
3
2
1

Figure 36

function of the copper concentration. The same is done for the polarization potential. When these two curves are added they result in the top curve which represents the cell voltage. (The scale on the voltage axis is there only to serve as a general indication of the relative magnitudes of the three curves. They are not absolute values.)

These same results were found by Fink and Phillippi (Fink and Phillippi, 1926) during their study of voltages in copper refining cells. Rouse and Aubel (Rouse and Aubel, 1927) also found this to be the case in their more comprehensive study of the cell voltages in copper refining.

The IR drop is linear with respect to the copper concentration. This has been shown to be true by many investigators, (Rouse and Aubel, 1927), (Skowronski and Reinoso, 1927), (Kern and Chang, 1922) and (Fink and Phillippi, 1926). Rouse and Aubel (Rouse and Aubel, 1927) demonstrated that the polarization curve assumes a shape similar to that shown in Figure 36.

Figure 17 indicated that the cell voltage decreased with a decrease in current density. This is due to a lower IR drop at the lower current densities. This is not the only factor however, that lowers the voltage. If it were,then the curves in Figure 17 should be equally spaced since they are all separated by equal amounts of current density. This indicates that the polarization effect becomes less at the lower current densities. This has also been shown to be true many times: e.g. (Edwards and Wall, 1966), (Bockris and Kita, 1962), (Mattsson and Bockris, 1959), (Sheir and Smith, 1952), and (Hunt, Chittum and Ritchey, 1938). It was also shown by the polarization experiments in

this investigation.

Rouse and Aubel (Rouse and Aubel, 1927) reported that nickel had an effect of reducing the polarization voltages in copper refining cells. This fact along with the fact that nickel increases the resistance of the electrolyte in the same way as copper (Kern and Chang, 1926) and (Skowronski and Reinoso, 1927) explains the shape of the curves in Figures 18, 19 and 20. The curves in Figure 18 show that the cell voltage with an electrolyte having no nickel is lower than with an electrolyte with 1 to 15 gpl nickel. This indicates that the polarization effect is not sufficient to overcome the effect of an increase in electrolyte resistance.

At 37.0 asf, Figure 19 shows a somewhat different result. For a nickel concentration of 1 gpl the depolarization effect of the nickel is greater than the effect of an increase in the electrolyte resistance so the cell voltage is lowered. However, for nickel concentrations of 5 and 15 gpl the increase in the electrolyte resistance is larger than the decrease in voltage due to the depolarization effect. In the case of a current density of 56.1 asf the situation is such that the decrease in the cell voltage due to the depolarization effect is sufficient at all nickel concentrations to overcome the increase in cell voltage due to the increase in resistance of the electrolyte.

So, it can be seen that at the higher current densities although the absolute amount of IR drop and polarization is greater than for a lower current density, the relative change is such that the depolarization effect of the nickel is gradually increasing to such a point that it is sufficient to overcome the effect of an increase in the electrolyte

resistance. The reason for this phenomena is the increased concentration of nickel ions in the diffuse layer with an increase in the current density.

Cell Voltage as a Function of Current Density

Figure 21 shows how the cell voltage changed with the current density. The curves in this figure are only another way of expressing the data shown in Figures 17 to 20. The same explanation will be true for the curves in this figure as for the curves in Figures 17 to 20.

One important point should be brought out. In Figure 21 the curves for 0 gpl nickel and 40 gpl copper and for 0 gpl nickel and 20-30 gpl copper show a non-linear relationship. If further data is added to these curves to give points at higher current densities then the curves seem to be more linear. This is shown in Figure 37. The points in this curve for 40 gpl copper could lie on a curve that would resemble that given in Figure 21. However, this is not really important. The important point is to compare Figure 37 to Figure 38, which shows a plot of the IR drop as a function of the current density for the same system as in Figure 37. Figure 38 shows a similar relationship between the two curves as is shown in Figure 37.

Polarization phenomena other than the IR drop are taking place at the electrode. These other polarization potentials would change the shape and position of the curves given in Figure 38 so that they would more closely resemble those in Figure 37.

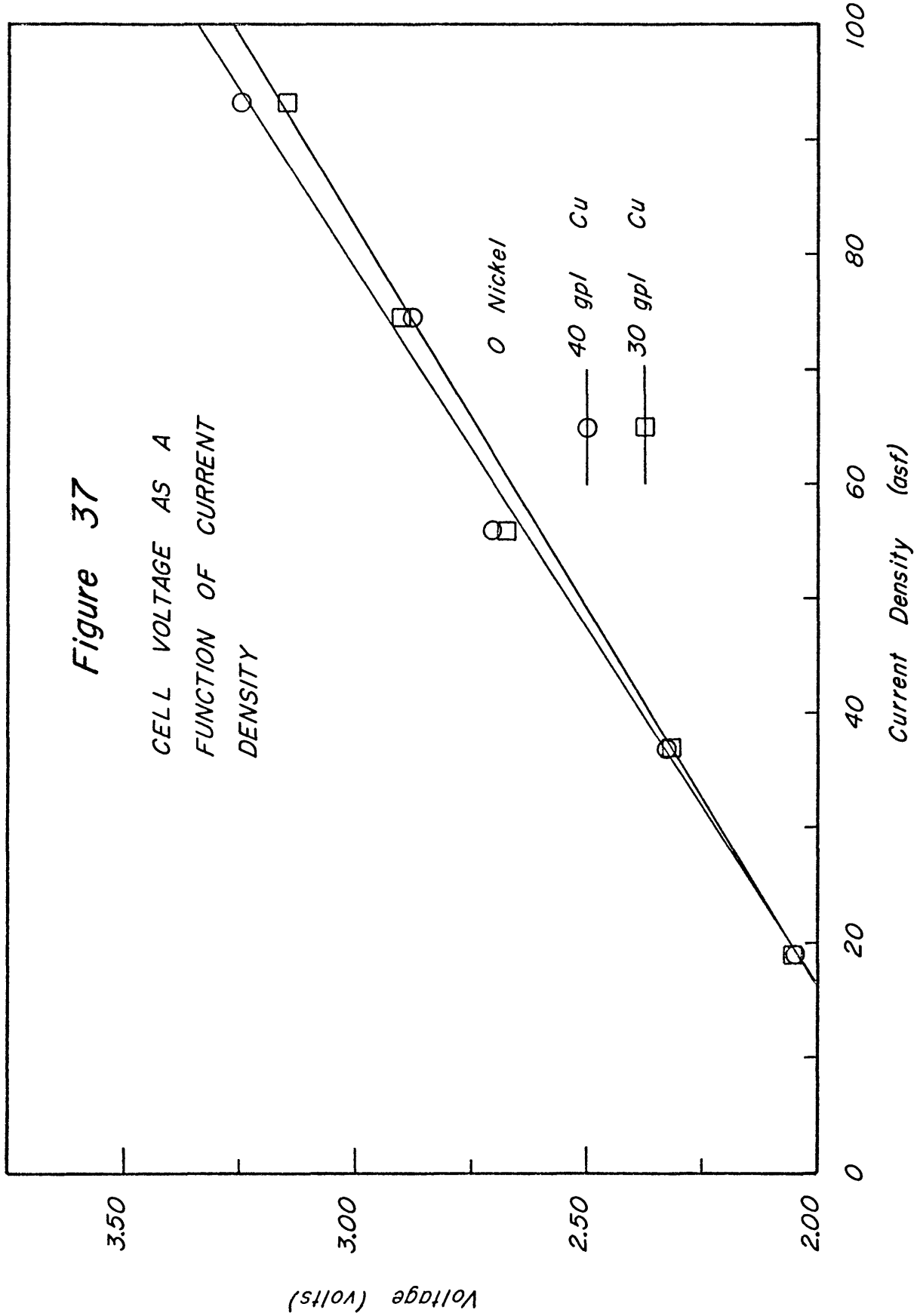
Figure 37
CELL VOLTAGE AS A FUNCTION OF CURRENT DENSITY
O Nickel
40 gpl Cu
30 gpl Cu
Voltage (volts)
3.50
3.00
2.50
2.00
0
20
40
60
80
100
Current Density (asf)

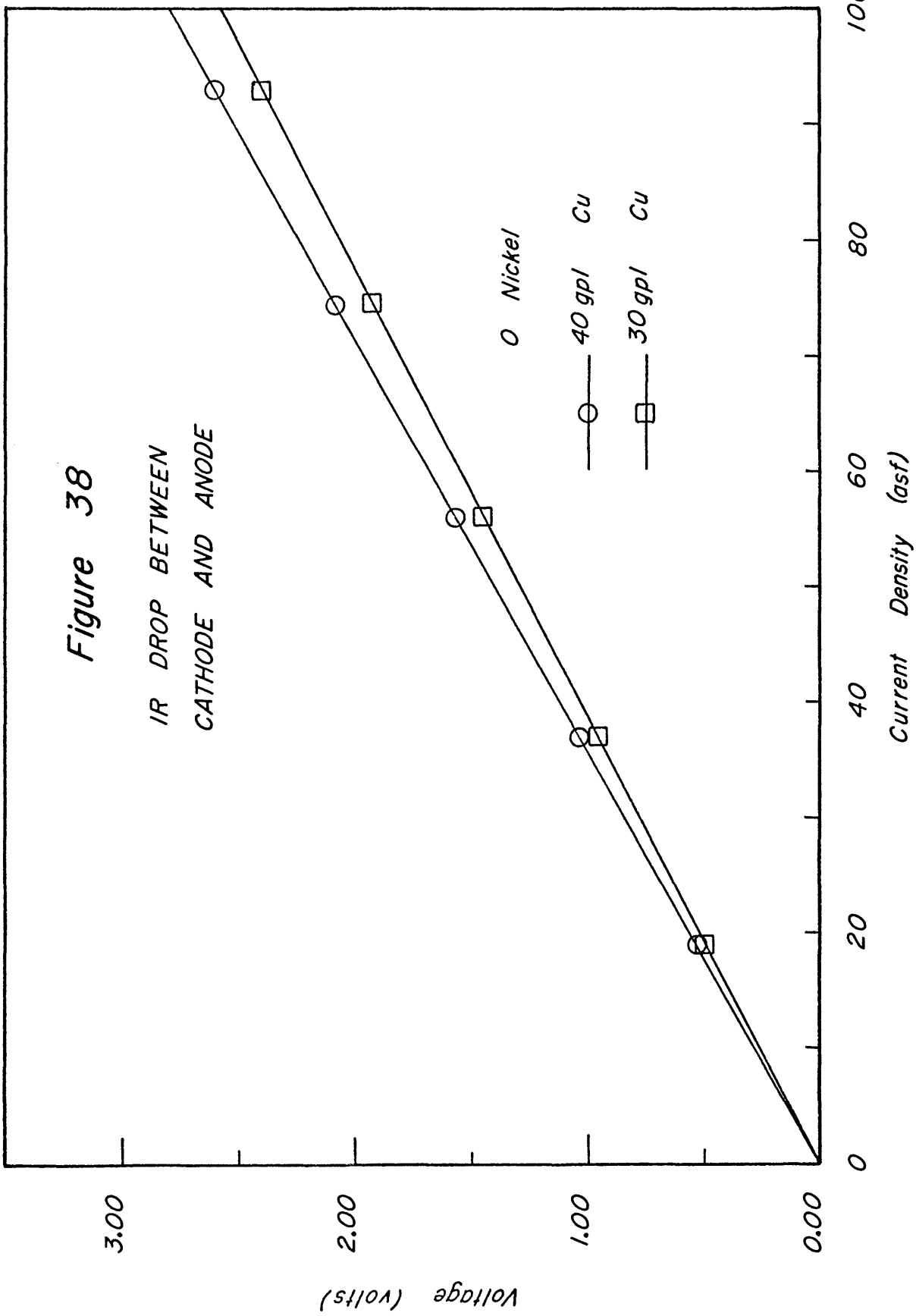
Figure 38
IR DROP BETWEEN
CATHODE AND ANODE
O Nickel
40 gpl Cu
30 gpl Cu
Voltage (volts)
3.00
2.00
1.00
0.00
0
20
40
60
80
100
Current Density (asf)

CONCLUSIONS

The results of the empirical experiments show that nickel does have an important effect on the cell voltage and morphology of the deposit. It does not effect the current efficiency of the deposition process nor the purity of the deposit. The effect on the cell voltage is small at the low current density of 19.1 amps/ft^2. At a current density of 37.0 amps/ft^2 there is a larger effect. A nickel concentration of 1 gram per liter lowered the cell voltage over what the cell voltage was with no nickel present. Nickel concentrations of 5 and 15 grams per liter raised the cell voltage over the no nickel values. At a current density of 56.1 amps/ft^2 the nickel lowered the cell voltage at all nickel concentrations. A concentration of 1 gram per liter nickel had the greatest effect on the lowering of the cell voltage at 56.1 amps.ft^2. The raising and lowering of the cell voltage is explained on the basis of an increase in the resistance of the electrolyte while at the same time the nickel acts as a depolarizing agent. At all current densities the nickel tended to stabilize the cell voltage at a value that was independent of the copper concentration.

Nickel affected the morphology of the deposit and gave less satisfactory deposits at higher nickel concentrations. This effect was greater at higher current densities. At the low current density of 19.1 amps/ft^2 the nickel concentration had very little effect on the morphology of the deposit. At the higher current densities of 37.0 and 56.1 amps/ft^2 the copper concentration was critical when the nickel

concentrations were high. Acceptable deposits at 37.0 amps/ft^2 could only be made when the copper concentration was carefully controlled. At 56.1 amps/ft^2 the quality of the deposit was very dependent on the nickel and copper concentrations.

The two methods for describing the system and resulting deposit, the Reference Number, R, and the Surface Index, Q, gave results which were very satisfactory. Correlation between R and Q were good. It should be possible to predict the type of deposit that would be obtained under any specified experimental coditions.

The kinetic studies indicated that the presence of nickelous ion had a very definite effect on the exchange current density. The results on the exchange current densities indicated that the presence of nickel had a very definite effect on the type of mechanism that the charge-transfer process followed. It was shown that the charge-transfer process is by a two-step mechanism at low nickel concentrations of 0 to 5 grams per liter. At higher nickel concentrations of approximately 10 grams per liter the charge-transfer process reverted to a one-step mechanism. Further additions of nickel resulted in still another change in the mechanism- back to a two-step mechanism.

A theory was proposed to explain the effects of nickel on the morphology and type of mechanism of the charge-transfer process. This theory stated that the effect of nickel was two-fold: 1) the first effect is to lower the amount of energy required for the charge-transfer process and thus enabling the process to occur by a one-step mechanism. This lowering of the energy is produced by either or a combination of the stretching of the copper-water bond or the lowering of the work

function of the metal electrode, by the presence of nickel ions; 2) the second effect is that of the nickel ions producing a barrier that the copper ions must pass in order to reach the electrode surface. The sum of these two effects was used to explain the experimental results of both the polarization and empirical experiments.

BIBLIOGRAPHY

Agar, J.N.,and Bowden, F.P., The kinetics of electrode reactions, I andII: Proc. of the Roy. Soc. of London, v.A169, p. 206-219 (1938-39).

Barnartt, S., Magnitude of IR-drop corrections in electrode polarization measurements made with a Luggin-Haber capillary: Jour. of the Electrochem. Soc., v. 108, p. 102-104 (1961).

Barnartt, S., Primary current distribution around capillary tips used in the measurement of electrolytic polarization: Jour. of the Electrochem. Soc., v. 99, p. 549-553 (1952).

Basolo, F. and Pearson, R.G., Mechanisms of inorganic reactions-a study of metal complexes in solution: John Wiley and Sons, Inc., New York, N.Y. (1967).

Bauer, H.H., The electrochemical transfer-coefficient: Electroanalytical Chem. and Interfac. Electrochem., v. 16, p. 419-432 (1968).

Bockris, J. O'M., and Kita, H., The dependence of charge transfer and surface diffusion rates on the structure and stability of an electrode surface: Jour. Electrochem. Soc., v. 109, p. 928-939 (1962).

Bockris, J. O'M., and Razumney, G.A., Fundamental aspects of electrocrystallization: Plenum Press, New York, N.Y. (1967).

Bockris, J. O'M., Hydrogen overpotential and the thermionic work function: Nature, v. 159, p. 539-540 (1947).

Bockris, J. O'M., and Potter, E.C., The mechanism of the cathode hydrogen evolution reaction: Jour. Electrochem. Soc., v. 99, p. 556-557 (1952).

Bockris, J. O'M., and Matthews, D.B., The mechanism of charge transfer at electrodes: Proc. Roy. Soc. of London, v. A292, p. 479-488 (1966).

Bockris, J. O'M., and Conway, B.E., Modern aspects of electrochemistry, v. 6: Plenum Press, New York, N.Y. (1966).

Bockris, J. O'M., and Devanathan, M.A.V., and Muller, K., On the structure of charged interfaces: Proc. Roy. Soc. of London, v. A274, p. 55-79 (1963).

Bowden, F.P., and Agar, J.N., Ann. Rep. Progr. Chem., v. 35, p. 90, (1938).

Butler, J.A.V., Proc. Roy. Soc. of London, v.A157, p. 423, (1936).

Conway, B.E., and Bockris, J. O'M., Electrolytic hydrogen evolution kinetics and its relation to the electronic and adsorptive properties of the metal: Jour. Chem. Phys., v. 26, p. 532-541 (1957).

Conway, B.E., and Bockris, J. O'M., The mechanism of electrolytic metal deposition: Proc. Roy. Soc. of London, v. A248, p. 394-403 (1958).

Delahay, P., and Tobias, C.W., Advances in electrochemistry and electrochemical engineering: Interscience Publishers, New York, N.Y. (1963).

Edwards, J., and Wall, A.J., Energy requirements in the electrodeposition of copper: Trans. A. I. M. E., v. 88, p. 307-317 (1966).

Fink, C.G., and Phillippi, C.A., Voltage studies in copper refining cells: Trans. Electrochem. Soc., v. 50, p. 267-279 (1926).

Gauvin, W.H., and Winkler, C.A., The effect of chloride ions on copper deposition: Jour. Electrochem. Soc., v. 99, p. 71-77 (1952).

Gerischer, H., Z. Physik. Chem. (Frankfurt), v. 26, p. 223 (1960).

Gold, L.B., A table of thermodynamic functions of ionic hydration: Trans. Faraday Soc., v. 50, p. 797-799 (1954).

Graham, A.K., A study of the influence of variables on the structure of electrodeposited copper: Trans. Electrochem. Soc., v. 52, p. 157-175 (1927).

Gurney, R.W., Proc. Roy. Soc. of London, v. A125, p. 446 (1937).

Hampel, A., The encyclopedia of electrochemistry: Reinhold Publishing Corporation, New York, N.Y., p. 586-589 (1964).

Hardesty, D.W., Anion effects in copper deposition: Jour. Electrochem. Soc., v. 117, p. 168 (1970).

Hunt, H., Chittum, J.F., and Ritchey, H., Overvoltage: Trans. Electrochem. Soc., v. 73, p. 299-314 (1938).

Hunt, L.B., A study of the structure of electrodeposited metals: Jour. of Phys. Chem., v. 36, p. 1006-10021 (1932).

Hurlen, T., Kinetics of metal/metal-ion electrodes-iron, copper, zinc: Electrochimia Acta., v. 7, p. 653-668 (1962).

Ives, D.J.G., and Rawson, A.E., Copper corrosion-I. thermodynamic aspects: Jour. Electrochem. Soc., v. 109, p. 447-451 (1962).

Ives, D.J.G., and Rawson, A.E., Copper corrosion-II. Kinetic studies: Jour. Electrochem. Soc., v. 109, p. 452-457 (1962).

Ives, D.J.G., and Rawson, A.E., Copper corrosion-III. electrochemical theory of general corrosion: Jour. Electrochem. Soc., v. 109, p. 458-462 (1962).

Ives, D.J.G., and Rawson, A.E., Copper corrosion-IV. the effects of saline additions: Jour. Electrochem. Soc., v. 109, p.462 (1962).

Jenkins, L.H., and Stiegler, J.O., Electrochemical dissolution of single crystalline copper: Jour. Electrochem. Soc., v. 109, p. 467-475 (1962).

Kasper, C., The theory of the potential and the technical practice of electrodeposition: Trans. Am. Electrochem. Soc., v. 77, p. 353-359 (1940).

Kern, E.F., and Chang, M.Y., Conductivity of copper refining electrolytes: Trans. Am. Electrochem. Soc., v. 41, p. 181-200 (1922).

Landolt, D., Muller, R.H., and Tobias, C.W., Anode potentials in high rate dissolution of copper: Jour. Electrochem. Soc., v. 118, p.40-46 (1971).

Leckie, H.P., The anodic polarization behavior of copper: Jour. Electrochem. Soc., v. 117, p.1478-1483 (1970).

Lingane, J.J., Electroanalytical Chemistry: Interscience Publishers, Inc.: New York, N.Y. (1966).

Mantell, C.L., Industrial electrochemistry: McGraw-Hill Book Company, New York, N.Y., second edition (1950).

Mattsson, E., and Bockris, J.O'M., Galvanostatic studies of the kinetics of deposition and dissolution in the copper+copper sulfate system: Trans. Faraday Soc., v. 55, p. 1586-1601 (1959).

Meites, L., Polarigraphic techniques: John Wiley and Sons, Inc., New York, N.Y., second edition (1967).

Parsons, R., General equations for the kinetics of electrode processes: Trans. Faraday Soc., v. 47, p. 1332-1344 (1951).

Power, K.L., Operation of the first commercial copper liquid ion exchange and electrowinning plant, Copper metallurgy: Proc. Extr. Met. Div. Symp. on Copper, A.I.M.M.P.E., New York, N.Y. (1970).

Rawling, J.R.,and Costello, L.D., Mixing characteristics of a copper refinery tankhouse cell: A.I.M.E. Preprint No. A69-25 (1969).

Rogers, L.B., and Stehney, A.F., The electrodeposition behavior of a simple ion: United States Atomic Energy Commision Paper No. AECD-2239 (1948).

Rosenbaum, J.B., Application of electrometallurgy in processing of minerals, copper metallurgy: Proc. Extr. Met. Div. Symp. on Copper, A.I.M.M.P.E., New York, N.Y. (1970).

Rouse, E.W., and Aubel, P.K., Analysis of copper refining cell voltages: Trans. Electrochem. Soc., v. 52, p. 189-203 (1927).

Shreir, L.L., and Smith, J.W., Cathode polarization potential during electrodeposition of copper. I. Nonreproducibility in acid copper sulfate solutions:Jour. Electrochem. Soc., v. 98, p. 193-202 (1951).

Shreir, L.L., and Smith, J.W., Cathode polarization potential during electrodeposition of copper. II. Variation of the cathode polarization potentials with current density and electrolyte concentration, III. Effect of the cathode base upon the cathode polarization potential and the crystal structure of the deposit: Jour. Electrochem. Soc., v. 99, p. 64-70 and p. 450-456 (1952).

Skowronski, S.,and Reinoso, E.A., The specific resistivity of copper refining electrolytes and method of calculation: Trans. Electrochem. Soc., v. 52, p. 205-231 (1927).

Sundheim, B.R., Two remarks on the resistive contribution to overpotential: Jour. Electrochem. Soc., v. 115, p. 158-160 (1968).

Tuddenham, W.M., Lewis, D.M., and Sorenson, W.R., A study of variables affecting the quality of electrowon copper: A.I.M.E. Preprint No. A69-21 (1969).

Turner, D.R., and Johnson, G.H., The effect of some addition agents on the kinetics of copper electrodeposition from a sulfate solution: Jour. Electrochem. Soc., v. 109, p. 798 (1962).

Valeev, A.Sh., and Knlopotina, L.V., and Chugunova, L.V., Mechanism of the anodic dissolution of copper in sulfuric acid. I. Concentration changes in the electrolyte in the diffusion layer and their role in the mechanism of the process: Soviet Electrochemistry, v. 5, p. 1307-1308 (1969).

Verney, L.R., and Harper, J.E., and Vernon, P.N., Development and operation of the Chambishi Process for the roasting, leaching and electrowinning of copper: Electrometallurgy, Proc. Extr. Met. Div. Sysmp. on Electromet., A.I.M.M.P.E., New York, N.Y. (1968).

Vetter, K.J., Electrochemical kinetics-theoretical and experimental aspects: Academic Press, New York, N.Y. (1967).

Wagner, C., The role of natural convection in electrolytic processes: Jour. Electrochem. Soc., v. 95, p. 161-173 (1949).

APPENDIX A

Summary of Experimental Data

The following table(s) give a summary of the data obtained for both the empirical and the polarization experiments. Values for the empirical experiments are listed in Table 1.A. The temperature and acid concentration for the empirical experiments were held constant at 25°C and 100 gpl respectively. The stirring speed was also held constant.

Data from tests 1-40 of the empirical experiments was not used in any results or conclusions. The problems with this data are explained in Appendix G.

Table 2.A lists the data for the polarization experiments. The acid (H_2SO_4), copper and nickel concentrations are given in grams per liter. The temperature is given in degrees centigrade. The current is given in milliamps. The potential (in millivolts) is the potential that has been corrected for electrometer errors and for IR drop. The Eo value is the potential when no current was flowing through the electrode. In order to find the polarization potential the Eo value is subtracted from each listed potential value.

TABLE 1.A

EMPIRICAL DATA

Test No.	Current (amps)	Time (min)	Electrode Spacing (cm)	Weight (g)	Current Density (asf)	Coulombs	Theo. Weight (g)	Current Eff. (%)	Copper (gpl)	Nickel (gpl)	Cell Volt. (v)
1	0.093	2140.7	5.0	1.72747 1.90165	4.65	11945.05	3.93279	92.28	~40	0.00	1.86
2	0.093	890.0	5.0	0.72970 0.78490	4.65	4966.20	1.63507	92.63	41.91	0.00	1.85
3	0.185	1014.9	5.0	1.70495 1.89371	9.25	11266.39	3.70935	97.02	41.49	0.00	1.99
4	0.372	735.0	5.0	2.51504 2.85246	18.60	16405.20	5.40125	99.37	40.20	0.00	2.20
5	0.372	300.0	5.0	1.02556 1.16042	18.60	6697.12	2.20496	99.14	40.03	0.00	2.25
6	0.557	195.0	5.0	1.01276 1.13245	27.87	6522.75	2.14755	99.89	40.55	0.00	2.45
7	0.745	230.0	5.0	1.58780 1.79388	37.25	10281.00	3.38492	99.90	40.87	0.00	2.66
8	0.930	232.0	5.0	1.94134 2.14943	46.50	12948.39	4.26313	95.96	40.34	0.00	2.80

TABLE 1.A

Test No.	Current (amps)	Time (min)	Electrode Spacing (cm)	Weight (g)	Current Density (asf)	Coulombs	Theo. Weight (g)	Current Eff. (%)	Copper (gpl)	Nickel (gpl)	Cell Volt. (v)
9*	-----	------	---	-------	----	--------	-------	-----	-----	----	----
10*	-----	------	---	-------	----	--------	-------	-----	-----	----	----
11	0.093	1070.0	5.0	0.85721 0.94702	4.65	5970.60	1.96756	91.78	39.44	0.00	1.88
12	0.185	1193.0	5.0	2.01989 2.22679	9.25	13242.30	4.35989	97.40	-----	0.00	2.01
13	0.375	632.0	5.0	2.17575 2.45212	18.75	14220.00	4.68179	98.85	39.73	0.00	2.24
14	0.557	505.0	5.0	2.59388 2.93727	27.87	16892.25	5.56170	99.45	38.58	0.00	2.42
15	0.745	575.0	5.0	3.97483 4.46477	37.25	25702.50	8.46229	99.73	~40	0.00	2.59
16	0.930	259.0	5.0	2.23372 2.52520	46.50	14450.20	4.75758	100.03	~40	0.00	2.88
17	1.115	210.0	5.0	2.16910 2.45083	55.75	14049.00	4.62549	99.88	~40	0.00	3.08
18	1.300	127.0	5.0	1.52319 1.73305	65.00	9906.00	3.26145	99.84	~40	0.00	3.26

*Tests numbers 9 and 10 were not run.

TABLE 1.A

Test No.	Current (amps)	Time (min)	Electrode Spacing (cm)	Weight (g)	Current Density (asf)	Coulombs	Theo. Weight (g)	Current Eff. (%)	Copper (gpl)	Nickel (gpl)	Cell Volt. (v)
19	1.485	161.0	3.8	2.19569 2.45398	74.25	14345.10	4.72298	98.45	~40	0.00	3.37
20*	-----	------	---	-------	-----	--------	-------	-----	-----	----	----
21	0.046	1117.0	3.8	0.93036 0.93036	4.60	3082.92	1.01502	91.66 91.66	38.29	0.00	1.86
22	0.092	630.0	3.8	1.11010 1.09585	9.25	3496.60	1.15132	96.42 95.18	38.29	0.00	1.97
23	0.185	317.0	3.8	1.15266 1.14696	18.50	3518.70	1.15850	99.50 99.00	38.29	0.00	2.15
24	0.280	190.0	3.8	1.05040 1.03947	28.00	3192.00	1.05093	99.95 98.91	38.29	0.00	2.35
25	0.375	150.0	3.8	1.12196 1.10941	37.50	3375.00	1.11118	100.97 99.84	38.29	0.00	2.41
26	0.465	120.0	3.8	1.11346 1.11346	46.50	3348.00	1.10233	101.01 101.01	38.29	0.00	2.51
27	0.557	108.0	3.8	1.20221 1.19004	55.75	3612.60	1.18951	101.07 100.04	38.29	0.00	2.67

*Test number 20 was not run.

TABLE 1.A

Test No.	Current (amps)	Time (min)	Electrode Spacing (cm)	Weight (g)	Current Density (asf)	Coulombs	Theo. Weight (g)	Current Eff. (%)	Copper (gpl)	Nickel (gpl)	Cell Volt. (v)
28	0.648	90.0	3.8	1.16570 1.15350	64.80	3499.20	1.15218	101.17 100.11	38.29	0.00	2.83
29	0.742	89.0	3.8	1.32343 1.30491	74.25	3964.95	1.30542	101.38 99.96	38.29	0.00	2.88
30	0.930	61.0	3.8	1.13649 1.10589	93.00	3403.80	1.12067	101.41 98.68	38.29	0.00	3.09
31	0.045	1105.0	3.8	0.89920 0.89003	4.50	2983.50	0.98229	91.54 90.60	36.90	0.00	1.86
32	0.092	528.0	3.8	0.91888 0.91383	9.25	2914.56	0.95959	95.61 95.02	36.90	0.00	1.99
33	0.185	303.0	3.8	1.09482 1.09139	18.50	3363.30	1.10733	98.87 98.56	36.90	0.00	2.19
34	0.279	201.0	3.8	1.11636 1.10160	27.90	3364.74	1.10791	100.76 99.43	36.90	0.00	2.31
35	0.375	151.0	3.8	1.12371 1.10920	37.50	3397.50	1.11859	100.46 99.16	36.90	0.00	2.73
36	0.463	133.0	3.8	1.21638 1.21163	46.30	3694.74	1.21646	99.99 99.60	36.90	0.00	2.68

TABLE 1.A

Test No.	Current (amps)	Time (min)	Electrode Spacing (cm)	Weight (g)	Current Density (asf)	Coulombs	Theo. Weight (g)	Current Eff. (%)	Copper (gpl)	Nickel (gpl)	Cell Volt. (v)
37	0.557	108.0	3.8	1.18960 1.18275	55.75	3612.60	1.18941	100.02 99.44	36.90	0.00	2.84
38	0.650	93.0	3.8	1.19796 1.19390	65.00	3627.00	1.19415	100.32 99.97	36.90	0.00	2.82
39	0.745	86.0	3.8	1.26440 1.25910	74.50	3844.20	1.26566	99.90 99.48	36.90	0.00	3.10
40	0.930	60.0	3.8	1.10765 1.05759	93.00	3348.00	1.1.030	100.48 95.94	36.90	0.00	3.24
41	0.933	165.0	3.8	3.02925	93.30	9236.70	3.04109	99.61	39.21	0.00	3.22
42	0.933	165.0	3.8	2.92695	93.30	9236.70	3.04109	96.25	37.42	0.00	3.11
43	0.933	-----	3.8	3.03553	93.30	-------	-------	-----	35.27	0.00	----
44	0.933	180.0	3.8	3.27820	93.30	10076.40	3.31755	98.81	32.96	0.00	3.03
45	0.933	165.0	3.8	3.01767	93.30	9236.70	3.04109	99.23	30.03	0.00	3.03
46	0.933	165.0	3.8	3.01033	93.30	9236.70	3.04109	98.99	27.72	0.00	2.96
47	0.933	165.0	3.8	2.99275	93.30	9236.70	3.04109	98.41	25.60	0.00	2.94

TABLE 1.A

Test No.	Current (amps)	Time (min)	Electrode Spacing (cm)	Weight (g)	Current Density (asf)	Coulombs	Theo. Weight (g)	Current Eff. (%)	Copper (gpl)	Nickel (gpl	Cell Volt. (v)
48	0.933	165.0	3.8	3.08467	93.30	9236.70	3.04109	101.43	23.64	0.00	2.94
49	0.933	165.0	3.8	3.10145	93.30	9236.70	3.04109	101.91	21.60	0.00	2.93
50	0.933	165.0	3.8	3.11682	93.30	9236.70	3.04109	102.49	19.25	0.00	2.93
51	0.745	201.0	3.8	2.94510	74.50	8984.70	2.95812	99.56	38.69	0.00	2.88
52	0.745	201.0	3.8	2.94430	74.50	8984.70	2.95812	99.53	37.23	0.00	2.83
53	0.745	255.0	3.8	3.73195	74.50	11383.20	3.74780	99.58	36.27	0.00	2.85
54	0.745	220.0	3.8	3.22048	74.50	9834.00	3.23775	99.47	32.57	0.00	2.85
55	0.745	201.0	3.8	2.91718	74.50	8984.70	2.95812	98.62	31.57	0.00	2.84
56	0.745	201.0	3.8	2.94632	74.50	8984.70	2.95812	99.60	30.34	0.00	2.90
57	0.745	264.0	3.8	3.85425	74.50	11800.80	3.88529	99.20	26.53	0.00	2.78
58	0.745	147.0	3.8	2.04880	74.50	6570.90	2.16340	94.70	23.48	0.00	2.78
59	0.745	284.0	3.8	4.20775	74.50	12694.80	4.17963	100.67	22.18	0.00	2.75
60	0.745	215.0	3.8	3.12357	74.50	9610.50	3.16426	98.71	-----	0.00	2.82

TABLE 1.A

Test No.	Current (amps)	Time (min)	Electrode Spacing (cm)	Weight (g)	Current Density (asf)	Coulombs	Theo. Weight (g)	Current Eff. (%)	Copper (gpl)	Nickel (gpl)	Cell Volt. (v)
61	0.560	486.0	3.8	5.34560	56.00	16329.60	5.37646	99.43	39.04	0.00	2.75
62	0.560	470.0	3.8	5.15287	56.00	15792.00	5.19946	99.10	35.80	0.00	2.72
63	0.560	433.0	3.8	4.76445	56.00	14548.80	4.79005	99.46	33.84	0.00	2.71
64	0.560	473.0	3.8	5.20595	56.00	15892.80	5.23265	99.49	30.14	0.00	2.68
65	0.560	482.0	3.8	5.30501	56.00	16195.50	5.33211	99.49	27.89	0.00	2.72
66	0.560	460.0	3.8	5.05969	56.00	15456.00	5.08873	99.43	23.77	0.00	2.68
67*	0.560	827.0	3.8	0.02820	56.00	27787.20	9.14866	-----	17.67	0.00	2.66
68*	0.560	510.0	3.8	0.17283	56.00	17136.00	5.64186	84.84	11.70	0.00	2.64
69	0.370	710.0	3.8	5.13945	37.00	15762.00	5.18948	99.04	39.44	0.00	2.37
70	0.370	700.0	3.8	5.06991	37.00	15540.00	5.11639	99.09	38.77	0.00	2.33
71	0.370	705.0	3.8	5.10450	37.00	15651.00	5.15293	99.06	32.92	0.00	2.31
72	0.370	820.0	3.8	5.94462	37.00	18204.00	5.99358	99.18	27.94	0.00	2.32

The deposits from tests numbers 67 and 68 were very powdery and did not adhere to the electrode. The total powder from both tests was 12.16705 g. The current efficiency given for test 68 is the combined efficiency.

TABLE 1.A

Test No.	Current (amps)	Time (min)	Electrode Spacing (cm)	Weight (g)	Current Density (asf)	Coulombs	Theo. Weight (g)	Current Eff. (%)	Copper (gpl)	Nickel (gpl)	Cell Volt. (v)
73	0.370	703.0	3.8	5.09490	37.00	15606.60	5.13832	99.15	24.76	0.00	2.37
74	0.370	684.0	3.8	4.95118	37.00	15184.80	4.99954	99.03	20.78	0.00	2.34
75	0.370	1615.0	3.8	11.66788	37.00	35853.89	11.80453	98.84	16.71	0.00	2.63
76	0.191	1441.0	3.8	5.27953	19.10	16513.86	5.43702	97.10	39.79	0.00	2.11
77	0.191	1503.0	3.8	5.51181	19.10	17224.38	5.67095	97.19	37.88	0.00	2.09
78	0.191	1426.0	3.8	5.22793	19.10	16341.96	5.38043	97.16	33.65	0.00	2.10
79	0.191	1430.0	3.8	5.25549	19.10	16387.80	5.39552	97.40	30.35	0.00	2.08
80	0.191	1435.0	3.8	5.27838	19.10	16445.10	5.41144	97.54	26.26	0.00	2.10
81	0.191	1420.0	[illegible]	[illegible]35	19.10	16273.20	5.35779	97.58	22.00	0.00	2.09
82	0.191	4265.0	3.8	15.66019	19.10	48876.90	16.09223	97.31	17.74	0.00	2.08
83	0.191	1410.0	3.8	5.16714	19.10	16158.60	5.32006	97.13	40.19	0.99	2.10
84	0.190	1410.0	3.8	5.17008	19.00	16074.00	5.29220	97.69	36.52	0.99	2.09
85	0.190	1420.0	3.8	5.20788	19.00	16188.00	5.32974	97.71	34.96	0.99	2.09

TABLE 1.A

Test No.	Current (amps)	Time (min)	Electrode Spacing (cm)	Weight (g)	Current Density (asf)	Coulombs	Theo. Weight (g)	Current Eff. (%)	Copper (gpl)	Nickel (gpl)	Cell Volt. (v)
86	0.190	1480.0	3.8	5.43060	19.00	16872.00	5.55494	97.76	31.28	0.99	2.11
87	0.190	1315.0	3.8	4.84097	19.00	14991.00	4.93563	98.08	25.93	0.99	2.11
88	0.190	1385.0	3.8	5.10394	19.00	15789.00	5.19837	98.18	22.29	0.99	2.11
89	0.190	1450.0	3.8	5.34736	19.00	16530.00	5.44234	98.25	18.54	0.99	2.11
90	0.190	1465.0	3.8	5.41628	19.00	16701.00	5.49864	98.50	14.65	0.99	2.16
91	0.190	1380.0	3.8	5.06395	19.00	15732.00	5.17960	97.77	40.19	5.10	2.11
92	0.190	1375.0	3.8	5.04598	19.00	15675.00	5.16084	97.77	37.70	5.10	2.11
93	0.190	1450.0	3.8	5.32620	19.00	16530.00	5.44234	97.87	34.82	5.10	2.10
94	0.190	1353.0	3.8	4.96874	19.00	15424.20	5.07826	97.84	30.48	5.10	2.11
95	0.190	1475.0	3.8	5.42265	19.00	16815.00	5.53617	97.95	25.87	5.10	2.10
96	0.190	1430.0	3.8	5.26495	19.00	16302.00	5.36727	98.09	23.27	5.10	2.10
97	0.190	1450.0	3.8	5.35030	19.00	16530.00	5.44244	98.31	-----	5.10	2.12
98	0.190	1410.0	3.8	5.22058	19.00	16074.00	5.29220	98.65	14.56	5.10	2.12

TABLE 1.A

Test No.	Current (amps)	Time (min)	Electrode Spacing (cm)	Weight (g)	Current Density (asf)	Coulombs	Theo. Weight (g)	Current Eff. (%)	Copper (gpl)	Nickel (gpl)	Cell Volt. (v)
99	0.190	1445.0	3.8	5.31877	19.00	16473.00	5.42357	98.07	40.24	17.66	2.12
100	0.190	1405.0	3.8	5.17437	19.00	16017.00	5.27344	98.12	35.18	17.66	2.12
101	0.190	1411.0	3.8	5.19625	19.00	16085.40	5.29596	98.12	33.31	17.66	2.10
102	0.190	1506.0	3.8	5.54608	19.00	17168.40	5.65262	98.12	29.06	17.66	2.11
103	0.190	1390.0	3.8	5.12683	19.00	15846.00	5.21714	98.27	24.69	17.66	2.08
104	0.190	1434.0	3.8	5.29469	19.00	16347.60	5.38228	98.37	20.87	17.66	2.10
105	0.190	1417.0	3.8	5.24090	19.00	16153.80	5.31858	98.54	17.84	17.66	2.13
106	0.190	1490.0	3.8	5.50803	19.00	16986.00	5.59247	98.49	13.47	17.66	2.17
107	0.370	738.0	3.8	5.34189	37.00	16383.60	5.39414	99.03	40.08	1.01	2.28
108	0.370	702.0	3.8	5.08357	37.00	15584.40	5.13101	99.07	36.54	1.01	2.24
109	0.370	725.0	3.8	5.25419	37.00	16095.00	5.29912	99.15	32.90	1.01	2.28
110	0.370	720.0	3.8	5.22122	37.00	15984.00	5.26257	99.21	29.54	1.01	2.28
111	0.370	725.0	3.8	5.25805	37.00	16095.00	5.29912	99.22	25.45	1.01	2.28

TABLE 1.A

Test No.	Current (amps)	Time (min)	Electrode Spacing (cm)	Weight (g)	Current Density (asf)	Coulombs	Theo. Weight (g)	Current Eff. (%)	Copper (gpl)	Nickel (gpl)	Cell Volt. (v)
112	0.370	750.0	3.8	5.43690	37.00	16650.00	5.48185	99.18	21.40	1.01	2.28
113	0.370	1045.0	3.8	7.56618	37.00	23199.00	7.63804	99.06	17.60	1.01	2.33
114	0.370	750.0	3.8	5.42498	37.00	16650.00	5.48185	98.96	40.08	6.24	2.35
115	0.370	758.0	3.8	5.48787	37.00	16827.60	5.54032	99.05	38.39	6.24	2.31
116	0.370	771.0	3.8	5.58187	37.00	17116.20	5.63534	99.05	33.64	6.24	2.31
117	0.370	722.0	3.8	5.20510	37.00	16028.40	5.27710	98.63	28.30	6.24	2.38
118	0.370	760.0	3.8	5.49438	37.00	16872.00	5.55494	98.91	25.61	6.24	2.35
119	0.370	690.0	3.8	4.98713	37.00	15318.00	5.04330	98.87	21.20	6.24	2.37
120	0.370	730.0	3.8	5.36692	37.00	16206.00	5.33566	100.58	17.36	6.24	2.37
121	0.370	872.0	3.8	6.25101	37.00	19358.40	6.37356	98.08	13.13	6.24	2.37
122	0.370	720.0	3.8	5.19673	37.00	15984.00	5.26257	98.75	39.33	13.38	2.37
123	0.370	785.0	3.8	5.67800	37.00	17427.00	5.73766	98.96	-----	13.38	2.35
124	0.370	686.0	3.8	4.96230	37.00	15229.20	5.01406	98.97	37.21	13.38	2.37

TABLE 1.A

Test No.	Current (amps)	Time (min)	Electrode Spacing (cm)	Weight (g)	Current Density (asf)	Coulombs	Theo. Weight (g)	Current Eff. (%)	Copper (gpl)	Nickel (gpl)	Cell Volt. (v)
125	0.370	785.0	3.8	5.68237	37.00	17427.00	5.73766	99.04	29.80	13.38	2.34
126	0.370	690.0	3.8	4.99216	37.00	15318.00	5.04330	98.99	25.49	13.38	2.37
127	0.370	725.0	3.8	5.25044	37.00	16095.00	5.29912	99.08	18.60	13.38	2.37
128	0.370	1380.0	3.8	9.90989	37.00	30636.00	10.08660	98.25	17.36	13.38	2.35
129	0.562	480.0	3.8	5.28122	56.20	16185.60	5.32895	99.10	40.29	1.26	2.56
130	0.562	545.0	3.8	5.98875	56.20	18378.40	6.05090	98.97	36.51	1.26	2.51
131	0.562	600.0	3.8	6.58848	56.20	20232.00	6.66118	98.91	32.24	1.26	2.56
132	0.562	445.0	3.8	4.90499	56.20	15005.40	4.94038	99.28	27.54	1.26	2.57
133	0.562	486.0	3.8	5.34559	56.20	16387.92	5.39556	99.07	24.02	1.26	2.57
134	0.562	755.0	3.8	8.32182	56.20	25458.60	8.38199	99.28	20.21	1.26	2.57
135	0.562	470.0	3.8	5.18720	56.20	15848.40	5.21793	99.41	40.08	6.27	2.61
136	0.562	515.0	3.8	5.68460	56.20	17365.80	5.71751	99.42	36.37	6.27	2.53
137	0.562	475.0	3.8	5.23943	56.20	16017.00	5.27344	99.35	32.31	6.27	2.56

TABLE 1.A

Test No.	Current (amps)	Time (min)	Electrode Spacing (cm)	Weight (g)	Current Density (asf)	Coulombs	Theo. Weight (g)	Current Eff. (%)	Copper (gpl)	Nickel (gpl)	Cell Volt. (v)
138	0.562	490.0	3.8	5.39720	56.20	16522.80	5.43997	99.21	28.57	6.24	2.63
139	0.562	440.0	3.8	4.85463	56.20	14836.80	4.88487	99.38	24.71	6.24	2.61
140	0.562	632.0	3.8	7.01044	56.20	21311.04	7.01645	99.91	21.25	6.24	----
141	0.562	485.0	3.8	5.35362	56.20	16354.20	5.38446	99.43	39.73	14.93	2.63
142	0.562	492.0	3.8	5.42900	56.20	16590.24	5.46217	99.39	35.91	14.93	2.64
143	0.562	390.0	3.8	2.91445	56.20	13150.80	4.32977	67.31	32.03	14.93	2.68
144	0.562	475.0	3.8	5.24563	56.20	16017.00	5.27344	99.47	29.94	14.93	2.63
145	0.562	440.0	3.8	4.85543	56.20	14836.80	4.88487	99.40	26.20	14.93	2.67
146	0.562	532.0	3.8	5.12490	56.20	17939.04	5.90625	86.77	22.72	14.93	2.65

TABLE 2.A

Test No. 1 Nickel Conc. 0.0 gpl

Acid Conc. 49 gpl Temp. 25 °C

Copper Conc. 0.0 gpl Eo 0.0 mv

Current (ma)	Potential (mv)	Current (ma)	Potential (mv)	Current (ma)	Potential (mv)
0.1	2.7	20	91.6	92.5	141.7
0.2	11.8	30	99.9	100	142.3
0.3	17.5	40	107.2	110	144.6
0.5	26.3	50	114.6	120	127.9
0.7	31.6	62	120.9	125	141.8
1.0	37.1	65	121.1	140	183.4
2.0	49.2	70	124.8	150	175.2
3.0	56.9	72.5	126.8	160	177.4
4.0	61.5	75	128.6	175	196.9
5.0	66.1	80	132.4	180	231.1
7.0	71.4	82.5	134.3	190	217.9
10	77.1	87.5	138.0	200	235.3

TABLE 2.A

Test No. 2 Nickel Conc. 0.0 gpl

Acid Conc. 49 gpl Temp. 25 °C

Copper Conc. 0.0 gpl Eo 0.0 mv

Current (ma)	Potential (mv)	Current (ma)	Potential (mv)	Current (ma)	Potential (mv)
0.2	6.3	15	82.8	77.5	109.9
0.4	16.1	17.5	84.6	80	111.8
0.6	23.2	22.5	90.3	85	115.5
0.8	26.8	25	93.2	90	114.1
1.0	30.6	27.5	96.1	95	112.7
2.0	42.2	30	95.8	97.5	114.6
3.0	49.9	35	98.5	100	111.4
4.0	55.0	37.5	99.3	110	113.7
5.0	60.1	40	101.1	125	116.2
6.0	63.8	45	103.8	130	135.1
7.0	67.9	50	103.3	150	139.4
8.0	70.5	55	105.0	160	136.4
9.0	70.6	60	105.5	170	143.7
10	74.0	70	109.4	175	161.2
12.5	76.8	75	107.9		

TABLE 2.A

Test No. 3 Nickel Conc. 0.0 gpl

Acid Conc. 49 gpl Temp. _____ °C

Copper Conc. 0.0 gpl Eo 0.0 mv

Current (ma)	Potential (mv)	Current (ma)	Potential (mv)	Current (ma)	Potential (mv)
0.1	4.8	8.0	80.7	70	114.5
0.2	12.9	9.0	82.5	75	113.1
0.4	24.5	10	83.3	80	113.8
0.6	33.0	12.5	88.1	85	117.5
0.8	35.3	30	101.9	90	119.3
1.0	39.6	35	106.7	95	117.9
1.5	47.4	40	107.2	100	121.7
2.0	53.2	45	109.9	110	124.0
3.0	61.4	50	112.5	125	131.6
4.0	67.5	55	112.1	150	144.5
5.0	72.6	60	117.3	175	171.4
6.0	76.8	65	116.0	200	204.6
7.0	77.4				

TABLE 2.A

Test No. 4 Nickel Conc. 0.0 gpl

Acid Conc. 100 gpl Temp. 25 °C

Copper Conc. 0.0 gpl Eo 7.6 mv

Current (ma)	Potential (mv)	Current (ma)	Potential (mv)	Current (ma)	Potential (mv)
0.1	11.9	4.5	68.1	30	102.2
0.2	16.2	5.0	70.2	40	106.2
0.3	20.5	5.5	72.3	50	111.2
0.4	24.3	6.0	73.5	60	114.2
0.5	27.8	6.5	74.6	70	117.2
0.6	28.9	7.0	76.7	80	118.0
0.8	33.6	7.5	77.3	90	121.0
1.0	37.2	8.0	78.4	100	124.0
1.5	44.9	8.5	80.1	110	136.7
2.0	50.5	9.0	80.2	125	125.9
2.5	55.0	10	82.4	150	138.7
3.0	58.7	15	89.6	175	146.3
3.5	62.3	20	97.2	200	154.0
4.0	66.0	25	99.7		

TABLE 2.A

Test No. 5 Nickel Conc. 0.0 gpl

Acid Conc. 100 gpl Temp. 25 °C

Copper Conc. 0.0 gpl Eo 2.7 mv

Current (ma)	Potential (mv)	Current (ma)	Potential (mv)	Current (ma)	Potential (mv)
0.1	10.8	6.0	75.5	60	127.5
0.2	18.9	7.0	78.2	70	132.6
0.3	24.2	8.0	80.9	75	133.0
0.4	28.8	9.0	83.7	80	136.5
0.6	34.9	10	83.4	85	139.0
0.8	38.6	15	92.6	90	141.5
1.0	43.2	20	100.3	95	135.9
1.5	50.4	25	104.9	100	144.0
2.0	55.5	30	109.4	110	147.0
2.5	59.6	35	112.9	125	146.5
3.0	63.2	40	116.4	150	159.3
4.0	68.5	45	120.0	175	172.1
5.0	72.2	50	122.5	200	191.5

TABLE 2.A

Test No. 6 Nickel Conc. 0.0 gpl

Acid Conc. 100 gpl Temp. 25 °C

Copper Conc. 10.0 gpl Eo 41.0 mv

Current (ma)	Potential (mv)	Current (ma)	Potential (mv)	Current (ma)	Potential (mv)
0.1	44.8	4.0	76.5	40	120.7
0.2	48.6	5.0	80.6	45	122.6
0.3	50.9	6.0	84.7	50	126.5
0.4	52.2	7.0	86.8	60	129.3
0.5	53.0	8.0	85.9	70	133.0
0.6	54.4	10	88.9	80	137.8
0.8	56.5	15	99.0	90	138.5
1.0	58.1	20	105.0	100	141.8
1.5	62.7	25	110.0	110	148.8
2.0	66.3	30	113.9	125	151.5
2.5	68.8	35	118.9	150	166.4
3.0	71.8				

TABLE 2.A

Test No. 7 Nickel Conc. 0.0 gpl

Acid Conc. 100 gpl Temp. 25 °C

Copper Conc. 10.0 gpl Eo 42.5 mv

Current (ma)	Potential (mv)	Current (ma)	Potential (mv)	Current (ma)	Potential (mv)
0.1	44.8	2.5	66.3	35	110.7
0.2	49.1	3.0	68.8	40	112.6
0.3	50.9	4.0	73.5	45	115.5
0.4	51.7	5.0	77.1	50	116.2
0.5	52.5	6.0	80.2	60	120.0
0.6	53.9	7.0	82.8	70	124.8
0.7	54.7	8.0	84.9	80	127.5
0.8	55.0	10	86.9	90	133.4
0.9	55.8	15	94.9	100	131.5
1.0	56.1	20	99.9	110	143.6
1.5	60.2	25	102.8	125	141.2
2.0	63.2	30	107.8	150	171.5

TABLE 2.A

Test No. 9 Nickel Conc. 0.0 gpl

Acid Conc. 100 gpl Temp. 25 °C

Copper Conc. 10.0 gpl Eo 40.0 mv

Current (ma)	Potential (mv)	Current (ma)	Potential (mv)	Current (ma)	Potential (mv)
0.1	43.8	7.0	80.8	55	116.1
0.2	47.6	8.0	82.9	60	116.9
0.3	49.4	9.0	84.1	65	118.8
0.4	50.3	10	84.8	70	119.7
0.6	52.4	15	91.8	75	120.5
0.8	54.0	20	96.8	80	121.4
1.0	54.1	25	100.7	85	125.3
2.0	61.3	30	103.7	90	127.2
3.0	65.8	35	108.6	95	127.0
4.0	70.5	40	109.5	100	131.5
5.0	74.6	45	111.4	110	133.3
6.0	77.7	50	113.1	125	136.1

TABLE 2.A

Test No. 10 Nickel Conc. 1.0 gpl

Acid Conc. 100 gpl Temp. 25 °C

Copper Conc. 10.0 gpl Eo 45.0 mv

Current (ma)	Potential (mv)	Current (ma)	Potential (mv)	Current (ma)	Potential (mv)
0.1	46.8	8.0	84.4	65	120.3
0.2	48.6	9.0	84.0	70	122.1
0.3	49.9	10	86.8	75	125.0
0.4	51.2	15	93.7	80	125.7
0.6	52.9	20	99.7	85	128.6
0.8	54.5	25	102.5	90	130.4
1.0	56.1	30	105.4	95	134.8
2.0	61.2	35	108.2	100	132.6
3.0	65.3	40	110.1	110	137.4
4.0	71.4	45	111.9	125	139.9
5.0	76.0	50	113.7	140	147.7
6.0	79.1	55	116.6	150	180.3
7.0	82.3	60	117.3		

TABLE 2.A

Test No. 11 Nickel Conc. 1.0 gpl

Acid Conc. 100 gpl Temp. 25 °C

Copper Conc. 10.0 gpl Eo 45.5 mv

Current (ma)	Potential (mv)	Current (ma)	Potential (mv)	Current (ma)	Potential (mv)
0.1	47.3	9.0	84.0	75	129.1
0.2	49.1	10	87.8	80	131.1
0.4	52.2	15	95.7	85	134.8
0.6	54.7	20	100.7	90	134.5
0.8	56.5	25	104.5	95	140.0
1.0	58.1	30	108.5	100	140.8
2.0	64.2	35	112.3	110	142.5
3.0	68.8	40	115.2	125	145.1
4.0	72.4	45	117.0	140	147.7
5.0	76.5	50	119.8	150	170.0
6.0	79.6	55	121.7	160	182.1
7.0	82.8	60	124.5	175	206.7
8.0	84.4	65	125.4		

TABLE 2.A

Test No. 12 Nickel Conc. 1.0 gpl

Acid Conc. 100 gpl Temp. 25 °C

Copper Conc. 10.0 gpl Eo 47.2 mv

Current (ma)	Potential (mv)	Current (ma)	Potential (mv)	Current (ma)	Potential (mv)
0.1	49.8	10	97.0	70	126.1
0.3	54.9	15	99.8	75	126.0
0.4	57.2	20	104.8	80	129.8
0.6	60.9	25	108.6	85	131.7
0.8	64.5	30	112.6	90	132.5
1.0	66.1	35	113.3	96	138.1
2.0	76.2	40	116.3	100	140.8
3.0	82.8	45	117.0	110	142.5
4.0	87.9	50	118.8	125	139.9
7.0	95.6	55	120.7	140	142.5
8.0	96.7	60	122.5	150	170.0
9.0	96.9	65	124.4	160	192.4

TABLE 2.A

Test No. 13 Nickel Conc. 5.0 gpl

Acid Conc. 100 gpl Temp. 25 °C

Copper Conc. 10.0 gpl Eo 44.0 mv

Current (ma)	Potential (mv)	Current (ma)	Potential (mv)	Current (ma)	Potential (mv)
0.1	46.8	8.0	88.0	60	119.1
0.2	49.6	10	91.3	65	120.7
0.4	53.2	15	98.0	70	121.2
0.6	55.3	20	101.6	75	121.7
0.8	57.4	25	105.2	80	124.3
1.0	59.5	30	106.8	85	126.9
2.0	67.6	35	109.3	90	127.4
3.0	73.6	40	111.9	95	122.8
4.0	78.2	45	113.5	100	126.9
5.0	82.3	50	115.0	110	115.7
6.0	84.8	55	117.6		

TABLE 2.A

Test No. 14 Nickel Conc. 5.0 gpl

Acid Conc. 100 gpl Temp. 25 °C

Copper Conc. 10.0 gpl Eo 44.0 mv

Current (ma)	Potential (mv)	Current (ma)	Potential (mv)	Current (ma)	Potential (mv)
0.1	45.8	8.0	82.4	65	119.6
0.2	47.6	9.0	81.5	70	121.2
0.4	50.7	15	89.8	75	121.7
0.6	52.3	20	94.5	80	124.3
0.8	53.4	25	100.1	85	126.9
1.0	54.5	30	103.7	90	127.4
2.0	59.6	35	107.2	95	123.8
3.0	63.6	40	109.9	100	124.8
4.0	69.7	45	111.4	110	131.2
5.0	73.8	50	114.0	125	127.8
6.0	77.3	55	115.5	140	134.6
7.0	80.4	60	118.0	150	171.8

TABLE 2.A

Test No. 15 Nickel Conc. 10.0 gpl

Acid Conc. 100 gpl Temp. 25 °C

Copper Conc. 10.0 gpl Eo 44.0 mv

Current (ma)	Potential (mv)	Current (ma)	Potential (mv)	Current (ma)	Potential (mv)
0.1	45.8	9.0	82.8	65	131.5
0.2	47.6	10	85.9	70	133.7
0.4	51.2	15	93.8	75	136.9
0.6	53.8	20	100.2	80	138.1
0.8	55.9	25	105.4	85	136.2
1.0	57.0	30	109.7	90	137.9
2.0	64.5	35	114.0	95	133.0
3.0	69.4	40	117.2	100	143.5
4.0	73.4	45	119.4	105	143.7
5.0	76.9	50	123.7	110	140.8
6.0	80.4	55	125.9	125	160.0
7.0	82.4	60	129.1	150	219.3
8.0	84.3				

TABLE 2.A

Test No. 16 Nickel Conc. 10.0 gpl

Acid Conc. 100 gpl Temp. 25 °C

Copper Conc. 10.0 gpl Eo 43.0 mv

Current (ma)	Potential (mv)	Current (ma)	Potential (mv)	Current (ma)	Potential (mv)
0.1	44.8	8.0	81.3	60	126.1
0.2	46.6	9.0	80.8	65	129.4
0.4	49.7	10	84.4	70	130.5
0.6	51.8	15	89.7	75	134.8
0.8	53.4	20	97.1	80	136.0
1.0	55.0	25	102.4	85	138.7
2.0	62.0	30	106.6	90	137.9
3.0	66.4	35	110.9	95	140.1
4.0	69.9	40	114.1	100	140.4
5.0	73.9	45	117.4	110	140.8
6.0	76.4	50	120.6	125	149.7
7.0	79.4	55	123.8	140	160.6

TABLE 2.A

Test No. 17 Nickel Conc. 15.0 gpl

Acid Conc. 100 gpl Temp. 25 °C

Copper Conc. 10.0 gpl Eo 42.5 mv

Current (ma)	Potential (mv)	Current (ma)	Potential (mv)	Current (ma)	Potential (mv)
0.1	44.8	8.0	83.8	60	130.1
0.2	47.1	9.0	84.8	65	130.9
0.4	49.7	10	85.8	70	135.8
0.6	52.2	15	93.8	75	138.8
0.8	53.8	20	99.8	80	139.6
1.0	55.4	25	105.7	85	142.0
2.0	61.8	30	107.6	90	143.9
3.0	66.7	35	112.5	95	143.8
4.0	70.6	40	116.5	100	146.7
5.0	75.0	45	119.3	110	148.5
6.0	78.5	50	123.3	125	153.3
7.0	81.4	55	126.1	140	181.7

TABLE 2.A

Test No. 18 Nickel Conc. 15.0 gpl

Acid Conc. 100 gpl Temp. 25 °C

Copper Conc. 10.0 gpl Eo 43.0 mv

Current (ma)	Potential (mv)	Current (ma)	Potential (mv)	Current (ma)	Potential (mv)
0.1	44.8	8.0	80.8	60	122.9
0.2	46.6	9.0	84.2	65	124.7
0.4	49.2	10	83.7	70	130.7
0.6	51.7	15	89.7	75	130.6
0.8	53.3	20	95.7	80	130.3
1.0	54.9	25	101.6	85	136.8
2.0	61.3	30	105.6	90	131.5
3.0	65.7	35	109.4	95	131.4
4.0	69.6	40	111.3	100	131.2
5.0	73.0	45	114.2	110	136.1
6.0	75.5	50	117.1	125	161.5
7.0	78.9	55	119.9		

TABLE 2.A

Test No. 19 Nickel Conc. 0.0 gpl

Acid Conc. 100 gpl Temp. 25 °C

Copper Conc. 30.0 gpl Eo 64.0 mv

Current (ma)	Potential (mv)	Current (ma)	Potential (mv)	Current (ma)	Potential (mv)
0.1	65.8	8.0	94.9	55	124.1
0.2	67.6	9.0	96.9	60	125.9
0.4	71.1	10	97.9	65	127.6
0.6	72.7	15	101.8	70	129.4
0.8	74.3	20	104.5	75	132.3
1.0	74.9	25	108.4	80	134.0
2.0	81.3	30	111.1	85	132.2
3.0	86.2	35	115.0	90	135.0
4.0	89.6	40	116.8	95	134.8
5.0	88.4	45	119.5	100	139.7
6.0	93.0	50	121.3	110	165.0
7.0	92.9				

TABLE 2.A

Test No. 20 Nickel Conc. 0.0 gpl

Acid Conc. 100 gpl Temp. 25 °C

Copper Conc. 30.0 gpl Eo 61.0 mv

Current (ma)	Potential (mv)	Current (ma)	Potential (mv)	Current (ma)	Potential (mv)
0.1	62.8	7.0	89.8	50	130.5
0.2	64.6	8.0	90.8	55	133.3
0.4	67.1	9.0	91.8	60	135.1
0.6	68.7	10	93.8	65	139.9
0.8	69.8	15	102.8	70	142.8
1.0	70.4	20	108.6	75	144.6
2.0	75.3	25	114.5	80	145.7
3.0	79.7	30	116.2	85	155.9
4.0	82.6	35	121.1	90	168.0
5.0	85.4	40	125.0	95	183.2
6.0	88.4	45	127.7		

TABLE 2.A

Test No. 21 Nickel Conc. 0.0 gpl

Acid Conc. 100 gpl Temp. 25 °C

Copper Conc. 30.0 gpl Eo 61.0 mv

Current (ma)	Potential (mv)	Current (ma)	Potential (mv)	Current (ma)	Potential (mv)
0.1	62.3	8.0	90.8	55	117.9
0.2	63.6	9.0	91.8	60	119.7
0.4	65.1	10	93.8	65	120.4
0.6	66.7	15	100.7	70	119.2
0.8	68.3	20	104.5	75	121.0
1.0	69.4	25	108.4	80	123.7
2.0	74.8	30	109.1	85	124.5
3.0	78.7	35	111.9	90	124.6
4.0	82.1	40	112.7	95	124.5
5.0	85.9	45	113.4	100	126.3
6.0	88.3	50	115.2	110	139.3
7.0	88.8				

TABLE 2.A

Test No. 22 Nickel Conc. 1.0 gpl

Acid Conc. 100 gpl Temp. 25 °C

Copper Conc. 30.0 gpl Eo 62.0 mv

Current (ma)	Potential (mv)	Current (ma)	Potential (mv)	Current (ma)	Potential (mv)
0.1	63.8	8.0	95.3	60	132.3
0.2	65.6	9.0	95.8	65	135.0
0.4	69.1	10	95.7	70	138.8
0.6	70.2	15	103.6	75	142.5
0.8	72.8	20	108.4	80	141.7
1.0	74.4	25	114.2	85	144.5
2.0	81.2	30	115.9	90	149.3
3.0	85.6	35	120.7	95	159.3
4.0	89.5	40	122.4	100	169.4
5.0	89.4	45	126.3	105	179.4
6.0	91.9	50	128.8	110	204.9
7.0	93.8	55	130.6		

TABLE 2.A

Test No. 23 Nickel Conc. 1.0 gpl

Acid Conc. 100 gpl Temp. 25 °C

Copper Conc. 30.0 gpl Eo 61.0 mv

Current (ma)	Potential (mv)	Current (ma)	Potential (mv)	Current (ma)	Potential (mv)
0.1	62.8	7.0	89.7	45	128.3
0.2	64.6	8.0	91.8	50	129.9
0.4	66.6	9.0	93.8	55	132.6
0.6	68.2	10	94.7	60	135.4
0.8	70.3	15	103.6	65	139.1
1.0	71.4	20	109.4	70	143.9
2.0	76.2	25	114.2	75	145.6
3.0	80.1	30	118.0	80	146.8
4.0	83.8	35	120.7	85	149.6
5.0	87.7	40	124.5	90	157.6
6.0	88.3				

TABLE 2.A

Test No. 24 Nickel Conc. 5.0 gpl

Acid Conc. 100 gpl Temp. 25 °C

Copper Conc. 30.0 gpl Eo 62.0 mv

Current (ma)	Potential (mv)	Current (ma)	Potential (mv)	Current (ma)	Potential (mv)
0.1	63.8	7.0	92.4	45	121.2
0.2	65.6	8.0	93.3	50	123.6
0.4	69.1	9.0	94.2	55	125.0
0.6	70.7	10	96.1	60	126.4
0.8	72.7	15	102.6	65	129.8
1.0	73.3	20	108.1	70	132.2
2.0	80.6	25	109.5	75	134.7
3.0	85.4	30	112.9	80	138.5
4.0	87.2	35	117.4	85	139.0
5.0	90.1	40	118.8	90	143.5
6.0	90.5				

TABLE 2.A

Test No. 25 Nickel Conc. 5.0 gpl

Acid Conc. 100 gpl Temp. 25 °C

Copper Conc. 30.0 gpl Eo 60.5 mv

Current (ma)	Potential (mv)	Current (ma)	Potential (mv)	Current (ma)	Potential (mv)
0.1	61.8	5.0	84.1	35	118.4
0.2	63.1	6.0	85.9	40	119.8
0.4	65.1	7.0	88.3	45	123.2
0.6	66.2	8.0	88.2	50	125.6
0.8	67.7	9.0	90.1	55	129.1
1.0	68.8	15	99.5	60	134.5
2.0	73.6	20	105.1	65	145.2
3.0	77.4	25	109.5	70	150.7
4.0	80.7	30	112.9	75	153.7

TABLE 2.A

Test No. 26 Nickel Conc. 5.0 gpl

Acid Conc. 100 gpl Temp. 40 °C

Copper Conc. 30.0 gpl Eo 72.0 mv

Current (ma)	Potential (mv)	Current (ma)	Potential (mv)	Current (ma)	Potential (mv)
0.1	72.8	7.0	90.4	50	124.4
0.2	73.6	8.0	91.6	55	126.3
0.4	74.7	9.0	92.9	60	130.3
0.6	75.9	10	94.1	65	132.1
0.8	76.5	15	100.0	70	135.1
1.0	77.1	20	106.0	75	139.0
2.0	80.7	25	111.0	80	141.9
3.0	83.3	30	112.9	85	144.8
4.0	86.5	35	115.8	90	147.2
5.0	88.6	40	118.7	95	151.2
6.0	87.7	45	121.7	100	162.4

TABLE 2.A

Test No. 27 Nickel Conc. 5.0 gpl

Acid Conc. 100 gpl Temp. 40 °C

Copper Conc. 30.0 gpl Eo 73.0 mv

Current (ma)	Potential (mv)	Current (ma)	Potential (mv)	Current (ma)	Potential (mv)
0.1	73.8	7.0	90.4	50	126.5
0.2	74.6	8.0	90.6	55	129.5
0.4	75.7	9.0	91.9	60	132.3
0.6	76.9	10	94.1	65	136.2
0.8	77.5	15	100.0	70	138.1
1.0	78.1	20	106.0	75	142.1
2.0	80.2	25	111.0	80	145.0
3.0	82.8	30	113.9	85	147.9
4.0	86.0	35	117.8	90	151.3
5.0	88.1	40	120.7	95	161.5
6.0	88.7	45	123.7		

TABLE 2.A

Test No. 28 Nickel Conc. 10.0 gpl

Acid Conc. 100 gpl Temp. 40 °C

Copper Conc. 30.0 gpl Eo 72.0 mv

Current (ma)	Potential (mv)	Current (ma)	Potential (mv)	Current (ma)	Potential (mv)
0.1	73.8	8.0	93.2	60	121.1
0.2	75.6	9.0	93.3	65	123.7
0.4	77.2	10	93.4	75	125.8
0.6	77.8	15	100.1	80	129.4
0.8	79.4	20	104.6	85	132.0
1.0	80.0	25	107.3	90	132.5
2.0	83.6	30	108.8	95	132.5
3.0	86.6	35	113.4	100	135.1
4.0	89.2	40	115.0	110	141.5
5.0	91.3	45	116.6	125	148.4
6.0	91.9	50	119.1	150	166.7
7.0	92.1	55	118.6	175	181.4

TABLE 2.A

Test No. 29 Nickel Conc. 10.0 gpl

Acid Conc. 100 gpl Temp. 25 °C

Copper Conc. 30.0 gpl Eo 63.0 mv

Current (ma)	Potential (mv)	Current (ma)	Potential (mv)	Current (ma)	Potential (mv)
0.1	63.8	7.0	92.9	50	137.9
0.2	64.5	8.0	94.7	55	139.9
0.4	67.1	9.0	96.5	60	145.0
0.6	68.6	10	98.4	65	150.0
0.8	70.2	15	106.5	70	153.6
1.0	71.7	20	112.6	75	154.6
2.0	77.5	25	117.7	80	160.8
3.0	82.2	30	121.7	90	161.8
4.0	86.9	35	124.7	95	173.1
5.0	89.6	40	129.8	100	195.8
6.0	91.0	45	133.9		

TABLE 2.A

Test No. 30 Nickel Conc. 10.0 gpl

Acid Conc. 100 gpl Temp. 25 °C

Copper Conc. 30.0 gpl Eo 63.5 mv

Current (ma)	Potential (mv)	Current (ma)	Potential (mv)	Current (ma)	Potential (mv)
0.1	63.8	8.0	92.6	55	137.9
0.2	64.0	9.0	94.5	60	141.9
0.4	65.6	10	97.3	65	146.0
0.6	67.1	15	105.5	70	149.0
0.8	68.7	20	112.6	75	149.4
1.0	69.2	25	116.7	80	153.5
2.0	75.0	30	120.7	85	152.5
3.0	79.2	35	123.7	90	156.6
4.0	82.9	40	127.8	95	160.7
5.0	86.6	45	131.8	100	164.9
6.0	86.4	50	135.9	105	169.0
7.0	90.8				

TABLE 2.A

Test No. 31 Nickel Conc. 15.0 gpl

Acid Conc. 100 gpl Temp. 25 °C

Copper Conc. 30.0 gpl Eo 63.0 mv

Current (ma)	Potential (mv)	Current (ma)	Potential (mv)	Current (ma)	Potential (mv)
0.1	64.3	8.0	94.0	60	141.1
0.2	65.5	9.0	95.8	65	143.7
0.4	68.0	10	98.6	70	143.2
0.6	70.6	15	106.3	75	148.4
0.8	71.6	20	113.0	80	150.1
1.0	73.1	25	117.7	85	150.7
2.0	79.3	30	121.3	90	151.3
3.0	83.4	35	125.0	95	152.9
4.0	86.6	40	128.6	100	156.7
5.0	89.2	45	131.2	105	157.3
6.0	90.5	50	134.8	110	169.2
7.0	92.3	55	136.4	125	180.4

TABLE 2.A

Test No. 32 Nickel Conc. 15.0 gpl

Acid Conc. 100 gpl Temp. 25 °C

Copper Conc. 30.0 gpl Eo 62.0 mv

Current (ma)	Potential (mv)	Current (ma)	Potential (mv)	Current (ma)	Potential (mv)
0.1	63.8	9.0	96.8	65	142.7
0.2	65.5	10	99.6	70	143.2
0.4	68.0	15	108.4	75	143.3
0.6	70.1	20	114.0	80	147.0
0.8	71.6	25	118.7	85	145.5
1.0	73.1	30	122.3	90	149.2
2.0	78.8	35	125.0	95	152.9
3.0	82.9	40	127.6	100	154.6
4.0	86.6	45	130.2	105	155.2
5.0	89.2	50	133.8	110	164.1
6.0	91.6	55	135.4	125	180.4
7.0	93.3	60	139.0	140	215.6
8.0	96.1				

TABLE 2.A

Test No. 33 Nickel Conc. 15.0 gpl

Acid Conc. 100 gpl Temp. 40 °C

Copper Conc. 30.0 gpl Eo 74.0 mv

Current (ma)	Potential (mv)	Current (ma)	Potential (mv)	Current (ma)	Potential (mv)
0.1	74.8	15	103.1	85	135.1
0.2	75.6	20	108.4	90	134.8
0.4	76.7	25	112.6	95	136.0
0.6	77.8	30	114.9	100	135.2
0.8	79.4	35	119.1	105	134.4
1.0	80.0	40	119.3	110	138.7
2.0	84.0	45	119.5	125	139.4
3.0	86.4	50	121.7	140	145.2
4.0	88.4	55	124.9	150	150.8
5.0	90.4	60	127.1	160	156.4
6.0	91.5	65	128.3	175	162.2
7.0	92.6	70	129.5	190	159.1
8.0	93.6	75	131.7	200	164.5
9.0	95.7	80	134.0	210	175.0
10	96.8				

TABLE 2.A

Test No. 34 Nickel Conc. 15.0 gpl

Acid Conc. 100 gpl Temp. 40 °C

Copper Conc. 30.0 gpl Eo 75.0 mv

Current (ma)	Potential (mv)	Current (ma)	Potential (mv)	Current (ma)	Potential (mv)
0.1	75.8	9.0	95.7	70	129.5
0.2	76.6	10	96.8	75	131.7
0.4	78.2	15	104.6	80	131.9
0.6	79.8	20	108.4	85	134.1
0.8	80.9	25	112.6	90	134.8
1.0	81.5	30	114.9	95	136.0
2.0	85.0	35	119.1	100	135.2
3.0	87.9	40	119.3	105	133.4
4.0	90.4	45	121.5	110	133.6
5.0	90.9	50	123.7	125	136.3
6.0	93.6	55	124.9	140	140.0
7.0	94.6	60	126.1	150	150.8
8.0	95.7	65	128.3	160	156.4

TABLE 2.A

Test No. 35 Nickel Conc. 15.0 gpl

Acid Conc. 100 gpl Temp. 60 °C

Copper Conc. 30.0 gpl Eo 90.0 mv

Current (ma)	Potential (mv)	Current (ma)	Potential (mv)	Current (ma)	Potential (mv)
0.1	90.8	30	118.5	105	145.1
0.2	91.6	35	122.0	110	146.6
0.4	92.3	40	124.5	125	151.1
0.6	92.9	45	124.9	140	155.6
0.8	93.6	50	127.4	150	163.8
1.0	94.2	55	128.9	160	166.8
2.0	95.5	60	131.4	175	171.3
3.0	94.7	65	133.9	190	175.8
4.0	97.6	70	135.3	200	180.4
5.0	98.9	75	136.8	210	183.3
6.0	99.2	80	138.2	225	184.5
8.0	100.8	85	141.7	240	191.9
10	103.5	90	142.2	250	196.8
15	109.0	95	144.1	275	207.1
20	112.5	100	145.6	300	228.1
25	116.0				

TABLE 2.A

Test No. 36 Nickel Conc. 15.0 gpl

Acid Conc. 100 gpl Temp. 60 °C

Copper Conc. 30.0 gpl Eo 89.5 mv

Current (ma)	Potential (mv)	Current (ma)	Potential (mv)	Current (ma)	Potential (mv)
0.1	89.8	25	113.0	100	143.6
0.2	90.1	30	115.4	105	143.0
0.4	90.8	35	117.9	110	146.6
0.6	91.9	40	121.4	125	149.0
0.8	92.1	45	122.9	140	155.6
1.0	92.2	50	125.4	150	160.7
2.0	94.0	55	127.9	160	163.7
3.0	94.7	60	130.3	175	168.2
4.0	96.6	65	132.8	190	175.8
5.0	96.9	70	134.3	200	175.3
6.0	98.2	75	135.7	210	183.3
8.0	98.8	80	138.2	225	187.6
10	101.4	85	141.7	250	196.8
15	107.0	90	142.2	260	202.8
20	109.5	95	143.1	275	202.0

TABLE 2.A

Test No. 37 Nickel Conc. 0.0 gpl

Acid Conc. 49 gpl Temp. 30 °C

Copper Conc. 4.76 gpl Eo 40.5 mv

Current (ma)	Potential (mv)	Current (ma)	Potential (mv)	Current (ma)	Potential (mv)
0.1	41.2	20	98.7	90	144.1
0.2	42.8	25	104.6	95	146.1
0.4	45.7	30	106.5	100	147.0
0.6	48.3	35	111.4	105	145.8
0.8	50.8	40	114.3	110	149.8
1.0	52.7	45	117.2	125	159.9
2.0	59.8	50	122.1	140	167.4
3.0	66.0	55	123.9	150	174.1
4.0	70.7	60	130.5	160	182.8
5.0	72.4	65	132.4	175	186.8
7.0	75.7	70	128.1	190	198.2
8.0	79.1	75	129.0	200	205.9
9.0	80.9	80	136.1	210	226.8
10	82.7	85	140.1	225	253.6
15	92.7				

APPENDIX B

Cell Designs for Empirical Experiments

The cells and electrode holders used for the empirical experiments were constructed of plexiglas. This was done in order to insure that no metal parts except the electrode surface were exposed to the electrolyte. Figures B.1, B.2, and B.3 show the details of the cells, electrode holders and electrode jig respectively.

The cell provided versatility in changing both the horizontal and vertical spacing of the electrodes. The electrode guide provided a means of locating the electrode holder within the cell in the same manner for each test. It was rigid and thus prevented any movement of the electrode holders during the course of an experiment.

The electrode holder shown in Figure B.2 also provided a rigid and repeatable method of holding the electrode within the cell. Electrical contact for the electrode was provided via the copper contact in the electrode holder. This copper contact was bent so that as the retainer plate was screwed onto the body of the electrode holder it pressed the electrode against the copper contact. Silicone stopcock grease was used to seal the electrode in the electrode holder. This prevented any electrolyte from reaching the copper contact. The screws used to fasten the retainer plate were made of nylon.

The electrode jig consisted of a back and front piece which were screwed together loosely. A taped electrode was inserted into the jig by slipping it into the 0.006" groove. Next,two plexiglas blocks measuring 1.2" x 1.2" were placed against the electrode by positioning them as shown by the shaded area in Figure B.3. These blocks were then clamped onto the electrode using a small C-clamp. The electrode was then removed from the jig by simply pulling it out of the groove. It was then ready to have a taped area of 1.2" x 1.2" cut and removed. By using this jig it was possible to produce electrodes which all had identical geometric characteristics. Each electrode had the same exposed area and could be positioned in the electrode holder the same way each time.

Figure B.4 shows the details of the magnetic stirrer that was constructed in order to insure reproducible stirring characteristics. It to was constructed of plexiglas. The copper tubes shown were there to provide a means of connecting the magnetic stirrer to its necessary power and to provide a means of cooling, via forced air, should the stirrer become overheated. All screws used in the construction of the magnetic stirrer were brass and were countersunk.

The positioning bar as shown in Figure B.5 was placed in the 3/8" groove of the guide also shown in Figure B.5. Once this positioning bar was located in the guide it provided a means of placing the cell onto the magnetic stirrer in a reproducible manner. This insured that the stirring bar within the cell was located in the same manner and position relative to the stirrer for each test.

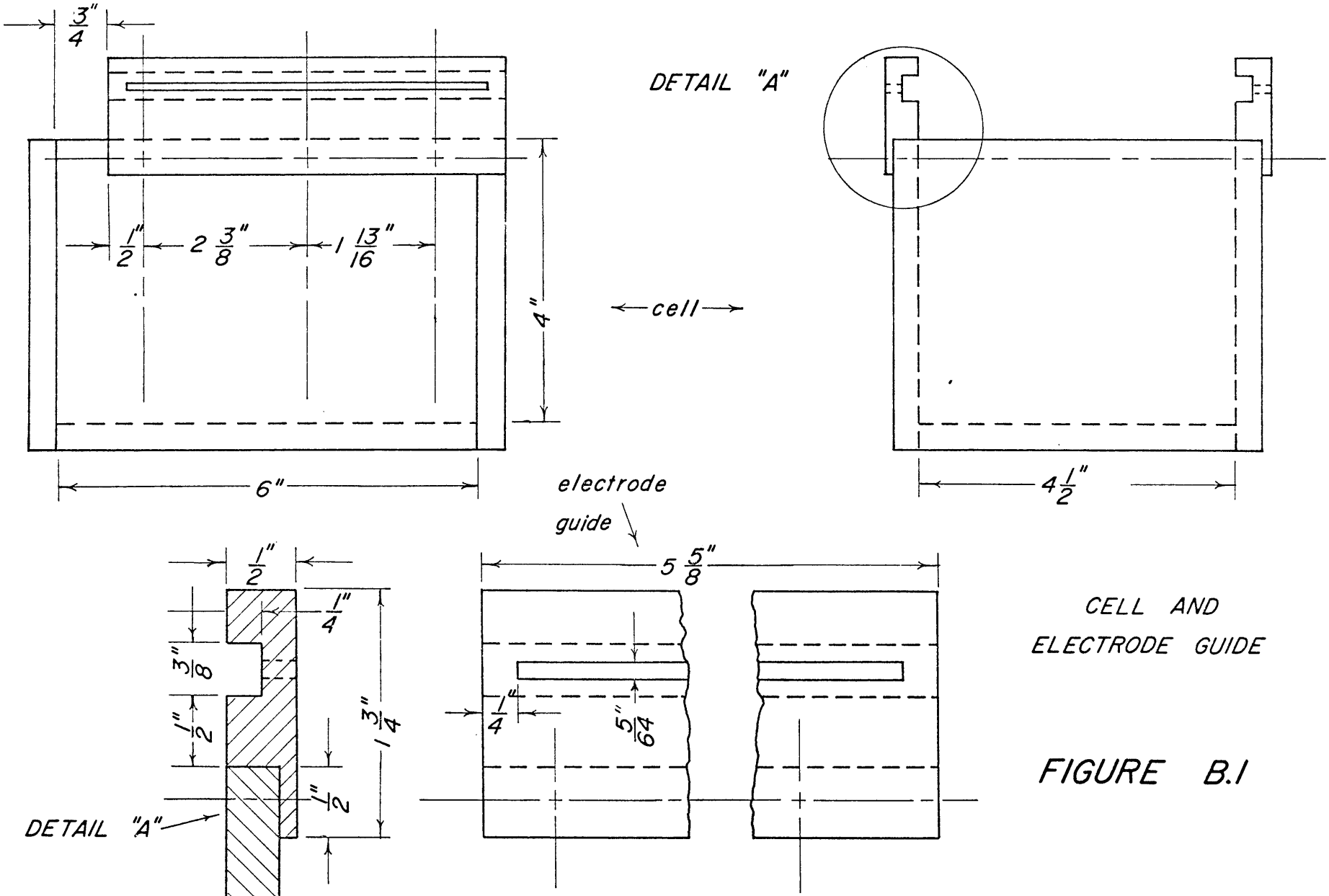

CELL AND
ELECTRODE GUIDE

FIGURE B.1

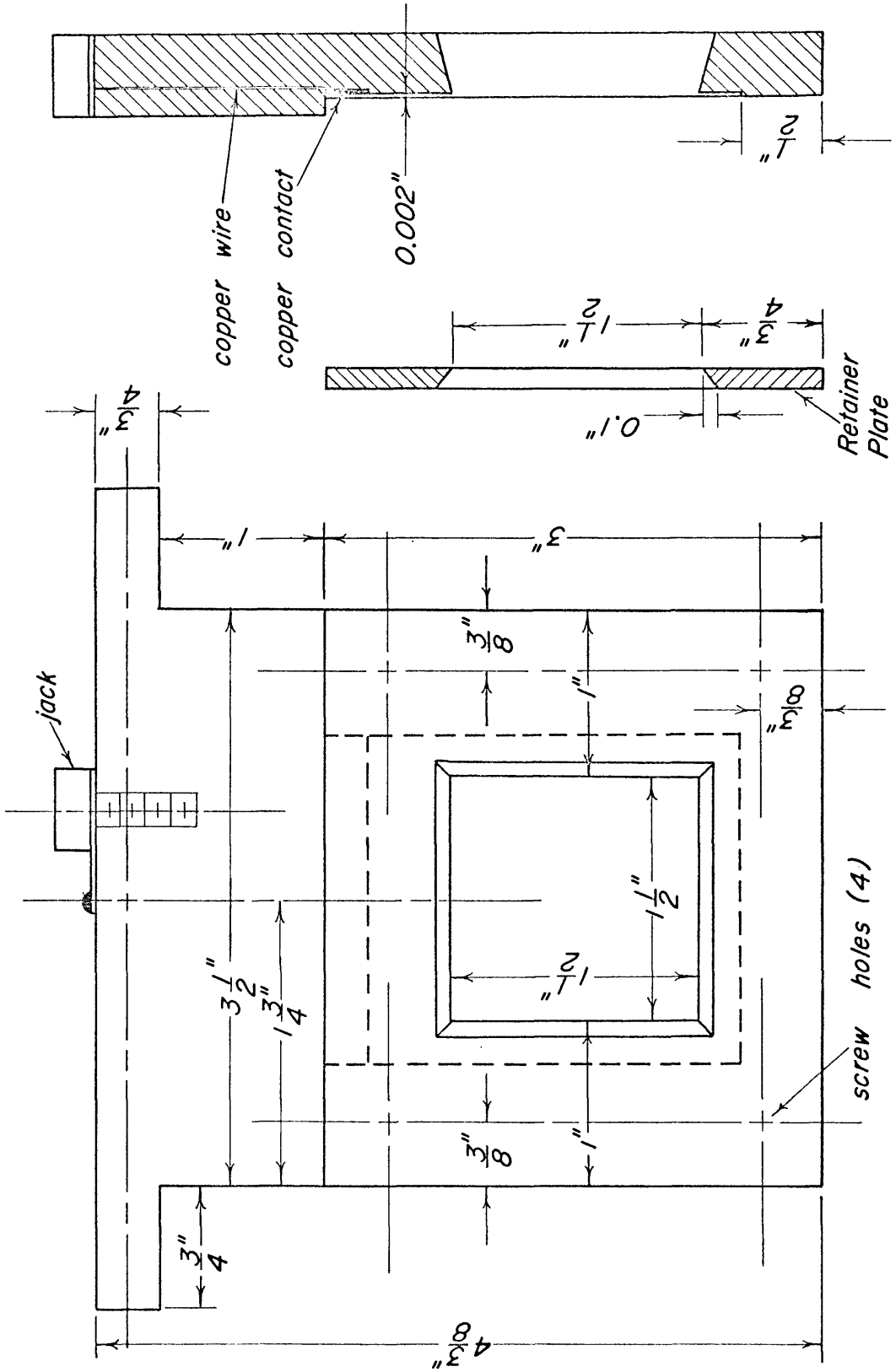

ELECTRODE HOLDER

FIGURE B.2

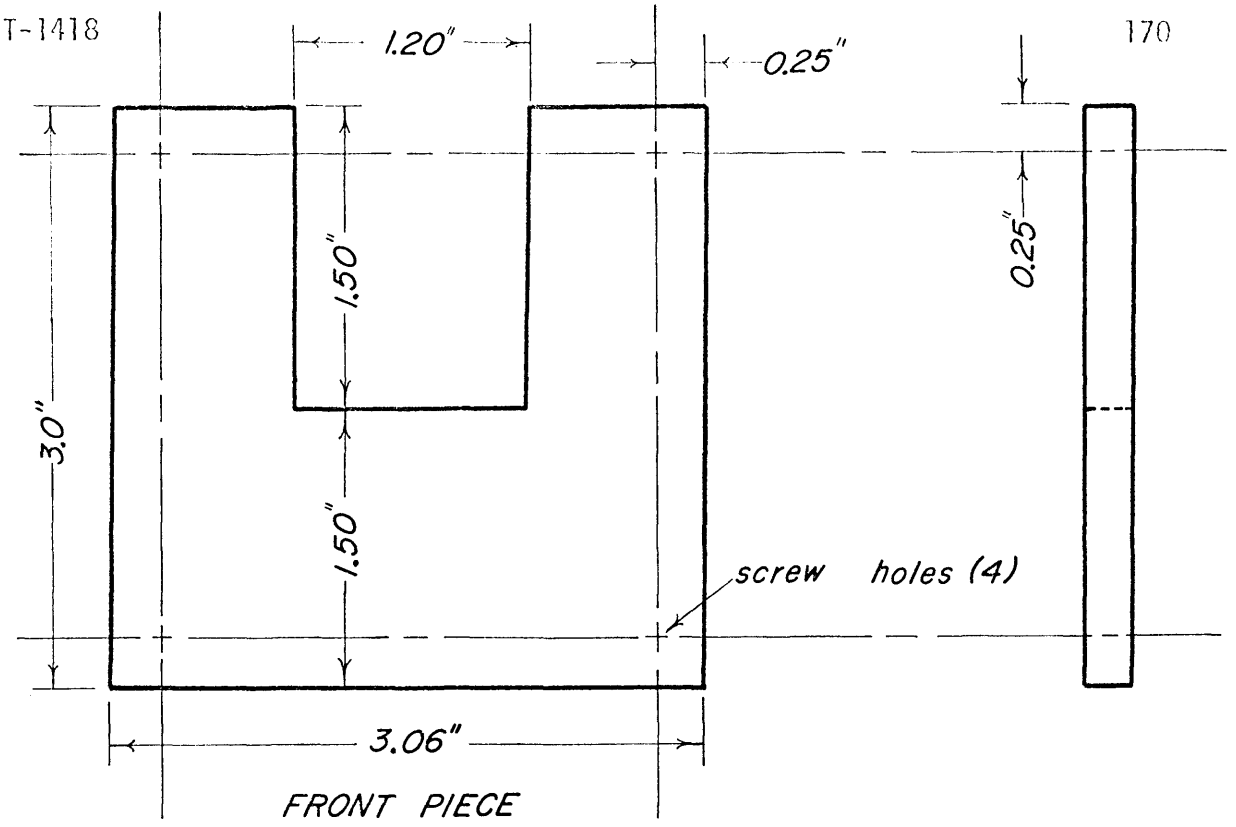

FRONT PIECE

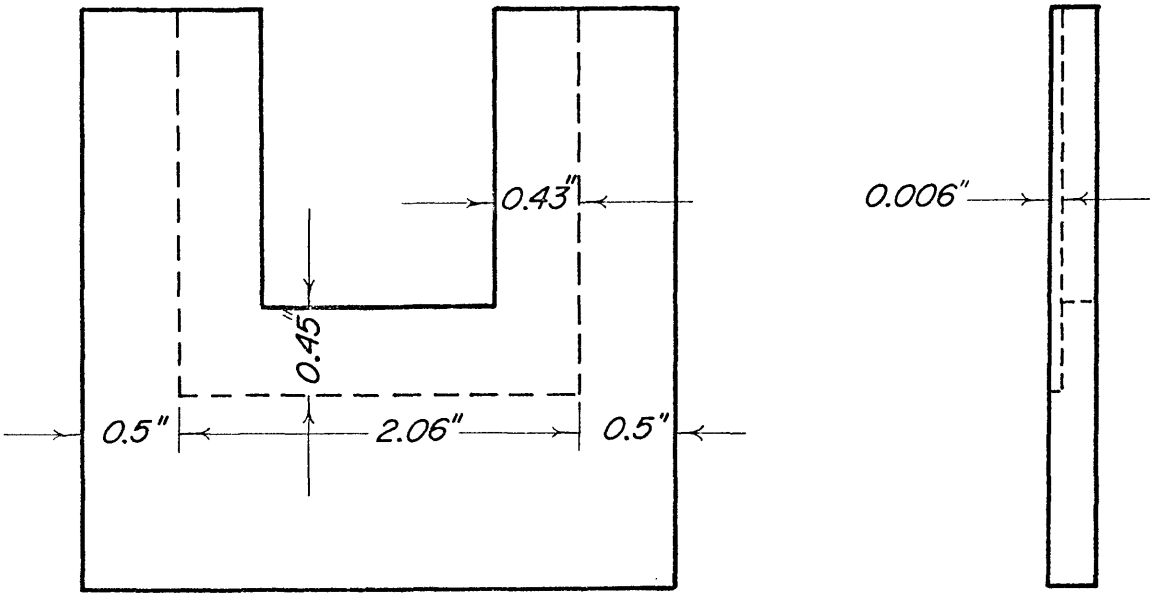

BACK PIECE

ELECTRODE JIG

FIGURE B.3

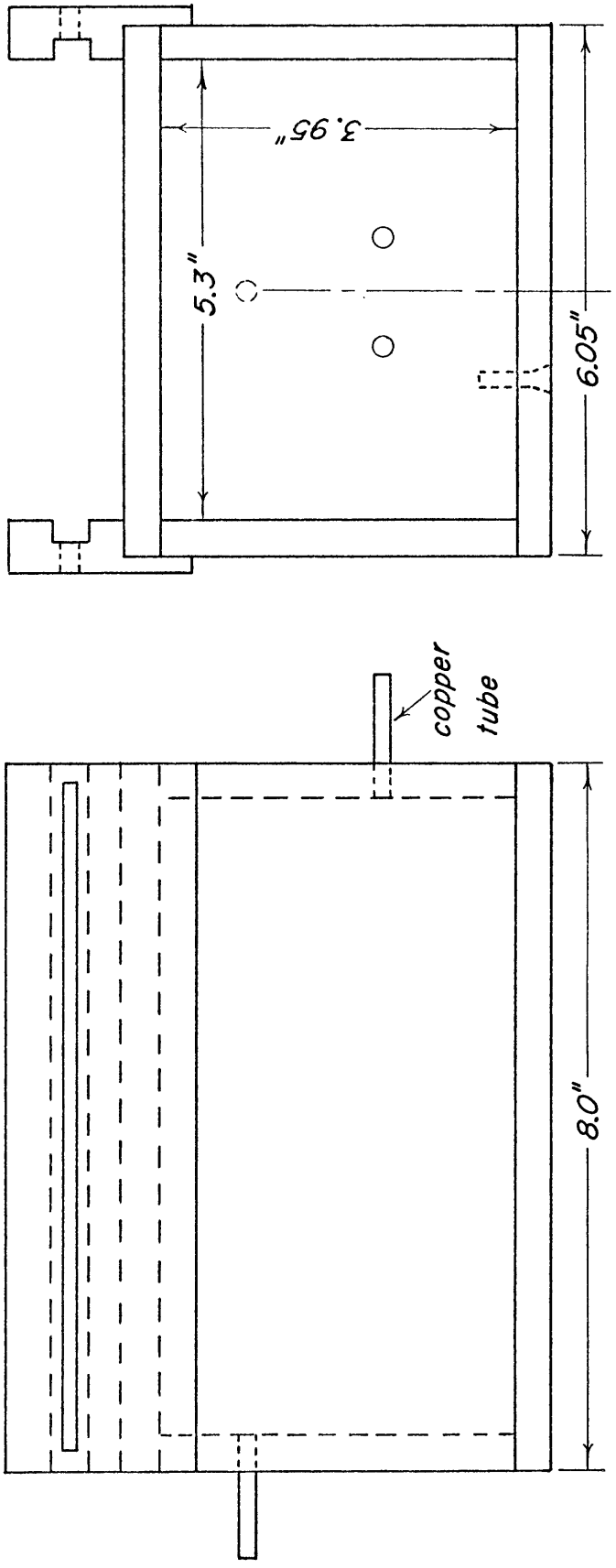

MAGNETIC STIRRER

FIGURE B.4

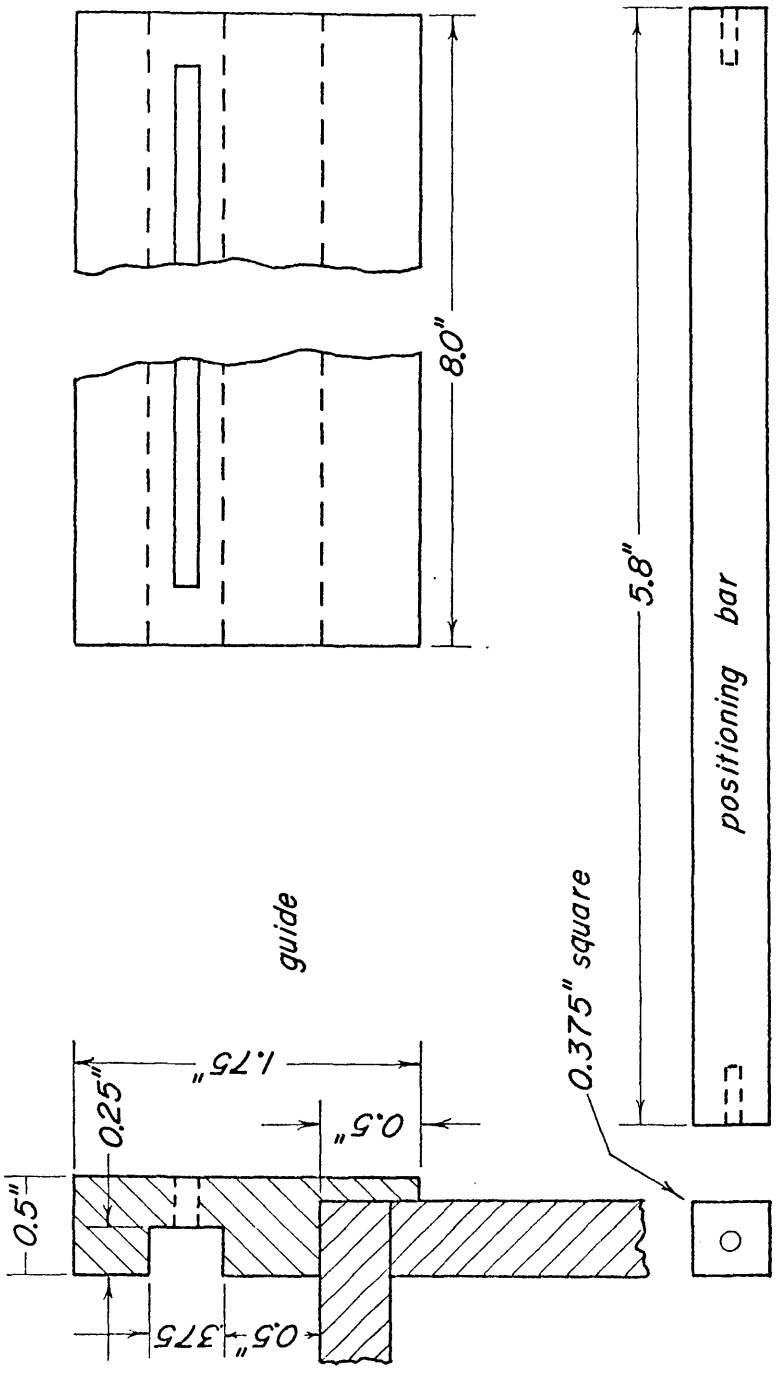

CELL GUIDE & POSITIONING BAR

FIGURE B.5

APPENDIX C

Construction of and Problems With the U-tube.

Detailed drawings of the U-tube and electrode holder are shown in Figures C.1 and C.2 respectively. When designing the U-tube and electrode holder several factors had to be considered. The basic design factors were simplicity and economy. The cell also had to be versatile. It had to have the capabilities of a controlled atmosphere, measurements at elevated temperatures, lack of contamination and ease in cleaning.

U-tube

The U-tube itself was constructed of Pyrex brand glass. A fritted glass (coarse grit) gas inlet tube was positioned in each arm of the tube. This was done in order to allow a purging atmosphere to be introduced into the electrolyte. The fritted glass permitted a more rapid purging by dispersing the purging gas through the solution in the form of many small bubbles. The electrode holder was fitted with an outlet hole which enabled the purging atmosphere to be directly vented into the atmosphere. The fritted glass disc (fine grit) dividing the two arms of the U-tube was needed in order to minimize mixing by convection. Division of the U-tube by such a method is standard practice in polarization studies and in no way disturbs the current flow.

Electrode Holder

The electrode holder was designed for use in the U-tube and for

use with the type of sample material available. The holder was constructed of glass tubing 0.3" outside diameter upon which a larger, threaded glass tube was attached at a 90° angle. A bakelite cap with a 0.4" hole drilled through the center was used to secure the sample to the holder. An o-ring was used to prevent leakage. Electrical contact was mad via a thin copper contact which in turn was attached to a shielded wire which lead through the stem of the holder.

The stem of the holder was mounted eccentrically in the nylon stopper which was machined to fit the ground joint of the U-tube. The eccentricity in the mounting provided a great deal of versatility when positioning the electrode. This mounting provided for both vertical and horizontal movement.

Figure C.3 shows in detail the method used to connect the Luggin-Haber probe to the reference electrode. The probe itself was filled with a special agar gel (see Appendix H). It was held to the U-tube by Tygon tubing. The tubing was filled with saturated potassium chloride making sure that no air bubbles were trapped in the solution. This tubing was then connected to a large diameter glass vial which also contained saturated potassium chloride and in which there was a saturated calomel electrode.

Shortcomings of the U-tube

Although the tube was designed with many factors in mind it did have some shortcomings. Many problems arose during use of the U-tube. The provisions made for the Luggin-Haber probe were not entirely satisfactory. Two main problems arose in this area. The probe was

hard to maintain and quite often failed because of air entrapment in the saturated potassium chloride solution or because of loss of the agar gel plug. It was also difficult to position the probe exactly equidistant from the electrode surface each time the electrode was changed. This factor introduced some random error in the IR drop corrections applied to the potential readings since these corrections depend on the probe to electrode distance.

Another serious problem arose because of the geometry of the U-tube. If it is supposed that the surfaces of the anode and cathode are two parallel and infinite planes, each of which is an equipotential plane, then it is obvious from geometrical considerations that the potential distribution between them can also be represented by a series of planes parallel to the two electrode surfaces. This is shown in Figure C.4, where planes A and B are electrodes and planes 1 - 7 are equipotential planes.

Two terms should now be defined. A "line of current flow" is a line which at all times is in the direction of current flow. A second useful term is that of "surfaces of current flow", which is a surface that at no time intersects a line of current flow. So, if any one point of a line of current flow lies in a given surface of current flow then the entire line lies within the surface. It also follows that a surface of current flow is necessarily always perpendicular to every equipotential surface.

Figure C.4 represents a situation in which the two electrode surfaces are parallel. This situation is called a linear conductor

and may be thought of as a wire of constant cross-section. In this instance a line of current flow is represented by a line perpendicular to the two electrode surfaces. A surface of current flow would be a plane perpendicular to and intersecting both electrode surfaces.

An example of another situation is shown in Figure C.5. Here the electrode surfaces are inclined to each other. In this situation AD may be considered to be an equipotential plane some distance from the electrode surface represented by BC. As the plane AD is approached the system tends to simulate a linear conductor; that is to say, the equipotential surfaces are parallel planes and the per unit potential differences are equally space.

However, as the plane BC is approached the equipotential surfaces tend to bend until at BC they assume the shape of BC. From previous definitions it then follows that the lines of current flow must also bend in order to remain perpendicular to the equipotential surfaces. This means that there will be a higher current density at B than there will be at C.

The same type of situation was present in the U-tube. From Figure C.6 it is possible to see that if the Luggin-Haber probe was positioned at point A, then the probe would be intersecting only one equipotential surface. However, at point B the probe might be intersecting two or more equipotential surfaces. This would give potential readings that were of a mixed nature. The likelyhood of this having occurred during any of the polarization experiments was small, since the probe was always positioned at the center of the electrode surface.

A second problem with the probe that arises in this situation is that of the IR drop corrections. All IR drop corrections were made assuming a rectangular volume of electrolyte between the probe tip and the electrode surface. However, Figure C.6 shows there to be a non-rectangular volume with a cross-section of abcd. This would certainly introduce some errors.

The actual presence of a higher current density at the bottom of the electrode surface was shown to be true experimentally. Figure C.7 shows a photograph of an actual electrode sample. It can be seen that a small portion of the electrode was corroded through. This portion had been the bottom of the electrode and theoretically had the highest current density.

The preceding discussion was based on the assumption that the electrodes are infinite planes. In actual practice the electrodes were finite and this made a difference. By looking at Figure C.5 it is evident that theoretically the highest current density should occur at the very bottom of the electrode, however, Figure C.7 shows that in actual practice the highest current density occurred not at the extreme bottom of the electrode but at some point higher up and more towards the center of the electrode.

This is due to some shielding effects of the electrode holder as shown in Figure C.8. From this figure it can be seen that the bakelite cap and o-ring interfered with the lines of current flow by introducing a sharper corner for them to go around. This meant the point of highest current density was moved upward. This situation also produced the rounded corners as pointed out in Figure C.8 and shown in Figure C.7

U-TUBE CELL

Figure C.1

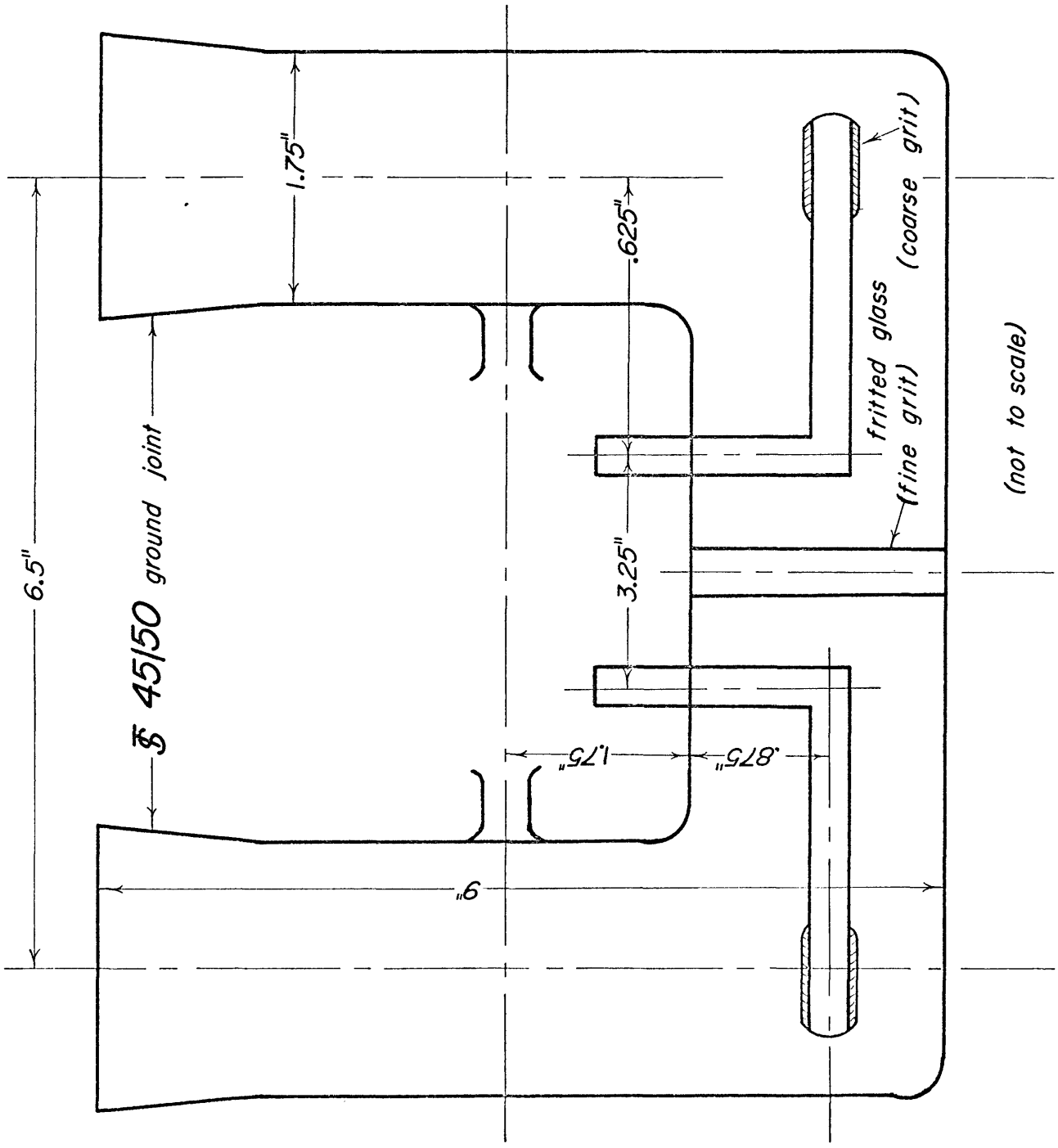

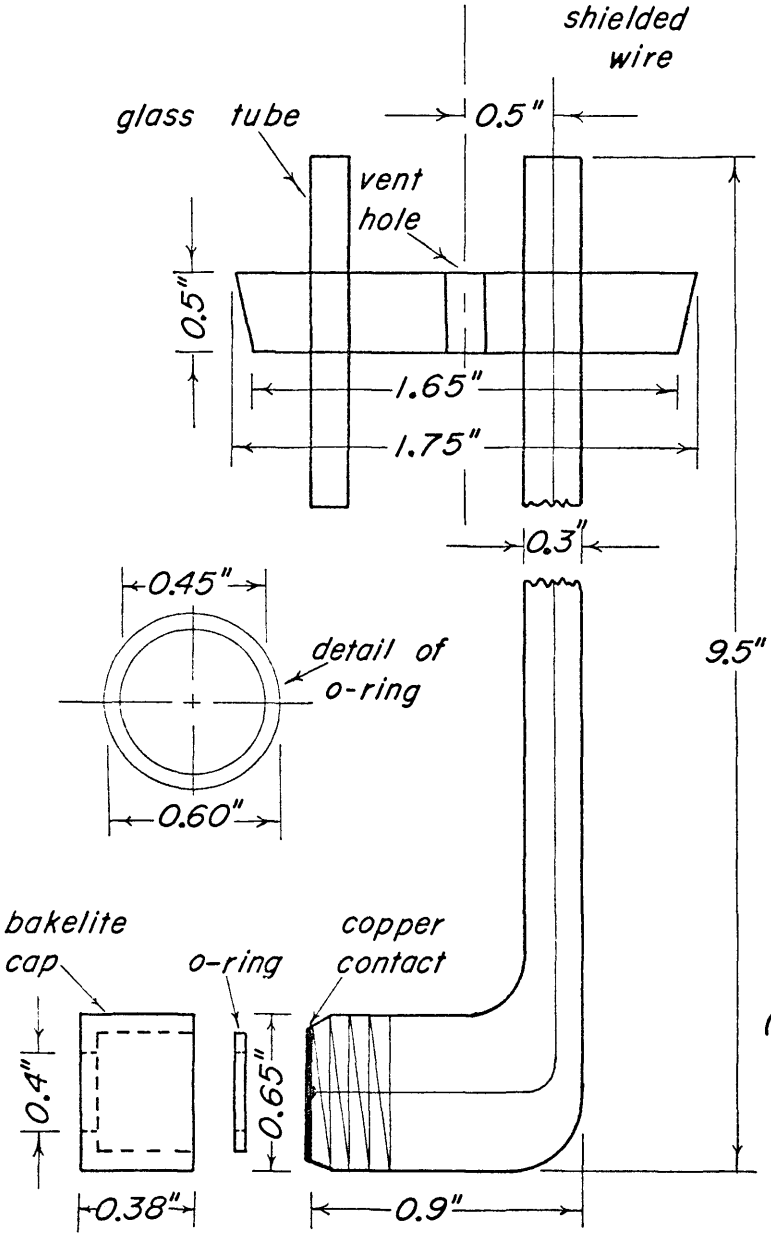

ELECTRODE HOLDER

LUGGIN-HABER CAPILLARY PROBE ASSEMBLY

(not to scale)

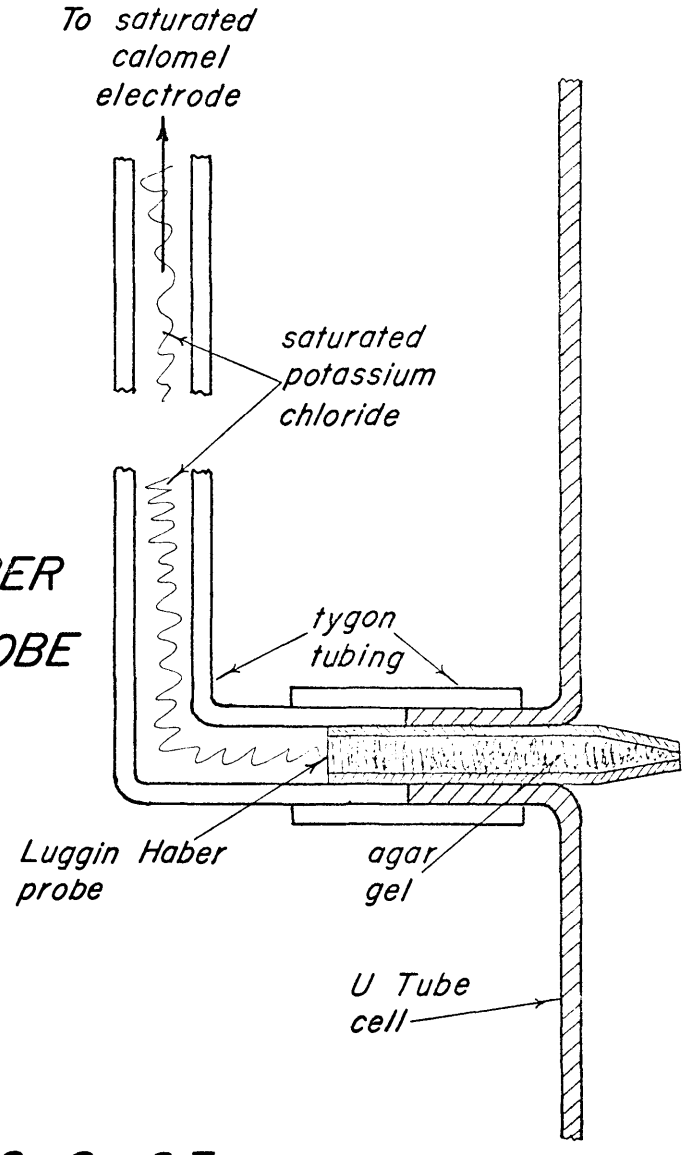

Figures C.2 & C.3

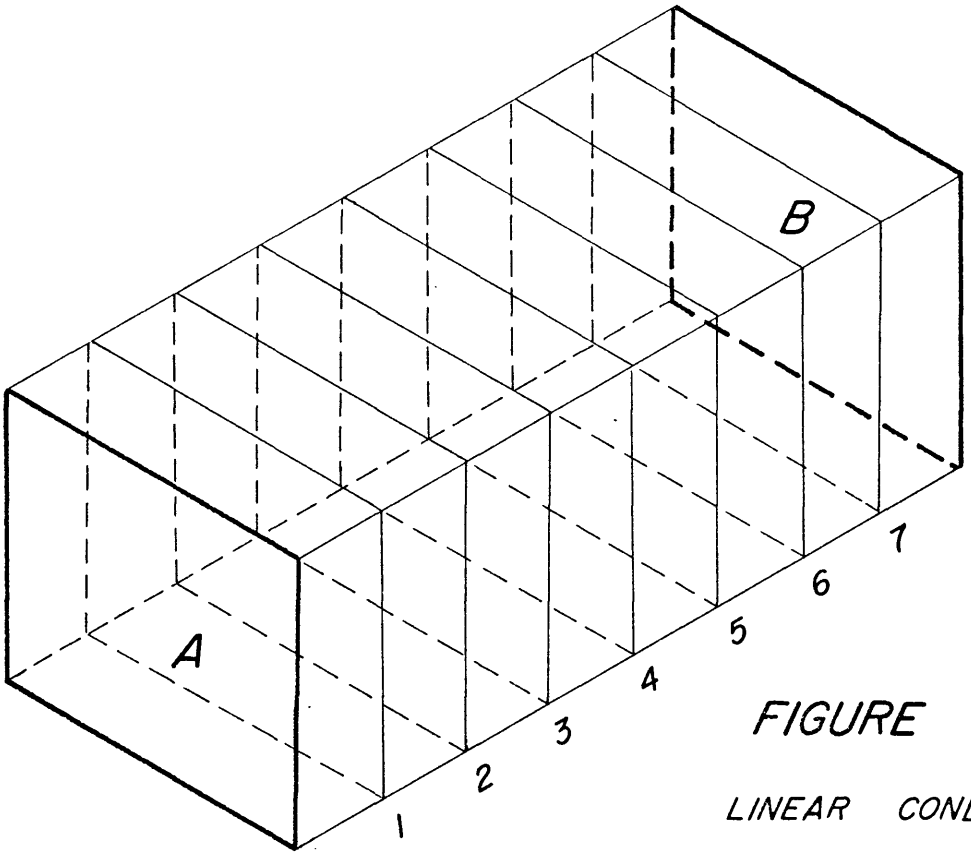

FIGURE C.4

LINEAR CONDUCTOR

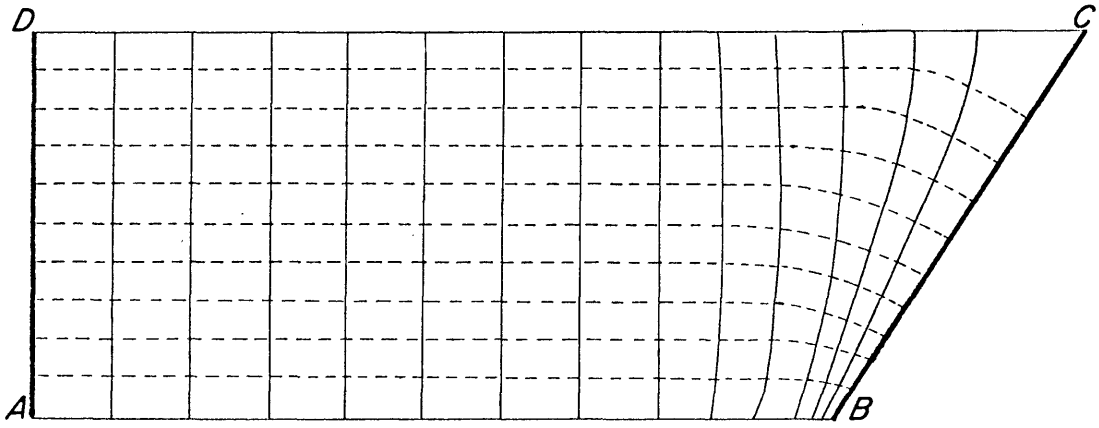

FIGURE C.5

INCLINED ELECTRODE

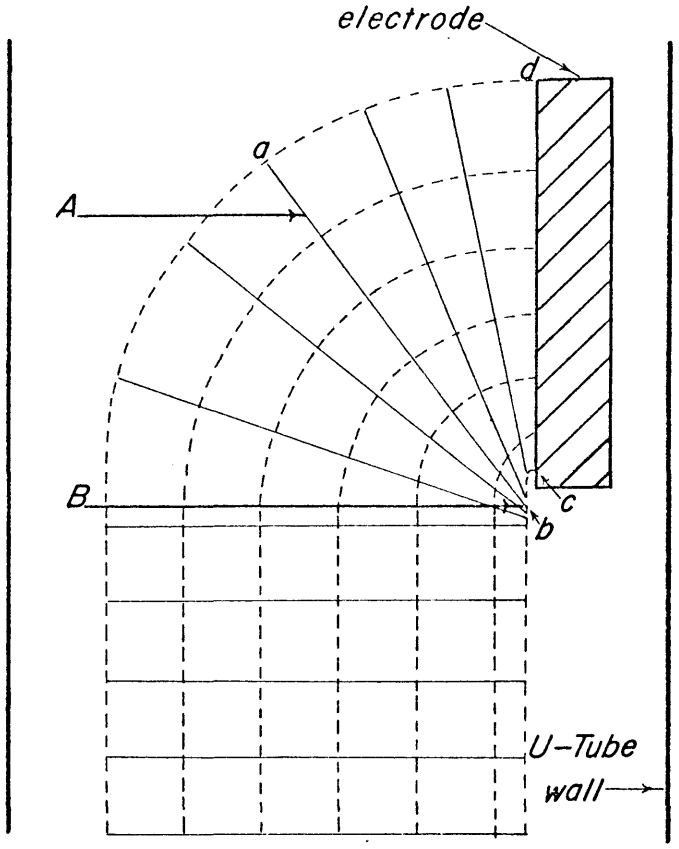

PROBE POSITION AND IR DROP ERRORS

FIGURE C.6

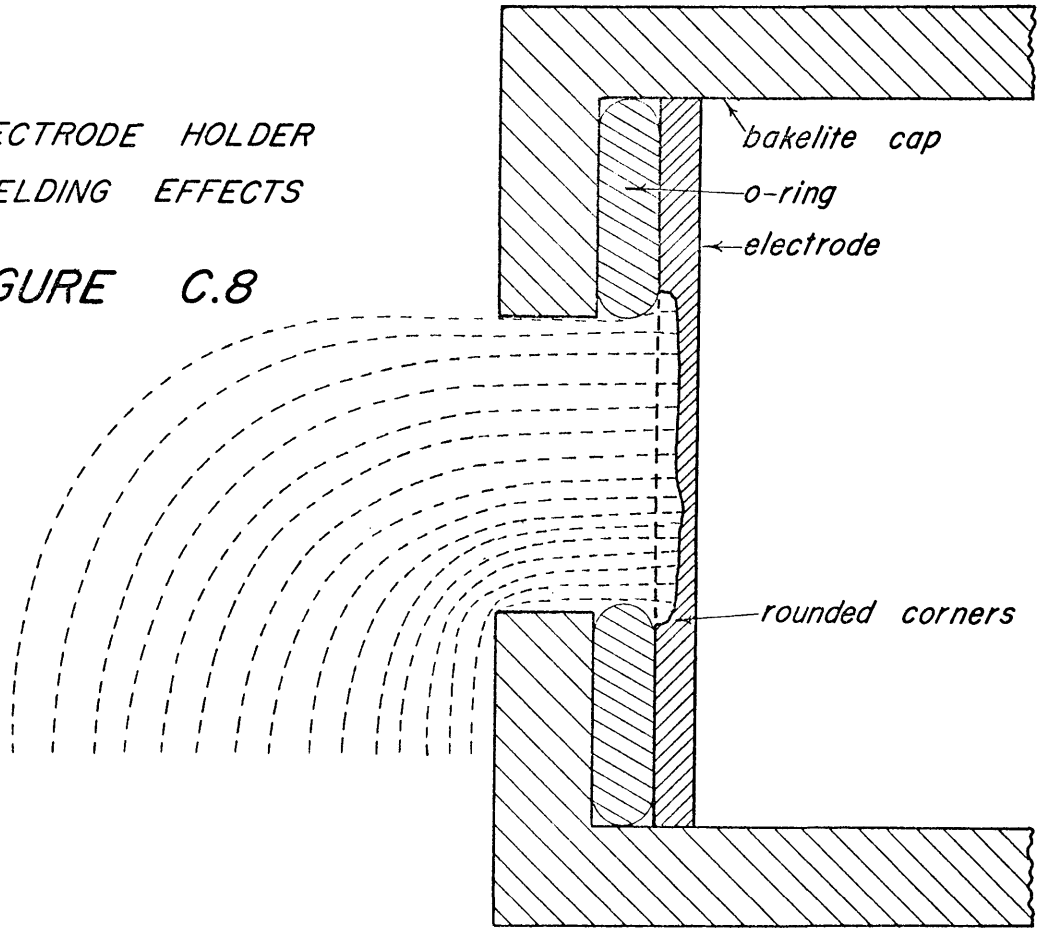

ELECTRODE HOLDER SHIELDING EFFECTS

FIGURE C.8

FIGURE C.7 Photograph Of An Actual Electrode Surface

APPENDIX D

Sample Preparation

A standard method of electrode preparation was devised in order to assure identical electrode surfaces throughout the empirical tests. The method is as follows:

Step 1. Each electrode consisting of a piece of copper foil measuring 2" x 2 1/2" was given an initial cleaning and etch by immersing it in a near boiling 30% nitric acid solution for a period of 10 seconds.

Step 2. After the initial cleaning and etch each electrode was completely taped on both sides using Scotch brand Electroplating Tape No. 470. The taped electrode was then passed between a set of steel rollers to insure that the tape was adhering securely.

Step 3. Next an area of tape measuring 1.2" x 1.2" was removed in order to expose a working surface. This was done by using a jig as shown in Figure B.3, Appendix B. The taped electrode was slipped into the jig by inserting it into the recessed area shown. Next two blocks of plexiglas measuring 1.2" x 1.2" were clamped onto the electrode. The electrode was then removed from the jig and a razor blade used to cut the tape around one block. The blocks were then removed and the cut tape pulled off to expose the working area.

Step 4. The electrode was then given a final cleaning and etch by again immersing it in a near boiling 30% nitric acid solution for a period of 10 seconds.

Step 5. A small strip of tape was then removed from the top back part of the electrode. This was necessary in order to assure electrical contact with the copper strip in the electrode holder. The sample was then loaded into the electrode holder. Silicone grease was used to seal the electrode in the electrode holder. This insured that the electrolyte was in contact only with the working surface of the electrode.

Step 6. The last step was to load the electrode holders containing the electrodes into the cell. Spacing of the electrode holders was accomplished by using spacing bars made of plexiglas held between the electrode holders as they were fastened into the cell. These spacing bars were then removed. The use of these bars assured a constant spacing of the electrodes from test to test. They also assured that the electrodes would be identically spaced in relationship to the stirring bar from test to test.

APPENDIX E

Calculation of Specific Conductance Values Used in IR Drop Corrections

To properly correct the data of the polarization tests for IR drop, the specific conductance of each solution had to be known. These values were not experimentally measured and therefore had to be calculated. This was done by using a method proposed by Skowronski and Reinoso (Skowronski and Reinoso, 1927). By using their data and data collected earlier by Kern and Chang (Kern and Chang, 1922) it was possible to readily determine the specific conductance of the test solutions involved.

Skowronski and Reinoso found that within the limits of their electrolyte composition the effect of copper, nickel, arsenic and iron on increasing the resistivity of the electrolyte was directly proportional to the amount added. They developed a term which they called the "percentage resistivity". This factor is used to express the percentage difference in resistivity of any electrolyte as compared to a standard electrolyte.

By using such a system it was possible for Skowronski and Reinoso to determine that even though the addition of copper, nickel, iron and arsenic to a sulfuric acid electrolyte increased the resistivity at varying acid concentrations the percentage resistivity remained constant as if no metallic salts had been added.

From their data they found the following percentage resistivities using a base electrolyte of 150 gpl H_2SO_4 at a temperature of 55°C (this electrolyte had a specific resistance $\rho = 1/\kappa = 1.364$ ohms/cm^3)

Percentage resistivity of copper = 100.000 + 0.657 (gpl Cu)

Percentage resistivity of nickel = 100.000 + 0.766 (gpl Ni)

A comparison of specific conductance values calculated by this method for actual refining electrolytes and measured values show an error of less than 1%.

Sample Calculation

A sample calculation for the electrolyte of tests 13 and 14 is shown below. The electrolyte composition was:

Copper = 10 gpl

Nickel = 5 gpl

H_2SO_4 = 100 gpl

Temperature = 25 °C

Percentage resistivity of Copper = 100.000 + 0.657 (10)

Percentage resistivity of Copper = 106.57 %

Percentage resistivity of Nickel = 100.000 + 0.766 (5)

Percentage resistivity of Nickel = 103.83 %

Percentage resistivity of H_2SO_4 = 180.37 % *

Total percentage resistivity = 106.57 % x 103.83 % x 180.37 %

Total percentage resistivity = 199.47 %

Specific resistance = 1.9947 x 1.364

Specific resistance = 2.722 = ρ

Specific conductance = $1/\rho$ = 1/2.722 = 0.367 = κ

*The value of percentage resistivity for the H_2SO_4 is arrived at by first finding the percentage resistivity of 100 gpl H_2SO_4 at 55 °C and then correcting this for 25 °C.

Percentage resistivity of 100 gpl H_2SO_4 at 55 °C = 139.48 % (as against the standard of 150 gpl H_2SO_4 at 55 °C)

Percentage resistivity of loo gpl H_2SO_4 at 25 °C = 129.32 %

Total percentage resistivity = .39.48 % x 129.32 %

Total percentage resistivity = 180.37 %

TABLE 1.E

Specific Conductance Values

Used in IR Drop Corrections

Test No.	κ (ohm^{-1}/cm)	Test No.	κ (ohm^{-1}/cm)
1	0.212	20	0.339
2	0.212	21	0.339
3	0.212	22	0.337
4	0.407	23	0.337
5	0.407	24	0.327
6	0.380	25	0.327
7	0.380	26	0.380
8	0.380	27	0.380
9	0.380	28	0.367
10	0.378	29	0.315
11	0.378	30	0.315
12	0.378	31	0.304
13	0.367	32	0.304
14	0.367	33	0.354
15	0.354	34	0.354
16	0.354	35	0.406
17	0.342	36	0.406
18	0.342	37	0.215
19	0.339		

APPENDIX F

Computer Programs Used in Polarization Calculations

Various calculations for the polarization tests were done using a computer. A listing of each program in Basic Language is given in this appendix.

Program Number 1

This program was used to correct the potential readings as read on the electrometer. It was found by comparing the electrometer to a secondary standard that it did not give accurate measurements. This program took the data from the electrometer and corrected it for the errors present in the readings.

Program Number 2

This program was used to make the IR drop corrections on the potential readings corrected in Program Number 1.

Program Number 3

This program is a curve fitting program using a least-squares polynomial method and was used to smooth some of the data from Program Number 2.

Program Number 4

This program is also a curve fitting program using least-squares and was also used to smooth some of the data from Program Number 2.

Program Number 5

This program was used to calculate exchange current densities and overvoltages using both theoretical and experimental parameters.

PROGRAM NUMBER 1

```
 10 PRINT "************************************************"
 20 PRINT "*                                              *"
 30 PRINT "*   PROGRAM FOR THE CORRECTION OF ELECTROMETER  *"
 40 PRINT "*   POTENTIAL READINGS FOR ANODIC POLARIZATION  *"
 50 PRINT "*                                              *"
 60 PRINT "************************************************"
 70 PRINT
 80 PRINT
 90 PRINT "C1 = CORRECTION COEFFICIENT FOR 100-300 MILLIVOLTS"
100 PRINT "C2 = CORRECTION COEFFICIENT FOR 300-500 MILLIVOLTS"
110 PRINT "C3 = CORRECTION COEFFICIENT FOR 500-700 MILLIVOLTS"
120 PRINT "C4 = CORRECTION COEFFICIENT FOR 700-1000 MILLIVOLTS"
130 PRINT
140 PRINT
150 READ T
160 DATA 18
170 PRINT "TEST NO. "; T
180 PRINT
190 PRINT
200 PRINT "MEASURED", "CORRECTED"
210 PRINT "POTENTIAL", "POTENTIAL"
220 READ C1, C2, C3, C4
230 DATA 1.026, 1.031, 1.024, 1.022
240 READ P
250 IF P>30 THEN 280
260 LET P1 = P
270 GO TO 410
280 IF P>100 THEN 310
290 LET P1 = P + 1
300 GO TO 410
310 IF P>300 THEN 340
320 LET P1 = P*C1
330 GO TO 410
340 IF P>500 THEN 370
```

```
350 LET P1 = P*C2
360 GO TO 410
370 IF P>700 THEN 400
380 LET P1 = P*C3
390 GO TO 410
400 LET P1 = P*C4
410 PRINT P, P1
420 GO TO 240
430 DATA
440 DATA
450 DATA
460 DATA
500 END
```

PROGRAM NUMBER 2

```
 10 DIM I(50), C(50), P(50), U(50), R(50), D(50)
 20 READ T
 30 DATA 2
 40 READ L, A, K
 50 DATA 0.8, 1.1193, 0.212
 60 READ N
 70 DATA 45
 80 PRINT "PROGRAM FOR THE CALCULATION AND CORRECTION OF THE"
 90 PRINT "IR DROP WHEN USING THE LUGGIN-HABER CAPILLARY"
100 PRINT
110 PRINT
120 PRINT
130 REM THE FOLLOWING LIST IS THAT OF THE NOMENCLATURE USED
140 REM IN THIS PROGRAM
150 REM N = NUMBER OF POINTS
160 REM L = DISTANCE OF CAPILLARY TIP FROM ELECTRODE, CM
170 REM A = CROSS-SECTIONAL AREA OF IR DROP, CM2
180 REM I(N) = CURRENT, AMPS
190 REM C(N) = CURRENT DENSITY, AMPS/CM2
200 REM D(N) = CURRENT DENSITY, MA/CM2
210 REM K = SPECIFIC CONDUCTANCE, OHM-1 CM-1
220 REM T = TEST NUMBER
230 REM P(N) = MEASURED POTENTIAL, MV
240 REM U(N) = CORRECTED POTENTIAL, MV
250 REM R(N) = IR DROP, MV
260 PRINT "TEST NUMBER"; T
270 PRINT
```

```
280 PRINT "NUMBER OF POINTS ="; N
290 PRINT "A = ";A;"CM2"
300 PRINT "K = ";K;"OHM-1 CM-1"
310 PRINT "L = ";L;"CM"
320 PRINT
330 PRINT
340 PRINT
350 PRINT "AMPS", "MA/CM2", IR DROP","MEAS. P", "CORR. P"
360 PRINT
370 FOR S = 1 TO N
380 READ I(S), P(S)
390 NEXT S
400 GO TO 450
450 FOR W = 1 TO N
460 LET C(W) = I(W) / (A*1000)
470 LET R(W) = (C(W)*L*1000)/K
480 LET U(W) = P(W) - R(W)
490 LET D(W) = C(W)*1000
500 PRINT I(W), D(W), R(W), P(W), U(W)
510 NEXT W
520 PRINT
530 PRINT
540 PRINT
550 DATA
560 DATA
570 DATA
900 END
```

PROGRAM NUMBER 3

```
10 DATA 14, 1
15 READ M, N
20 DIM A(15), B(15), S(15), G(15), U(15)
25 DIM Q(100), P(100), X(100), Y(100), C(100)
30 LET Z = 0
35 LET O = 1
40 LET K = 12
45 LET N = N+1
50 IF N>12 THEN 576
55 IF M<N THEN 616
60 IF M>100 THEN 570
70 LET T7 = Z
75 LET T8 = Z
80 LET W7 = Z
```

```
100 DATA
101 DATA
102 DATA
103 DATA
300 FOR I = 1 TO M
302 READ X(I), Y(I)
304 LET W7 = W7 + X(I)
306 LET T7 = T7 + Y(I)
308 LET T8 = T8 + Y(I)↑2
310 NEXT I
312 LET T9 = (M*T8-T7↑2)/(M↑2 - M)
314 PRINT
316 PRINT "L E A S T - S Q U A R E S  P O L Y N O M I A L S"
318 PRINT
320 PRINT "       NUMBER OF POINTS = "; M
322 PRINT "        MEAN VALUE OF X = "; W7/M
324 PRINT "        MEAN VALUE OF Y = "; T7/M
326 PRINT "         STD ERROR OF Y = "; SQR(T9)
328 PRINT
330 PRINT "   NOTE:  CODE FOR WHAT NEXT?  IS:"
332 PRINT
334 PRINT "            0 = STOP PROGRAM"
336 PRINT "            1 = COEFFICIENTS ONLY"
338 PRINT "            2 = ENTIRE SUMMARY"
340 PRINT "            3 = FIT NEXT HIGHER DEGREE"
342 PRINT
344 PRINT
346 FOR I = 1 TO M
348 LET P(I) = Z
350 LET Q(I) = 0
352 NEXT I
354 FOR I = 1 TO 11
356 LET A(I) = Z
358 LET B(I) = Z
360 LET S(I) = Z
362 NEXT I
364 LET E1 = Z
366 LET F1 = Z
368 LET W1 = M
370 LET N4 = K
372 LET I = 1
374 LET K1 = 2
376 IF N = 0 THEN 380
378 LET K1 = N4
380 LET W = Z
382 FOR L = 1 TO M
384 LET W = W + Y(L)*Q(L)
386 NEXT L
388 LET S(I) = W/W1
390 IF I-N4>= 0 THEN 428
```

```
391 IF I-11>= 0 THEN 428
392 LET E1 = Z
394 FOR L = 1 TO M
396 LET E1 = E1 + X(L)*Q(L)*Q(L)
398 NEXT L
400 LET E1 = E1/W1
402 LET A(I+1) =E1
404 LET W = Z
406 FOR L = 1 TO M
408 LET V = (X(L) - E1)*Q(L) - F1*P(L)
410 LET P(L) = Q(L)
412 LET Q(L) = V
414 LET W = W + V*V
416 NEXT L
418 LET F1 = W/W1
420 LET B(I+2) = F1
422 LET W1 = W
424 LET I = I+1
426 GO TO 380
428 FOR L = 0 TO 12
430 LET G(L) = Z
432 NEXT L
434 LET G(1) = 0
436 FOR J = 1 TO N
438 LET S1 = Z
440 FOR L = 1 TO N
442 IF L = 1 THEN 446
444 LET G(L) = G(L) - A(L)*G(L-1) - B(L)*G(L-2)
446 LET S1 = S1 + S(L)*G(L)
448 NEXT L
450 LET U(J) = S1
452 LET L = N
454 FOR I2 = 2 TO N
456 LET G(L) = G(L-1)
458 LET L = L-1
460 NEXT I2
462 LET G(1) = Z
464 NEXT J
466 PRINT
468 LET T = Z
470 FOR L = 1 TO M
472 LET C(L) = Z
474 LET J = N
476 FOR I2 = 1 TO N
478 LET C(L) = C(L)*X(L) + U(J)
480 LET J = J-1
482 NEXT I2
484 LET T3 = Y(L) - C(L)
486 LET T = T + T3↑2
488 NEXT L
```

```
490 IF M<>N THEN 496
492 LET T5 = 0
494 GO TO 498
496 LET T5 = T/(M-N)
498 LET Q7 = 1-T/(T9*(M-1))
500 PRINT
502 PRINT " POLYFIT OF DEGREE ";N-1;
504 PRINT " INDEX OF DETERM = ";Q7;
506 GOSUB 622
508 PRINT
510 PRINT
512 IF R = 0 THEN 628
514 IF R = 3 THEN 564
516 PRINT " TERM", "COEFFICIENT"
518 PRINT
520 FOR J = 1 TO N
522 LET I2 = J-1
524 PRINT I2, U(J)
526 NEXT J
528 IF R = 1 THEN 558
530 PRINT
532 PRINT "X-ACTUAL", "Y-ACTUAL", "Y-CALC", "DIFF", "PCT-DIFF"
534 PRINT
536 FOR L = 1 TO M
538 LET Q8 = Y(L) - C(L)
540 PRINT X(L), Y(L), C(L), Q8
542 IF C(L) = 0 THEN 548
544 PRINT 100*Q8/C(L)
546 GO TO 550
548 PRINT "INFINITE"
550 NEXT L
552 PRINT
554 PRINT"          STD ERROR OF ESTIMATE FOR Y = "; SQR(T5)
556 IF K = N THEN 628
558 PRINT
560 GOSUB 622
562 GO TO 512
564 LET N = N+1
565 IF N>12 THEN 576
566 IF M<N THEN 616
568 GO TO 428
570 PRINT
572 PRINT "PROGRAM SIZE LIMIT IS 100 POINTS"
574 GO TO 628
576 PRINT "ELEVENTH DEGREE IS THE LIMIT"
578 GO TO 628
580 PRINT
582 PRINT "THIS PROGRAM FITS LEAST-SQUARES POLYNOMIALS TO BIVARIATE"
584 PRINT "DATA, USING AN ORTHOGONAL POLYNOMIAL METHOD.  LIMITS ARE"
586 PRINT "11-TH DEGREE FIT AND A MAX OF 100 DATA POINTS.  PROGRAM"
```

```
588 PRINT "ALLOWS USER TO SPECIFY THE LOWEST DEGREE POLYNOMIAL TO BE"
590 PRINT "FIT, AND THEN FITS THE POLYNOMIALS IN ORDER OF ASCENDING"
592 PRINT "DEGREE.  AT EACH STAGE, THE INDEX OF DETERMINATION IS"
594 PRINT "PRINTED, AND THE USER HAS THE CHOICE OF GOING TO THE NEXT"
596 PRINT "HIGHER DEGREE FIT, SEEING EITHER OF TWO SUMMARIES OF FIT"
598 PRINT "AT THAT STAGE, OR OF STOPPING THE PROGRAM.  TO USE, TYPE:"
600 PRINT
602 PRINT "   10 DATA N, D"
604 PRINT "            (WHERE N = NUMBER OF DATA POINTS TO BE READ"
606 PRINT "            AND D = INITIAL (LOWEST) DEGREE TO BE FIT)"
608 PRINT "   100 DATA X(1), Y(1), X(2), Y(2), . . . . , X(N), Y(N)"
610 PRINT "          (CONTINUATION OF LINES 101 - 299 AS NEEDED)"
612 PRINT "  RUN"
614 GO TO 628
616 PRINT
618 PRINT "TOO FEW POINTS FOR FITTING DEGREE"; N-1
620 GO TO 628
622 PRINT "WHAT NEXT?"
624 INPUT R
626 RETURN
628 END
```

PROGRAM NUMBER 4

```
  1 REM  THIS PROGRAM FITS A POLYNOMIAL TO A SET OF POINTS.  IT
  2 REM  WILL FIT UP TO THE FIFTH DEGREE BUT WILL PRESENT ROUNDOFF
  3 REM  ERRORS AT THIS LEVEL.  IT IS VERY RELIABLE UP TO THE
  4 REM  FOURTH DEGREE.  THE MAXIMUM NUMBER OF POINTS TO BE USED
  5 REM  IS 50 UNLESS MODIFICATIONS ARE MADE.
 10 DATA 13, 3
 12 DATA
 13 DATA
 14 DATA
100 DIM X(50), Y(50), B(50), A(7,7)
110 READ N, K
120 FOR J = 1 TO N
130 READ Y(J)
140 NEXT J
150 FOR J = 1 TO N
160 READ X(J)
170 NEXT J
180 LET K1 = K+1
190 LET K2 = K+2
```

```
200 LET K3 = K+K
210 FOR M = 1 TO K3
220 LET S = 0
230 FOR I1 = 1 TO N
240 LET S = S + X(I1)↑M
250 NEXT I1
260 LET I1 = 1 + (M+1)/2
270 FOR I = 1 TO I1
280 LET J = M - I+2
290 IF J>6 THEN 320
300 LET A(I,J) = S
310 LET A(J,I) = S
320 NEXT I
325 NEXT M
330 FOR I = 1 TO K
340 LET S = 0
350 FOR I1 = 1 TO N
360 LET S = S + Y(I1)*X(I1)↑I
370 NEXT I1
380 LET A(I+1,K2) = S
390 NEXT I
400 LET S = 0
410 FOR I1 = 1 TO N
420 LET S = S + Y(I1)
430 NEXT I1
440 LET A(1,K2) = S
450 LET A(1,1) = N
460 FOR I = 1 TO K
470 LET I1 = I + 1
480 FOR J = I1 TO K1
490 LET K3 = K2 + 1
500 FOR M = I1 TO K2
510 LET K3 = K3 - 1
520 LET A(J,K3) = A(J,K3) - A(J,I)*A(I,K3)/A(I,I)
530 NEXT M
540 NEXT J
550 NEXT I
560 LET K3 = K2
570 FOR J = 1 TO K1
580 LET M = K3
590 LET K3 = K3 - 1
600 LET S = 0
610 FOR I = M TO K2
620 IF K2<= I THEN 650
630 LET S = S + A(K3,I)*B(I)
640 NEXT I
650 LET B(K3) = (A(K3,K2)-S)/A(K3,K3)
655 NEXT J
660 PRINT " NUMBER OF POINTS = "; N
670 PRINT
```

```
680 PRINT "DEGREE OF EQUATION = "; K
690 PRINT
700 PRINT "COEFFICIENTS"
710 FOR J = 0 TO K
720 PRINT "B(";J+1;") = "; B(J+1)
730 NEXT J
740 PRINT
750 PRINT
760 PRINT "INDEPENDENT", "PREDICTED", "OBSERVED", "PERC. ERROR"
770 PRINT
780 LET A(7,1) = 0
790 FOR I1 = 1 TO N
800 LET S = 0
810 FOR I = 1 TO K1
820 LET J = K1 - I + 1
830 LET S = S*X(I1) + B(J)
840 NEXT I
850 LET A(7,2) = S - Y(I1)
860 LET A(7,1) = A(7,1) + A(7,2)*A(7,2)
870 PRINT X(I1), S, Y(I1), A(7,2)*100/S
880 NEXT I1
890 PRINT
900 PRINT "SUM OF THE SQUARES = "; A(7,1)
910 END
```

PROGRAM NUMBER 5

```
 10 REM  THIS PROGRAM IS FOR THE CALCULATION OF OVERVOLTAGES AND
 20 REM  EXCHANGE CURRENT DENSITIES.  IN PART 1 THE PROGRAM FIRST
 30 REM  CALCULATES THE EXCHANGE CURRENT DENSITIES USING THE
 40 REM  THEORETICAL SLOPE VALUE.  IT THEN TAKES THE AVERAGE OF THESE
 50 REM  EXCHANGE CURRENT DENSITIES AND CALCULATES THE CORRESPONDING
 60 REM  OVERVOLTAGE VALUES.  IN PART 2 THE PROGRAM USES EXPERIMENTALLY
 70 REM  DETERMINED SLOPE AND INTERCEPT VALUES AND FIRST CALCULATES
 80 REM  OVERVOLTAGE VALUES.  IT THEN CALCULATES EXCHANGE CURRENT
 90 REM  DENSITIES USING EXPERIMENTAL OVERVOLTAGES.  IT THEN RECALCU-
100 REM  LATES THE EXCHANGE CURRENT DENSITIES USING THE PREVIOUSLY
110 REM  CALCULATED OVERVOLTAGE VALUES.
120 REM ..........................................................
130 REM ..........................................................
140 DIM I(25), O(25), L(25), X(25), G(25), H(25), C(25), P(25)
150 DIM D(25), K(25), F(25), M(25), Q(25), R(25), U(25)
160 PRINT "TEST NO. ";
170 INPUT T
```

```
180 IF T = 0 THEN 1380
190 PRINT "NUMBER OF POINTS IS = ";
200 INPUT N
210 PRINT "SLOPE FACTOR = ";
220 INPUT S
230 PRINT "EQUILIBRIUM POTENTIAL = ";
240 INPUT E
250 PRINT
260 PRINT
270 PRINT
280 FOR J = 1 TO N
290 READ C(J)
300 NEXT J
310 FOR J = 1 TO N
320 READ P(J)
330 NEXT J
340 REM  THIS IS THE BEGINNING OF PART 1 CALCULATIONS
350 LET G(0) = 0
360 FOR J = 1 TO N
370 LET I(J) = C(J)/1.1193
380 LET O(J) = P(J) - E
390 LET L(J) = LOG (I(J)) - (O(J)/S)
400 LET X(J) = EXP(L(J))
410 LET G(J) = G(J-1) + X(J)
420 NEXT J
430 LET V = G(N)/N
440 FOR J = 1 TO N
450 LET H(J) = (-S*LOG(V)) + (S*LOG(I(J)))
460 NEXT J
470 PRINT
480 PRINT
490 PRINT "THE FOLLOWING VALUES ARE THEORETICAL USING AN EQUILIBRIUM"
500 PRINT "POTENTIAL OF";E;"MV. AND A SLOPE OF";S
510 PRINT
520 PRINT
530 PRINT "CURRENT", "C.D. MA/CM2", "POTENTIAL", "OVERVOLTAGE", "EXCHANGE C.D."
540 FOR J = 1 TO N
550 PRINT C(J), I(J), P(J), O(J), X(J)
560 NEXT J
570 PRINT
580 PRINT
590 PRINT "THE AVERAGE EXCHANGE CURRENT DENSITY = ";V;"MA/CM2"
600 PRINT
610 PRINT
620 PRINT "USING AN EXCHANGE CURRENT DENSITY OF";V;"MA/CM2 AND A"
630 PRINT "SLOPE OF";S;"THEN THE CALCULATED OVERVOLTAGES WILL BE:"
640 PRINT
650 PRINT
660 PRINT "CURRENT","C.D.MA/CM2","POTENTIAL","O.V. EXP.","O.V. CALC."
670 FOR J = 1 TO N
```

```
 680 PRINT C(J), I(J), P(J), O(J), H(J)
 690 NEXT J
 700 PRINT
 710 PRINT
 720 PRINT "EXPERIMENTAL SLOPE =";
 730 INPUT B
 740 PRINT "EXPERIMENTAL INTERCEPT =";
 750 INPUT A
 760 PRINT
 770 PRINT
 780 PRINT "THE FOLLOWING VALUES ARE BASED ON EXPERIMENTAL"
 790 PRINT "DETERMINED VALUES, WITH AN EQUILIBRIUM POTENTIAL OF"
 800 PRINT E;"MV., AND A SLOPE OF";B;"."
 810 PRINT
 820 PRINT
 830 REM  THIS IS THE BEGINNING OF PART 2 CALCULATIONS
 840 LET R(0) = 0
 850 LET U(0) = 0
 860 FOR J = 1 TO N
 870 LET D(J) = (A-E) + (B*LOG(I(J)))
 880 LET F(J) = LOG(I(J)) - (O(J)/B)
 890 LET K(J) = LOG(I(J)) - (D(J)/B)
 900 LET M(J) = EXP(F(J))
 910 LET Q(J) = EXP(K(J))
 920 LET R(J) = R(J-1) + M(J)
 930 LET U(J) = U(J-1) + Q(J)
 940 NEXT J
 950 LET W = R(N)/N
 960 LET Y = U(N)/N
 970 PRINT "CURRENT","C.D.MA/CM2","POTENTIAL","O.V. EXP.","O.V. CALC."
 980 FOR J = 1 TO N
 990 PRINT C(J), I(J), P(J), O(J), D(J)
1000 NEXT J
1010 PRINT
1020 PRINT "THE FOLLOWING EXCHANGE CURRENT DENSITIES ARE CALCULATED"
1030 PRINT "USING EXPERIMENTAL OVERVOLTAGES AND EXPERIMENTAL"
1040 PRINT "SLOPE AND INTERCEPT VALUES"
1050 PRINT
1060 PRINT
1070 PRINT "CURRENT","C.D.MA/CM2","POTENTIAL","O.V. EXP.","EXCHANGE C.D."
1080 FOR J = 1 TO N
1090 PRINT C(J), I(J), P(J), O(J), M(J)
1100 NEXT J
1110 PRINT
1120 PRINT "AVERAGE EXCHANGE CURRENT DENSITY = ";W;"MA/CM2"
1130 PRINT
1140 PRINT
1150 PRINT "THE FOLLOWING EXCHANGE CURRENT DENSITIES ARE CALCULATED"
1160 PRINT "USING CALCULATED OVERVOLTAGE VALUES AND EXPERIMENTAL"
1170 PRINT "SLOPE AND INTERCEPT VALUES"
1180 PRINT
```

```
1190 PRINT
1200 PRINT "CURRENT","C.D.MA/CM2","POTENTIAL","O.V. CALC.","EXCHANGE C.D."
1210 FOR J = 1 TO N
1220 PRINT C(J), I(J), P(J), D(J), Q(J)
1230 NEXT J
1240 PRINT
1250 PRINT "AVERAGE EXCHANGE CURRENT DENSITY = ";Y;"MA/CM2"
1260 PRINT
1270 PRINT
1280 PRINT
1290 PRINT
1295 PRINT
1300 PRINT
1310 GO TO 160
1320 DATA
1330 DATA
1340 DATA
1350 DATA
1360 DATA
1370 DATA
1380 END
```

APPENDIX G

Early Experimental Problems

Two Cathode System

Much of the early work was plagued with experimental problems. Initial plans called for the use of two cathodes with one anode spaced equally between them. Tests were to be run using the same solution analysis but by preparing a new solution for each test and varying the current density for each test. It was also planned to deposit only a total of four grams of copper (two grams on each cathode). The data for these tests are listed in Table 1.A, Appendix A and are tests 1 to 20.

It soon became evident however, that this type of system would not work satisfactorily because of three shortcomings. In no case was there an equal amount of copper deposited on each cathode. The average variance was approximately 12 % . Nor were the morphological characteristics of both cathodes the same. Current efficiencies were erratic and did not follow the usual pattern. Instead of decreasing with increasing current density the current efficiency increased to a peak and then decreased.

It was felt that these shortcomings were due to a combination of several factors. One such factor was the difference in hydrodynamic flow to which each electrode was exposed. This is illustrated in Figure G.1. As can be seen from this figure each electrode surface was placed an equal distance from its corresponding anode surface.

However, because of the way the electrode holders were designed the hydrodynamics in the area A to B were not the same as those in the corresponding area C to D. It was very possible that some turbulence was present in the area A since this area was shielded from the solution more than areas B, C and D. The magnetic stirring bar shown in the figure was always located in the same manner with relation to the electrodes.

When looking at Figure G.1 it would seem that between cathode number one and its corresponding anode surface there would be better hydrodynamic flow and thus if there were a difference in the amount of copper deposited between the two cathodes then cathode number one would have the greatest amount of deposit (owing to a slightly better current efficiency). This was indeed found to be the case experimentally, with cathode number one having on the average 12% more copper deposited on it than was deposited on cathode number two.

It was also realized that with the present system the spacing of the cathodes equally distant from the anode was impossible. This explained the difference in morphology and possibly the difference in the amounts of deposits.

A more important explanation of the current efficiency deviations was felt to lie in the method of sample weighing. These weighings were made by first weighing the sample and then applying the masking tape as explained in Appendix D. The sample was then reweighed. The etched sample was then reweighed to determine the amount of weight loss due to etching. This amount lost was used to correct the initial

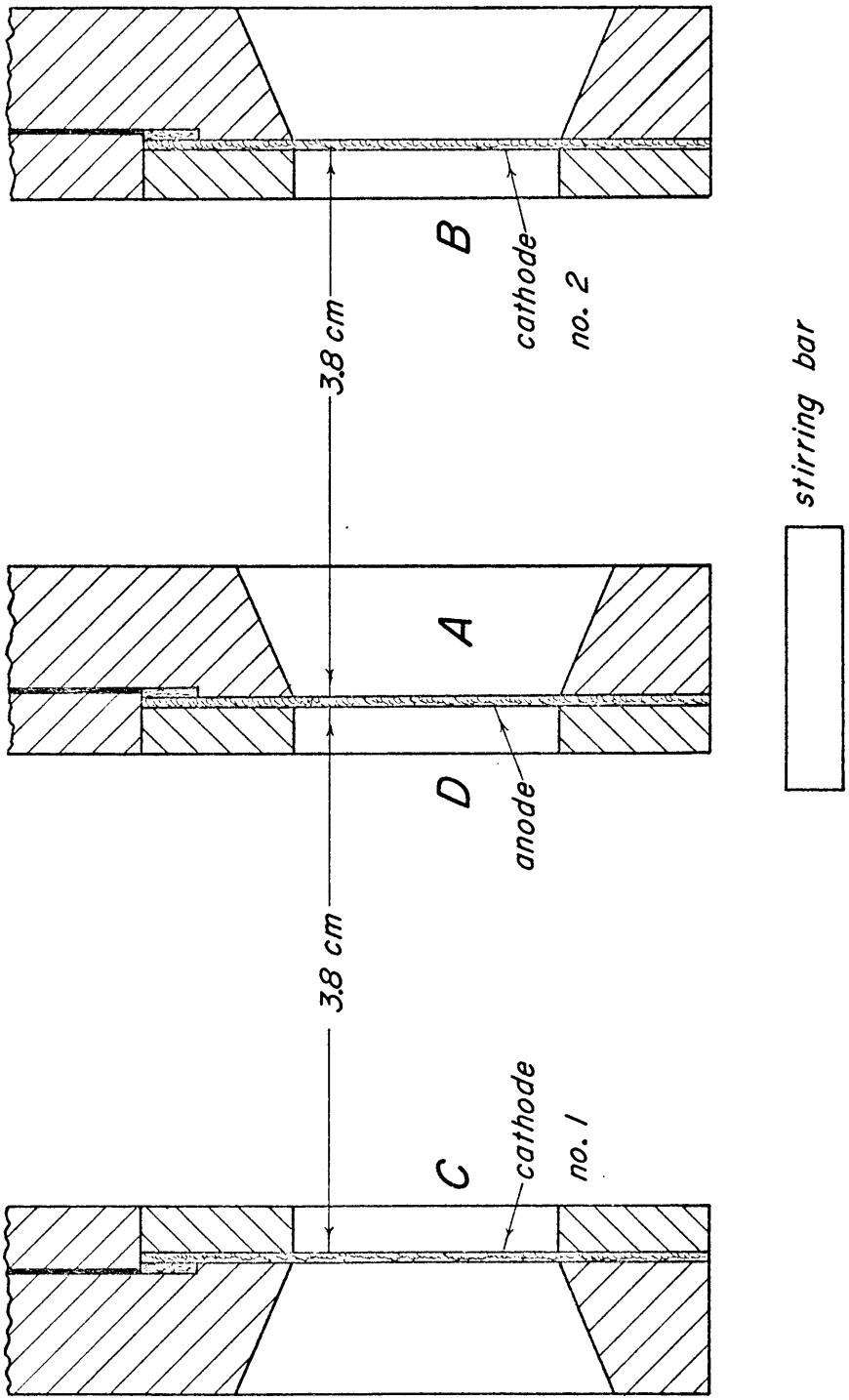

CROSS-SECTIONAL VIEW OF 3-ELECTRODE SYSTEM

FIGURE G.1

weight of the sample. After a test the sample was dried with a blast of air and the tape was stripped off. A final weighing was made and this weight together with the corrected initial weight was used to determine the weight of deposit and therefore the current density. This system was both tedious and susceptible to errors. These errors could combine to produce the results already noted.

One Cathode System

A new procedure was then used in which only one cathode was used, and only one gram of copper was deposited (tests 21 to 40, Table 1.A, Appendix A). Changes were also made in the weighing procedures to see if more reliable results could be obtained. The only difference in procedure over the previous one was that a final weight of the sample was also measured with the tape still on. It was therefore possible to compare results using weights made without any tape and those with tape.

This procedure produced current efficiency results which although were not in agreement with an acceptable trend they did not deviate as badly as in the previous tests. However, another phenomenon was encountered. Current efficiencies of greater than 100 % were obtained. These were obtained only when using those weights obtained with the tape still on the sample. Current efficiencies calculated by using weights obtained without any tape differed from those with tape and were consistently lower. This could be easily explained if the tape was porous enough to absorb some electrolyte and therefore itself gain weight during a test.

Absorbtion and Dissolution Tests

Tests were then run to see if in fact the tape was capable of absorbing electrolyte. At this same time tests were also run to see if any dissolution of copper might have occurred during the previous tests. If dissolution had occurred this could explain the low efficiencies of low current densities, since at low current densities the samples had to remain in solution for as long as twenty hours in order to obtain the same amount of deposit as in higher current density tests.

Five electrode sample without any tape were suspended in a cell which was operating at 30 amps/ft^2 and which had an electrolyte of 40 gpl copper, 100 gpl H_2SO_4 and a temperature of 25 °C. The samples were kept in the solution for a period of 1387 minutes after which they were removed, rinsed and dried. The results show an average weight loss of 11%. The results are shown in Table 1.G.

TABLE 1.G

Sample	Initial Weight (g)	Final Weight (g)	Weight Change (g)	% Wt Change (%)
1	3.11287	2.72447	-0.3884	-12.477
2	2.78374	2.45733	-0.3264	-11.725
3	3.11038	2.82100	-0.2894	- 9.304
4	3.15941	2.85355	-0.3059	- 9.681
5	3.20705	2.81842	-0.3886	-12.118

The next step was to determine the rate of dissolution as a function of time. This was accomplished by using fourteen electrode samples that were taped and etched in the usual manner. An initial weight with the tape on was used as was a final weight with tape. The fourteen samples were suspended in a bath containing 40 gpl copper, 100 gpl H_2SO_4 and at 25 °C. Two samples were removed every two hours. These samples were rinsed and air dried and then allowed to dry further in a dessicator for a period of twenty-four hours before a final weight measurement was made. The results are shown in Table 2.G and indicate an average weight loss of 0.02% per hour.

Next tests were run to indicate the degree of absorption if any. These tests were run by using prepared electrode samples with tape and soaking them in distilled water for a twenty-four hour period. After removal from the water they were dried in a blast of air and weighed. They were then allowed to dry in a dessicator for twenty-four hours and then reweighed. The results are shown in Table 3.G and indicate a small degree of absorption.

The net result of all of these tests was an indication that a change in procedure was necessary. The final procedure that was used is outlined in the main text. The data for tests 1 to 40 listed in Table 1.A, Appendix A, are those tests in which the trouble in experimental procedure was realized. The data for these tests was not used in any way in the results of the empirical experiments. They are listed only for the benefit of the reader.

TABLE 2.G

Rate of Dissolution

Sample	Time (hr)	Weight Change (g)	% Weight Change (%)	Rate of Dissolu. (%/hr)
1.1	2	-0.0017	-0.0404	0.0202
1.2	2	-0.0021	-0.0510	0.0255
2.1	4	-0.0027	-0.0648	0.0162
2.2	4	-0.0036	-0.0851	0.0213
3.1	6	-0.0040	-0.0917	0.0153
3.2	6	-0.0048	-0.1134	0.0189
4.1	8	-0.0062	-0.1431	0.0179
4.2	8	-0.0071	-0.1663	0.0208
5.1	10	-0.0085	-0.1973	0.0197
5.2	10	-0.0093	-0.2165	0.0216
6.1	12	-0.0082	-0.1920	0.0160
6.2	12	-0.0106	-0.2458	0.0204
7.1	72	-0.0547	-1.2564	0.0174
7.2	72	-0.0718	-1.6958	0.0235
			Average	0.020

TABLE 3.G

Absorbtion Data

Sample	Weight Change Air Dry (g)	% Change	Weight Change Dessicator (g)	% Change
1.1	+0.0052	+0.1205	+0.0010	+0.0231
1.2	+0.0055	+0.1311	+0.0010	+0.0247
2.1	+0.0054	+0.1279	+0.0012	+0.0296
2.2	+0.0058	+0.1346	+0.0014	+0.0326
3.1	+0.0058	+0.1332	+0.0023	+0.0530
3.2	+0.0046	+0.1076	+0.0020	+0.0468
4.1	+0.0054	+0.1243	+0.0022	+0.0505
4.2	+0.0056	+0.1329	+0.0023	+0.0543
5.1	+0.0060	+0.1387	+0.0021	+0.0485
5.2	+0.0061	+0.1441	+0.0024	+0.0565
6.1	+0.0066	+0.1529	+0.0021	+0.0496
6.2	+0.0064	+0.1488	+0.0024	+0.0558
7.1	+0.0067	+0.1569	+0.0028	+0.0651
7.2	+0.0066	+0.1573	+0.0025	+0.0605

Calculation of Current Efficiencies With Dissolution Considered

In all of the low current density tests it was found that the current efficiencies were lower than those for the higher current density tests. The cause for this anomalous behavior was attributed to redissolution. In order to show this, calculations were made using data from tests 76 to 82 which were all made at a low current density (19.1 amps/ft^2) and for time periods that were of the order of 24 hours. A sample calculation is given below and the results are shown in Table 4.G.

These results show that if some allowance is made for redissolution having occurred then the current efficiencies are more in accord with what should be expected, i.e. an equal or higher current efficiency than those determined at higher current densities. It should be noted when looking at the results in Table 4.G that although they show current efficiencies greater than 100 % these results are only comparitive and not absolute values. They were calculated using an average dissolution rate of 0.020 %/hr. In actual practice the dissolution rate may have been lower than this value and indeed it would take only a slightly smaller dissolution rate to give current efficiency values below 100%.

Sample Calculation

For test number 76 and using an average dissolution rate of 0.020 %/hr then:

Time of test = 24.05 hours

Weight of deposit = 5.279 g

Theoretical weight of deposit = 5.437 g

Percent dissolution = 24.05 hr x 0.020 %/hr = 0.481 %

Corrected weight of deposit = 1.048 x 5.279 = 5.532 g

Corrected current efficiency =(5.532 g / 5.437 g) x 100 = 101.6 %

TABLE 4.G

Dissolution Corrections For Current Efficiencies*

Test No.	Time (hr)	Experimental Current Efficiency (%)	Experimental Weight of Deposit (g)	Theoretical Weight of Deposit (g)	Calc. Wt. of Depos. (g)	Calc. Current Effic. (%)
76	24.05	97.1	5.279	5.437	5.532	101.6
77	25.05	97.2	5.512	5.671	5.960	105.1
78	23.75	97.2	5.228	5.380	5.480	101.8
79	23.85	97.4	5.255	5.395	5.510	102.2
80	23.92	97.5	5.278	5.411	5.530	102.3
81	23.68	97.6	5.228	5.358	5.470	102.1
82	71.08	97.3	15.660	16.092	17.880	111.1

* An example of results is given only for tests 76 to 82.

APPENDIX H

Preparation of Agar Gel

The agar gel used as a salt bridge in the polarization experiments was prepared in the following manner.

Preparation

Warm a flask containing 4 g agar and 90 ml of water using a double boiler arrangement. When the agar is completely dissolved add 30 g of potassium chloride (KCl) and stir throughly. Solidified gel should be white in color. Use a good grade of agar in order to obtain the best results. When the potassium chloride has dissolved pipette the liquid gel into the probe. Allow the gel to set-up before using (this requires a period of approximately 10 minutes).

Precautions

Special precautions should be taken in order to insure that the probe does not dry out. This is best prevented by keeping both ends immersed in a solution of saturated potassium chloride. Never use distilled water for this purpose as it leaches the potassium chloride from the gel and reduces the effectiveness of the probe by increasing its resistance.

Best results are also obtained when the gel in the probe contains as few air bubbles as possible. The entrapment of air bubbles

can be minimized by getting the gel as fluid as possible before introducing it into the probe (however, do not allow the gel to overheat as this will cause it to burn and again be less effective).

Any gel that is not used in the probe can be saved by keeping it stored in an air tight container. To use the gel after storage remelt it in the same double boiler arrangement. Occasionally during the remelting process it is necessary to add a few drops of saturated potassium chloride solution in order to get the gel sufficiently fluid.

APPENDIX I

Examples Of Corrections Made To Polarization Data

All the experimental data from the polarization tests were processed in three distinct steps in order to arrive at what was considered the final form of the data.

Step Number One

The first step was to correct the potential readings for the error that was present in the electrometer used in the measurements. It was found by comparing the electrometer to a secondary standard that the electrometer consistently read values that were lower than the actual potential. The deviation was different for the various ranges on the electrometer. For this reason it was necessary to correct the potential readings according to the range upon which it had been read. Corrections were made via computer and the correction factors for each range are as follows:

0 - 100 millivolts,	no factor
100 - 300 millivolts,	1.026
300 - 500 millivolts,	1.031
500 - 700 millivolts,	1.024
700 - 999 millivolts,	1.022

The program used for these corrections is listed in Appendix F, Program

Number One. An example of the changes in potentialsis shown in Table 1.I using data from test number 33.

Step Number Two

The second step in the correction process was to take the data from step number one and correct for the IR drop that occurred between the tip of the Luggin-Haber probe and the electrode surface.

This ohmic potential drop was first recognized by F.P. Bowden and J.N. Agar (Agar and Bowden, 1938). They referred to it as "resistance overpotential". This term is currently being replaced by the more correct term of "resistance polarization". This ohmic potential drop in no way influences the electrode process and likewise is not influenced by the electrode process. It is only a function of the conductivity of the electrolyte and the applied current. However, if the true overvoltage values are to be known it is necessary to compensate for the resistance polarization. This is especially true for potentials read at higher current densities.

For a system in which the electrode is a plane surface and the tip of the probe is separated from the electrode surface by a distance l, then the resistance polarization will be :

$$R = l \cdot i/\kappa \text{ millivolts}$$

Where i is the current density (ma/cm^2), κ is the specific conductivity (ohm^{-1}/cm) and R is the resistance polarization (millivolts).

This method of correcting for the resistance polarization depends on two assumptions, which for the case at hand, should be applicable. First, this method of correction assumes that the conductivity of the

elec yte is constant between the tip of the probe and the surface of the electrode. It is known that this is not absolutely true since there are concentration changes in this region. However, for these experiments this assumption will introduce very little error.

A second assumption is that the electrolyte is of the "no migration" type. This means that there must be an excess of some electrolyte. In this case there was an excess of sulfuric acid.

The reader is referred to the following references for more details on the subject of resistance polarization: (Barnartt, 1952), (Barnartt, 1961) and (Sundheim, 1968).

An example of the changes in the data when the corrections for resistance polarization are made is shown in Table 2.I. A graphic illustration is shown in Figure I.1 in which the top curve is the data corrected only for the electrometer errors and the bottom curve is the data when the resistance polarization corrections are made. The data for Table 2.I and Figure I.1 is again from test number 33.

Step Number Three

The third step in the process of correcting the experimental data was to take the data from step number two and use a least-squares method for curve fitting. This was done by using either of the two programs listed in Appendix F. Table 3.I and Figure I.2 show the resulting changes (data taken from test number 33).

TABLE 1.I

Electrometer Corrections For Test Number 33

Measured Potential (mv)	Corrected Potential (mv)	Measured Potential (mv)	Corrected Potential (mv)
74.0	75.0	185	189.8
75.0	76.0	195	200.1
76.5	77.5	205	210.3
78.0	79.0	217	222.6
80.0	81.0	230	236.0
81.0	82.0	242	248.3
87.0	88.0	253	259.6
91.5	92.5	264	270.9
95.5	96.5	276	283.2
99.5	100.5	288	295.5
101	103.6	299	306.8
104	106.7	307	316.5
107	109.8	318	327.8
111	113.9	327	337.1
114	117.0	336	346.4
130	133.4	350	360.8
145	148.8	380	391.8
159	163.1	415	427.9
171	175.4	440	453.6

TABLE 1.I (cont.)

Measured Potential (mv)	Corrected Potential (mv)	Measured Potential (mv)	Corrected Potential (mv)
465	479.4	555	568.3
500	515.5	585	599.0
530	542.7		

TABLE 2.I

Resistance Polarization Corrections For Test Number 33

Current (ma)	Current Density (ma/cm^2)	IR Drop (mv)	Measured Potential (mv)	Corrected Potential (mv)
0.1	0.089	0.202	75.0	74.8
0.2	0.179	0.40	76.0	75.6
0.4	0.357	0.81	77.5	76.7
0.6	0.536	1.21	79.0	77.8
0.8	0.715	1.61	81.0	79.4
1.0	0.893	2.02	82.0	80.0
2.0	1.787	4.04	88.0	84.0
3.0	2.680	6.06	92.5	86.4
4.0	3.574	8.08	96.5	88.4
5.0	4.467	10.09	100.5	90.4
6.0	5.360	12.11	103.63	91.5
7.0	6.254	14.13	106.70	92.6
8.0	7.147	16.15	109.78	93.6
9.0	8.041	18.17	113.89	95.7
10	8.934	20.19	116.96	96.8
15	13.401	30.28	133.38	103.1
20	17.868	40.38	148.77	108.4
25	22.335	50.47	163.13	112.6
30	26.802	60.57	175.45	114.9

Table 2.I (cont.)

Current (ma)	Current Density (ma/cm^2)	IR Drop (mv)	Measured Potential (mv)	Corrected Potential (mv)
35	31.269	70.66	189.81	119.1
40	35.737	80.76	200.07	119.3
45	40.204	90.85	210.33	119.5
50	44.671	100.95	222.64	121.7
55	49.138	111.05	235.98	124.9
60	53.605	121.14	248.29	127.1
65	58.072	131.44	259.58	128.3
70	62.539	141.33	270.86	129.5
75	67.006	151.43	283.88	131.7
80	71.473	161.52	295.49	134.0
85	75.940	171.62	306.77	135.1
90	80.407	181.71	316.52	134.8
95	84.874	191.81	327.86	136.0
100	89.432	201.90	337.14	135.2
105	93.809	211.10	346.42	134.4
110	98.276	222.09	360.85	138.7
125	111.677	252.38	391.78	139.4
140	125.078	282.66	427.86	145.2
150	134.012	302.85	453.64	150.8
160	142.946	323.04	479.41	156.3

TABLE 3.I

Curve Fitted Data

(third degree equation)

Current (ma)	Observed Overvoltage (mv)	Predicted Overvoltage (mv)
10	22.77	26.74
15	29.09	30.24
20	34.39	33.45
25	38.65	36.50
30	40.88	39.31
35	45.14	41.93
40	45.31	44.36
45	45.47	46.63
50	47.69	48.73
55	50.94	50.68
60	53.15	52.50
65	54.34	54.18
70	55.53	55.76
75	57.75	57.23
80	59.97	58.61
85	61.15	59.91
90	60.81	61.14
95	62.05	62.31

TABLE 3.I (cont.)

Current (ma)	Observed Overvoltage (mv)	Predicted Overvoltage (mv)
100	61.24	63.44
105	60.42	64.53
110	64.76	65.60
125	65.40	68.78
140	71.20	72.16
150	76.79	74.68
160	62.37	77.53
175	68.17	82.59
190	65.11	88.89
200	70.52	93.92
210	81.05	99.74

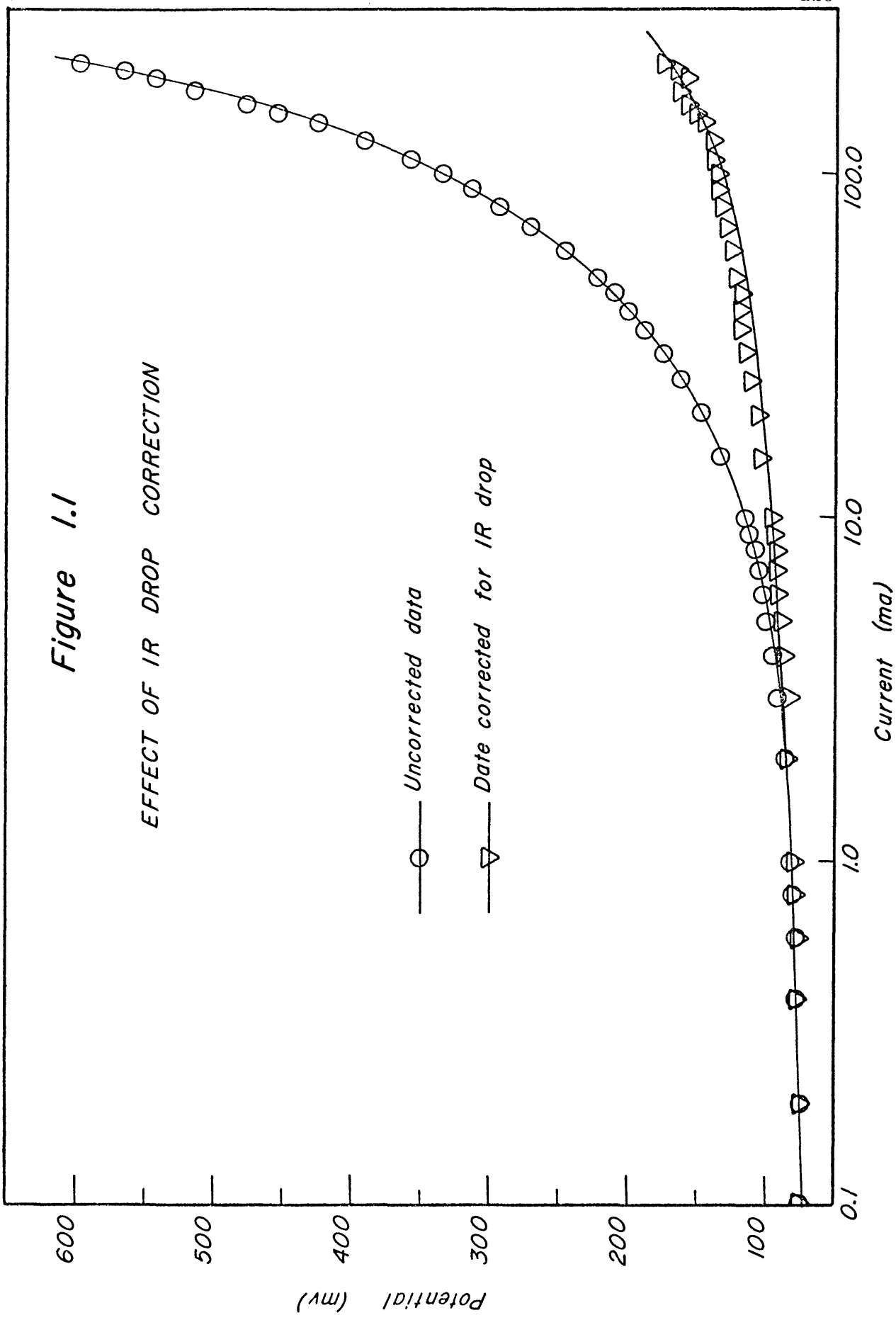
Figure 1.1
EFFECT OF IR DROP CORRECTION
Uncorrected data
Date corrected for IR drop
Potential (mv)
600
500
400
300
200
100
0.1
1.0
10.0
100.0
Current (ma)

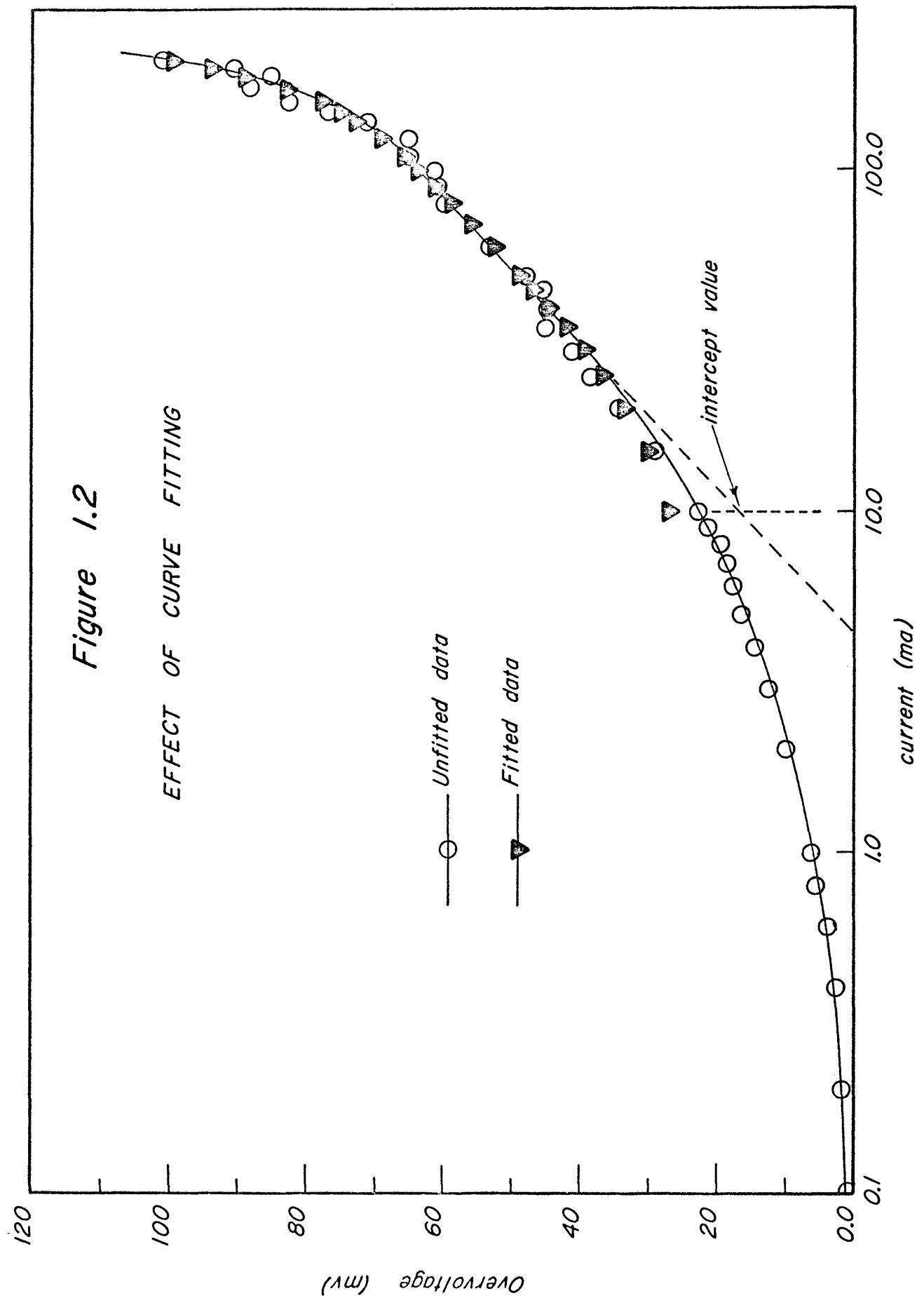
Figure 1.2
EFFECT OF CURVE FITTING
Unfitted data
Fitted data
intercept value
Overvoltage (mv)
current (ma)
120
100
80
60
40
20
0.0
0.1
1.0
10.0
100.0

APPENDIX J

Example Illustrations of Surface Indexes

The following photographs are example illustrations of actual electrode surfaces having different surface indexes. The photographs are listed in ascending order of surface indexes. Along with each photograph is a list of the surface index, the test number and the magnification of the photograph.

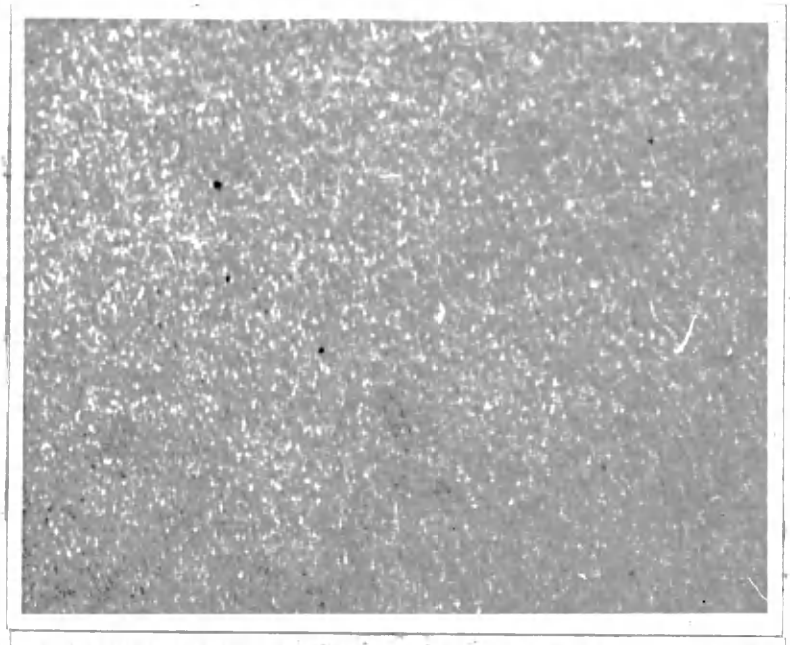

FIGURE J.1

Surface Index = 1.0

Test Number 76

Magnification 8

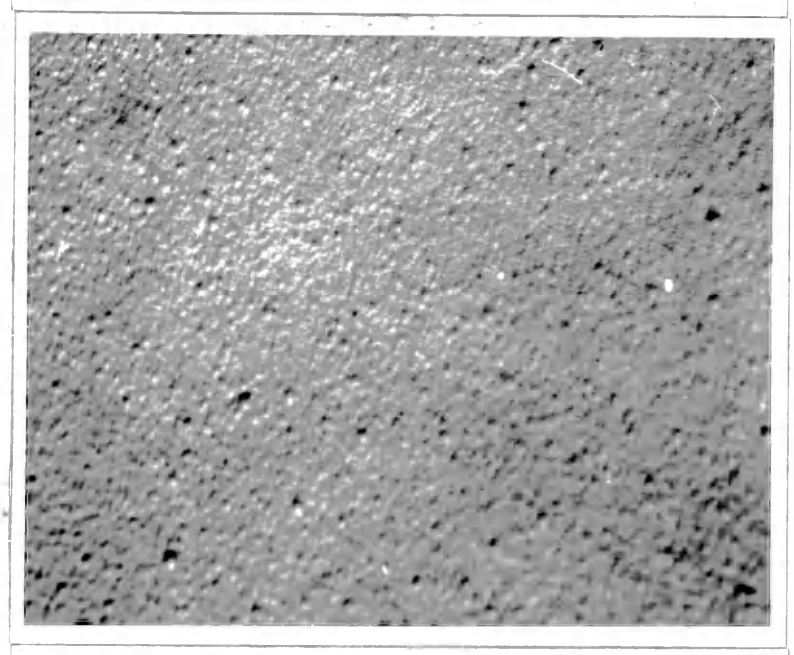

FIGURE J.2

Surface Index = 1.5

Test Number 81

Magnification 8

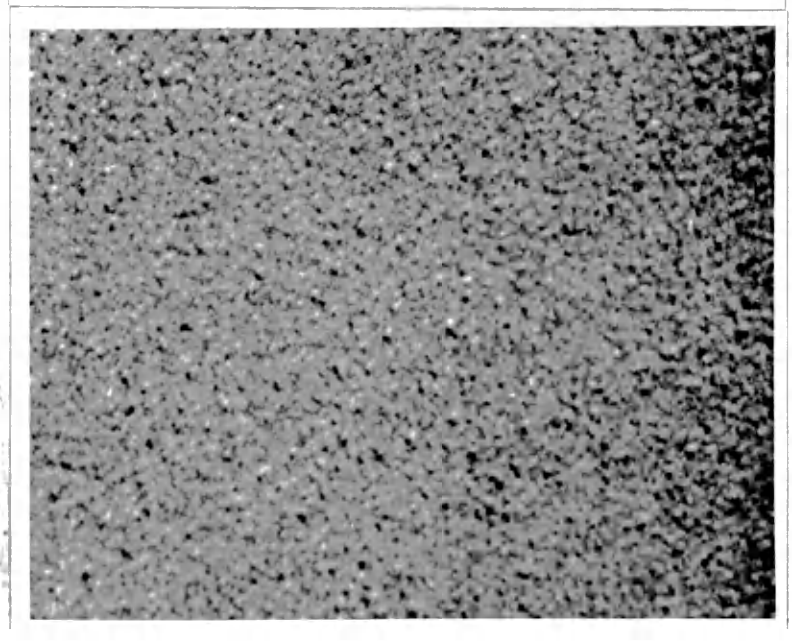

FIGURE J.3

Surface Index = 2.0

Test Number 104

Magnification 8

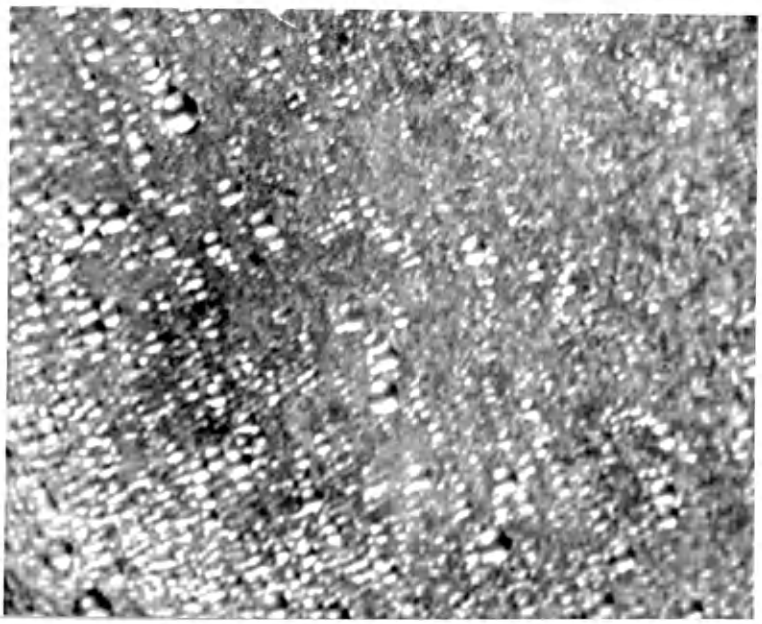

FIGURE J.4

Surface Index = 2.5

Test Number 124

Magnification 8

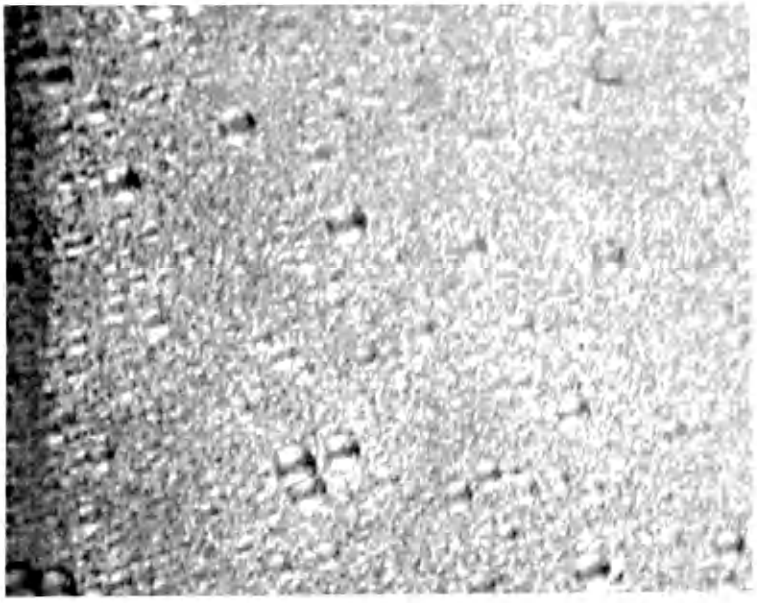

FIGURE J.5

Surface Index = 3.5

Test Number 117

Magnification 8

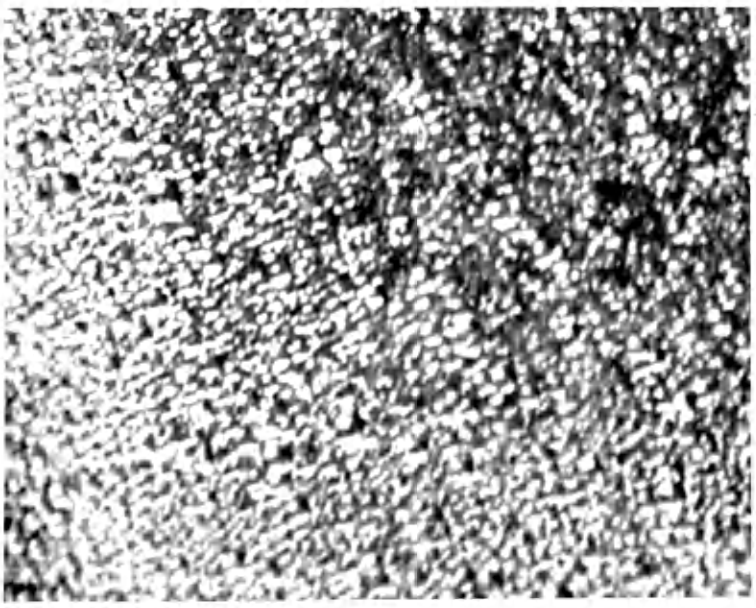

FIGURE J.6

Surface Index = 4.2

Test Number 61

Magnification 8

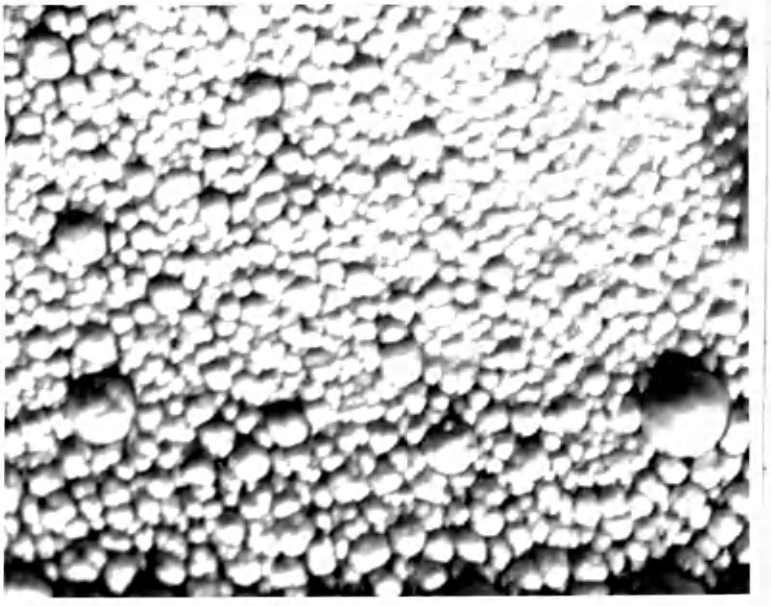

FIGURE J.7

Surface Index = 4.5

Test Number 135

Magnification 8

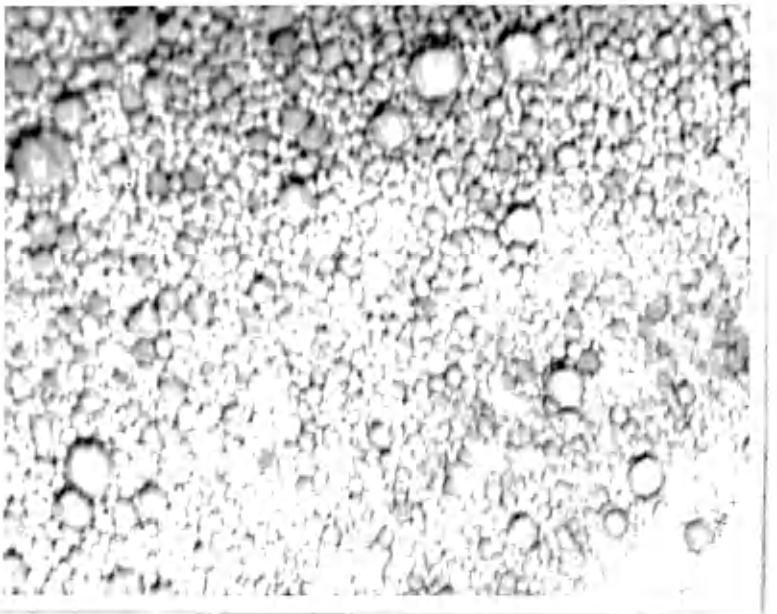

FIGURE J.8

Surface Index = 5.0

Test Number 74

Magnification 8

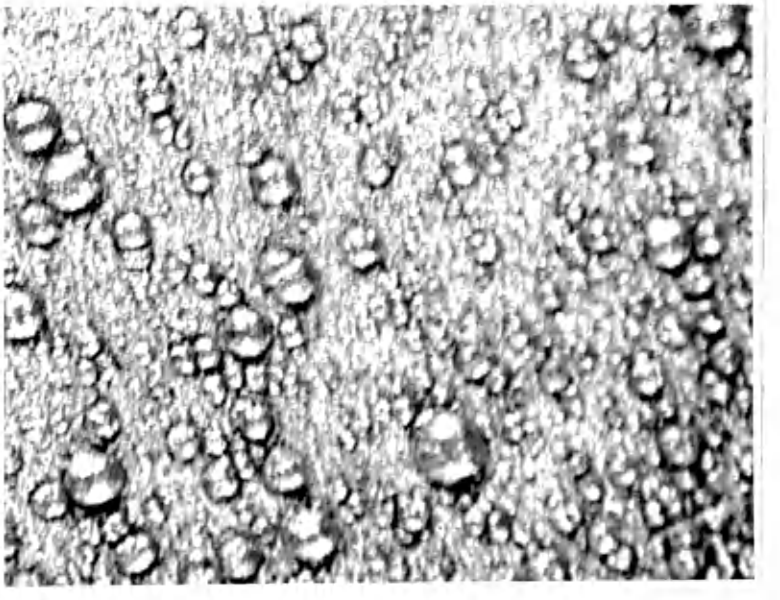

FIGURE J.9

Surface Index = 6.0

Test Number 90

Magnification 8

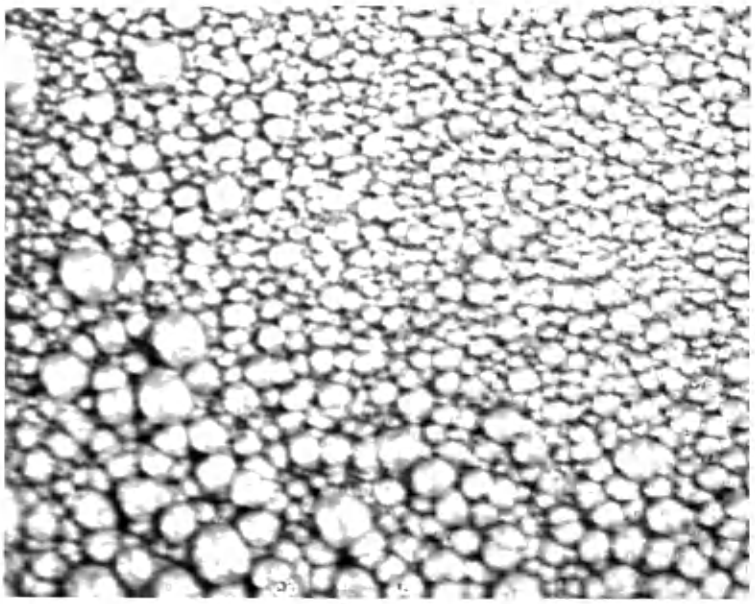

FIGURE J.10

Surface Index = 7.0

Test Number 138

Magnification 8

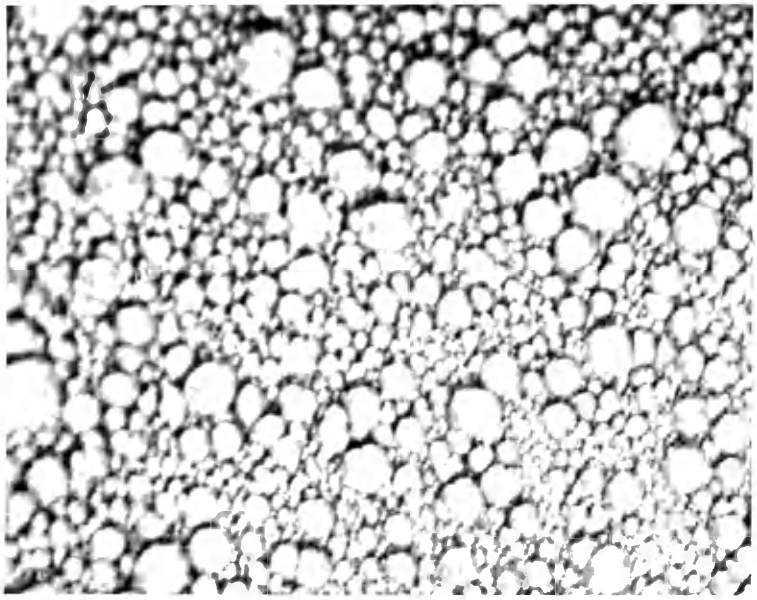

FIGURE J.11

Surface Index = 8.0

Test Number 119

Magnification 8

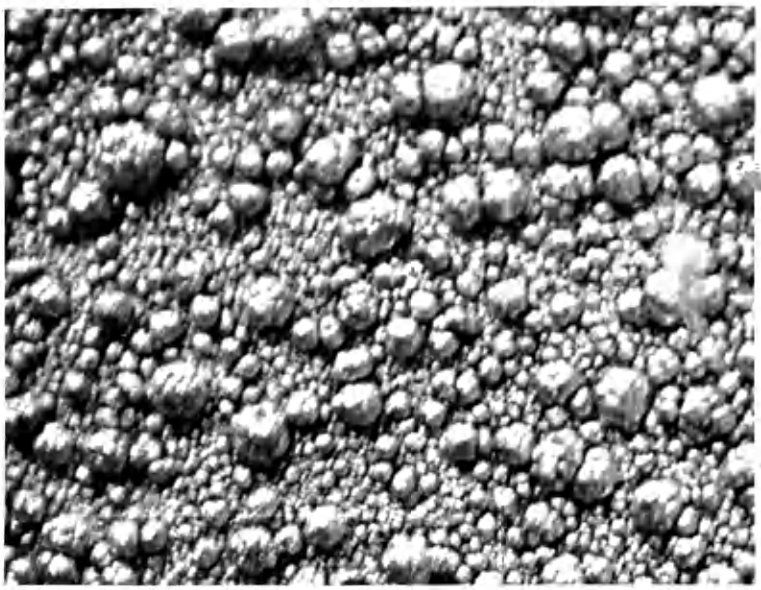

FIGURE J.12

Surface Index = 9.0

Test Number 106

Magnification 8

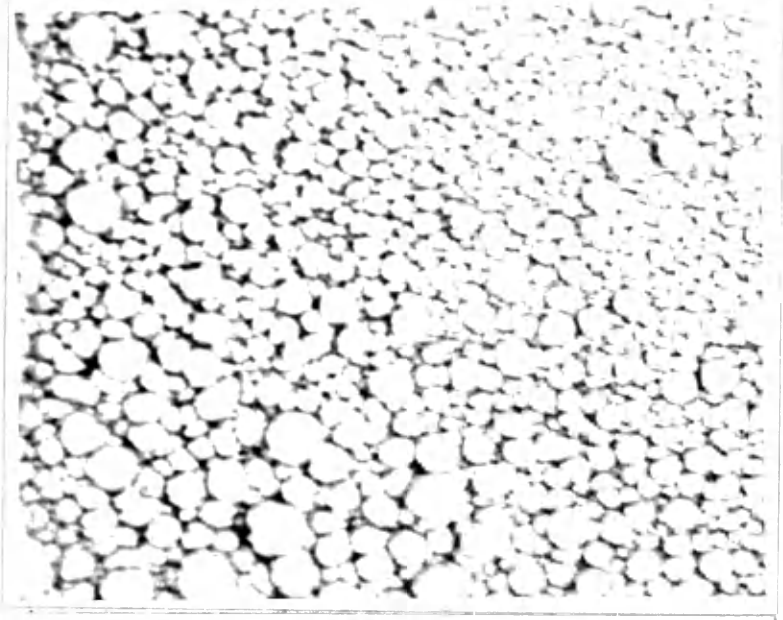

FIGURE J.13

Surface Index = 10.0

Test Number 144

Magnification 8

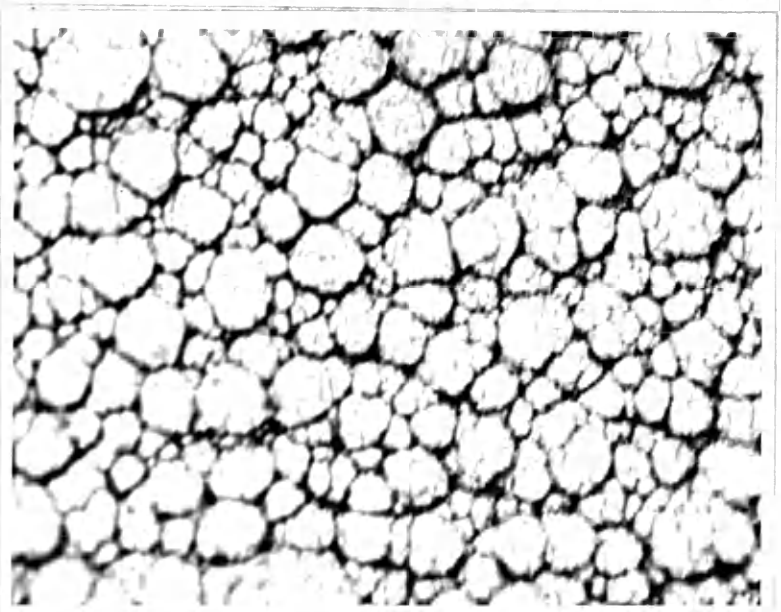

FIGURE J.14

Surface Index = 16.0

Test Number 75

Magnification 8

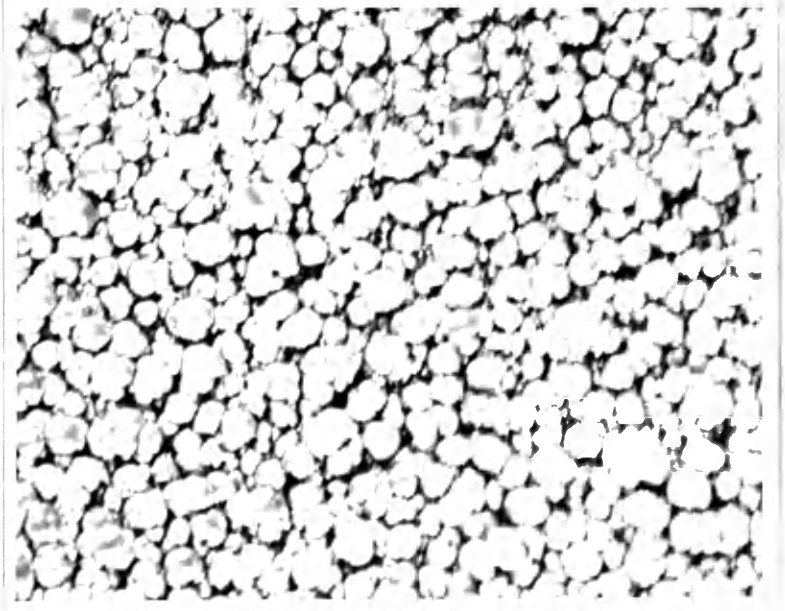

FIGURE J.15

Surface Index = 17.0

Test Number 66

Magnification 8

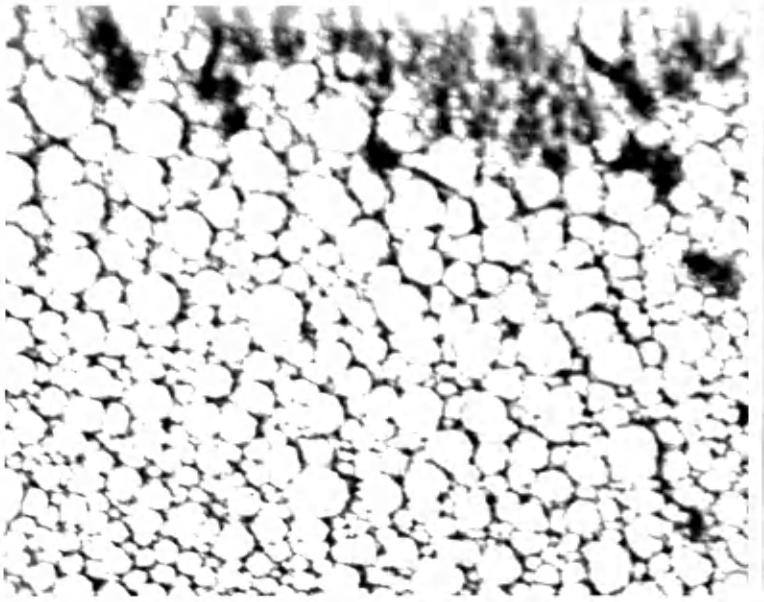

FIGURE J.16

Surface Index = 18.0

Test Number 133

Magnification 8

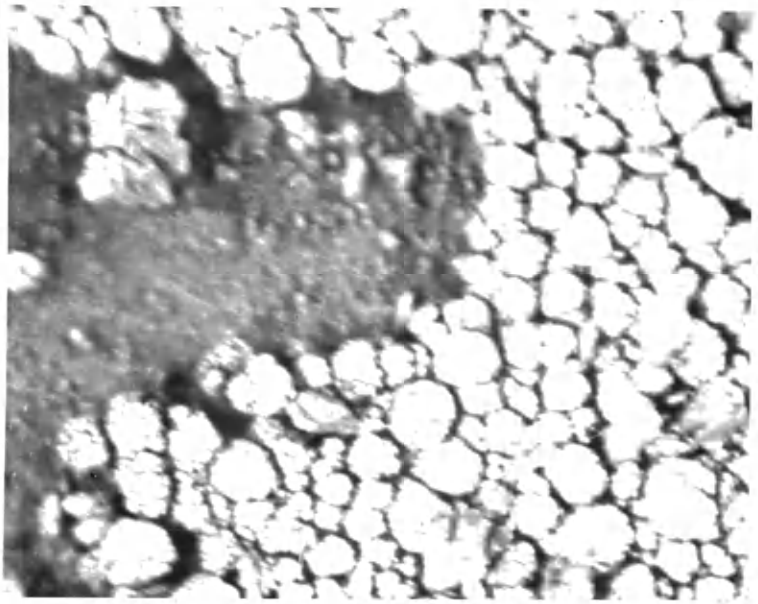

FIGURE J.17

Surface Index = 20.0

Test Number 140

Magnification 8

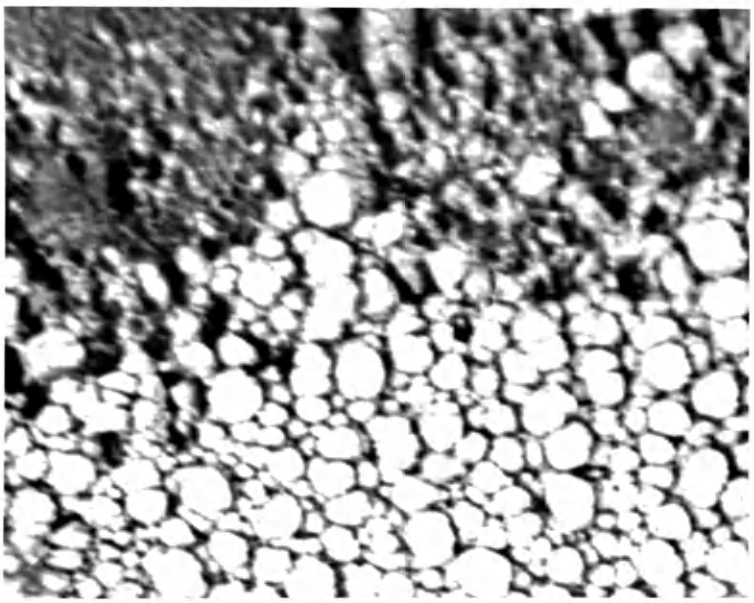

FIGURE J.18

Surface Index = 20.0

Test Number 146

Magnification 8